UNIVERSITY OF LONDON THESIS

Degree PhD Year 2006 Name of Author HORAN, Susannah Jane

CYTOCHROME OXIDASE ASSEMBLY, AND CELLULAR AND GENOMIC EFFECTS OF NITRIC OXIDE, STUDIED IN YEAST

Thesis submitted to the University of London
for the degree of Doctor of Philosophy,
April 2006

by Susannah Jane Horan

Wolfson Institute for Biomedical Research
University College London
The Cruciform Building
Gower Street
London WC1E 6BT

ProQuest LLC
789 East Eisenhower Parkway
P.O. Box 1346
Ann Arbor, MI 48106-1346

ABSTRACT

Cytochrome oxidase is the terminal proton pumping enzyme of the respiratory chain, catalysing the reduction of oxygen to water. This complex enzyme is composed of up to thirteen subunits of both nuclear and mitochondrial genetic origin, but the order in which they assemble is not fully understood. To investigate assembly I utilised blue native gel electrophoresis to analyse *Saccharomyces cerevisiae* strains with mutations in cytochrome oxidase causing assembly defect. I identified novel subcomplexes incuding, for the first time, a subcomplex containing mitochondrially encoded subunits.

The respiratory chain is a target of the free radical nitric oxide (NO), which reversibly inhibits cytochrome oxidase through competition with oxygen at its active site. NO also has a myriad of other targets, and many of its actions are mediated through reactive nitrogen species (RNS) formed on reaction of NO with other species. NO is released as part of the immune response to infection and has antimicrobial action. Here, I found that prolonged incubation of yeast with an NO donor inhibited growth and caused a decrease in cytochrome oxidase content in dividing cells, which may be due to NO interfering with the assembly of the enzyme. I have also analysed gene expression in yeast after short NO exposure, to gain insight into the stress sensed by the cell and the transcription factors involved. The data suggest that NO causes a general stress response, in addition to specific effects such as repression of respiratory chain genes and activation of antioxidant/detoxification systems. Many genes known to be regulated by Hap1p were repressed, suggesting that NO might interfere with this transcription factor.

ACKNOWLEDGEMENTS

First of all, special thanks to Brigitte Meunier for her supervision and support over the last few years, and for always making time for discussions with me. Also thanks to past members of the lab, both recent and more distant, especially Ingrid Bourges and Nick Fisher, for sharing their knowledge, skills and friendship.

Particular thanks go to Jan-Willem Taanman, for allowing me to utilise his expertise and resources to produce the western blots in Chapter 3. Thank you also to Peter Piper and Mehdi Mollapour, for generously providing many of the strains and plasmids used in Chapters 4 and 5, and Bernard Guiard and Alexander Tzagoloff, who also kindly provided plasmids.

Thank you to all at the WIBR, for providing an excellent working environment. In particular, thank you to the Scientific Support team, for their expertise in sequencing, microarray and (RT)-qPCR.

Finally, thank you to James, for doing everthing non thesis-related, so I didn't have to.

This work was funded by the Biotechnology and Biological Sciences Research Council, and Nicox, France.

PUBLICATIONS

Horan,S., Bourges,I., and Meunier,B. (2006) Transcriptional response to nitrosative stress in *Saccharomyces cerevisiae*. Yeast. *23*, 519-535.

Horan,S., Bourges,I., Taanman,J.-W., and Meunier,B. (2005). Analysis of *COX2* mutants reveals cytochrome oxidase subassemblies in yeast. Biochem. J. *390*, 703-8.

Bourges,I., **Horan,S.**, and Meunier,B. (2005). Effect of inhibition of the bc_1 complex on gene expression profile in yeast. J. Biol. Chem. *280*, 29743-9.

TABLE OF CONTENTS

ABSTRACT 2
ACKNOWLEDGEMENTS 3
PUBLICATIONS 4
TABLE OF CONTENTS 5
LIST OF FIGURES AND TABLES 9
ABBREVIATIONS 11
Chapter 1 INTRODUCTION 13
1.1. MITOCHONDRIA AND THE RESPIRATORY CHAIN 14
1.1.1. The chemiosmotic hypothesis 14
1.1.2. Components of the respiratory chain 15
1.2. CYTOCHROME OXIDASE 15
1.2.1. Structure of cytochrome oxidase 16
1.2.2. Catalysis and proton translocation 17
1.3. ASSEMBLY OF CYTOCHROME OXIDASE 18
1.3.1. Import of nuclear encoded subunits into the mitochondria 18
1.3.2. Export of protein domains from the mitochondrial matrix 19
1.3.2.1. Subunit-specific membrane-bound translational activators 19
1.3.2.2. Oxa1p 20
1.3.2.3. Mba1p 22
1.3.2.4. Removal of the Cox2p N-terminal presequence 22
1.3.2.5. Cox18p, Mss2p and Pnt1p 22
1.3.3. Recruitment and insertion of cofactors 23
1.3.3.1. Heme 23
1.3.3.2. Copper 24
1.3.4. Quality control systems 26
1.3.5. Association of subunits 28
1.3.6. Cytochrome oxidase disorders 29
1.4. NITRIC OXIDE 30
1.4.1. Physiological functions of NO 30
1.4.2. Reversible inhibition of cytochrome oxidase by NO 31
1.4.3. Antimicrobial action of NO 32
1.5. REACTIVE NITROGEN SPECIES AND THEIR TARGETS 32
1.5.1. Irreversible inhibition of respiratory chain enzymes by NO/RNS 33
1.5.2. Other protein targets 34
1.5.3. DNA and lipid damage 35
1.5.4. Production of ROS by the respiratory chain 36
1.6. ROS/RNS DEFENCE IN YEAST 37
1.6.1. Superoxide dismutase 37
1.6.2. Yhb1p 37
1.6.3. Glutathione 38
1.6.4. Removal of peroxides 38
1.6.5. Transcription factors involved in the response to stress 39
1.7. AIMS OF THIS THESIS 40
1.7.1. Cytochrome oxidase assembly 40
1.7.2. Antimicrobial action of nitric oxide 41
Chapter 2 MATERIALS AND METHODS 46
2.1. CELL BIOLOGY 47
2.1.1. Yeast growth 47
2.1.2. Bacterial growth 47

2.1.3. Crossing yeast strains 48
2.1.4. Generation of ρ^0 (mtDNA-less) cells 48
2.1.5. Mapping mutations to the *COX2* gene 48
2.1.6. Cytoduction 48
2.1.7. Generation of revertants 49
2.1.8. Incubation with nitric oxide donor 50
2.1.9. Methylene blue staining 51
2.1.10. Fluorimetry 51
2.1.11. Confocal microscopy 52
2.2. MOLECULAR BIOLOGY 53
2.2.1. DNA extraction 53
2.2.2. PCR 53
2.2.3. Sequencing 53
2.2.4. Bacterial transformation 54
2.2.5. Yeast transformation 54
2.2.6. Site-directed mutagenesis 54
2.3. BIOCHEMICAL METHODS 57
2.3.1. Preparation of mitochondrial membranes 57
2.3.2. Spectroscopy 57
2.3.3. Oxygen consumption/cytochrome oxidase activity 58
2.3.4. Nitric oxide detection 58
2.4. WESTERN BLOTTING 59
2.4.1. Denaturing electrophoresis 59
2.4.1.1. Gel preparation 59
2.4.1.2. Sample preparation 59
2.4.1.3. Gel running and processing 59
2.4.2. Blue native electrophoresis 60
2.4.2.1. Gel preparation 60
2.4.2.2. Sample preparation 60
2.4.2.3. Gel running and processing 60
2.4.3. Two-dimensional native/denaturing electrophoresis 61
2.4.4. Immunodetection 61
2.4.5. *In situ* cytochrome oxidase activity assay 62
2.4.6. Electroelution 63
2.5. GENE EXPRESSION 65
2.5.1. Microarray 65
2.5.1.1. RNA extraction 65
2.5.1.2. mRNA isolation 66
2.5.1.3. Synthesis of double-stranded cDNA 66
2.5.1.4. In vitro transcription 66
2.5.1.5. Hybridisation and initial analyses 67
2.5.1.6. Data analysis 67
2.5.2. Quantitative real-time PCR 67
2.5.3. β-Galactosidase assay 68
Chapter 3 SUBCOMPLEXES OF CYTOCHROME OXIDASE 85
3.1. INTRODUCTION 86
3.1.1. Temporal pathway of cytochrome oxidase assembly 86
3.1.2. Aims 86
3.2. RESULTS 87
3.2.1. Selection and initial characterisation of the mutant strains 87
3.2.2. Analysis of cytochrome oxidase assembly by optical spectroscopy 87
3.2.3. Activity of cytochrome oxidase in the mutants R159K and G156E 88

3.2.4. Reversion mutations in the copper-binding domain of Cox2p 88
3.2.5. No evidence for a role of Oxa1p or Sco1p in the suppression of the defect caused by R159K. 89
3.2.6. Steady state subunit levels 90
3.2.7. Subcomplexes of cytochrome oxidase 91
3.2.7.1. Major subcomplexes present in the wild type 91
3.2.7.2. Subcomplex c identified only in the mutants and revertants 92
3.2.7.3. Other subcomplexes 93
3.2.8. Membrane insertion of the Cox2p N-terminal domain by Oxa1p 94
3.3. DISCUSSION 96
3.3.1. *COX2* mutations abolishing cytochrome oxidase assembly 96
3.3.2. *COX2* mutations allowing partial cytochrome oxidase assembly 97
3.3.3. Origin of band *c* 98
3.3.3.1. Degradation product 98
3.3.3.2. Assembly intermediate 98
3.3.3.3. Partially degraded assembly intermediate 99
3.3.4. Band *d* 100
3.3.5. Conclusions 100
Chapter 4 EFFECT OF NO/RNS ON CELL PROLIFERATION AND THE RESPIRATORY CHAIN 115
4.1. INTRODUCTION 116
4.1.1. Antimicrobial activity of nitric oxide 116
4.1.2. Aims 116
4.2. RESULTS 117
4.2.1. Inhibition of yeast respiration by NO donor 117
4.2.2. Inhibition of yeast proliferation by NO donor 117
4.2.3. NO donor does not impair cell viability 119
4.2.4. NO donor does not cause rho$^-$ accumulation 120
4.2.5. ROS do not appear to be involved in the effect of NO donor on cell proliferation 121
4.2.6. The NO donor has a deleterious effect on cell proliferation in the absence of a respiratory chain 121
4.2.7. Sites of ROS production in yeast 122
4.2.8. Prolonged treatment with NO donor severely decreased cytochrome oxidase content 123
4.2.9. The decrease in cytochrome oxidase content is specific to NO donor 124
4.2.10. NO donor has little effect on cytochrome content in stationary phase cells 125
4.3. DISCUSSION 126
4.3.1. Inhibitory effect of NO on cell proliferation 126
4.3.2. Possible mechanisms for the inhibition of proliferation 127
4.3.3. Severe decrease in cytochrome oxidase level after NO donor exposure 128
4.3.4. Possible disruption of cytochrome oxidase synthesis 129
4.3.4.1. mRNA changes 129
4.3.4.2. Alterations in cytochrome oxidase assembly 130
4.3.5. Conclusions 132
Chapter 5 TRANSCRIPTIONAL CHANGES INDUCED BY NO/RNS 143
5.1. INTRODUCTION 144
5.1.1. Aims 144
5.2. RESULTS 145
5.2.1. W303-1B Δ*yhb1* sensitivity to NO donor 145
5.2.2. Time-course response to NO donor treatment 145

5.2.3. Validation of microarray results by (RT)q-PCR 146
5.2.4. Effect of different concentrations of NO donor on gene expression 147
5.2.5. Dependence of NO donor-induced gene expression on the respiratory chain 147
5.2.6. Comparison with transcriptional changes induced by myxothiazol treatment 148
5.2.6.1. Genes commonly altered by NO donor and myxothiazol 149
5.2.6.1. Genes specifically altered in response to NO donor 149
5.2.7. Role of the transcription factors Yap1p, Msn2p and Msn4p 150
5.2.8. Role of the transcription factor Hap1p 152
5.3. DISCUSSION 154
5.3.1. Overview of results 154
5.3.2. Activation of antioxidant/detoxification enzymes 155
5.3.2.1. Yhb1p 155
5.3.2.2. Superoxide dismutase, catalase and cytochrome c peroxidase 155
5.3.2.3. Glutathione 155
5.3.2.4. Peroxiredoxins 156
5.3.2.5. Lipid peroxidation 156
5.3.2.6. DNA repair system 158
5.3.3. Modification of iron homeostasis 158
5.3.4. Induction of transporters 159
5.3.5. Repression of fatty acid and sterol synthesis 159
5.3.6. Severe repression of respiratory chain genes 160
5.3.7. Transcription factors involved in the genomic response to NO/RNS 161
5.3.7.1. Hap1p 161
5.3.7.2. Msn2/4p 162
5.3.7.3. Yap1p 162
Chapter 6 CONCLUSIONS AND FUTURE DIRECTIONS 178
6.1. CYTOCHROME OXIDASE ASSEMBLY 179
6.1.1. Mutations in *COX2* abolishing assembly 179
6.1.2. Subcomplexes of cytochrome oxidase 180
6.1.3. Perspectives 181
6.2. ANTIMICROBIAL EFFECT OF NO/RNS 182
6.2.1. Yeast are extremely resistant to NO/RNS 182
6.2.3. General considerations about the microarray analysis 183
6.2.4. Targets of NO/RNS and mechanisms of defence 184
6.2.5. Involvement of ROS in the effect of NO/RNS 186
6.2.6. Downregulation of Hap1p-activated genes by NO donor 187
6.2.7. Conclusions 189
6.3. FINAL REMARKS 189
REFERENCE LIST 191
APPENDICES 229

LIST OF FIGURES AND TABLES

Figure 1.1. The respiratory chain 42
Figure 1.2. Structure of bovine cytochrome oxidase 43
Figure 2.1. Mapping of mutations to the *COX2* gene 70
Figure 2.2. Mapping of reversions 71
Figure 2.3. Excitation/emission spectra 72
Figure 2.4. Annealing sites of primers used in the amplification of the *S. cerevisiae* *COX2* gene 73
Figure 2.5. Screening of transformants 74
Figure 2.6. Typical standard curve used to determine protein concentration of membrane preparations 74
Figure 2.7. Porin signal intensities of a wild type dilution series 75
Figure 2.8. Assembly of two-dimensional native/denaturing gels 76
Figure 2.9. Determining band identity in denaturing gels 77
Figure 2.10. RNA integrity assessed by the Agilent Technologies 2100 Bioanalyser 78
Figure 2.11. Relative efficiency plots to assess suitability of primer pairs for analysis using the comparative Ct (ΔΔCt) method 79
Figure 3.1. The R159K mutation in *COX2* 101
Figure 3.2. Location of Cox2p mutations and reversions 102
Figure 3.3. Cytochrome levels in mutant and wild type cells 103
Figure 3.4. Cytochrome oxidase activity in mutants and wild type 104
Figure 3.5. Steady state levels of cytochrome oxidase subunits in mutants and revertants 105
Figure 3.6. Subcomplexes of cytochrome oxidase in wild type and Cox2p mutants and revertants 106
Figure 3.7. Cytochrome oxidase activity of complexes *a* and *b* in the wild type 107
Figure 3.8. Proximity of the N-terminal regions of COX6A and COX5B 108
Figure 3.9. Subunit composition of cytochrome oxidase subcomplexes in the R159K + S222Y revertant verified by two-dimensional electrophoresis 109
Figure 3.10. Identity of band *f* 110
Figure 3.11. Possible salt bridge between Cox2p and Cox7ap 111
Figure 3.12. Possible stabilising sidechain interaction between Cox2p and Cox5p 112
Figure 3.13. Formation of a partially degraded assembly intermediate of cytochrome oxidase 113
Figure 4.1. Effect of NO donor on oxygen consumption by yeast cells 133
Figure 4.2. Effect of NO donor on yeast proliferation 134
Figure 4.3. Effect of decomposed NO donor on yeast proliferation 135
Figure 4.4. NO released upon addition of 3 mM DETA NONOate to the culture medium 135
Figure 4.5. Viability of yeast cells after NO donor exposure 136
Figure 4.6. Effect of NO donor on the growth of cells with a non-functional respiratory chain, and on cells lacking components of the oxidative stress response system 137
Figure 4.7. Change in cytochrome content on NO donor treatment of cells in late exponential phase 138
Figure 4.8. Effect of NO donor on FY1679 proliferation 139
Figure 4.9. Cytochrome levels after NO donor treatment of FY1679 Δ*yhb1* 139
Figure 4.10. Tyrosine 244 in the bovine COX1 140
Figure 5.1. Effect of NO donor on yeast proliferation 164

Figure 5.2. Changes in gene expression after NO donor treatment 165
Figure 5.3. Effect of varying concentration of NO donor on gene expression 166
Figure 5.4. Genes commonly altered by NO donor and myxothiazol 166
Figure 5.5. Genes altered specifically by NO donor 167
Figure 5.6. STRE activation by Msn2/4p induced by NO donor 167
Figure 5.7. *CYC1* repression in the presence of NO donor and myxothiazol 168
Figure 6.1. Mammalian cytochrome oxidase assembly pathway 190
Figure 6.2. Sequence comparison of the *COX2* gene showing the conserved residues G156 and R159 190

Table 1.1. Yeast cytochrome oxidase subunits and their mammalian counterparts 43
Table 1.2. Accessory proteins involved in cytochrome oxidase assembly 44
Table 2.1. Yeast strains used in this study 80
Table 2.2. Primers used for amplification of mitochondrial and nuclear genes 81
Table 2.3. Gel recipes 81
Table 2.4. Solutions used in western blotting 82
Table 2.5. Antibodies 83
Table 2.6. Primers used for amplification in (RT)q-PCR 84
Table 3.1. Mutations and reversions in *COX2* 114
Table 3.2. Cytochrome oxidase content and activity in mutants and revertants 114
Table 4.1. Variation in cytochrome levels and oxygen consumption in control cells 141
Table 4.2. Cytochrome levels after myxothiazol treatment 141
Table 4.3. Change in cytochrome content on NO donor treatment of cells in early stationary phase 141
Table 4.4. Gene expression changes after treatment with 3 mM DETA NONOate 142
Table 5.1. Number of genes with altered expression as a result of incubation with NO donor 169
Table 5.2. Validation of microarray results by (RT)qPCR analysis 170
Table 5.3. Dependence of NO donor-induced changes in gene expression on the respiratory chain, and on the transcription factors Msn2/4p and Yap1p 171
Table 5.4. Genes with altered expression after NO donor treatment but not myxothiazol treatment 172
Table 5.5. Expression changes of known and putative Hap1p and Rox1p-regulated genes after NO donor and myxothiazol treatment 177

ABBREVIATIONS

AAA protease	ATPase Associated with a variety of cellular Activities
ABC transporter	ATP-binding cassette transporter
Acetyl CoA	acetyl coenzyme A
ADP	adenosine monophosphate
ATP	adenosine triphosphate
BSA	bovine serum albumin
Carboxy-H_2DCFDA	2',7'-dichlorodihydrofluorescein diacetate
DEA NONOate	2-(N,N-diethylamino)-diazenolate-2-oxide diethylammonium salt
DETA NONOate	(Z)-1-[2-(2-aminoethyl)-N-(2-ammonioethyl)amino]diazen-1-ium-1,2-diolate
DMSO	dimethylsulfoxide
dpIX	deuteroporphyrin IX
DNA	deoxyribonucleic acid
ssDNA	single-stranded DNA
DPTA NONOate	dipropylenetriamine NONOate
DTT	dithiothreitol
FAD/$FADH_2$	flavin adenine dinucleotide
FCCP	carbonyl cyanide 4-(trifluoromethoxy)phenylhydrazone
FMN	flavin mononucleotide
FPLC	fast protein liquid chromatography
GAPDH	glyceraldehyde-3-phosphate dehydrogenase
GSH	reduced glutathione
GSSG	oxidised glutathione
GSNO	S-nitrosoglutathione
HMC	high molecular weight complex
HRP	horse radish peroxidase
IMM	inner mitochondrial membrane
IMS	intermembrane space
LHON	Leber's hereditary optical neuropathy
LPS	lipopolysaccharide
MELAS	myopathy, encephalopathy, lactic acidosis and stroke-like syndrome

MPP	mitochondrial processing peptide
MRP	multidrug associated resistance protein
mtDNA	mitochondrial DNA
NAD^+/NADH	nicotinamide adenine dinucleotide
NO	nitric oxide
NOS	nitric oxide synthase
OMM	outer mitochondrial membrane
ORF	open reading frame
PAP	peroxidase anti-peroxidase
PBS	phosphate buffered saline
PCR	polymerase chain reaction
PMSF	phenylmethylsulphonylfluoride
PVDF	polyvinylidene fluoride
RNA	ribonucleic acid
tRNA	transfer RNA
rRNA	ribosomal RNA
RNS	reactive nitrogen species
ROS	reactive oxygen species
SAGE	serial analysis of gene expression
SDS	sodium dodecyl sulfate
SNAP	S-nitroso-N-acetylpenicillamine
TEMED	N,N,N',N'-Tetramethylethylenediamine
TIM	translocase of the inner membrane
TMPD	N,N,N',N'-Tetramethylbenzene-1,4-diamine
TOM	translocase of the outer membrane
TRAM	translocating chain-associating membrane protein
UTR	untranslated region

Chapter 1
INTRODUCTION

In this thesis I began by studying the assembly of the respiratory chain enzyme cytochrome oxidase, using the yeast *Saccharomyces cerevisiae* as a model system. I next moved on to assess the effect of nitric oxide (NO), an inhibitor of cytochrome oxidase, on the respiratory chain and on the growth of yeast. This then led me to investigate the antimicrobial action of NO, again using yeast as a model.

1.1. MITOCHONDRIA AND THE RESPIRATORY CHAIN

In eukaryotic cells, mitochondria occupy a central position in the extraction of energy from nutrients and its trapping as adenosine triphosphate (ATP). Each cell can contain hundreds of mitochondria, spread throughout the cytosol. The organelle is enclosed by an outer membrane (OMM) which, together with the highly convoluted inner membrane (IMM) encloses the intermembrane space (IMS). The OMM is permeable due to the presence of porin, which allows solutes of less than 10 kDa molecular weight (most ions and metabolites, but not proteins) to pass, hence the composition of the IMS is similar to that of the cytosol. The IMM holds the components of the respiratory chain (Figure 1.1) and surrounds the mitochondrial matrix, containing the mitochondrial DNA (mtDNA) alongside a multitude of enzymes involved in the citric acid cycle, β-oxidation of fatty acids, and the final steps of degradation of other nutrients. The mtDNA encodes several polypeptides which form part of the respiratory chain complexes, in addition to mitochondrial rRNAs and tRNAs. In yeast, these polypeptides are Cox1p, Cox2p, Cox3p, cytochrome *b*, Atp6p, Atp8p and Atp9p.

1.1.1. The chemiosmotic hypothesis

Controlled oxidation of nutrients begins in the cytosol and terminates in the mitochondria, converging in the formation of mitochondrial acetyl coenzyme A (acetyl CoA). The citric acid cycle, in which acetyl CoA is oxidised, is the final common pathway for the oxidation of fuel molecules. The electrons released during these processes are transferred to the molecules NAD^+ and FAD, which carry the electrons to the mitochondrial respiratory chain (Figure 1.1). Respiratory chains are found in biological systems from mammals to bacteria and plants, and play a major role in the generation of energy, through ATP synthesis, by aerobic cells.

The essential premise of the respiratory chain is that electron flow through the respiratory chain complexes leads to proton pumping from the matrix to the IMS, generating a gradient of protons which return to the matrix through the ATP synthase, with the concomitant generation of ATP from ADP and inorganic phosphate (Figure 1.1). This is known as the chemiosmotic hypothesis (Mitchell and Moyle, 1967). The

components of the respiratory chain are arranged roughly in order for electron flow from compounds with low redox potential to compounds with higher redox potential. The proton electrochemical gradient, or proton motive force, generated has two components: the Δ_{pH} caused by different concentrations of protons across the membrane, and the Δ_{ψ} due to the difference in electrical potential. Establishment of the proton gradient relies on the impermeability of the IMM to nearly all ions and polar molecules; movement across the IMM relies on specific ion and metabolite transporters, for example, the pyruvate produced in cytosolic glycolysis is transported from the intermembrane space to the matrix *via* a pyruvate carrier.

1.1.2. Components of the respiratory chain

In mammals, the respiratory chain comprises five enzyme complexes embedded in the IMM (Figure 1.1). Electrons from NADH are transferred to NADH dehydrogenase (complex I, NADH:ubiquinone oxidoreductase, EC 1.6.5.3). The soluble carrier ubiquinone transports electrons from NADH dehydrogenase and from the $FADH_2$ produced by succinate dehydrogenase (complex II, succinate:quinone oxidoreductase, EC 1.3.5.1), which is part of the citric acid cycle, to the bc_1 complex (complex III, ubiquinol cytochrome *c* oxidoreductase, EC 1.10.2.2). Finally soluble cytochrome *c* transports electrons to cytochrome oxidase (complex IV, cytochrome *c* oxidase, ferrocytochrome *c*:O_2 oxidoreductase, EC 1.9.3.1) where oxygen is reduced to water. NADH dehydrogenase, the bc_1 complex and cytochrome oxidase pump protons across the IMM, and the ATP synthase (complex V, F_1-ATPase, EC 3.6.3.14) utilises these to generate ATP.

In *S. cerevisiae* the system is slightly different in that there are not one but three NADH dehydrogenases, none of which span the membrane or pump protons, but which are exposed to either the cytosolic or the matrix side of the IMM. Yeast succinate dehydrogenase is composed of four subunits and contains three iron-sulfur clusters, FAD and cytochrome *b*. The yeast bc_1 complex contains three catalytic subunits which include cytochrome *b*, cytochrome c_1 and an iron-sulfur centre, together with seven other non-catalytic subunits. The yeast ATP synthase contains 16 subunits. The structure of cytochrome oxidase is reviewed below.

1.2. CYTOCHROME OXIDASE

The cytochrome *c* oxidases are members of a large family of terminal oxidases present in prokaryotes and eukaryotes, all of which contain heme and copper. Cytochrome oxidase catalyses the reduction of oxygen to water using electrons from cytochrome *c*,

and the multisubunit enzyme is the terminal proton pumping component of the respiratory chain.

1.2.1. Structure of cytochrome oxidase

Mammalian cytochrome oxidase is composed of thirteen subunits, while yeast cytochrome oxidase is composed of eleven. Most of the yeast subunits have a mammalian counterpart (Taanman and Capaldi, 1992; Taanman 1997), as detailed in Table 1.1. The crystal structure of *Paracoccus denitrificans* cytochrome oxidase was determined by Iwata in 1995 (Iwata et al., 1995), and that of bovine heart cytochrome oxidase by Tsukihara in 1996 (Tsukihara et al., 1996) (Figure 1.2). Three subunits, Cox1p, Cox2p and Cox3p, form the core of the enzyme and are encoded by the mtDNA itself, while the remaining subunits are encoded by the nuclear genome. The core subunits are highly conserved, being found in both eukaryotic and bacterial oxidases. *P. denitrificans* cytochrome oxidase, for example, contains homologs to Cox1p, Cox2p and Cox3p, in addition to a further non-homologous subunit. Therefore it is not surprising that the catalytic site and the region thought to be involved in proton pumping are located in these mitochondrially encoded subunits. Cox3p does not appear to be involved in proton pumping or catalysis, but is conserved and may be required for assembly or stability of the enzyme (Haltia et al., 1989). The role of the nuclear subunits has not been clearly established, but they are believed to be involved in assembly or stability of the complex, or in allosteric modification of activity through nucleotide binding (Kadenbach et al., 1998); some of them exist as isoforms.

Cytochrome oxidase is embedded in the IMM. In the bovine structure the core Cox2p is comprised of a C-terminal ten-stranded β-barrel globular domain protruding into the IMS, anchored to the IMM by two transmembrane helices (Tsukihara et al., 1996) (Figure 1.2A). The globular domain contains the initial acceptor of electrons from cytochrome *c*, the binuclear Cu_A site. The transmembrane region of Cox2p associates with Cox1p, the largest subunit, having twelve membrane-spanning helices which contain the redox-active heme *a* and heme a_3-Cu_B centres but no appreciable extramembrane region. Cox3p also associates with the transmembrane region of Cox1p, but does not make direct contact with Cox2p. Cox3p spans the membrane seven times and contains no prosthetic groups. The nuclear-encoded subunits are smaller and either have one transmembrane region or are extramembrane polypeptides (Table 1.1, Figure 1.2B). Cytochrome oxidase operates as a dimer, and the total molecular weight of each monomer is around 200,000 kDa.

In addition to the redox active cofactors mentioned above, other metal sites are also present (Tsukihara et al., 1995). A magnesium binding site (to which manganese can also bind) is located at the interface between Cox1p and Cox2p, and may be involved in the exit of water from the catalytic site (Schmidt et al., 2003). Another binding site, for a calcium or sodium ion, has also been identified in Cox1p (Ostermeier et al., 1997; Kirichenko et al., 1998). A zinc ion is located in mammalian COX5B, ligated by 4 cysteine residues. Substitution of some of the cysteine ligands in the corresponding Cox4p impairs assembly of the yeast enzyme (Lightowlers et al., 1991).

1.2.2. Catalysis and proton translocation

Cytochrome oxidase uses electrons from cytochrome *c* to reduce molecular oxygen to water. The overall reaction is:

$$O_2 + 4e^- + 8H^+_{in} \rightarrow 2H_2O + 4H^+_{out}$$

Protons for water formation are sourced from the matrix side of the IMM while electrons from cytochrome *c* originate from the IMS side, hence this creates a Δ_{pH} and a Δ_{ψ} over the IMM, which the active translocation of protons out of the matrix adds to. The transfer of electrons occurs in several steps. The docking site for cytochrome *c* is believed to be located primarily in the Cox2p C-terminal extramembrane domain, but may also involve residues in Cox3p and other subunits (Tsukihara et al., 1996). Docking is thought to involve mainly electrostatic interactions between acidic residues on cytochrome oxidase and lysine residues surrounding the heme crevice of cytochrome *c*. Optimisation of the interaction may then be mediated by hydrophobic interactions (Maneg et al., 2004). Electrons from cytochrome *c* enter the protein at the Cu_A site in the C-terminal region of Cox2p, which comprises two copper atoms and is located close to the cytochrome *c* docking site. Electrons move from here to heme *a* in Cox1p, then to the Cox1p heme a_3-Cu_B site where the reaction with oxygen takes place.

The fully reduced heme a_3-Cu_B site is known as the R species. Once this is formed, the iron of heme a_3 binds oxygen to form the A species, then the O-O bond breaks and dioxygen is reduced. Electron and proton transfer to the heme a_3-Cu_B site forms the F state then the O state. Formation of the F and O species is associated with the translocation of two protons across the IMM. Finally, in the reductive part of the cycle, two molecules of water are released *via* the intermediate E, requiring two further protons and two electrons, to reform species R (see (Michel et al., 1998; Wikström, 2000)). The mechanism by which this is coupled to proton translocation is still unclear. Two possible proton translocating pores, the D- and K-channels formed of hydrophilic

residues linked by a network of water molecules, are located in Cox1p (Rich et al., 1998; Wikström et al., 1998).

1.3. ASSEMBLY OF CYTOCHROME OXIDASE

Cytochrome oxidase is a large multisubunit complex. Its assembly is complicated first by the fact that its composite polypeptides are synthesised in two separate cellular compartments (mitochondria and cytosol), and second by the requirement for incorporation of metal groups and cofactors. An array of nuclear encoded assembly proteins are required to coordinate assembly. These factors are involved in all aspects of assembly, from processing of mRNAs, to insertion of polypeptides into the membrane, to recruitment of cofactors. Some of the assembly factors have a general function and are also involved in the biogenesis of other respiratory complexes, while some are more specifically required for cytochrome oxidase assembly. Many of the assembly factors were first identified in *S. cerevisiae*, and much of the functional analysis has been performed in yeast. Table 1.2 summarises current knowledge on the more specific assembly factors required, and in the following sections I will expand on some of the information in this table.

1.3.1. Import of nuclear encoded subunits into the mitochondria

The three core catalytic subunits are encoded by the mitochondrial genome, so the synthesis of these subunits utilises the mitochondrial replication system. The remaining subunits (ten in mammals, eight in yeast) are encoded by the nuclear genome, so are synthesised on cytosolic ribosomes and must be targeted to the mitochondria. Mitochondrial targeting sequences can be in the form of a cleavable N-terminal sequence or, for many IMM proteins, an internal non-cleavable sequence. Mammalian COX6C, for example, contains several basic amino acids in its N-terminus, which is not cleaved after import (Otsuka et al., 1988). Proteins pass first through the OMM *via* the translocase of the outer membrane (TOM) complex. Passage across or insertion into the IMM is facilitated by the translocase of the inner membrane (TIM) complex. Two such complexes have been identified (Pfanner and Geissler, 2001). The first, known as the Tim17p-23p complex, is the more general one, and is used by proteins with an N-terminal targeting presequence. This complex requires the cooperation of Tim44p, the ATP-dependent chaperone Hsp70p and its cochaperone Mge1p. The second complex, Tim22p-54p, is used by a set of polytopic IMM proteins containing internal mitochondrial targeting sequences and requires the soluble IMS proteins Tim8p, Tim10p, Tim12p and Tim13p. Some of those proteins whose final fate is to span the

IMM can utilise their topogenic signal (normally an integral part of the protein, i.e. the transmembrane section, though sometimes a section of protein removed by the Imp peptidase complex of the IMS after sorting) to cause translocation arrest and allow lateral sorting into the membrane. This is known as the 'stop transfer' mechanism, and import of Cox5ap has been shown to follow this route (Miller and Cumsky, 1993). Other IMM proteins continue to the matrix where their N-terminal target sequence is cleaved by the mitochondrial processing peptide (MPP), before they are then exported to the IMM. Here, the mechanism of export converges with that used by the mtDNA-encoded proteins destined for the IMM (Hell et al., 1998).

1.3.2. Export of protein domains from the mitochondrial matrix

The export of Cox2p, synthesised on mitochondrial ribosomes in the matrix has been most widely studied. Cox2p becomes tethered to the IMM by two transmembrane helices, with its small N-terminal and large C-terminal domains protruding into the IMS. In yeast Cox2p is synthesised as a precursor with a 15 amino acid N-terminal presequence, although this leader sequence is not present in mammalian *COX2* (Pratje et al., 1983). Assembly of Cox2p requires insertion of the hydrophobic membrane domains into the IMM, and translocation of the hydrophilic regions across to the IMS.

1.3.2.1. Subunit-specific membrane-bound translational activators

There is evidence to suggest that, in yeast at least, subunit insertion into the IMM is cotranslational, which would prevent aggregation of subunits in the matrix. mRNAs are thought to be recruited to the IMM by subunit-specific membrane-bound translational activators which interact with the 5' UTR of transcripts. Pet111p is required for translation of *COX2* mRNA (Mulero and Fox, 1993). Mss51p is required for *COX1* mRNA translation but, unusually, does not recognise the mRNA simply through its 5' UTR (Perez-Martinez et al., 2003). Mss51p also physically interacts with the Cox1p polypeptide, and is required for insertion of Cox1p into the membrane. Pet309p is also involved in Cox1p translation (Manthey and McEwan, 1995). Cox3p translation requires Pet54p (Costanzo et al., 1986), Pet122p (Kloeckener-Gruissem et al., 1988) and Pet494p (Costanzo and Fox, 1986), all of which have been shown to interact with each other (Brown et al., 1994). Some of the translational activators for different subunits have also been shown to interact, suggesting that the synthesis of all three core subunits could be directed to occur at particular sites in the IMM, rather than the subunits diffusing freely until an interaction partner is found (Naithani et al., 2003).

1.3.2.2. Oxa1p

Translocation of Cox2p from the matrix to the IMS is mediated by the highly conserved protein Oxa1p, which spans the membrane five times in an N_{out}-C_{in} orientation. A temperature-sensitive mutant of yeast Oxa1p displayed accumulation of the precursor form of Cox2p in the matrix. Since the presequence is cleaved by enzymes in the IMS this indicated that Oxa1p is essential for the insertion of Cox2p into the IMM (Bauer et al., 1994; Hell et al., 2001). Oxa1p has been specifically implicated as essential in transfer of the N-terminal transmembrane domain of Cox2p. Export of the Cox2p C-terminal domain was also defective in the absence of Oxa1p (Hell et al., 1997; He and Fox, 1997), however this could be due to a requirement for prior translocation of the N-terminal domain (Hell et al., 1998). Oxa1p may facilitate membrane insertion of Cox2p by sandwiching the N-terminal region between its own transmembrane helices until stable integration with the lipid bilayer is attained, in a similar manner to mammalian TRAM (translocating chain-associating membrane protein) (Saint-Georges et al., 2001).

Though Cox2p has been identified as the polypeptide most highly dependent on Oxa1p, the function of Oxa1p appears to be not restricted to Cox2p, but to form part of a more general mitochondrial export machinery (Hell et al., 1998; Hell et al., 2001). When the yeast *OXA1* gene is deleted the resulting strain is respiratory deficient due to a complete loss of cytochrome oxidase content, in addition to decreased cytochrome *b* content and bc_1 complex activity, and diminished ATP synthase activity (Altamura et al., 1996). The temperature-sensitive Oxa1p mutant mentioned above also had defects in the insertion of Cox1p, Cox3p, cytochrome *b* and Atp6p into the IMM, albeit to a lesser extent than Cox2p (Hell et al., 2001). Additionally, membrane insertion of Oxa1p itself utilises Oxa1p (Hell et al., 1998).

Crosslinking experiments by Hell *et al.* have demonstrated direct interaction of Oxa1p with several substrates, both nascent mitochondrial polypeptide chains (including Cox1p, Cox2p, Cox3p and cytochrome *b*) and newly imported nuclear encoded proteins (Hell et al., 1998; Hell et al., 2001). The association with nascent mitochondrial polypeptides was enhanced in the presence of ribosomes. When puromycin (which causes premature release of the polypeptide chain from the ribosome) was used to inhibit protein synthesis, the number of nascent chains found associated with Oxa1p decreased. However, when chloramphenicol (which stalls elongation of the polypeptide chain) was used this was not the case (Hell et al., 2001). It was suggested that membrane insertion may be cotranslational, and that Oxa1p may make direct contact with the ribosomes themselves, or with translational activator

proteins. A pool of Oxa1p was found to copurify with mitochondrial ribosomes in sucrose gradient centrifugation, and the C-terminal matrix domain of Oxa1p may interact with the ribosomes (Szyrach et al., 2003).

Oxa1p was first thought to be involved in the export of only N-terminal regions, but several of its substrates contain IMS loops adjacent to two transmembrane regions, suggesting that it is not the location of a protein domain that determines the requirement for Oxa1p in translocation, but the nature of that domain. Oxa1p may be of particular importance in the translocation of transmembrane domains which have a high proportion of negatively charged residues, a feature of the N-terminal transmembrane domain of Cox2p (Saint-Georges et al., 2001; Herrmann and Bonnefoy, 2004). In the absence of Oxa1p, mutations which introduced positively charged residues into the transmembrane region of cytochrome c_1 restored translocation of the Cox2p N-terminal transmembrane domain (Hamel et al., 1998). The introduction of a single positively charged residue into the transmembrane region of another bc_1 complex subunit Qcr9p had a similar effect (Saint-Georges et al., 2001). The authors of these studies propose that the positive charges promote interaction of cytochrome c_1 or Qcr9p with negatively charged residues in Cox2p and allow coinsertion of Cox2p into the membrane. In another study the absence of the N-terminal presequence of Cox2p abolished assembly (Torello et al., 1997). However a suppressor mutant expressing Cox2p with its N-terminal presequence replaced by a large portion of cytochrome *b* was identified. In this fusion protein the N-terminus of Cox2p was required to be exported effectively as a hairpin loop adjacent to two transmembrane domains. The presence of Oxa1p was essential for export of the fusion protein, suggesting that the specific properties (in particular net charge) of the domain to be transported, rather than its final topology, determines its dependence on Oxa1p (Herrmann and Bonnefoy, 2004). Additionally, when the IMS domain of Atp9p was made more positively charged by mutagenesis the export of this protein did not subsequently require Oxa1p (Herrmann and Bonnefoy, 2004). The Cox2p N-terminal IMS domain is highly acidic, with a net charge of -5, as opposed to the loops in the other (less dependent) known substrates of Oxa1p, which have net charges of -2 or -3. Other proteins, which insert into the membrane in the absence of Oxa1p, are uncharged or have a positive net charge. Therefore the number of charged residues in a domain seems to determine its dependence on Oxa1p (Herrmann and Bonnefoy, 2004).

1.3.2.3. Mba1p

The extent of dependency of Oxa1p substrates on Oxa1p varies considerably. Cox2p displays a high requirement for Oxa1p, while Cox1p, Cox3p, Atp6p and cytochrome *b* are less dependent and can insert into the membrane in the absence of Oxa1p, albeit with lower efficiency (Hell et al., 2001). These substrates may be more easily able to spontaneously insert into the membrane, or may require another translocation machinery, perhaps of partially overlapping function with Oxa1p, to mediate their insertion (Herrmann and Bonnefoy, 2004). Mba1p, an IMM protein, was isolated along with Oxa1p as a multicopy suppressor of an *AFG3* (encoding a mitochondrial protease) deletion mutant (Rep et al., 1996). Preuss *et al.* found that deletion of *MBA1* caused a defect in Cox2p N-terminal export, and, like Oxa1p, Mba1p interacted with Cox1p, Cox2p, Cox3p and cytochrome *b* during their synthesis (Preuss et al., 2001). However, Mba1p did not interact with Oxa1p and is unlikely to be part of an Oxa1p complex. Mba1p is partially dispensable and cannot replace Oxa1p, but there seems to be some overlap in the function of the two proteins (Preuss et al., 2001). Mba1p has been suggested to be involved in export of protein domains less charged than those exported by Oxa1p (Herrmann and Bonnefoy, 2004).

1.3.2.4. Removal of the Cox2p N-terminal presequence

After translocation the Cox2p presequence is cleaved by the IMM Imp peptidase complex (Behrens et al., 1991; Bauer et al., 1994), containing at least two subunits, Imp1p and Imp2p (Nunnari et al., 1993). Cleavage is dependent on another protein Cox20p, since *COX20* deletion leads to an accumulation of the precursor form of Cox2p with its N-terminus in the IMS (Hell et al., 2000). Cox20p was found in association with both the precursor and the mature form of Cox2p, therefore it has been proposed that Cox20p somehow presents Cox2p as a substrate to the Imp peptidase complex and then acts as a chaperone during subsequent assembly (Hell et al., 2000).

1.3.2.5. Cox18p, Mss2p and Pnt1p

Less is known about the protein components involved in transfer of the C-terminal domain of Cox2p. C-terminal extrusion, unlike N-terminal extrusion, is dependent upon IMM potential (He and Fox, 1997). Saracco and Fox demonstrated that Cox18p is required for export of the C-terminal domain of Cox2p (Saracco and Fox, 2002). Cox18p deficiency causes a lack of cytochrome oxidase but does not affect other components of the respiratory chain (Souza et al., 2000). The *Neurospora crassa*

homologue of Cox18p, Oxa2p, interacts with newly synthesised Cox2p and Cox3p and is not necessary for N-terminal extrusion, since in the absence of Cox18p the targeting sequence of Cox2p was removed as normal (Funes et al., 2004). Cox18p is an integral IMM protein with five predicted helices and a similar structure to Oxa1p but a shorter C-terminal domain, and may act as a posttranslational translocase (Preuss et al., 2005).

Cox18p immunoprecipitates with Mss2p and Pnt1p (Saracco and Fox, 2002). Pnt1p is an integral IMM protein. Its deletion in yeast did not affect respiratory growth, though less cytochrome oxidase was assembled (He and Fox, 1999). However, deletion of the homologous gene in the yeast *Kluyveromyces lactis* abolished cytochrome oxidase activity due to a defect in Cox2p C-terminal export and some decrease in N-terminal export (He and Fox, 1999). Mss2p is a matrix side peripherally bound IMM protein. Deletion of Mss2p caused respiratory deficiency through inhibiting export of the Cox2p C-terminal domain but not the N-terminal domain, and subsequent degradation of Cox2p and cytochrome oxidase (Broadley et al., 2001). Since Mss2p does not span the membrane and therefore is unlikely to be a translocase, the authors proposed that it may be involved in delivery of the Cox2p C-terminus to its translocation machinery, or in folding the C-terminal domain prior to export.

1.3.3. Recruitment and insertion of cofactors

1.3.3.1. Heme

Both hemes of cytochrome oxidase bind non-covalently to the transmembrane region of Cox1p. The difference between heme *a* and heme a_3 arises because of their different protein environments, and in particular because one coordination position of heme a_3 is unoccupied to enable binding of oxygen. Heme *a* is low-spin, ligated with two histidine residues, while heme a_3 is high-spin, and ligated by only one histidine residue (Tsukihara et al., 1995). Heme *a* is a modified form of the more common heme *b*, having a 15 carbon farnesyl side chain instead of a vinyl at C-2, and replacement of the methyl group at C-8 of the porphyrin ring by a formyl group (Caughey et al., 1975). Heme *a* is formed from heme *b* in two steps. The farnesyl transferase Cox10p converts heme *b* to heme *o* (containing the farnesyl side chain) (Tzagoloff et al., 1993) which is then oxidized at the methyl by a three component monooxygenase comprising the heme synthase Cox15p, the ferredoxin Yah1p and the ferredoxin reductase Arh1p (Barros et al., 2001).

Since the hemes are located within the membrane domain of the core subunit Cox1p, it seems probable that their insertion would occur early on in assembly, prior to

interaction of Cox1p with other subunits and likely during translation of Cox1p (Carr and Winge, 2003). Consistent with this, human *COX10* mutant cells did not accumulate a subassembly containing COX1, COX4 and COX5A (mammalian numbering), thought to be an early assembly intermediate of cytochrome oxidase (Williams et al., 2004). In particular, the insertion is very likely to occur prior to interaction with Cox2p since the farnesyl group of heme a_3 is packed between the two subunits (Carr and Winge, 2003). SURF1, homologous to yeast Shy1p, has recently been implicated in the insertion of heme a_3 in *Rhodobacter sphaeroides* (Smith et al., 2005).

1.3.3.2. Copper

Copper insertion at the Cu_A site of Cox2p and the Cu_B site of Cox1p has been more widely investigated. In the crystal structures of bovine and *P. denitrificans* cytochrome oxidase, the two copper atoms at Cu_A are bridged by two cysteine residues and each atom is ligated by a pair of histidine sidechains and either a methionine residue or a main chain carbonyl oxygen (Tsukihara et al., 1995; Iwata et al., 1995). In yeast the copper atoms are likely to be bound in a similar manner. The single copper atom of the Cu_B site has three histidine ligands (Tsukihara et al., 1995), one of which is covalently cross-linked to a tyrosine residue (Ostermeier et al., 1997).

Assembly of both copper sites requires the soluble protein Cox17p. Absence of Cox17p was shown by Glerum *et al.* to cause respiratory deficiency in yeast due to a lack of cytochrome oxidase, and was rescued by the addition of high concentration of exogenous copper (Glerum et al., 1996a). The Cox17p protein is small (8 kDa), has a CCXC consensus sequence allowing binding of up to three copper ions per monomer, and exists as a dimer or tetramer (Beers et al., 1997; Heaton et al., 2001). Cox17p is found in the cytoplasm and the IMS, consistent with its proposed role as a shuttler of copper from the cytoplasm to the mitochondria (Beers et al., 1997). However, Maxfield *et al.* demonstrated that Cox17p is functional even when its location is restricted to the mitochondria. Expression of a form of Cox17p tethered to the IMM through fusion with the transmembrane domain of another protein Sco2p was sufficient to rescue respiratory growth in a *COX17* deletion strain, even in a low copper environment. This suggests that Cox17p does not function as a transporter and its presence in the cytosol may be simply due to poor uptake or retention by the mitochondria (Maxfield et al., 2004).

Cox17p is thought to deliver copper ions to the Cu_A site of Cox2p and the Cu_B site of Cox1p *via* two different proteins, Sco1p and Cox11p, respectively. Sco1p, along with the homologous Sco2p, was shown by Glerum *et al.* to be a high copy suppressor

of *COX17* mutations (Glerum et al., 1996b). Evidence for copper transfer from Cox17p to Sco1p has been provided by Horng *et al.* These authors showed that the luminescence of copper-bound Cox17p was quenched in the presence of the soluble domain of Sco1p, and that the Sco1p recovered afterwards contained bound copper (Horng et al., 2004). Unlike deletion of *COX17*, deletion or mutation of yeast *SCO1* is not rescued by high concentrations of copper in the growth medium (Glerum et al., 1996b).

Sco1p consists of an IMS soluble domain tethered to the IMM by a single transmembrane helix (Balatri et al., 2003). Yeast Sco1p has been shown to form homomers both *in vitro* and *in vivo*, and binds the C-terminal region of Cox2p (Lode et al., 2000). Homomer formation might allow the two copper atoms required by the Cu_A site to be delivered simultaneously (Nittis et al., 2001). Sco1p has a CXXXC consensus in its IMS domain, similar to that found in the copper-binding site of Cox2p (Glerum et al., 1996b), and binds one copper ion per monomer through three ligands: the two cysteines and a conserved C-terminal histidine. Mutation of any of these residues produces non-functional cytochrome oxidase and leads to decreased levels of Cox2p (Nittis et al., 2001; Lode et al., 2000). Yeast also contain a homologous protein Sco2p, the role of which is still not understood. When *SCO1* is deleted cytochrome oxidase is not assembled (Krummeck and Rödel, 1990) but this is not the case for deletion of *SCO2* (Glerum et al., 1996b). Two human genes, *SCO1* and *SCO2*, show homology to both yeast *SCO1* and *SCO2* (Petruzzella et al., 1998; Paret et al., 1999). Both are required for cytochrome oxidase function, and pathogenic mutations have been identified in both genes (for example (Vesela et al., 2004)). Copper supplementation of cultured cells derived from such patients has been reported to rescue cytochrome oxidase activity and COX2 protein levels (Jaksch et al., 2001; Salviati et al., 2002).

Sco1p is generally thought to act by accepting copper ions from Cox17p and transferring them to Cox2p. However in addition to its copper binding motif Sco1p has several conserved residues in its active site similar to those found in peroxiredoxins and thiol:disulfide oxidoreductases, and its secondary structure has a typical thioredoxin fold. Therefore it was suggested that it might act not as a copper carrier, but to facilitate reduction of the cysteine residues in the Cox2p copper binding site to allow concomitant transfer of copper directly from Cox17p to Cox2p (Chinenov, 2004; Balatri et al., 2003). However, human SCO2, containing these conserved active site residues, did not reduce disulfide bridges in a thioredoxin assay (Jaksch et al., 2001).

The presence of the copper-binding region of Sco1p in the IMS, and the binding of Sco1p to the IMS region of Cox2p, suggest that Cu_A site formation occurs after

translocation of the Cox2p C-terminal domain through the IMM. Dickinson *et al.* have suggested that Cu_A site assembly occurs after the cytochrome oxidase complex is formed, since the mutation S240F in yeast *SCO1* allows assembly of the enzyme, albeit with a selective decrease in Cox2p (Dickinson et al., 2000). Conflicting evidence in humans has been provided by Williams *et al.* who found that fibroblasts with a *SCO1* mutation did not form subassemblies containing both Cox1p and Cox2p, indicating that Cu_A assembly is a prior requirement for the interaction of Cox1p with Cox2p, at least in the mammalian system (Williams et al., 2004).

Delivery of copper to Cox1p requires Cox11p, identified by Tzagoloff (Tzagoloff et al., 1990). Deletion of the *COX11* gene in *R. sphaeroides* led to diminished accumulation of the aa_3 type cytochrome oxidase, which lacked Cu_B but contained Cu_A and both hemes (Hiser et al., 2000). Since the oxidase formed was relatively stable, Cu_B insertion may be a late step in enzyme assembly. However, on deletion of *COX11* in yeast no stable cytochrome oxidase is present, perhaps reflecting the differing complexity of the two organisms (Tzagoloff et al., 1990). Cox11p has been shown to interact with mitochondrial ribosomes, indicating a possible cotranslational insertion of copper into the Cu_B site (Khalimonchuk et al., 2005), which would make sense since the site is located deep within the membrane. Cox11p has a similar structure to Sco1p and binds a single copper atom (Carr et al., 2002). Direct transfer of copper from Cox17p to Cox11p has been demonstrated in the same way as described for Sco1p (Horng et al., 2004). Horng *et al.* provided evidence to suggest that Cox17p utilised two different areas of its surface in binding to its two substrates Sco1p and Cox11p. However, no stable interaction has been identified between Cox17p and either Sco1p or Cox11p.

1.3.4. Quality control systems

Quality control of the assembly of IMM proteins is essential, since potentially deleterious aggregates of mitochondrial translation products could otherwise form in the membrane, disrupting cellular function. The degradation of unassembled subunits or incompletely assembled complexes is an important part of the assembly machinery. In yeast, this degradation process has proven especially efficient, and cytochrome oxidase assembly in yeast is regarded as an all or nothing process, with the mitochondrial subunits in particular being rapidly degraded if assembly cannot proceed.

A family of highly conserved ATP-dependent proteases termed the AAA proteases (ATPases Associated with a variety of cellular Activities) are believed to be

of major importance in the degradation of unassembled subunits. In yeast, two such complexes exist. Both are located in the IMM and are around 1000 kDa in mass. The first, *i*-AAA, is a homo-oligomeric complex of Yme1p which exposes its catalytic domain to the IMS. Yme1p has been implicated specifically in the degradation of Cox2p. Cytochrome *c*-deficient yeast mutants are deficient in cytochrome oxidase, and lack Cox1p, Cox2p and Cox3p. Pulse chase experiments revealed that Cox2p is rapidly degraded *in vivo* in such strains. However when *YME1* was deleted the levels of Cox2p and Cox3p were seen by western analysis to be partially restored (Pearce and Sherman, 1995). Similarly, Cox2p is degraded in Cox4p-deficient yeast, but mutation of *YME1* partially restored Cox2p levels (though not, in this experiment, Cox3p levels, which were also decreased by Cox4p deficiency) (Nakai et al., 1995). The second complex, *m*-AAA, is a hetero-oligomer of Afg3p and Rca1p, with its catalytic site exposed to the matrix side. This complex has been implicated in the degradation of several cytochrome oxidase subunits. For example, disruption of the proteolytic domain of yeast Afg3p reduced degradation of Cox1p and Cox3p compared to the wild type (Guelin et al., 1996).

There are two models currently under consideration to explain the mechanism of protein degradation by the Afg3p/Rca1p complex and the Yme1p complex (Leonhard et al., 2000). The 'shedding' model suggests that the exposed loops of membrane-bound proteins are cleaved, destabilising the membrane-spanning segments and allowing proteolytic attack from the surface of the membrane. The two complexes could work together in this model, one acting from the IMS side and the other from the matrix side. Alternatively, the 'pulling' model suggests that the proteases actively remove membrane-spanning proteins from their hydrophobic environment for degradation, this made possible by an ATP-dependent conformational change of the protease on binding of the target protein.

AAA proteases show similarity to chaperones, and it has been suggested that in addition to their proteolytic activity they may play a chaperone-like role. They interact specifically with unfolded proteins but not with their folded counterparts. The interaction of Yme1p with a correctly folded model protein and a counterpart in which the extramembrane C-terminal domain was only loosely folded was analysed *in vitro* by Leonhard *et al.* (Leonhard et al., 1999). Yme1p associated with and degraded only the incorrectly folded protein, and the AAA domain was crucial for binding. Additionally, the AAA domain prevented the aggregation of denatured dihydrofolate reductase, presumed by the authors to be due to mediation of refolding. Loss of Afg3p abolished

respiratory growth by impairing activity of the yeast respiratory chain complexes, indicating its importance in the assembly of cytochrome oxidase (Tauer et al., 1994). The simultaneous absence of both Afg3p and Yme1p is lethal in yeast, but when the proteolytically inactive variant of Afg3p is present this is not the case, suggesting that a chaperone-like function is in operation (Lemaire et al., 2000).

The existence of proteolytic activities in the mitochondria other than those described above is highly likely. The sensitivity of cytochrome oxidase subunits to degradation appears to be variable. The steady state levels of subunits may reflect both their intrinsic stability and protective associations with other subunits or assembly factors. The soluble subunits Cox4p and Cox6p appear to have a higher intrinsic stability than some of the membrane-bound subunits; they are relatively stable in assembly-arrested mutants (Glerum and Tzagoloff, 1997).

1.3.5. Association of subunits

It is not clear whether individual subunits diffuse in the membrane to find each other, or whether they are inserted at particular membrane sites. As discussed earlier, membrane-bound translational activators may direct synthesis of mitochondrially-encoded subunits to particular membrane sites in yeast, but no homologues have been identified in mammals. There appears to be no regulatory system coordinating synthesis of nuclear and mitochondrial subunits of cytochrome oxidase, in humans at least. When mitochondrial protein synthesis was persistently inhibited no decrease in nuclear protein synthesis was observed, and instead the excess of nuclear subunits was dealt with by enhanced degradation (Nijtmans et al., 1995).

The temporal order of subunit interaction is still not well understood. As discussed above, unassembled or incompletely assembled subunits in yeast are rapidly degraded in the face of assembly problem, hence yeast has so far not proven useful in the identification of assembly intermediates. However, degradation of unassembled mammalian subunits seems less severe, and several intermediates have been identified in human cells. Nijtmans *et al.* blocked cytosolic protein synthesis with cycloheximide to deplete pools of nuclear-encoded subunits and cause the accumulation of assembly intermediates (Nijtmans et al., 1998). This strategy allowed the detection of two intermediates. The first was a subcomplex containing COX1 and COX4 (yeast Cox1p and Cox5p), while the second contained all subunits except COX6A and COX7A or B (yeast Cox6ap and Cox7p). Williams *et al.* took this further and looked for accumulation of subcomplexes in cells derived from patients with mutations in the

assembly factors SCO1, SURF1 (homologous to yeast Shy1p) and COX10 (Williams et al., 2004). The previously identified subassemblies accumulated in these cells, and use of additional antibodies demonstrated that the first subcomplex contained COX5A (yeast Cox6p) in addition to COX1 and COX4. It seems therefore that an early assembly step involves formation of a complex between COX1, COX4 and COX5A (yeast Cox1p, Cox5p and Cox6p), and the peripheral polypeptides COX6A and COX7A or B (yeast Cox6ap and Cox7p) are added in a final step. Although assembly of mammalian cytochrome oxidase is believed to be a sequential process, this is not necessarily the case for lower organisms. Cox1p in *R. sphaeroides* can form a complex with either Cox2p or Cox3p, suggesting that several pathways may be possible (Hiser and Hosler, 2002).

Cytochrome oxidase exists as a dimer, and the presence of cardiolipin may be required for dimer formation (Sedlák and Robinson, 1999). There is also evidence to suggest that cytochrome oxidase associates with the bc_1 complex to form a supracomplex within the IMM, leaving little enzyme present in free form (Schagger and Pfeiffer, 2000; Cruciat et al., 2000). The supracomplex would consist of the bc_1 complex together with either one or two cytochrome oxidase dimers, and is thought to allow cytochrome *c* to be channelled quickly from the bc_1 complex to cytochrome oxidase, improving efficiency. However the association is not required for stability of either enzyme. The stability of such supracomplexes is also promoted by cardiolipin (Zhang et al., 2002; Pfeiffer et al., 2003).

1.3.6. Cytochrome oxidase disorders

The importance of the study of assembly of cytochrome oxidase lies partly in its relevance to human disease. Many of the assembly factors identified in yeast have human homologues. Mitochondrial disease is associated with a wide range of clinical presentations, even for mutation of a single gene, and phenotypes are commonly tissue-specific. Mammalian cells contain hundreds of mitochondria, and therefore thousands of copies of mtDNA; a cell can contain mutant mtDNA in addition to wild type mtDNA (heteroplasmy; this is not the case in yeast), and the relative proportions of these are likely to contribute to the tissue specificity. Those tissues with high energy demand (muscle, heart, brain) tend to be most affected. Phenotypes include myopathy, encephalomyopathy, MELAS (mitochondrial encephalopathy, lactic acidosis, and stroke-like episodes), LHON (Leber's hereditary optical neuropathy) and Leigh

syndrome (an early-onset fatal neurodegenerative disorder). Defects tend to be early-onset and prognosis is generally unfavourable.

Cytochrome oxidase deficiency is one of the most frequent causes of respiratory chain defect in humans (Barrientos et al., 2002). It can be caused by mutation in the mitochondrial genome (subunits of the enzyme or tRNA or rRNA mutations) or the nuclear genome. No mutation in any of the nuclear encoded subunits of cytochrome oxidase has ever been identified, although autosomal recessive mutations in several of the nuclear-encoded assembly factors required for synthesis have been found. Several mutations of the mitochondrial subunits have been reported, and their effects have been studied using the yeast and *R. sphaeroides* models (Meunier, 2001; Bratton et al., 2003).

1.4. NITRIC OXIDE

The second part of my thesis relates to nitric oxide (NO), a gaseous uncharged free radical which has intricate connections with the respiratory chain and in particular cytochrome oxidase. NO is synthesised from L-arginine by a family of NO synthase (NOS) enzymes (Alderton et al., 2001), and has several physiological and pathophysiological roles. NO can diffuse between cells (Lancaster, Jr., 1994), though its hydrophobicity means that it has a tendency to partition into membranes (Liu et al., 1998). NO coordinates transition metals such as iron, manganese and copper (Henry et al., 1993). Of particular importance, NO can easily bind Fe^{2+}, either in free form, in iron sulfur centres, or in hemoproteins where the heme has a free ligand position (Cooper, 1999). In mammalian cells the main mechanism of NO breakdown is through its reaction with hemoglobin (Wennmalm et al., 1993).

1.4.1. Physiological functions of NO

NO has several physiological functions in mammalian cells. Its physiological importance was first recognised when it was identified as EDRF (endothelium derived relaxing factor), an intracellular messenger causing relaxation of smooth muscle (Palmer et al., 1987; Ignarro et al., 1987). NO produced in endothelial cells on activation with, for example, acetylcholine, diffuses to the smooth muscle to cause relaxation and dilation, part of the normal regulation of blood flow. NO is also produced post-synaptically by neurons, and is involved in neurotransmission and neuromodulation, particularly in memory formation (Susswein et al., 2004). Additionally, NO inhibits platelet aggregation and adhesion (Moncada et al., 1991). All of these physiological effects are primarily mediated through activation of the soluble guanylate cyclase: NO binds Fe^{2+} in the heme group of this enzyme, triggering the

production of cGMP from GTP, which can then act on cGMP-dependent protein kinases or cGMP-gated ion channels (Denninger and Marletta, 1999). Yeast do not appear to have a homologue to the soluble guanylate cyclase. A further possible physiological role of NO in regulating respiration at the level of cytochrome oxidase is discussed below.

1.4.2. Reversible inhibition of cytochrome oxidase by NO

NO has been known for many years to bind cytochrome oxidase, and was widely used to study the effects of inhibition of cytochrome oxidase. NO competes with oxygen for the active site of cytochrome oxidase, binding reduced heme a_3 or oxidised Cu_B (Sarti et al., 2003). However, only in recent years has the possibility that this might have biological relevance been considered. There is now increasing evidence to suggest that inhibition of cellular respiration through the action of NO on cytochrome oxidase may have a physiological role in mammalian cells. Several investigations have demonstrated that physiological concentrations of NO can rapidly and reversibly inhibit cell respiration at the level of cytochrome oxidase in mammalian cells.

In 1994, Cleeter *et al.* showed that NO inhibited respiration through inhibition of cytochrome oxidase activity in isolated mitochondria (Cleeter et al., 1994). Subsequently, Brown and Cooper demonstrated that sub-micromolar levels of NO, likely to be present in some physiological conditions, rapidly and reversibly inhibited respiration in rat brain synaptosomes and isolated bovine cytochrome oxidase, through competition with oxygen for the cytochrome oxidase active site (Brown and Cooper, 1994). Brown *et al.* also showed that the addition of activated macrophages to a fibroblast or non-activated macrophage culture reversibly inhibited respiration in the second cell population, and that this was due to NO but did not involve the soluble guanylate cyclase (Brown et al., 1998), demonstrating that the inhibition of cytochrome oxidase could be caused by endogenously produced NO and was not confined to the NO-producing cell.

Brown has suggested that the acute reversible inhibition of cytochrome oxidase by NO may physiologically regulate mitochondrial respiration. NO increases the K_m of cytochrome oxidase for oxygen, and could allow cytochrome oxidase to act as an oxygen sensor, regulating its consumption at the point where it is consumed (Brown, 1995a). This has been suggested to lead to 'metabolic hypoxia', meaning that cytochrome oxidase cannot use the available oxygen, which could have pathophysiological consequences (Moncada and Erusalimsky, 2002). Additionally,

since cytochrome oxidase is responsible for virtually all cellular oxygen consumption, it would result in increased cellular oxygen levels which could have implications for signalling pathways regulated by oxygen concentration (Moncada and Erusalimsky, 2002).

1.4.3. Antimicrobial action of NO

In yeast there is no clear evidence for the existence of a NOS enzyme, therefore NO is unlikely to play any physiological role in this organism. However, NO is released in high concentrations by the macrophages of the mammalian innate immune system upon infection with pathogenic bacteria, viruses, parasites and fungi (Hibbs, Jr. et al., 1987; Marletta et al., 1988; MacMicking et al., 1997). Three NOS enzymes, eNOS (endothelial), nNOS (neuronal) and iNOS (inducible), as well as the controversial mtNOS (mitochondrial) have been described (Ghafourifar and Richter, 1997; Tatoyan and Giulivi, 1998; Alderton et al., 2001). In macrophages, NO is synthesised by the inducible iNOS (MacMicking et al., 1997). NO has cytotoxic and cytostatic properties against pathogens and, together with reactive oxygen species (ROS), which are also generated by cells of the immune system by the enzyme NADPH oxidase (Klebanoff, 1971; Nathan and Root, 1977), provides a first line of defence against pathogen infection (Mastroeni et al., 2000). The release of NO by activated macrophages has also been implicated in mammalian pathology, including inflammatory diseases such as arthritis (McCartney-Francis et al., 1993) and neurodegenerative diseases such as Parkinson's disease (Shergill et al., 1996).

The mechanism by which the NO produced by macrophages gives rise to antimicrobial action is unclear. At high concentrations and/or on prolonged exposure, NO can react with other molecules, including ROS, to form species collectively described as reactive nitrogen species (RNS), which can react with a wide variety of cellular targets. It is likely that such species contribute to the effect. In the next few sections I will discuss the formation of RNS, their targets, the formation of ROS, which may also be involved in the antimicrobial effect of NO, and the mechanisms of defence the cell employs against RNS and ROS.

1.5. REACTIVE NITROGEN SPECIES AND THEIR TARGETS

RNS are formed in the reaction of NO with other species. NO reacts slowly with oxygen to produce nitrogen dioxide (NO_2), which can react with another NO radical to generate dinitrogen trioxide (N_2O_3). These reactions are particularly prevalent within membranes, where NO tends to accumulate (Liu et al., 1998). NO_2 can nitrate several

molecules, including tyrosine. Tyrosine nitration can cause protein dysfunction and has been identified in diseases such as atherosclerosis (Leeuwenburgh et al., 1997). A proteomic study of nitrated proteins after cytokine induction of iNOS in rat cells or tissues identified over forty nitrated proteins, and a third of these were mitochondrial, for example glutamate dehydrogenase, aconitase, creatine kinase, COX5 and ATP synthase (Aulak et al., 2001). N_2O_3 can nitrosate (add NO^+ to) thiols or amines. Nitrosation of thiols generates S-nitrosothiols, and the NO^+ group is directly transferable from one thiol to another, in a process called transnitrosation. S-nitrosation of cysteine thiols has been implicated in redox-based signalling, regulating a wide variety of pathways (Hess et al., 2005).

NO also reacts with the radical superoxide anion ($O_2^{\cdot-}$) to produce peroxynitrite ($ONOO^-$), a highly reactive oxidant and strong nitrating agent. Peroxynitrite has been implicated in many of the deleterious cellular actions of NO. It can mediate oxidation of deoxyribose (Beckman et al., 1990), methionine (Moreno and Pryor, 1992), thiols (Radi et al., 1991a), phospholipids (Radi et al., 1991b) and causes DNA strand cleavage (King et al., 1992). It can also nitrate tyrosine residues (Beckman et al., 1992).

1.5.1. Irreversible inhibition of respiratory chain enzymes by NO/RNS

The enzymes of the respiratory chain are perhaps the most widely studied targets of NO/RNS. Irreversible or persistent inhibition has been found to occur under high concentrations or on prolonged periods of incubation with NO, and evidence suggests that RNS rather than NO itself mediates the inhibition. The antimicrobial effect of NO could be partly mediated through inhibition of the respiratory chain, either irreversible, or reversible at cytochrome oxidase.

Using the NO donor DETA NONOate, Clementi *et al.* showed that prolonged exposure to NO causes persistent inhibition of NADH dehydrogenase (Clementi et al., 1998). The inhibition was reversible by light and thiols (glutathione or DTT); S-nitrosation can be reversed by light or reduced thiols, so the mechanism of inhibition has been proposed to be *via* S-nitrosation of critical thiol residues (Clementi et al., 1998). In support of this, the S-nitrosothiol NO donors SNAP and GSNO inhibit NADH dehydrogenase even in conditions where little NO is released, in a manner which is reversible by light or thiols (Borutaite et al., 2000). However, other evidence suggests that peroxynitrite might be involved. Addition of peroxynitrite causes NADH dehydrogenase inhibition and in some studies this is also partly relieved by light and thiols (Cassina and Radi, 1996; Borutaite et al., 2000; Riobo et al., 2001). Peroxynitrite

scavengers were not found to prevent inhibition of respiration in the study by Clementi *et al.* (Clementi et al., 1998), but another study found partial prevention of the NO-induced NADH dehydrogenase inhibition (Riobo et al., 2001). Since peroxynitrite is a poor nitrosating agent this suggests that mechanisms other than S-nitrosation are involved. There is some evidence to suggest that peroxynitrite can nitrate tyrosines in NADH dehydrogenase (Yamamoto et al., 2002). As discussed earlier, *S. cerevisiae* does not contain a conventional NADH dehydrogenase, instead having three non-membrane-spanning NADH dehydrogenases. However, the above discussion serves to illustrate the complexity of the chemistry which can result in consequence of NO.

Succinate dehydrogenase and the bc_1 complex, like NADH dehydrogenase, contain non-heme iron-sulfur centres. However, inhibition of these complexes has not been as consistently observed as has the inhibition of NADH dehydrogenase. Some studies have found that NO inhibits succinate dehydrogenase; both peroxynitrite (Cassina and Radi, 1996; Radi et al., 1994) and destruction of the iron-sulfur centres (Welter et al., 1996; Geng et al., 1992) has been implicated in this. Other authors find the bc_1 complex but not succinate dehydrogenase inhibited (Poderoso et al., 1996; Pearce et al., 2001).

Bolanos *et al.* have reported irreversible inhibition of cytochrome oxidase in astrocytes after prolonged incubation (over 18 hours) with NO, with no change in NADH dehydrogenase or succinate dehydrogenase activity (Bolanos et al., 1994). This was suggested to be due to the peroxidation of cardiolipin, which has been shown to inhibit cytochrome oxidase activity (Heales et al., 1994; Paradies et al., 2000). Irreversible inhibition of cytochrome oxidase activity by RNS has also been associated with a decrease in steady state enzyme level (Sharpe and Cooper, 1998; Leary et al., 2002; Ramachandran et al., 2004).

1.5.2. Other protein targets

Aside from the components of the respiratory chain, RNS are likely to have a myriad of other protein targets. Here, I review some of the major targets identified in mammalian cells. Mitochondrial aconitase, a component of the citric acid cycle catalysing the isomerisation of citrate to isocitrate, is inhibited in co-cultivated cells by activated macrophages (Drapier and Hibbs, 1986). The mechanism of inhibition may be through S-nitrosation of the aconitase iron-sulfur centre (Gardner et al., 1997) or disruption of the centre by peroxynitrite (Hausladen and Fridovich, 1994; Castro et al., 1998). Mitochondrial creatine kinase is involved in export of ATP from the mitochondrion.

Inhibition of the kinase was observed in the presence of NO donor, and was reversible on addition of the reducing agent DTT, therefore the mechanism of inhibition was suggested to be through S-nitrosation of a critical active site cysteine (Gross et al., 1996; Wolosker et al., 1996). However, peroxynitrite can also inhibit creatine kinase activity, and oxidation of the critical thiol has also been proposed (Stachowiak et al., 1998; Konorev et al., 1998). The glycolytic enzyme GAPDH, catalysing the rate-limiting step in glycolysis, is also inhibited by NO (Dimmeler et al., 1992). Peroxynitrite can oxidise the active-site cysteine (Souza and Radi, 1998) and S-nitrosation of the same cysteine has also been implicated in the inhibition (Padgett and Whorton, 1995; Beltran et al., 2000).

NO also causes reversible inhibition of catalase, the enzyme which converts hydrogen peroxide into water and molecular oxygen, probably by competitive inhibition with hydrogen peroxide at the active site heme (Brown, 1995b). This might be expected to lead to increased hydrogen peroxide levels and consequent cell damage. NO also inhibits glutathione reductase, *via* the formation of S-nitrosothiols (Butzer et al., 1999). This enzyme recycles oxidised glutathione (GSSG) to regenerate reduced glutathione (GSH) which, as will be seen later, is important in detoxification.

The cytochrome P450 superfamily contains heme iron, and NO has been found to decrease the activity of cytochrome P450 enzymes (Morgan et al., 2001). The inhibition can be both reversible at the heme iron of cytochrome P450, and irreversible, perhaps *via* modification of thiols or nitration of tyrosine residues by peroxynitrite (Minamiyama et al., 1997; Roberts et al., 1998; Quaroni et al., 2004). In yeast, cytochrome P450-containing enzymes are involved in the synthesis of ergosterol, an essential component of the fungal cell wall. Ribonucleotide reductase, the rate-limiting enzyme in DNA synthesis, is also inhibited by NO (Kwon et al., 1991). The enzyme catalyses the reduction of ribonucleotides to their corresponding deoxyribonucleotides, to be used as precursors in DNA synthesis. The inhibition may be due to S-nitrosation of one or more of the cysteine residues involved in electron transfer (Roy et al., 1995) and/or disruption of a stable tyrosyl free radical in the enzyme (Lepoivre et al., 1994; Lemaire et al., 1999).

1.5.3. DNA and lipid damage

RNS target other cellular components in addition to proteins. DNA damage has been reported, and is due to both deamination mediated by N_2O_3 and oxidation by peroxynitrite (Dedon and Tannenbaum, 2004). A yeast mutant deficent in DNA repair

was more sensitive to NO-induced toxicity than wild type yeast (Tamir et al., 1996). Since peroxynitrite production is likely to be concentrated in the mitochondria, mtDNA may be particularly at risk of mutagenesis. mtDNA is also inherently less protected from such damage due to the absence of protective histones and the apparent incapability of mitochondria to perform nucleotide-excision repair (Yakes and Van Houten, 1997). Peroxynitrite has been shown to cause a higher level of damage to mtDNA than nuclear DNA (Ballinger et al., 2000).

Lipids are another target of RNS. Lipid peroxidation is initiated by free radicals, which remove hydrogen from unsaturated lipids to generate lipid radicals, which combine with oxygen and propagate a chain of lipid peroxidation. Peroxynitrite and NO_2 can initiate this process (Pryor and Lightsey, 1981; Radi et al., 1991b; O'Donnell et al., 1997). As mentioned earlier, peroxidation of cardiolipin may be involved in the irreversible inhibition of cytochrome oxidase caused by NO.

1.5.4. Production of ROS by the respiratory chain

Inhibition of the respiratory chain by NO/RNS, whether reversible or irreversible, would lead to the respiratory chain being in a more reduced state. The respiratory chain is a major site of superoxide generation, and its inhibition by NO has been shown to increase the amount of superoxide generated (Poderoso et al., 1996). This might therefore be expected to increase peroxynitrite production (Packer et al., 1996). Synthesis of highly reactive peroxynitrite in close proximity to the respiratory chain is likely to further potentiate the action of NO (Moncada and Erusalimsky, 2002). It is not surprising that many of the enzymes identified to be inhibited by NO are located in the mitochondria, since this is where the formation of peroxynitrite will be at its highest.

When the respiratory chain is highly reduced, electrons can 'escape' and react with oxygen to form superoxide. Many of the redox centres of the electron transport chain are one electron carriers, so could potentially donate one electron to molecular oxygen, generating the superoxide radical. In particular, the oxidation of ubiquinol (UQH_2) to ubiquinone (UQ) at the Q_o site of the bc_1 complex takes place in two one-electron steps, allowing the transient formation of ubisemiquinone ($UQH^{\cdot}$). The unpaired electron can be transferred to molecular oxygen (Boveris et al., 1976; Cadenas et al., 1977). When the respiratory chain is reduced the existence of ubisemiquinone will be prolonged, increasing the likelihood of reaction with oxygen. Additionally, superoxide is generated by NADH dehydrogenase at the flavin mononucleotide group, the first electron carrier of the complex (Turrens and Boveris, 1980; Liu et al., 2002).

ROS include the superoxide anion, hydrogen peroxide (H_2O_2) and the hydroxyl radical ($OH^{\cdot}$). These are highly reactive and therefore transient species. Superoxide spontaneously dismutates to oxygen and hydrogen peroxide, a process which can be accelerated by the enzyme superoxide dismutase. On reaction with Fe^{2+} the hydroxyl radical is generated by hydrogen peroxide. This is a powerful oxidant, and can cause damage to proteins, lipids and DNA.

1.6. ROS/RNS DEFENCE IN YEAST

Microorganisms have developed numerous defence strategies, both enzymatic and non-enzymatic, to protect against damaging reactive species, involving both the detoxification of the reactive species themselves and the repair or removal of damaged cellular constituents. The defences against ROS have been well studied, however, defence mechanisms against RNS are less well defined. Below I review the major enzyme-based ROS and RNS defences.

1.6.1. Superoxide dismutase

One of the most important antioxidant activities in the cell is superoxide dismutase, which catalyses the conversion of one ROS (superoxide) into another ROS (hydrogen peroxide). The reaction can also proceed spontaneously in the absence of enzyme. Yeast contain a cytosolic copper,zinc superoxide dismutase encoded by the *SOD1* gene and a mitochondrial manganese superoxide dismutase encoded by the *SOD2* gene. When *SOD2* is deleted the cell is sensitive to high oxygen levels (van Loon et al., 1986), and when *SOD2* is mutated this causes severely increased sensitivity to conditions which enhance ROS production by the respiratory chain (Piper, 1999). Removal of superoxide would be expected to decrease the level of highly reactive peroxynitrite formed in the reaction between NO and superoxide, hence superoxide dismutase may protect against the actions of RNS in addition to its more obvious role in protection against ROS (De Groote et al., 1997).

1.6.2. Yhb1p

In yeast, the main defence mechanism against NO is thought to be the NO oxidoreductase Yhb1p, encoded by the *YHB1* gene. This is part of the widely conserved flavohemoglobin family, which contain a globin element containing heme b and a reductase element with binding sites for FAD and NAD(P)H, and are widely distributed in bacteria and fungi (Poole and Hughes, 2000). Evidence suggests that bacterial flavohemoglobins act as oxygenases consuming NO to produce nitrate under aerobic

conditions (Kim et al., 1999), and as NO reductases to form N_2O under anaerobic conditions (Hausladen et al., 1998). The yeast Yhb1p probably has the same function (Liu et al., 2000).

1.6.3. Glutathione

Glutathione (γ-glutamylcysteinylglycine) is an abundant low molecular weight thiol. Synthesis of glutathione requires γ-glutamylcysteine synthetase (Gsh1p) and glutathione synthetase (Gsh2p). The peptide has many functions including free radical scavenging, mediated by the redox-active sulfhydryl group of the cysteine residue (Meister, 1988). Glutathione cycles between a reduced form (GSH) and an oxidised form (GSSG), in which two peptides are linked by a disulfide bond. Reduced glutathione (GSH) is oxidised by ROS/RNS, forming a disulfide bond with another GSH to generate oxidised glutathione (GSSG). Regeneration of GSH from GSSG requires NADPH and is catalysed by glutathione reductase (Glr1p). GSH may scavenge RNS or reverse the modifications they make to proteins. S-nitrosation of thiols, and thiol oxidation, will deplete the cellular pool of GSH, making damage to other cellular components more likely (Radi et al., 1991a). Inhibition of NADH dehydrogenase seems to be preceded by a drop in reduced glutathione levels (Beltran et al., 2000).

GSH can also form conjugates with compounds requiring excretion, including epoxides (Meister 1988), in a reaction catalysed by glutathione S-transferase (Gtt1p, Gtt2p). The conjugates are then pumped out of the cytosol into the vacuole. In mammalian cells, this is achieved by the MRP (multidrug associated resistance protein) sub-family of ABC transporters. In yeast, the MRP-like Ycf1p family carries out the function (Li et al., 1996).

1.6.4. Removal of peroxides

Several systems are in place for removal of hydrogen peroxide and other peroxides. Catalase catalyses the conversion of hydrogen peroxide into water and molecular oxygen. Yeast contain two catalases: catalase A (Cta1p) is peroxisomal and involved in removal of hydrogen peroxide formed during fatty acid oxidation (Hiltunen et al., 2003), while catalase T (Ctt1p) is cytoplasmic and plays a more general antioxidant role. Mitochondrial cytochrome *c* peroxidase (Ccp1p) also degrades hydrogen peroxide, using electrons from cytochrome *c*. Expression of this enzyme increases during respiratory growth and on treatment with hydrogen peroxide (Kwon et al., 2003). Interestingly, expression also increases in the presence of peroxynitrite, suggesting a possible role in detoxification of RNS (Kwon et al., 2003).

Glutathione peroxidases use GSH as a reductant to break down both hydrogen peroxide and larger peroxides. Phospholipid hydroperoxide glutathione peroxidases differ functionally from classical glutathione peroxidases in that they are able to additionally break down lipid hydroperoxides, and are therefore involved in the repair of lipid peroxidation. Yeast does not contain any classical glutathione peroxidases, but contains three phospholipid hydroperoxide glutathione peroxidases, encoded by the genes *GPX1*, *GPX2* and *GPX3* (Avery and Avery, 2001).

Glutaredoxins also use GSH as a reductant. Like the glutathione peroxidases they reduce hydroperoxides, so have overlapping function (Collinson et al., 2002; Collinson and Grant, 2003). *S. cerevisiae* has two glutaredoxins (*GRX1* and *GRX2*) containing two redox active cysteines in the active site, and three glutaredoxin-related proteins (*GRX3*, *GRX4* and *GRX5*), each containing one active site cysteine. The glutaredoxins were also shown to have glutathione S-transferase activity (Collinson and Grant, 2003).

Peroxiredoxins, or thiol peroxidases, also scavenge peroxides. *S. cerevisiae* has five peroxiredoxins (Park et al., 2000). There are two types, 1-Cys peroxiredoxins and 2-Cys peroxiredoxins. When oxidised the 2-Cys variety forms an intramolecular disulfide bridge which requires thioredoxin for reduction. The regeneration of thioredoxin is, in turn, mediated by thioredoxin reductase. Tsa1p and Tsa2p, 2-Cys peroxiredoxins, both detoxify hydrogen peroxide, while Tsa2p can additionally scavenge peroxynitrite (Wong et al., 2002).

1.6.5. Transcription factors involved in the response to stress

ROS and RNS, as we have seen, interact with multiple cellular components, which will give rise to cellular stress. This will induce a response at the transcriptional level to enable the cell to adjust to the stress sensed. Three transcription factors which may be relevant in the cellular response to NO/RNS treatment are Msn2p, Msn4p and Yap1p. Msn2p and Msn4p are homologous zinc finger transcription factors which bind specifically to stress response elements (STREs; C_4T) to activate genes (Estruch and Carlson, 1993; Schmitt and McEntee, 1996). Their intracellular location is sensitive to environmental stress, and in conditions of stress the proteins accumulate in the nucleus. These transcription factors mediate the general response to stress (Schmitt and McEntee, 1996; Martinez-Pastor et al., 1996). Yap1p, a member of the AP-1 group of transcription factors, containing a bZIP (leucine zipper) domain, is specifically involved in the response to oxidative stress (Rodrigues-Pousada et al., 2004). Like Msn2/4p,

regulation of Yap1p takes place at the level of subcellular localisation. In conditions of oxidative stress the protein accumulates in the nucleus where it activates the transcription of oxidative stress response genes (Kuge et al., 1997). Another transcription factor Skn7p was identified in a screen of mutants sensitive to oxidative stress (Krems et al., 1996). Like Yap1p, it has been shown to regulate the transcription of several genes involved in the response to oxidative stress (Morgan et al., 1997; Lee et al., 1999).

1.7. AIMS OF THIS THESIS

1.7.1. Cytochrome oxidase assembly

Chapter 3 attempts to provide more information on the pathway of synthesis of cytochrome oxidase, using yeast as a model system. The structure of cytochrome oxidase of the yeast *S. cerevisiae* closely resembles that of its mammalian counterpart (see Table 1.1) (Taanman, 1997). Full genomic sequence data has been available for yeast since 1996, and yeast is amenable to genetic manipulation. Yeast are facultative anaerobes, so can ferment the pyruvate produced in glycolysis. This means that the organism is viable in the absence of a functional respiratory chain, allowing study of mutant strains. Unlike mammalian cells, yeast cells can tolerate only one type of mtDNA, hence manipulation of yeast mtDNA allows creation of homoplasmic cells and mutations in the mtDNA-encoded respiratory chain subunits can also be studied. Yeast has proven extremely useful in deciphering the roles of particular subunits and residues in the function of cytochrome oxidase, and in the identification of nuclear proteins involved in the cytochrome oxidase assembly process. However, as discussed earlier, when there is a defect in cytochrome oxidase assembly, unassembled subunits in yeast are rapidly degraded by mitochondrial proteases. Consequently the use of yeast to investigate the sequential assembly process of cytochrome oxidase has been limited because of the absence of partially assembled intermediates, and to date there is only one report of cytochrome oxidase subassemblies identified in yeast (Church et al., 2005).

I screened yeast strains with mutations in the *COX2* gene to identify assembly-defective strains. This was achieved by analysing the UV-Vis spectrum of the cells and assessing the concentration of cytochrome oxidase present as determined by absorbance of heme aa_3. I then characterised those strains with assembly defects. Two strains which, unusually, contained partially assembled cytochrome oxidase, were further analysed using blue native electrophoresis to investigate the presence of assembly

complexes, providing information on the sequential process of assembly of cytochrome oxidase.

1.7.2. Antimicrobial action of nitric oxide

Much research has concentrated on the physiological actions of NO occurring in mammalian cells in the presence of low concentrations of the gas. However, the antimicrobial actions of NO on pathogenic bacteria, viruses, parasites and fungi, resulting from its release in higher concentrations by macrophages, has been less well characterised. Here, I used *S. cerevisiae* as a model system to study the antimicrobial action. The action is likely to be mediated by RNS, formed on reaction of NO with other molecules such as molecular oxygen or the superoxide radical. Several studies have shown that the NO oxidoreductase Yhb1p is likely to be the main protective mechanism against NO in some microorganisms, including *S. cerevisiae*, limiting the exposure of cellular targets to damaging RNS (Liu et al., 2000; Hromatka et al., 2005; 2005; Sarver and DeRisi, 2005). Consequently, to detect other proteins contributing to the defence against NO/RNS, I analysed the effect of NO/RNS on yeast strains lacking the *YHB1* gene.

In Chapter 4 I characterised the effect of NO/RNS on yeast cell proliferation and viability, and on the components of the respiratory chain. In Chapter 5 I used a genomic approach to determine the systems/proteins which are targeted by RNS stress, and the strategies used by the cells to withstand the stress. I identified those genes which had altered expression on treatment with NO/RNS, and analysed the data in such a way as to exclude the contribution of the general stress response. I also studied the roles of the transcription factors Msn2/4p and Yap1p in the gene expression response to RNS treatment.

The formation of RNS and their actions in the cell involve complex chemistry, and I did not attempt to distinguish between NO and RNS involvement in the antimicrobial action. However, I did assess the contribution of the respiratory chain to the growth inhibition and gene expression changes. This provides information about the role of respiratory chain inhibition (both reversible and irreversible) in the stress sensed by the cell. Additionally, since the respiratory chain is the major source of ROS production, it gives clues as to whether ROS have a major involvement in the stress.

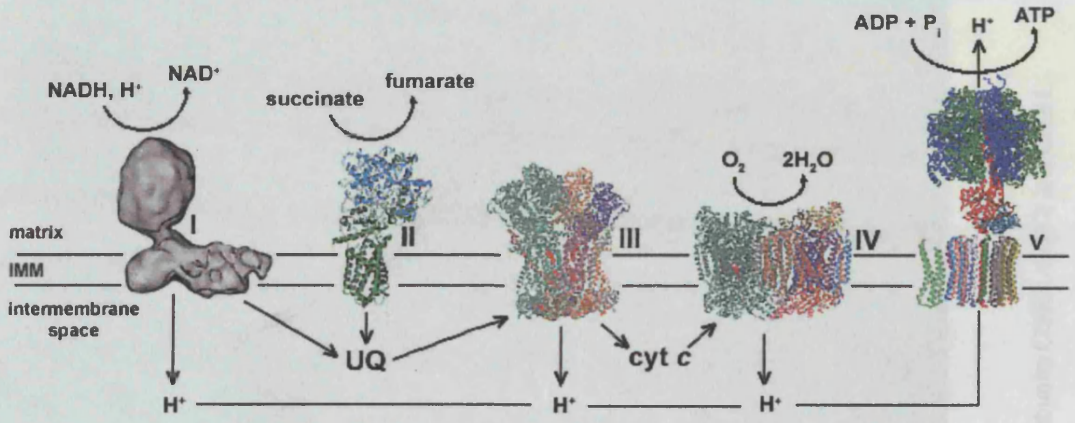

Figure 1.1. The respiratory chain.

Electron flow through the respiratory chain complexes leads to pumping of protons from the matrix to the IMS, generating a gradient of protons which return to the matrix through the ATP synthase (complex V), accompanied by the generation of ATP. UQ, ubiquinone.

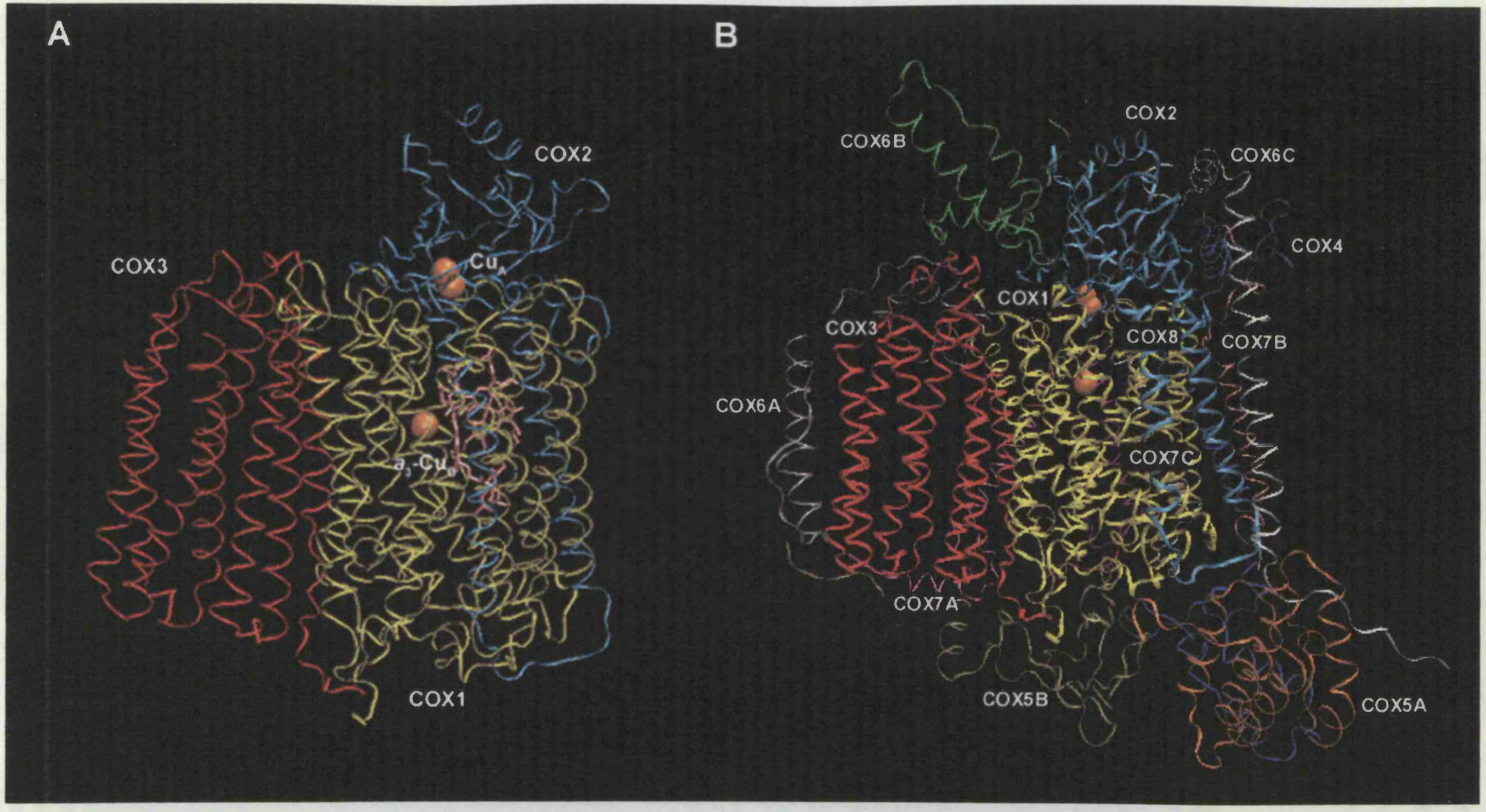

Figure 1.2. Structure of bovine cytochrome oxidase.

The atomic structure is from the bovine enzyme (PDB 1OCC) and bovine numbering is used. **A.** Structure of the core subunits COX1, COX2 and COX3. **B.** Structure of the entire cytochrome oxidase monomer.

Table 1.1. Yeast cytochrome oxidase subunits and their mammalian counterparts. [a]Data obtained from the Saccharomyces Genome Database (www.yeastgenome.org). [b]Data obtained from (Taanman, 1997). [c]Data obtained from the bovine structure (Tsukihara et al., 1996).[d]Size of full length transcript. [e]Interchangeable isoforms (Cumsky et al., 1985): Cox5ap is expressed at high oxygen tension, Cox5bp at low oxygen tension (Poyton and Burke, 1992). [f]Yeast Cox7ap also shows some homology to mammalian COX8. Yeast subunits corresponding to mammalian COX7B have not been identified.

Yeast subunit	Gene name[a]	Mammalian counterpart[b]	Interacts with[c]	Molecular weight (kDa)[d]	Location[c]	Disruption of fungal gene
Cox1p	*COX1*	COX1	COX2 COX3 COX4 COX7C	58.8	IMM	Assembly defect (Lemaire et al., 1998)
Cox2p	*COX2*	COX2	COX1 COX6B COX6C	28.6	IMM	Assembly defect (Slonimski and Tzagoloff, 1976; Lemaire et al., 1998)
Cox3p	*COX3*	COX3	COX1 COX4 COX6A COX6B COX7A	30.4	IMM	Assembly defect (Haltia et al., 1989; Lemaire et al., 1998)
Cox4p	*COX4*	COX5B	COX1 COX3	17.1	Matrix extrinsic	Assembly defect (Dowhan et al., 1985)
Cox5ap/ Cox5bp[e]	*COX5 A/B*	COX4	COX5A COX7B COX8	17.1/ 17.2	IMM	Assembly defect (McEwan et al., 2004) (Glerum and Tzagoloff, 1997)
Cox6p	*COX6*	COX5A	COX4 COX6C	17.3	Matrix extrinsic	Assembly defect (Glerum and Tzagoloff, 1997)
Cox6ap	*COX13*	COX6A	COX3 COX1 (other monomer)	15.0	IMM	Altered activity (dependent on ionic strength) (Taanman and Capaldi, 1993)
Cox6bp	*COX12*	COX6B	COX2 COX3 COX6B (other monomer)	9.8	IMS extrinsic	Partial assembly defect (LaMarche et al., 1992)
Cox7p	*COX7*	COX7A	COX3	6.9	IMM	Assembly defect (Aggeler and Capaldi, 1990; Calder and McEwen, 1990)
Cox7ap	*COX9*	COX6C[f]	COX2 COX5A	7.0	IMM	Assembly defect (Wright et al., 1986)
Cox8p	*COX8*	COX7C	COX1	8.9	IMM	Diminished activity (Patterson and Poyton, 1986)

Table 1.2. Accessory proteins involved in cytochrome oxidase assembly. Assembly factors specifically involved in the assembly of cytochrome oxidase are shown. Yeast nomenclature is used.

Protein	Function	Location	Reference
Arh1p	Heme *a* biosynthesis	IMM	(Barros et al., 2001)
Cox10p	Heme *a* biosynthesis	IMM	(Tzagoloff et al., 1993)
Cox11p	Delivery of copper to Cox1p	IMM	(Hiser et al., 2000)
Cox14p	Unknown	IMM	(Glerum et al., 1995)
Cox15p	Heme *a* biosynthesis	IMM	(Barros et al., 2001)
Cox16p	Unknown	IMM	(Carlson et al., 2003)
Cox17p	Delivery of copper to Sco1p and Cox11p	Cytosol; IMS	(Glerum et al., 1996a)
Cox18p	Translocation of Cox2p C-terminus into IMS	IMM	(Saracco and Fox, 2002)
Cox19p	May be involved in copper insertion; has homology to Cox17p	Cytosol; IMS	(Nobrega et al., 2002)
Cox20p	Required for Cox2p N-terminal presequence cleavage	IMM	(Hell et al., 2000)
Cox23p	May be involved in copper insertion; has homology to Cox17p	IMS	(Barros et al., 2004)
Cox24p	Translation of *COX1* mRNA	IMM	(Barros et al., 2006)
Imp1p, Imp2p	Cleavage of Cox2p N-terminal presequence	IMM	(Behrens et al., 1991) (Bauer et al., 1994)
Mba1p	Translocation of subunits	IMM	(Preuss et al., 2001)
Mia40p	Import of metal-containing proteins	IMS	(Chacinska et al., 2004; Terziyska et al., 2005)
Mss2p	Translocation of Cox2p	IMM	(Broadley et al., 2001)
Mss51p	Translation of *COX1* mRNA; insertion of Cox1p into the IMM	IMM	(Perez-Martinez et al., 2003) (Siep et al., 2000)
Oxa1p	Translocation of Cox2p N-terminus into the IMS	IMM	(Hell et al., 2001)
Pet54p	Translation of *COX3* mRNA	IMM	(Costanzo et al., 1986)
Pet100p	Matrix incorporation of a subcomplex containing Cox7p, Cox7ap and Cox8p	IMM	(Church et al., 1996) (Church et al., 2005)
Pet111p	Translation of *COX2* mRNA	IMM	(Mulero and Fox, 1993)
Pet117p	Unknown	IMM	(McEwen et al., 1993)
Pet122p	Translation of *COX3* mRNA	IMM	(Kloeckener-Gruissem et al., 1988)
Pet191p	Unknown	IMM	(McEwen et al., 1993)
Pet309p	Translation of *COX1* mRNA	IMM	(Manthey and McEwan, 1995)
Pet494p	Translation of *COX3* mRNA	IMM	(Costanzo and Fox, 1986)
Pnt1p	Translocation of Cox2p	IMM	(He and Fox, 1999)
Sco1p	Delivery of copper to Cox2p	IMM	(Glerum et al., 1996b)
Sco2p	May have similar function to Sco1p	IMM	(Lode et al., 2002)
Shy1p	May be involved in heme a_3 insertion	IMM	(Smith et al., 2005)
Yah1p	Heme *a* biosynthesis	matrix	(Barros et al., 2001)
Yme1p	Degradation of unassembled subunits	IMM	(Pearce and Sherman, 1995)
Afg3p, Rca1p	Degradation of unassembled subunits	IMM	(Guelin et al., 1996)

Chapter 2

MATERIALS AND METHODS

2.1. CELL BIOLOGY

2.1.1. Yeast growth

The yeast strains used in this study are listed in Table 2.1. Media components were obtained from Sigma or Becton Dickinson unless otherwise stated. YPDA (1% (w/v) yeast extract, 2% (w/v) peptone, 3% (w/v) glucose, supplemented with 10 mg/L adenine) was the standard growth medium. Adenine was omitted to allow detection of Ade^- auxotrophs. To assess respiratory competence glucose was replaced with glycerol (YPG). For the experiments involving nitric oxide, glucose was replaced with galactose and the medium was supplemented with 800 mg/L of CSM-Ura (complete supplement mixture minus uracil, BIO 101 systems) and 20 mg/L uracil (YPGal). In the presence of glucose mitochondrial functions are repressed, so cells rely only on fermentation for energy production. This repression of genes involved in metabolising other carbon sources is lifted in the absence of glucose. Glycerol cannot be fermented so cells growing in YPG must rely only on respiration for growth, allowing detection of respiratory deficient strains. Galactose can be used by the cell for both fermentation and respiration. For selective growth of diploids a minimal medium (0.7% (w/v) yeast nitrogen base, 3% (w/v) glucose or galactose, 2% (w/v) agar) was used. For the selection of auxotrophs, minimal medium containing 800 mg/L of CSM-(component) was used. Transformation medium (0.7% (w/v) yeast nitrogen base, 3% (w/v) glucose, 1M sorbitol, 800 mg/L CSM-Ura) was used for site-directed mutagenesis. 2% (w/v) agar was added for solid media, and all media were autoclaved at 121°C for 15 minutes prior to use.

Growth on solid medium was overnight at 28°C or at room temperature for 2-3 days. Growth in liquid culture was at 28°C with shaking at 170 rpm, routinely in 10 ml medium in 100 ml flasks. Cells were stored in the short term at 4°C on solid media. For long term storage at -80°C cells were resuspended in 50% YPDA, 25% glycerol.

2.1.2. Bacterial growth

Bacterial strains were grown in LBA medium (0.5% sodium chloride, 0.5% yeast extract, 1% tryptone, 100 μg/ml ampicillin added after autoclaving) with 2% agar added for solid media. Growth on solid medium was overnight at 37°C or at room temperature for 2-3 days. Growth in liquid culture was at 37°C with shaking at 170 rpm. Cells were stored in the short term at 4°C on solid media, or for long term storage in 50% LBA, 25% glycerol at -80°C.

2.1.3. Crossing yeast strains

Cells were grown on YPDA then physically mixed on a fresh YPDA plate. Alternatively when many clones were tested, they were resuspended in water in a 96-well plate and a replicator used to lay drops onto a YPDA plate spread with a lawn of the second strain. After 2 days growth plates were replicated on minimal medium and incubated for 2 days for selection of diploids.

2.1.4. Generation of ρ^0 (mtDNA-less) cells

Cells were subcloned then subjected to successive rounds of growth on YPDA supplemented after autoclaving with 1 mg/L ethidium bromide. Absence of mtDNA was confirmed by inability to grow on YPG.

2.1.5. Mapping mutations to the *COX2* gene

Haploid mutants were crossed with the respiratory deficient rho$^-$ tester strain CKDS 302 containing only *COX2* in its mitochondrial genome. Respiratory growth of the diploids formed indicated that recombination had occurred to introduce wild type *COX2* into the mutant mitochondrial genome and that the mutation must therefore be present in the *COX2* gene, while respiratory deficiency indicated that *COX2* recombination did not affect the mutation, which must therefore be located elsewhere (Figure 2.1). Since the *COX2* sequence present in the tester strain contained some sequence outside (upstream and downstream) of the *COX2* non-coding sequence, the existence of mutations outside the *COX2* coding region was excluded by crossing with W303-1B/pBM2, a rho$^-$ strain containing only the *COX2* coding region. This tester strain was constructed in our lab by biolistic transformation of W303-1B rho^0 (see 2.2.6) with the pBM2 plasmid generated in our lab by PCR cloning, using the product of amplification of the *COX2* gene with the primers PL32 and PL27 (see Table 2.2 and Figure 2.4.) and the Stratagene PCR-Script cloning kit.

2.1.6. Cytoduction

The respiratory deficient mutations were generated in the BM1/1-16 strain by moderate mutagenesis with 8 mM of the mtDNA mutagen manganese chloride. The strain harbours the *op1* mutation which affects the adenine nucleotide carrier of the IMM (Meunier et al., 1993). The *op1* mutation is lethal in combination with a rho^0 or rho$^-$ (complete deletion or large deletion of mtDNA) mutation, hence only mit$^-$ (point) mutants accumulated. Since the *op1* mutation itself causes respiratory deficiency,

screening for mit$^-$ mutants required diploids (*OP/op1*); mit$^-$ mutants were identified by the inability of diploids to grow on respiratory medium (YPG) (Meunier et al., 1993).

Due to the *op1* mutation causing respiratory deficiency, further genetic analysis of the respiratory deficient mutants required transfer of the mtDNA to another nuclear background. This was done in a two step manner. The BM1/1-16 mutants were used for cytoduction of the mitochondrial genome into the recipient strain JC8/56 rho^0, carrying the mutation *kar1-1* required for cytoduction (Conde and Fink, 1976). 12 hours after crossing single colonies were generated on YPD, the aim being to terminate crossing at the point where zygotes with mixed cytoplasm but unfused nuclei can be selected. After 2 days growth BM 1/1-16 haploid colonies (auxotroph for adenine) appeared red due to the absence of adenine. Blockage of the adenine biosynthetic pathway due to the *ade1* or *ade2* mutations causes accumulation of P-ribosylaminoimidazole, a pink intermediate of the adenine biosynthetic pathway. Diploids appeared as large white colonies. The smaller white colonies (Ade$^+$) present were either JC8/56 rho^0 or JC8 rho$^+$ mit$^-$ (i.e. with mitochondrial genome but mutation in *COX2*) mutant haploids, and these were transferred by toothpick onto YPD. To distinguish between them, colonies were crossed with the respiratory deficient rho$^-$ tester strain W303-1B/pBM2 containing only *COX2* in the mitochondrial genome. The resultant diploids were replicated onto YPG medium to select for respiratory competent colonies (derived from JC8 rho$^+$ mit$^-$ mutant haploids).

The corresponding haploids were selected and crossed with W303-1B rho^0 as described for the initial crossing. This time the red (Ade$^-$) colonies were selected and crossed with the respiratory deficient tester strain CKDS 302 to distinguish between W303-1B rho^0 and W303-1B mutant haploids. Haploid strains corresponding to the resultant respiratory competent diploids were used for subsequent analyses.

2.1.7. Generation of revertants

The mutant strain was subcloned on YPDA, then subclones were resuspended in 50 µl of sterile water, spread on YPG, and incubated for 1-2 weeks. Respiratory competent clones arising were then subcloned on YPDA, and subclones were replicated on YPG to confirm respiratory competence. In cases where few respiratory competent clones arose the procedure was repeated with the initial subclones (approx. 10^7 cells per ml) first incubated overnight in YPDA containing 8 mM manganese chloride to increase the frequency of mutagenesis.

Secondary mutations may arise at any location, in the nuclear as well as in the mitochondrial genome. To determine the mitochondrial or nuclear heredity of a reversion, the rho^0 was generated from the revertant, and crossed with the parent mutant of the correct mating type. Growth of the resultant diploid on YPG indicated a nuclear dominant reversion, while absence of growth indicated a nuclear recessive or mitochondrial mutation. To distinguish between the latter two possibilities the revertant was crossed with the rho^0 form of the parent mutant, and growth of the diploid on YPG indicated mitochondrial reversion (Figure 2.2).

2.1.8. Incubation with nitric oxide donor

The nitric oxide (NO) donor used was (Z)-1-[2-(2-aminoethyl)-N-(2-ammonioethyl)amino]diazen-1-ium-1,2-diolate (DETA NONOate), obtained from Alexis Biochemicals and dissolved to form a 500 mM aqueous solution. NO is released from DETA NONOate in a temperature- and pH-dependent manner, with higher temperature and lower pH resulting in quicker decomposition. The half life of DETA NONOate is 20 hours at 37°C and 57 hours at 24°C at pH 7.4 (Hrabie and Klose, 1993). The experiments described here were carried out at 28°C. Prior to culture the pH of YPGal media was approximately 5.85. Yeast growth caused media pH to drop, and DETA NONOate was added to cultures when a pH of around 5.6 was reached.

In Chapter 4, two culture conditions were used. In both cases, a 10 ml starter culture was grown in a 100 ml Erlenmeyer flask for 6 hours at 28°C with shaking at 170 rpm, and used to inoculate new YPGal cultures to A_{600nm} = 0.015 (or 0.05 for FY1679 Δ*yhb1* Δ*sod1*). For the first condition, after 15.5 hours growth the A_{600nm} of the cultures was measured to be around 2, a density of approximately 6.10^7 cells per ml (late exponential phase). Cultures were divided into 10 ml aliquots in new 100 ml flasks, and treatment was given immediately afterwards. For the second condition, cells were allowed to grow for a further 6 hours to allow early stationary phase (A_{600nm} around 10, approximately 3.10^8 cells per ml) to be reached prior to splitting and treatment.

0.1, 1 or 3 mM final concentration of DETA NONOate was added to the cultures. Where myxothiazol (Sigma) was added, the stock was 20 mM in ethanol and the final concentration was 8 μM. An ergosterol (Sigma) stock was 30 mg/ml in ethanol and the final concentration was 15, 50 or 120 μg/ml. In cases where both ergosterol and NO donor were required, ergosterol was added immediately prior to NO donor. Cultures were returned to the incubator for up to 26 hours and cell density was monitored by measuring absorbance at 600 nm. Cells were harvested for characterisation as required.

To harvest, cells were pelleted by centrifugation at 1,780 g at 4°C for 4 minutes, washed twice with ice-cold water, then resuspended to around 100 mg cells per ml in water (for oxygen consumption measurements) or 5% Ficoll pH 7.5 (for spectroscopy).

In the experiment involving carbon monoxide, the gas was bubbled slowly through a 120 ml aliquot of cells in a closed Erlenmeyer flask at a rate of approx. 1 bubble/8s; compressed air was also bubbled through at a faster rate to ensure the culture was aerobic. The experiment took place at room temperature with moderate stirring and the cells were harvested after 6.5 hours

2.1.9. Methylene blue staining

80 µl of a 0.1% solution of methylene blue was added to 5 µl of cells, which were then immediately visualised at 40x magnification with a light microscope. As positive control, cells were treated with 100% ethanol in a 1:1 (v/v) ratio for 5 minutes prior to the methylene blue addition. The numbers of blue and white cells were counted, for a sample size of at least 300.

2.1.10. Fluorimetry

The dyes tested were: dihydrorhodamine 123, dihydroethidium, 2',7'-dichlorodihydrofluorescein diacetate (carboxy-H_2DCFDA), all dissolved in DMSO. Excitation/emission spectra of the corresponding active fluorophores are shown in Figure 2.3. Assays were performed with minimal exposure to light. Yeast starter cultures were used to inoculate new 20 ml YPGal cultures so that after 17 hours of growth they reached an A_{600nm} of 1-2. The volume of cells required to give 3.10^5-2.10^8 cells per well of a 96-well plate was calculated and placed in an eppendorf. Preliminary experiments showed that YPGal medium had significant autofluorescence (due to peptone and yeast extract), so assays were carried out in PBS rather than YPGal. Cells were harvested at 1,780 g for 2 minutes, washed with 1 ml PBS then centrifuged again at 1,780 g for 2 minutes. Cells were resuspended to a volume of 95.7 µl/well in PBS, aliquoted into wells, then 2-250 µM dye was added as required. Reactions were incubated for 1 hour at 28°C in the dark. Alternatively, dye was added directly to an aliquot of culture with enough cells for 5 wells. After 1 hour incubation cells were harvested by 1,780 g centrifugation for 2 minutes, then washed twice in water and twice in PBS before resuspension in 500 µl PBS, then 100 µl was aliquoted into wells. Fluorescence was measured in a plate reader using filters allowing excitation at 485 nm and emission detection at 535 nm. Negative controls were: addition of DMSO in place of dye; assay with no cells. The positive control was incubation with 5 mM hydrogen

peroxide for 15 minutes at 28°C with 170 rpm shaking in the dark, before addition of dye (and corresponding negative control).

2.1.11. Confocal microscopy

Cultures were grown as described in 2.1.10 then a culture volume equating to 2.10^8 cells was removed and the volume made up to 5 ml. 2 μM dye (see above) or DMSO (control) was added and the cells were incubated at 28°C degrees for 1 hour with shaking at 170 rpm. Where antimycin was used this was added immediately prior to dye or DMSO. Cells were harvested by 1,780 g centrifugation for 2 minutes, then washed twice in water and twice in PBS before resuspension in 500 μl PBS. Varying volumes were mounted onto slides and visualised with a Leica confocal microscope at 40x and 63x magnification. Fluorophores were excited at 488 nm (dihydrorhodamine 123 and carboxy-H_2DCFDA) and 543 nm (dihydroethidium). Emission was measured at >500 nm for dihydrorhodamine 123 and carboxy-H_2DCFDA and >560 nm for dihydroethidium.

2.2. MOLECULAR BIOLOGY

2.2.1. DNA extraction

Cells were resuspended in 0.5 ml of a solution of 0.1 M Tris pH 8, 50 mM EDTA then approximately 0.25 ml glass beads (425-600 micron, Sigma) was added. 0.5 ml of phenol:chloroform:isoamyl alcohol (25:24:1) pH 8.0 was added and the mixture vortexed for 2 minutes then centrifuged for 5 minutes at 16,000 g. The upper aqueous phase containing the DNA was removed to a new tube and centrifuged again, then this step was repeated to remove all residual phenol. 50 µl of 3 M sodium acetate pH 5.5 and 1 ml of ethanol was added prior to incubation at -20°C for 30 minutes. The precipitated DNA was pelleted by 5 minute centrifugation at 16,000 g, washed with 70% ethanol then allowed to air dry. Finally, DNA was resuspended in 100 µl water and stored at -20°C.

2.2.2. PCR

Primer oligonucleotides were obtained from Sigma Genosys and resuspended to 10 µM. Routinely, PCR reactions were set up in a total volume of 50 µl containing 1X Taq buffer (Promega; 50 mM potassium chloride, 10 mM Tris-HCl pH 9, 1.5 mM magnesium chloride, 0.1% Triton X-100), dNTPs at 200 µM each, forward and reverse primer at 200 nM each, 0.5 µl of template DNA (prepared as in 2.2.1) and 5U of Taq DNA polymerase (Promega), in water. The primers routinely used are listed in Table 2.2 and the primer sites in the *COX2* gene are indicated in Figure 2.4. The standard PCR parameters used were 94°C for 2 minutes, then 35 cycles of 94°C for 1 minute, 35°C for 1 minute and 70°C for 1 minute, then 70°C for 20 minutes. For amplification of *OXA1* and *COX12* annealing was carried out at 45°C.

To confirm amplification a 5 µl aliquot of reaction product was mixed with 3 µl of PCR loading buffer (Sigma) and resolved alongside 5 µl of DNA ladder (Sigma; 50-2000 bp) on agarose gel (1% (w/v) agarose, 0.5 µg/ml ethidium bromide). Bands were visualised under UV light.

2.2.3. Sequencing

PCR products were purified using the Qiagen PCR Purification kit, according to the manufacturer's instructions. Purified product was quantified using a NanoDrop Technologies spectrophotometer and diluted to 4-8 fmoles/µl in water. Sequencing was performed by an in-house service using primers at 4 pmol/µl dilution.

Sequences were analysed with the aid of BioEdit (Ibis Therapeutics), and ClustalW (http://www.ebi.ac.uk/clustalw/) was used for alignments.

2.2.4. Bacterial transformation

SoloPack Gold Ultracompetent cells (Stratagene) were transformed with plasmid according to the manufacturer's protocol. For the site-directed mutagenesis 5 µl of digested PCR product (see 2.2.6) was used to transform XL10-Gold Ultracompetent cells (Stratagene) according to the manufacturer's protocol. To isolate plasmids from transformed bacteria, overnight LBA cultures (5 ml) were pelleted at 16,000 g for 1 minute then processed using the Qiagen Plasmid Miniprep kit, according to the manufacturer's instructions. The success of isolation was determined by resolving 5 µl of plasmid on agarose gel (see 2.2.2).

2.2.5. Yeast transformation (see 2.2.6 for biolistic transformation)

The method used was based on the Gietz and Woods protocol (Gietz and Woods, 2002). Briefly, cells were pelleted, resuspended in 1 ml of 100 mM lithium acetate, incubated at 28°C for 5 minutes, pelleted, then the supernatant removed. On top of the cell pellet was placed 240 µl of 50% (w/v) polyethylene glycol, 36 µl of 1 M lithium acetate, 50 µl of 2 mg/ml ssDNA, 5 µl of plasmid DNA and 20 µl of water. The pellet was vortexed well then incubated at 42°C for 40 minutes. Cells were then harvested and resuspended in 200 µl water for plating onto synthetic drop out medium (MinGlu-Ura).

2.2.6. Site-directed mutagenesis

The plasmids pJM2 (obtained from T. Fox (Mulero and Fox, 1993)) and pBM2, containing the *COX2* gene (from our lab, obtained by PCR cloning using the Stratagene PCR-Script cloning kit), were subjected to PCR-based mutagenesis to introduce the amino acid changes D41N and F45K, with the point mutations GAT → AAT and TTT → AAA, respectively. PCR reactions were set up in a total volume of 50 µl containing 1X reaction buffer (Stratagene; 10 mM potassium chloride, 20 mM Tris-HCl pH 8.8, 10 mM ammonium sulfate, 2 mM magnesium sulfate, 0.1% Triton X-100, 0.1 mg/ml nuclease-free BSA), dNTPs at 200 µM each, forward and reverse primer at 200 nM each, 0.5 µl plasmid, 2.5U Pfu Turbo high fidelity polymerase (Stratagene), in water. The primers used for introduction of D41N were $^{5'}$aaggtattttag**a**attacataataatattat (fwd) and $^{5'}$atatatttattatgtaat**t**ctaaaatacctt (rev). Primers used for introduction of F45K were $^{5'}$gataatattatg**aaa**tatttattagttattttagg (fwd) and $^{5'}$cctaaaataactaataaata**ttt**cataatattatc (rev).

The standard PCR parameters used were 94°C for 3 minutes, then 18 cycles of 94°C for 30 seconds, 35°C for 1 minute, 68°C for 14 minutes, then 68°C for 20 minutes. 1 µl of Dpn1 was added to the reaction mixture, which was then incubated at 37°C for 1 hour to degrade the template at methylated GATC sites. Success of the amplification was checked by resolving a 10 µl aliquot of reaction product on agarose gel (as described in 2.2.2); high molecular weight bands corresponding to plasmid should still be present after Dpn1 treatment. PCR product was used to transform bacterial cells as detailed in 2.2.4. Transformants were subcloned and plasmids were isolated from 12 subclones as described in 2.2.4. The *COX2* gene was fully sequenced to identify clones with only the required mutation. Bacterial transformant containing the correct plasmid was used to prepare more plasmid stock, which was then concentrated with an Amicon Microcon ultrafiltration device (Millipore), according to the manufacturer's instructions, for use in biolistic transformation.

3 µg of plasmids containing the mutated *COX2* and 0.5 µg of YEp352 plasmid containing the *URA3* gene (allowing selection of Ura^+ nuclear transformants) were mixed with 50 µl of 60 $mg.ml^{-1}$ 0.7 µm tungsten particles, and the particles coated with DNA according to the manufacturers protocol (BioRad). Aliquots were used for transformation of the recipient strain W303-1B rho^0, on transformation medium (selective for Ura^+ transformants). Particle bombardments were performed with a Biolistic PDS-1000/He Particle Delivery System (BioRad) at 1,300 psi. Plates were incubated for 4-5 days after which time Ura^+ transformants (which have received the YEp352 plasmid) arose from cells which were amenable to transformation. Screening the colonies arising from only this type of cell increases the likelihood of identifying mitochondrial transformants.

To identify the mitochondrial transformants, more than 1000 Ura^+ colonies were crossed with the tester strain CKL3 containing the complete mitochondrial genome but with the mutations *COX2* A189V and A220V, which cause respiratory deficiency and are far away from the sites of site-directed mutagenesis. On crossing, high frequency homologous recombination will occur if the modified pJM2 or pBM2 plasmid is present, producing diploid wild type (respiratory competent), diploid CKL3 (respiratory deficient) and diploid *COX2* mutant (respiratory competence unknown) (Figure 2.5). If the plasmid is absent no respiratory competent diploids will arise. Therefore selecting for respiratory competence allows identification of colonies transformed with the pJM2 or pBM2 plasmid.

Forty haploids corresponding to respiratory competent diploids were subcloned and approx. 100 subclones of each crossed again with the tester strain. Two of the resulting respiratory competent diploids were subcloned again and the *COX2* gene of 24 subclones sequenced. If sequences are all wild type this indicates that recombination leading to the mitochondrial mutation probably causes respiratory deficiency. In this case, the mutated gene was introduced into a rho^+ genome by crossing the corresponding haploids with the wild type CKWT, then the diploids diluted and plated on YPD (approx. 1000 colonies) then YPG to identify respiratory deficient diploids. These colonies may be either parental rho^- or recombinant mit^-, so spectra were measured (see 2.3.1) to identify mit^- colonies (rho^- has no cytochrome *b* or aa_3).

2.3. BIOCHEMICAL METHODS

2.3.1. Preparation of mitochondrial membranes

400 ml YPDA cultures were grown for 48 hours, pelleted at 1,780 g for 5 mins at 4°C, washed with phosphate buffer (50 mM potassium phosphate, 5 mM EDTA pH 7.5), then resuspended in 5 ml of the same buffer. All subsequent steps were carried out at 4°C. Glass beads (425-600 micron, Sigma) were added and cells broken by shaking at 30 Hz for 10 minutes in a Retsch bead-mill. Debris and beads were removed by centrifugation at 6,000 g for 20 mins, and the supernatant, containing the membranes, was centrifuged at 800,000 g for 1.5 hours. The pelleted membranes were resuspended in 1 ml of phosphate buffer containing 10% (v/v) glycerol using a hand homogeniser and stored in aliquots at -80°C.

Membranes were scanned and concentrations of cytochromes were measured as described below. Protein concentration of mitochondrial membrane preparations was determined with a modified Lowry method (Peterson, 1977) using the Protein Assay kit from Sigma, and a typical concentration was 20-40 mg per ml for wild type. A typical standard curve is shown in Figure 2.6.

2.3.2. Spectroscopy

Optical spectra of both cell suspensions and mitochondrial membranes were measured using a spectrophotometer built in house. Spectra were generated by scanning in the visible range with a single beam instrument built in-house. Cells were grown on YPDA plates for 48 hours then resuspended in 5% Ficoll pH 7.5 to around 100 mg cells per ml, or grown in YPGal liquid medium for up to 26 hours, pelleted and resuspended (as described in 2.1.8). For cell suspensions, a baseline was recorded using diluted milk, samples were reduced with sodium dithionite as required, and cytochrome contents were estimated from the dithionite reduced spectra. Alternatively, mitochondrial membranes were diluted up to 5 times in phosphate buffer and dithionite reduced minus ferricyanide oxidised spectra were used for cytochrome estimation. These were generated by first scanning oxidised sample, then adding dithionite to reduce the sample, and scanning again, then reduced minus oxidised spectra were computer-generated. Cytochrome contents were measured using the following formulae: cytochrome oxidase at 604-(594-614)/2 nm using an extinction coefficient of 14 mM^{-1} cm^{-1}; cytochrome *b* at 562-575 nm, ε=28.5 mM^{-1} cm^{-1}; cytochromes $c + c_1$ at 550-542 nm, ε=18 mM^{-1} cm^{-1} (van Gelder and Slater, 1962; Meunier and Rich, 1998).

2.3.3. Oxygen consumption/cytochrome oxidase activity

Oxygen consumption was measured with an oxygen electrode at 25°C. To measure cytochrome oxidase activity, mitochondrial membrane samples were diluted to 10 nM cytochrome oxidase in phosphate buffer containing 10 mM ascorbate and 50 μM TMPD. Consumption of oxygen by cytochrome oxidase was initiated by the addition of varying concentrations of cytochrome *c* and rates of oxygen consumption were measured as a function of cytochrome *c* concentration, and used to produce Lineweaver-Burk (1/V vs 1/[S]) plots from which K_m (cyt *c*) and V_m values were derived.

To measure oxygen consumption of whole cells, cells were harvested from liquid culture, resuspended to around 100 mg cells per ml in water, then added to YPGal containing 2 μM FCCP at a concentration of approximately 10 mg cells per ml. Respiratory activity is presented relative to the amount of cells or the amount of cytochrome oxidase present. Since the respiratory chain is the major site of oxygen consumption in yeast cells it was not necessary to add a respiratory chain inhibitor to measure the proportion of oxygen consumption due to cytochrome oxidase.

2.3.4. Nitric oxide detection

Cells were grown to an A_{600nm} of around 2, as described in 2.1.8, then a 1 ml aliquot was removed and placed in the chamber of an NO electrode (World Precision Instruments). The culture was stirred and was open to air. 3 mM DETA NONOate was added and the concentration of NO in the culture was measured over 24 hours.

2.4. WESTERN BLOTTING

2.4.1. Denaturing electrophoresis

2.4.1.1. Gel preparation

Denaturing SDS gels were prepared using the BioRad Mini-PROTEAN 3 electrophoresis system. 10% to 20% resolving gels were prepared as described in Table 2.3A. Urea was added to gel solutions since this assists in ensuring complete denaturation, resulting in sharper bands, and prevents aggregation. Gels were overlayed with 100 µl of water whilst setting to produce a uniform upper edge. After approx. 30 minutes gels were overlaid with stacking gel (Table 2.3A). 10-well combs were encased in stacking gel and removed once the gel had set.

2.4.1.2. Sample preparation

Analyses were performed on crude mitochondrial membranes, prepared as described in 2.3.1. Samples were diluted in dissociation buffer (Table 2.4) to give 2 µg/µl protein, as determined by Lowry assay (see 2.3.1), then incubated at 37°C for 30 minutes. Incubation at a low temperature for a long period prevents formation of aggregates. To assess quantities to load, an initial gel was loaded with 10 µg protein of each sample, blotted and probed with an antibody against porin. Signal intensities were quantified and a graph of intensity against wild type dilution plotted (Figure 2.7). Mutant signal intensities were compared to the graph allowing the percentage error in the Lowry assay to be determined. Sample preparations were subsequently adjusted by the dilution factors calculated, so that between 10 and 20 µg of total protein, as determined by Lowry assay, was loaded in each lane to represent 100% sample. Unused dissociated sample was stored at -80°C for up to one month.

2.4.1.3. Gel running and processing

For estimation of molecular mass, 5 µl of Precision Protein Standards (10-250 kDa, BioRad) was loaded. Protein was electrophoresed in running buffer (Table 2.4) at 100V, then 200V after samples had stacked, for around 1 hour depending on the percentage of acrylamide. After electrophoresis, protein was electroblotted onto PVDF membrane (Amersham Biosciences, pore size 0.45 µm) with the BioRad Mini Trans-Blot cell, as follows. The gel was placed on Whatman 3MM paper resting on a sponge piece. PVDF was placed on top and the sandwich was completed with further pieces of filter paper and sponge. The sandwich was placed inside the blotting cassette and protein transfer

was for 1 hour at 100V, in Towbin's buffer (Table 2.4). After blotting the membranes were allowed to dry completely overnight and were rewetted in methanol prior to immunodetection.

2.4.2. Blue native electrophoresis

2.4.2.1. Gel preparation

Native gels were prepared using Hoeffer gradient gel pouring apparatus connected to a Watson Marlow 4 way peristaltic pump. As with denaturing gels, the BioRad Mini-PROTEAN 3 electrophoresis system was used. Gels were prepared as described in Table 2.3B. To pour 8-16% gradient gels the 16% solution was allowed to flow about 10 cm towards the pump before the 8% solution was released from its chamber. After pouring the gels were overlaid with 100 µl of water-saturated butanol and allowed to set for around 30 minutes. After the stacking gel had been set around 10-well combs, gels were wrapped in clingfilm and stored at 4°C overnight for use within 24 hours. Gels were assembled with cathode buffer filling the inner chamber and anode buffer in the outer chamber, and wells were rinsed thoroughly with cathode buffer immediately prior to loading of samples (Table 2.4).

2.4.2.2. Sample preparation

Sample volume equating to one lane (approx. 60 µg protein) was mixed with 15 µl of solubilising solution containing 1 µg/ml leupeptin, 1 µg/ml pepstatin and 1 µM PMSF. 5 µl of 10% (w/v) laurylmaltoside was added to solubilise and the mixture was left on ice for 15 mins, then centrifuged for 20 minutes at 16,000 g. The supernatant was removed and 2.5 µl of loading buffer was added to it. Samples were prepared in multiples and either loaded directly onto 8-16% gradient gel or stored at -80°C for up to one month. Since large volumes were loaded, any empty lanes were loaded with an appropriate volume of loading mix (solubilising solution, 10% laurylmaltoside and loading buffer, 6:2:1) to avoid distortion during electrophoresis.

2.4.2.3. Gel running and processing

5 µl of HMW Native Markers 66-669 kDa (Amersham Biosciences) were used for estimation of molecular mass. Gels were run at 100 V until the dye front had migrated well into the stacking gel, then run at 8 mA fixed current (for 2 gels; 4 mA for 1 gel) for the remainder of the electrophoresis. Gels were electroblotted as described in 2.4.1.3.

Prior to immunodetection the Serva blue G was removed from membranes by short incubation in three changes of methanol.

2.4.3. Two-dimensional native/denaturing electrophoresis

Samples were prepared and separated on 8-16% polyacrylamide blue native gels as described above. Single sample lanes were excised and protein was dissociated by incubation in 1% β-mercaptoethanol, 1% SDS for 15 minutes, before washing twice for 10 minutes in 50 mM Tris-HCl pH 6.8, 1% SDS with gentle shaking, to remove β-mercaptoethanol, an inhibitor of polymerisation. The gel slice was placed horizontally between two glass plates, in the region where stacking gel would usually be poured. Resolving gel (20% polyacrylamide for detection of Cox8p, 15% polyacrylamide for detection of other subunits, Table 2.3A) was poured below it (Figure 2.8).

When resolving gel had set the native gel slice was encased in stacking gel, with a marker well created adjacent to it. A common problem in two-dimensional electrophoresis is streaking, in which bands merge and individual complexes are difficult to identify. The use of agarose as stacking gel has been suggested to overcome this problem and to be a more efficient method than using an acrylamide stacking gel, since proteins in the gel slice can be dissociated by adding agents to the agarose gel rather than in separate steps as described above, which allow substantial leaching of protein.(Brookes et al., 2002). I initially attempted to use a stacking gel of 0.7% (w/v) agarose, 0.5% (w/v) SDS and 15 mM β-mercaptoethanol, heated to 60°C and poured around the untreated gel slice. However, I did not find that this method prevented streaking, and instead obtained better results by dissociating the protein as initially described and using a 3% polyacrylamide stacking gel (Table 2.3A). The stacking gel had a tendency to reduce in volume prior to setting, so was topped up at regular intervals during the setting period. Also, residual β-mercaptoethanol occasionally impaired the setting process; this was remedied where necessary by placing the gel at 40°C for up to 30 minutes. Once set, electrophoresis apparatus was assembled and run as described in 2.4.1.3.

2.4.4. Immunodetection

Non-specific protein binding sites on the PVDF membranes were blocked by 1 hour incubation with gentle shaking in 10% (w/v) non-fat milk (Marvel) in PBS then the membranes were incubated with subunit-specific primary antibodies for 2 hours. After three 10 minute washes in PBST, membranes were incubated with HRP-conjugated secondary antibody for 1 hour. Where tertiary PAP (peroxidase anti-peroxidase)

antibody was used a further two 10 minute washes were performed and membranes were incubated with PAP antibody for 1 hour. Finally three 10 minute washes in PBST were carried out, plus a final 5 minute wash in PBS. Western Lightning Chemiluminescence Reagent Plus (Perkin Elmer) in conjunction with Hyperfilm ECL film (Amersham Biosciences) was used to visualise proteins.

Subunit-specific mouse monoclonal antibodies against the yeast cytochrome oxidase subunits Cox1p, Cox2p, Cox3p, Cox4p, Cox5p, Cox6p, Cox6ap and Cox8p, and porin were used, in addition to a polyclonal rabbit antiserum recognising the co-migrating subunits Cox7p and Cox7ap (Table 2.5). All these antibodies were generated in the laboratory of Prof. R. A. Capaldi (Institute of Molecular Biology, Eugene, OR) and are described in (Taanman and Capaldi, 1993); most of them are commercially available (Molecular Probes Inc., Eugene, OR). The polyclonal antiserum against cytochrome c_1 was generously supplied by Prof. B. L. Trumpower (Dartmouth Medical School, Hanover, NH, USA). HRP-conjugated anti-mouse secondary antibodies were obtained from BioRad, DakoCytomation and Jackson ImmunoResearch. Anti-rabbit secondary antibody was obtained from BioRad. Monoclonal mouse PAP tertiary antibody was obtained from DakoCytomation.

Some of the antibodies used gave rise to more than one strong band on blots from denaturing gels. To determine which of the bands corresponded to the cytochrome oxidase subunit the antibody was raised against, and to confirm the identity of single bands detected, the band pattern in wild type mitochondrial membrane preparations was compared to that of purified yeast cytochrome oxidase (kindly provided by J.-W. Taanman, isolated according to (Taanman and Capaldi, 1992)). Here, purified yeast cytochrome oxidase was mixed with an equivalent volume of 2x dissociation buffer then 4 times the volume of 1x dissociation buffer, before incubation at 37°C for 30 minutes, and 10 µl was loaded in each lane of a denaturing gel adjacent to wild type mitochondrial membrane preparation and molecular weight marker (Figure 2.9).

2.4.5. *In situ* cytochrome oxidase activity assay

An 8-16% native gel was prepared, loaded and run as described above, then a single gel strip was removed and destained with anode buffer for 10 minutes before being rinsed in water. The strip was incubated in staining solution (50 mM sodium phosphate buffer pH 7.4 containing 0.5 $mg.ml^{-1}$ diaminobenzidine, 1 $mg.ml^{-1}$ cytochrome *c* and 2 $\mu g.ml^{-1}$ catalase) at 37°C with gentle shaking overnight, then the reaction was stopped and

excess strain removed by replacing staining solution with 10% acetic acid and 40% methanol for several hours. The assay detects a colour change.

2.4.6. Electroelution

Blots derived from native gels exhibited a Cox1p-containing band running at approximately the level that Cox1p itself should be found. To determine the identity of the band I needed to resolve isolated Cox1p adjacent to the membrane sample on native gel. Purified yeast cytochrome oxidase was available but could not be simply dissociated then run on native gel as the SDS would diffuse and/or be drawn into the rest of the gel.

Prior to isolation of Cox1p from purified yeast cytochrome oxidase, the preparation was checked for purity. 20 µl was dissociated in 4 µl of a solution of 5x dissociation buffer at 37°C for 30 minutes. The entire dissociated sample was loaded on 15% denaturing gel adjacent to molecular weight markers, and the gel was run as described in 2.4.1.3. The gel was subsequently stained with Coomassie blue for 5 hours, then destained in water for approx. 24 hours to allow optimal band visualisation. A large band of the correct molecular weight for Cox1p was present, and contaminating bands (i.e. not components of cytochrome oxidase) were absent.

Another denaturing gel (10%, to allow good separation of bands) was prepared, with one large well of 67 mm width. Purified yeast cytochrome oxidase was prepared as above, but sample volume was scaled up by a factor of 14 and 250 µl sample was loaded into the well, adjacent to a molecular weight marker. The gel was run as normal, then the two edges were removed and stained as described above to determine the migration of Cox1p, while the central portion of the gel was wrapped in clingfilm and stored at -20°C. After staining, the edges were aligned and the Cox1p band excised from the central portion of the gel. This was placed in an electroelution tank with running buffer, glycerol and a few grains of bromophenol blue. Protein was eluted at 4 mA until all the dye had transferred to the positive terminus, and elution was allowed to continue for 30 minutes subsequent to this to ensure completion. Running buffer was carefully removed by pipette, then the protein solution was collected and the chamber rinsed twice with running buffer to collect residual protein.

To determine the correct quantity of purified Cox1p to load onto native gel a dilution series of purified yeast Cox1p was loaded onto 10% denaturing gel. One lane was excised and Coomassie-stained to confirm the absence of contaminating bands. The

remainder of the gel was blotted and probed with Cox1p antiserum, and 16x dilution of purified yeast Cox1p was judged the best signal.

2.5. GENE EXPRESSION

2.5.1. Microarray

The microarray strategy employed was as follows. mRNA was isolated from yeast cells (2.5.1.1 and 2.5.1.2) then reverse transcribed using a modified oligo(dT) primer with a T7 RNA polymerase promoter sequence in the first strand cDNA synthesis (2.5.1.3). Second strand cDNA synthesis was RNase H-mediated. Double-stranded cDNA was purified and used as template for *in vitro* transcription from T7 RNA polymerase promoters (in the presence of T7 RNA polymerase and a biotinylated nucleotide analog/ribonucleotide mix) for antisense cRNA amplification and biotin-labelling (2.5.1.4). Single stranded biotinlyated cRNA targets were fragmented (to 200 nucleotides or less) and hybridised to Affymetrix GeneChip expression arrays (2.5.1.5). The arrays contain several 25-mer DNA probes for each gene present on the chip (ORFs from the Yeast Genome Database (www.yeastgenome.org)), each present in hundreds of copies. Use of cRNA rather than cDNA targets results in improved target binding avidity, and better sensitivity as the melting temperature of RNA-DNA hybrids is higher; also the target population does not self-hybridise. Arrays are scanned to determine fluorescence of each probe, relating to the number of copies of labeled cRNA present.

2.5.1.1. RNA extraction

YPGal starter cultures which had been allowed to grow for 18 hours were used to inoculate 30 ml cultures of YPGal media to A_{600nm} = 0.08 in 250 ml Erlenmeyer flasks. After 8 hours incubation at 28°C with shaking at 170 rpm the cultures reached an A_{600nm} of around 0.5 (mid exponential phase), and 0.1, 1 or 3 mM DETA NONOate was added. Cultures were incubated for a further 10, 30, 60 or 120 minutes, then cells were harvested at 1,780 g for 4 minutes at 4°C. Control cells were not treated with NO donor but were harvested immediately. Pellets were washed with ice-cold water than flash frozen in liquid nitrogen and stored at -80°C. Cells were resuspended in 1.2 ml of AE buffer (50 mM sodium acetate, 10 mM EDTA pH 5.3) and RNA was extracted by a hot phenol method (Schmitt et al., 1990). Briefly, 1/10 volumes of 10% SDS and 1 volume of phenol were added and incubated at 65°C for 10 minutes, then tubes were rapidly chilled in a dry ice/ethanol bath before centrifugation at 16,000 g for 2 minutes. The aqueous phase was removed and an equal volume of phenol:chloroform:isoamyl alcohol (25:24:1) pH 6.6 added before centrifugation for 5 minutes at 16,000 g. The aqueous

phase was again removed, and 1/10 volumes of 3 M sodium acetate pH 5.3 and 2.5 volumes of 100% ethanol were added before precipitation at 65°C for 30 minutes. RNA was pelleted by 5 minute centrifugation at 16,000 g then washed in 80% ethanol and resuspended in 150 µl water. All steps involving RNA were carried out using RNase-free reagents and equipment. Absorbance at 260 and 280 nm of samples diluted in 10 mM Tris pH 7.5 was used for quantification and purity control (A_{260}/A_{280} ratio of 1.9-2.1 for pure RNA), and RNA integrity was assessed using the Agilent Technologies 2100 Bioanalyser. An example trace is shown in Figure 2.10.

2.5.1.2. mRNA isolation

Poly(A) mRNA was enriched in a single round using the Qiagen Oligotex mRNA kit, using the Batch protocol, according to the manufacturer's instructions. After analysis of mRNA quality with the Agilent Technologies 2100 Bioanalyser (Figure 2.10) and mRNA quantitation, mRNA was concentrated by precipitation as described in the Affymetrix GeneChip Expression Analysis Technical Manual (www.affymetrix.com). After air-drying the pellet was resuspended in 10 µl (for 0.2-1 µg mRNA) or 9 µl (for 1-2 µg mRNA) water and samples were stored at -20°C.

2.5.1.3. Synthesis of double-stranded cDNA

Double-stranded DNA was made from mRNA using the SuperScript II Reverse Transcriptase kit (Invitrogen) and a modified oligo(dT) primer with a T7 RNA polymerase promoter sequence (GeneChip), according to instructions given in the Affymetrix GeneChip Expression Analysis Technical Manual (www.affymetrix.com), but with incubations at 42°C taking place at 37°C instead. cDNA cleanup protocol was also as described in this manual.

2.5.1.4. In vitro *transcription*

In vitro transcription was performed, using the entire template, with T7 RNA polymerase and biotinylated ribonucleotides (BioArray High Yield RNA Transcript Labelling Kit, Enzo Diagnostics), according to the manufacturer's instructions. The biotinylated cRNA obtained was purified with the Affymetrix GeneChip Sample Cleanup Module, absorbance of samples at 260 and 280 nm was used for quantification and purity control, and RNA integrity was assessed using the Agilent Technologies 2100 Bioanalyser. The cRNA was fragmented using the GeneChip Sample Cleanup Module.

2.5.1.5. Hybridisation and initial analyses

Hybridisation and initial analyses were performed by an in-house service. 15 µg of fragmented cRNA was hybridized onto Affymetrix GeneChip Yeast Genome S98 arrays in a rotating hybridization oven at 45°C for 16 hours. This was followed by staining and washing on a GeneChip Fluidics Station 450, and scanning on a GeneChip Scanner 3000 with autoloader. Arrays were stained with streptavidin phycoerythrin and fluorescence was amplified by addition of biotinylated goat anti-streptavidin antibody (plus goat IgG), then restaining. Acquisition and quantification of array images as well as primary data analysis was performed using the GeneChip Operating System (GCOS) software version 1.2 from Affymetrix.

2.5.1.6. Data analysis

Microsoft Excel was used for further statistical analyses. Triplicate samples (independent cell preparations) were prepared for untreated control cells (W303-1B Δ*yhb1*), and duplicates for cells treated for 10, 60 or 120 minutes with 3 mM NO donor. For all other tests, one sample was prepared. Transcript number in treated cells was compared to transcript number in untreated cells, and fold change values (or average fold change values) at each time point were calculated relative to the gene expression (or average gene expression) in the respective strain without treatment. The transcript level was assumed significantly increased or decreased for a specific gene when its Z-score was higher than 1.96 compared with all the genes designated as present by the Affymetrix software. Replicates were compared with the average value for the time point and changes in expression of over 2-fold were noted. Categorisation of genes was performed using the Yeast Genome Database (www.yeastgenome.org). The genomic expression profiles were created using the software Cluster and TreeView (rana.lbl.gov/EisenSoftware.htm).

2.5.2. Quantitative real-time PCR

(RT)q-PCR allows quantitation of starting DNA because it measures PCR amplification during the exponential phase of a PCR reaction rather than using the less precise end-point measurement, which displays significant variability even with the same starting concentration of DNA. Total RNA extraction, mRNA purification and cDNA synthesis were carried out as described above. Where the effect of the heme precursor deuteroporphyrin IX (dpIX) was assessed, this was added to cells immediately prior to the NO donor. Quantitative PCR was performed using the ABI Prism 7700 Sequence

Detection System (Applied Biosystems). The primers used are listed in Table 2.6, and were designed using Primer Express version 2.0 software within the guidelines given by the supplier (Applied Biosystems). Reactions were carried out in a 25 µl mixture containing 24 pg/µl of cDNA, 1x SYBR Green PCR Master Mix (Applied Biosystems; containing SYBR green I dye, AmpliTaq Gold DNA polymerase, dNTPs with dUTP and optimised buffer components) and 300 nM of each primer. PCR parameters used were 50°C for 2 minutes, 95°C for 10 minutes (for optimal DNA polymerase activation), then 40 cycles of 90°C for 15 seconds, 60°C for 1 minute. Accumulation of PCR products was detected by monitoring the increase in fluorescence of the reporter dye SYBR green I.

The mean of the background fluorescence for all the tested wells measured between cycles 3 and 10 was recorded and used to set the baseline with Sequence Detector software version 1.7a. (Applied Biosystems). The threshold for amplification was set by drawing a line intersecting the exponential phase of the logarithmic amplification curves (fluorescence *vs* cycle number); a threshold of 0.04 was used in all assays. The cycle number at which the threshold line intersects the linear curve for each sample was used to determine the threshold cycle (Ct) value. Dissociation curves (change in fluorescence with time *vs* temperature) were run to confirm absence of contaminating products. All subsequent data analysis was performed in Excel. (RT)q-PCR products generated using primers amplifying the *ACT1* (actin) gene were used as endogenous control since *ACT1* expression did not alter between treatments in the microarray analysis. The quantity of mRNA of each gene of interest in each sample, indicated by the threshold cycle (Ct), was therefore normalised by the level of *ACT1* RNA: $Ct_{\text{gene of interest}} - Ct_{ACT1} = \Delta Ct$. Relative quantification of mRNA between treated and untreated cells was performed using the comparative Ct ($\Delta\Delta Ct$) method ($\Delta Ct_{\text{sample}} - \Delta Ct_{\text{reference}} = \Delta\Delta Ct$; relative quantity = $2^{-\Delta\Delta Ct}$), as suggested by the manufacturer (Applied Biosystems). This method is valid if amplification efficiencies of the target genes and the endogenous control gene are equivalent, as demonstrated in Figure 2.11 (Livak and Schmittgen, 2001). Each sample was assayed at least in triplicate, and each assay contained duplicates or triplicates. The exception was dpIX treatment, where only one assay (in duplicate) was performed.

2.5.3. β-Galactosidase assay

STRE-*LacZ* or *CYC1*^{P}-*LacZ* cells were grown in YPGal media as described for the microarray analysis. For the assays involving *CTT1* overexpression YPG was used, and

for the *SOD1* overexpression plasmid MinGal-Trp was used for induction and MinGlu-Trp for control. Where anaerobic cultures were required these were placed in closed tubes with no shaking. After 8 hours of growth cells were treated with 3 mM NO donor or 8 μM myxothiazol and incubated for 10, 60 or 120 minutes. Where deuteroporphyrin IX (dpIX) was required this was also added after 8 hours, and immediately prior to NO donor. Cells were harvested at 1,780 g at 4°C for 4 minutes (this step was not required for anaerobic cultures). The pellet was washed with ice-cold water then resuspended in ice-cold Z buffer (60 mM disodium hydrogen phosphate, 40 mM sodium dihydrogen phosphate, 10 mM potassium chloride, 1 mM magnesium sulfate, 50 mM β-mercaptoethanol, pH 7), then the A_{600nm} was measured. One drop of 0.1% SDS and two drops of chloroform were added, and the mix was equilibrated at 28°C for 15 minutes. *o*-Nitrophenyl-β-D-galactopyranoside was added to a final concentration of 0.64 $mg.ml^{-1}$ and, after incubation at 28°C for 15 minutes, the mix was centrifuged at 2,330 g at room temperature for 2 minutes, and the A_{420nm} and A_{550nm} of the supernatant were measured. β-galactosidase activity was expressed in Miller units, calculated as follows: $1000 \times [A_{420nm} - (1.75 \times A_{550nm})] / (15 \text{ min} \times \text{culture volume used in the assay in ml} \times A_{600nm})$. Experiments were repeated five times for the STRE-*LacZ* Δ*yhb1* assay, three times for the overexpression assays, and twice for the $CYC1^{P}$-*LacZ* assays.

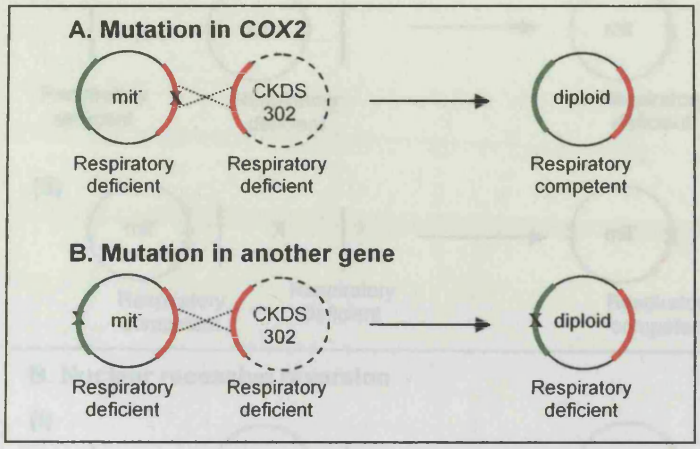

Figure 2.1. Mapping of mutations to the *COX2* gene.

Mitochondrial DNA is shown. CKDS 302 is a respiratory deficient rho⁻ strain and its mtDNA contains only the *COX2* gene, illustrated in red. The respiratory deficient mit⁻ strain contains mutation in the *COX2* gene (red) or another gene (green). Mutations are indicated by a cross. If the mit⁻ mutation is present in *COX2* homologous recombination will allow formation of respiratory competent diploids (**A**), while if present in another gene respiratory deficient diploids will be formed (**B**).

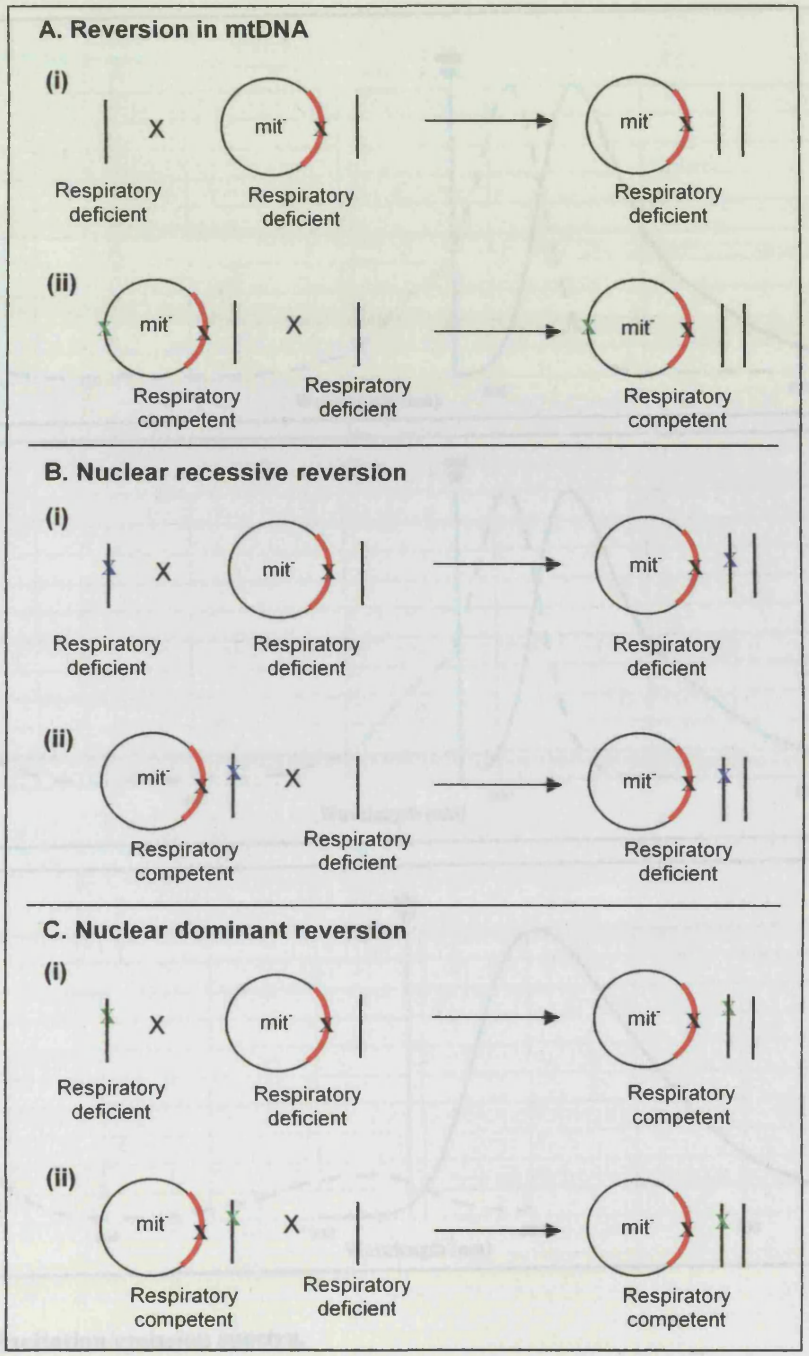

Figure 2.2. Mapping of reversions.

Two crosses were performed for each revertant to determine the genetic origin of the suppressor mutation. (i) Rho^0 revertants, in which mtDNA had been removed, were crossed with the corresponding original mutants. (ii) The revertants were crossed with a wild type rho^0 strain. Nuclear DNA is indicated by a solid line and mtDNA by a circle. The *COX2* gene is illustrated in red, and mutations by a cross (black = primary mutation causing respiratory deficiency; green = secondary mutation restoring respiratory competence).

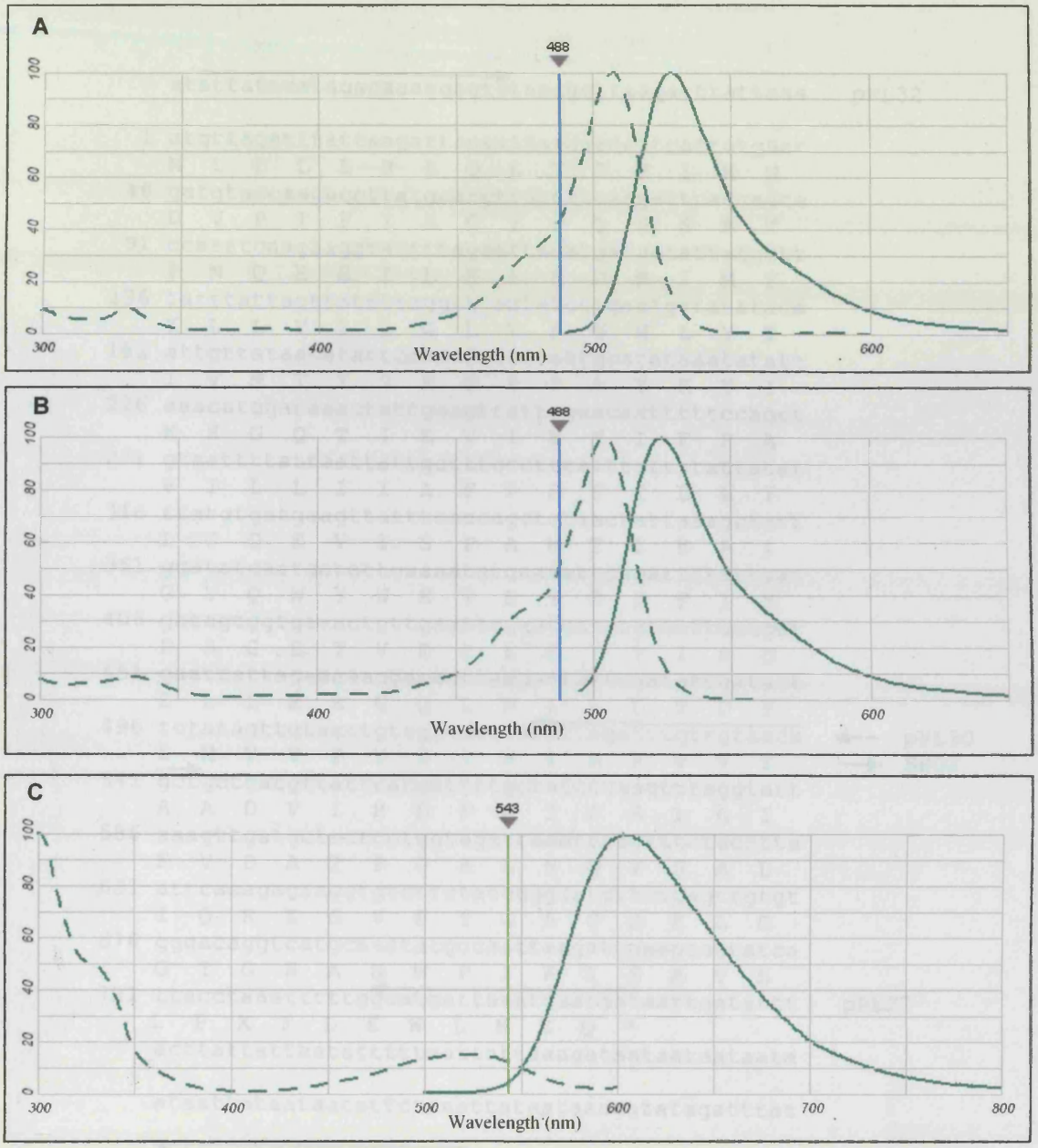

Figure 2.3. Excitation/emission spectra.

Spectra for the active fluorophores from **A.** dihydrorhodamine 123 (rhodamine 123) **B.** carboxy-H_2DCFDA (2',7'-dichlorofluorescein) and **C.** dihydroethidium (ethidium), obtained from Invitrogen (http://probes.invitrogen.com/resources/spectraviewer/). Excitation lasers used in confocal imaging are indicated.

Figure 2.4. Annealing sites of primers used in the amplification of the *S. cerevisiae COX2* gene.

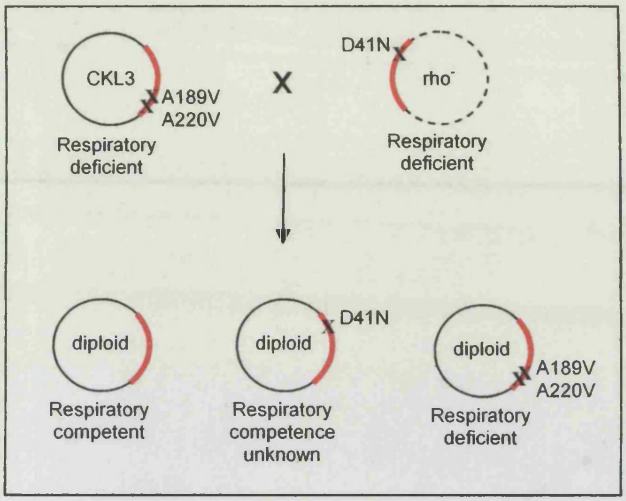

Figure 2.5. Screening of transformants.

The Ura$^+$ transformants were screened for the presence of the *COX2* plasmid. Recombination can occur between the mutated *COX2* gene in the tester strain CKL3 and the *COX2* plasmid if present in the Ura$^+$ transformant. Some of the rho$^+$ progeny will be respiratory competent. However, if no plasmid is present respiratory competent colonies will not arise. The *COX2* gene is shown in red, and mutations are indicated with a cross.

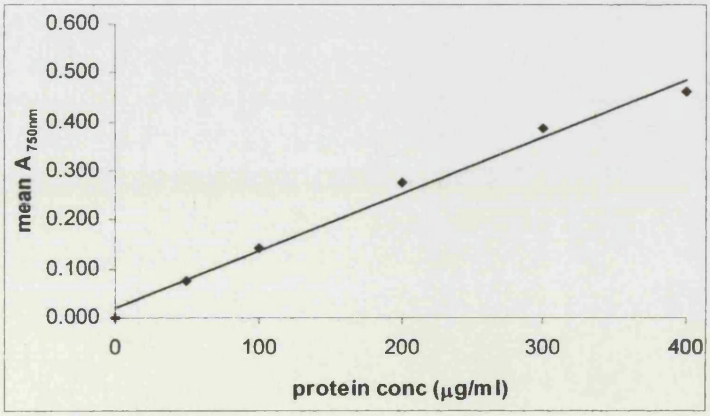

Figure 2.6. Typical standard curve used to determine protein concentration of membrane preparations.

The standard curve was generated using BSA standards ranging from 50 to 400 µg/ml, processed in duplicate.

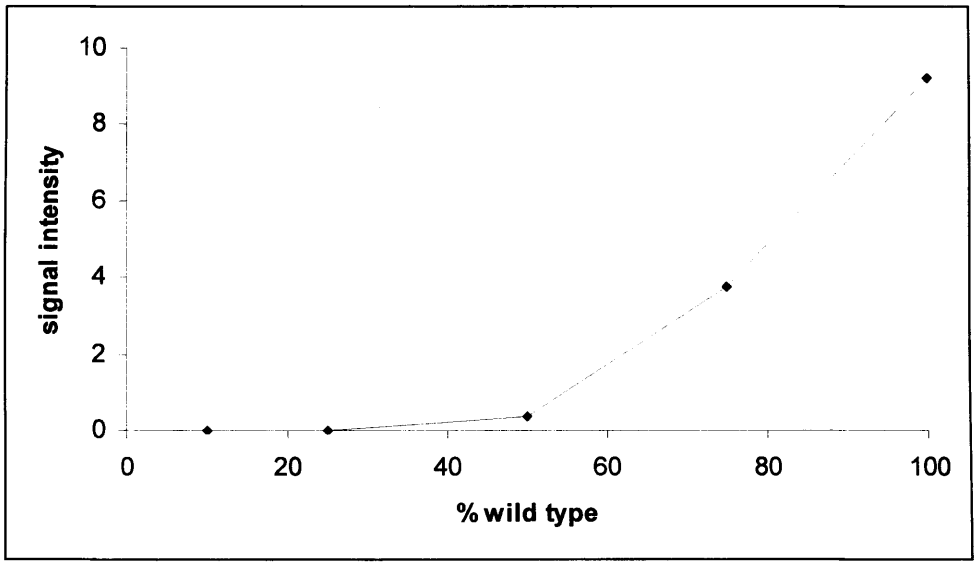

Figure 2.7. Porin signal intensities of a wild type dilution series.

Anti-porin antiserum was used to probe a blot of mutant samples loaded at 10 μg per well according to results of Lowry assay, and a wild type dilution series. Signal intensity was measured. All mutant signal intensities fell between 5 and 15 and the chart was used to calculate dilution factors for subsequent sample preparation.

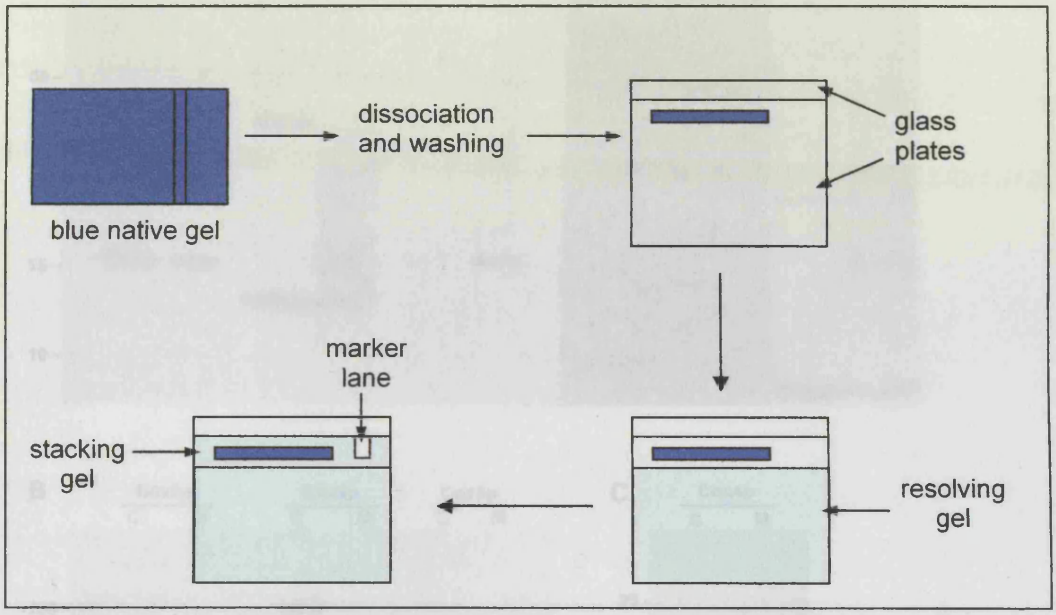

Figure 2.8. Assembly of two-dimensional native/denaturing gels.

A single gel slice was excised from a blue native gel, treated to dissociate protein, then placed horizontally between two glass plates. Resolving gel was poured beneath the slice before its enclosure in stacking gel.

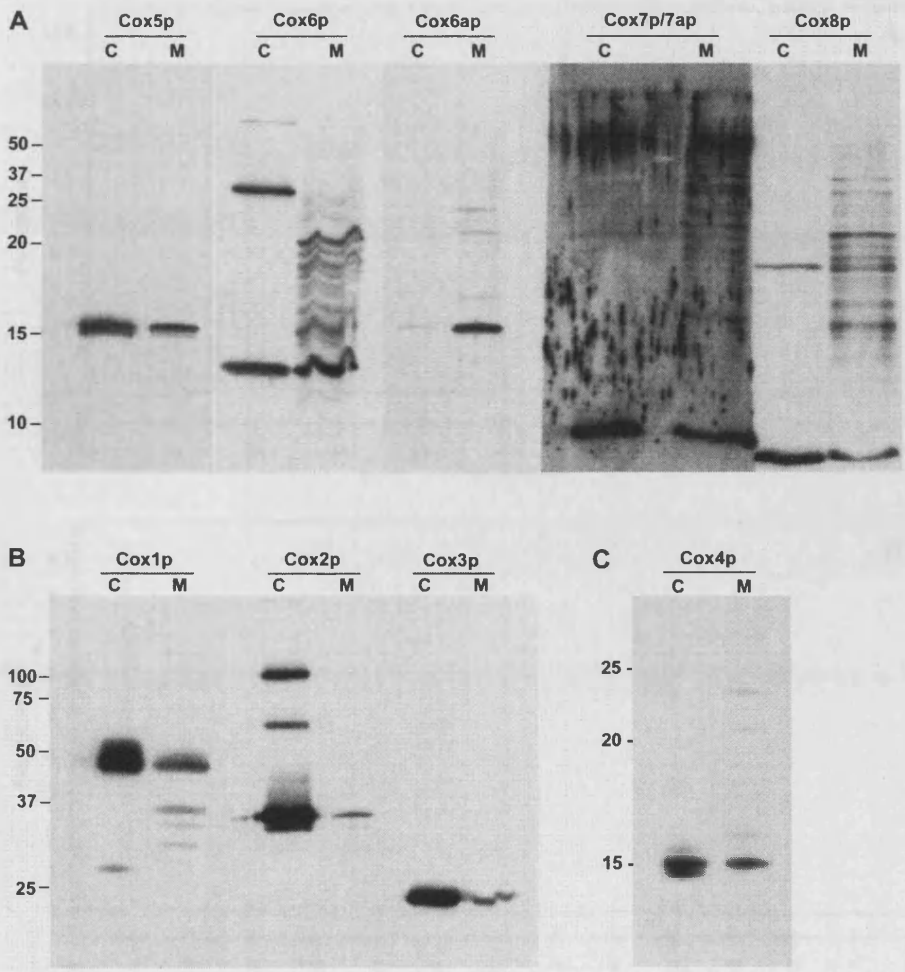

Figure 2.9. Determining band identity in denaturing gels.

Samples of purified yeast cytochrome oxidase (C) were electrophoresed adjacent to wild type mitochondrial membrane samples (M) and molecular weight markers. **A.** Subunits resolved on 15% gel. **B.** Subunits resolved on 10% gel. **C.** Subunits resolved on 12.5% gel.

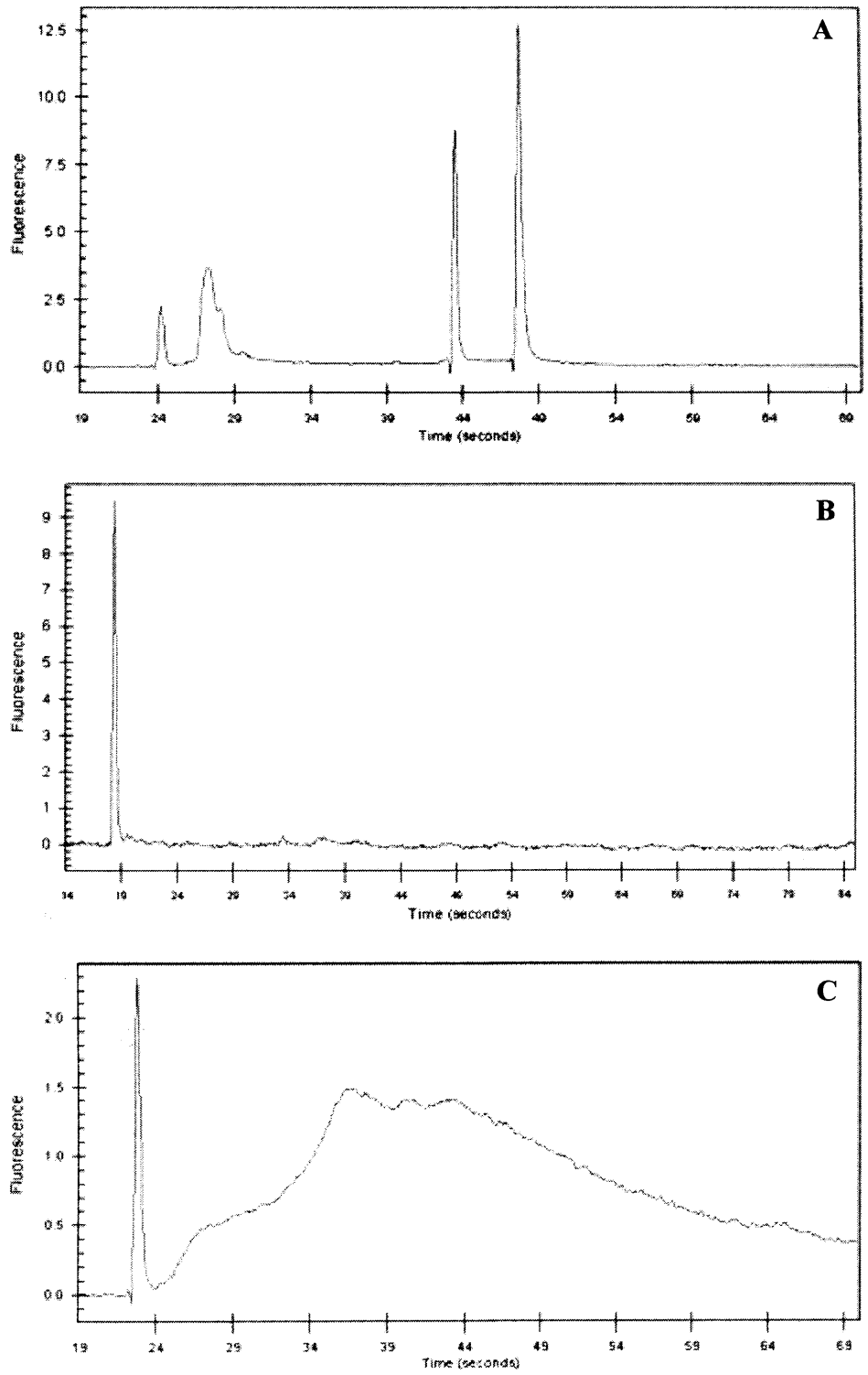

Figure 2.10. RNA integrity assessed by the Agilent Technologies 2100 Bioanalyser.
Example traces of total RNA (**A**), mRNA (**B**) and cRNA (**C**) are shown.

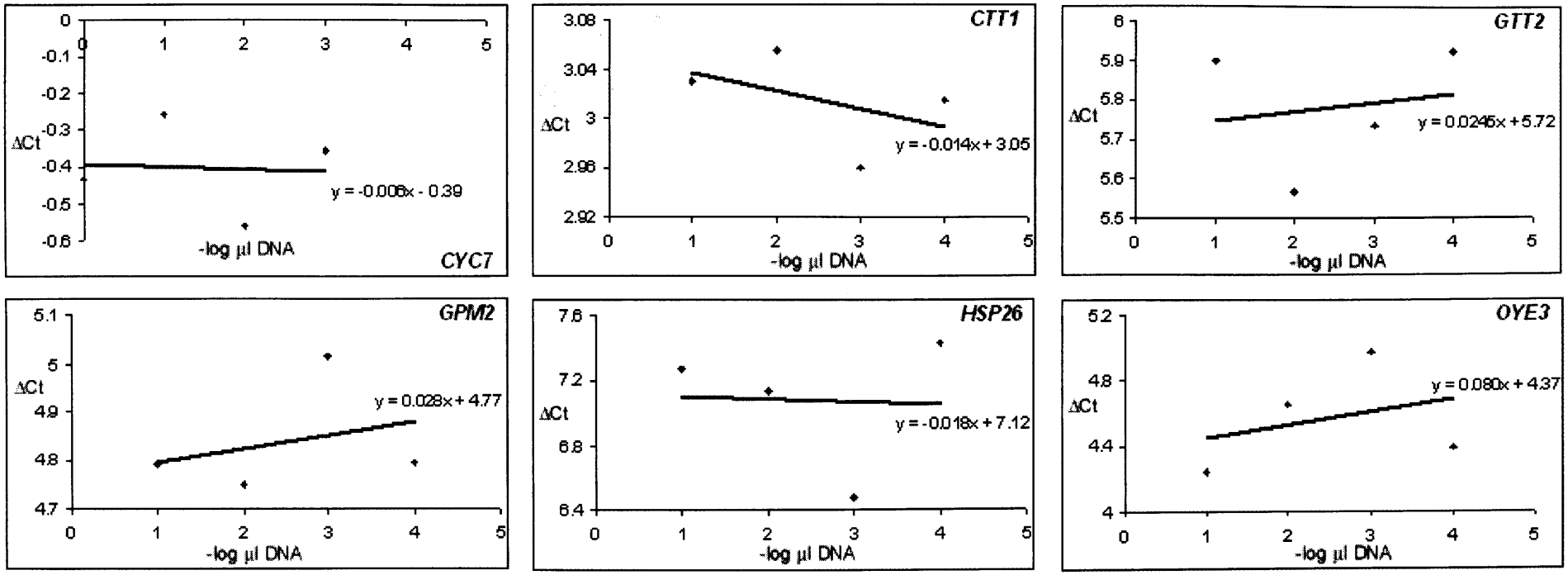

Figure 2.11. Relative efficiency plots to assess suitability of primer pairs for analysis using the comparative Ct (ΔΔCt) method.

Standard curves of ΔCt (using *ACT1* as endogenous control) for serial dilutions of DNA were drawn and linear regression lines calculated. Amplification efficiencies of target gene and endogenous control gene are judged equivalent, and therefore suitable for analysis using the comparative Ct (ΔΔCt) method, if gradient is <0.1 (Applied Biosystems).

Table 2.1. Yeast strains used in this study.

Strain	Genotype	Source
Strains used in Chapter 3		
BM 1/1-16	*MATα ade1 op1 [ery1 oli1 intronless]*	Our lab
JC8/56 rho^0	*MATa leu1 kar1-1 [rho^0]* [a]	Our lab
W303-1B rho^0	*MATα ura3-1 his3$^-$ leu2-3 ade2-1 trp1-1 [rho^0]*	Our lab
CKDS 302	*MATa leu1 kar1-1 [rho$^-$ COX2]* [b]	Our lab
W303-1B/pBM2	*MATα ura3-1 his3$^-$ leu2-3 ade2-1 trp1-1 [rho$^-$ COX2]*	Our lab
CK L3	*MATa leu1 kar1-1 [COX2 A189V A220V]* [c]	Our lab
CK WT	*MATa leu1 kar1-1*	Our lab
Strains used in Chapters 4 and 5		
BY4741	*MATa his3Δ1 leu2Δ0 met15Δ0 ura3Δ0*	Euroscarf
BY4741 Δ*yhb1*	*MATa his3Δ1 leu2Δ0 met15Δ0 ura3Δ0 yhb1::kanMX4*	Euroscarf
BY4741 Δ*yhb1* rho^0	*MATa his3Δ1 leu2Δ0 met15Δ0 ura3Δ0 yhb1::kanMX4 [rho^0]*	Euroscarf[d]
FY1679 Δ*yhb1*	*MATα his3-Δ200 ura3-52 leu2-Δ1 trp1-Δ63 yhb1::LEU2*	Our lab[e]
FY1679 Δ*yhb1* Δ*sod1*	*MATα his3-Δ200 ura3-52 leu2-Δ1 trp1-Δ63 sod1::kanMX4 yhb1::LEU2*	Our lab[e]
FY1679 Δ*yhb1* Δ*sod2*	*MATa his3-Δ200 ura3-52 leu2-Δ1 trp1-Δ63 sod2::kanMX4 yhb1::URA3*	Our lab[e]
FY1679 Δ*yhb1* Δ*ccp1*	*MATα his3-Δ200 ura3-52 leu2-Δ1 trp1-Δ63 ccp1::kanMX4 yhb1::LEU2*	Our lab[e]
FY1679 Δ*yhb1* Δ*ctt1*	*MATa his3-Δ200 ura3-52 leu2-Δ1 trp1-Δ63 ctt1::kanMX4 yhb1::URA3*	Our lab[e]
BY4741 Δ*nde1*	*MATa his3Δ1 leu2Δ0 met15Δ0 ura3Δ0 nde1::kanMX4*	Euroscarf
BY4741 Δ*nde2*	*MATa his3Δ1 leu2Δ0 met15Δ0 ura3Δ0 nde2::kanMX4*	Euroscarf
BY4741 Δ*ndi1*	*MATa his3Δ1 leu2Δ0 met15Δ0 ura3Δ0 ndi1::kanMX4*	Euroscarf
BY4741 Δ*sdh1*	*MATa his3Δ1 leu2Δ0 met15Δ0 ura3Δ0 sdh1::kanMX4*	Euroscarf
BY4741 Δ*sdh2*	*MATa his3Δ1 leu2Δ0 met15Δ0 ura3Δ0 sdh2::kanMX4*	Euroscarf
BY4741 Δ*cat5*	*MATa his3Δ1 leu2Δ0 met15Δ0 ura3Δ0 cat5::kanMX4*	Euroscarf
CW L65	*MATα ura3-1 his3$^-$ leu2-3 ade2-1 trp1-1 [CYTB T46K]*	Our lab
CW ΔF	*MATα ura3-1 his3$^-$ leu2-3 ade2-1 trp1-1 [COX3 ΔF94-F98]*	Our lab
W303-1B	*MATα ade2-1 his3$^-$ leu2-3,112 trp1-1 ura3-1 URA3-STRE-LacZ*	P. Piper
W303-1B Δ*yhb1*	*MAT α ade2-1 his3$^-$ leu2-3,112 trp1-1 ura3-1 URA3-STRE-LacZ yhb1::LEU2*	Our lab[e]
W303 Δ*yhb1* Δ*msn2/4*	*MAT α ade2-1 his3$^-$ leu2-3,112 trp1-1 ura3-1 URA3 STRE-LacZ yhb1::LEU2 msn2::HIS3 msn4::TRP1*	Our lab[e]
W303 Δ*yhb1* Δ*yap1*	*MAT α ade2-1 his3$^-$ leu2-3,112 trp1-1 ura3-1 yhb1::LEU2 yap1::TRP1*	Our lab[e]
W303 Δ*yhb1* rho^0	*MAT α ade2-1 his3$^-$ leu2-3,112 trp1-1 ura3-1 URA3-STRE-LacZ yhb1::LEU2 [rho^0]*	Our lab[d,e]
SOD1/CSS1 overexpression	W303-1B Δ*yhb1* transformed with a centromeric plasmid containing the *SOD1* and *CCS1* genes under the control of the *ADH2* promoter	Our lab[f]
CTT1 overexpression	W303-1B Δ*yhb1* transformed with an insertional vector pRS403 containing the *CTT1* gene under the control of the *ADH2* promoter	Our lab[f]
BY4741 Δ*yhb1* *CYC1^P-LacZ*	BY4741 Δ*yhb1* transformed with a multicopy vector containing the LacZ gene under the control of the *CYC1* promoter	Our lab[g]

[a] rho^0 mutation is the complete loss of mtDNA

[b] rho$^-$ mutation involves a large deletion of mtDNA, with amplification of the remaining sequence

[c] mit$^-$ mutation is a point mutation in a gene encoded by the mtDNA

[d] rho^0 produced by ethidium bromide treatment

[e] Δ*yhb1* strains obtained through PCR-mediated gene deletion from the strains given by P. Piper

[f] plasmid from P. Piper (Harris et al, 2003; Harris et al., 2005)

[g] plasmid from B. Guiard (Guarente and Ptashne, 1981; Ramil et al, 2000)

Table 2.2. Primers used for amplification of mitochondrial and nuclear genes.

Gene	Forward primer(s)		Reverse primer(s)	
COX1	PL50	atg gta caa aga tga tta tat tca ac	PL51	tta aga ttg tac agc tgg tgt att aaa tg
COX2	PL32	att ata aat aga caa aag agt c	PL27	att gtt cat tta atc att c
	SH02	tat tag att cgt tgt aac agc t	SH01	ata taa ggt gat tga ata gaa t
			PL30	agc tgt tac aac gaa tct aat a
COX3	BM09	tag aaa gaa gta gac atc aac	BM10	cct cat caa taa aat agt acg
COX12	Cox6bF	tca caa ata gga aca agc ac	Cox6bR	agg cta agt gca cat tact a
COX9	Cox7aF	gat att tgc aaa cta cta ac	Cox7aR	ata aga ata taa tgc gaa aa
OXA1	OXA1F	atg ttc aaa ctc acc tct cg	OXA1R	aat gaa gtt tga ttt gtg aa
SCO1	scof	ggg aaa cag aaa aaa cag caa	scor	aca aga acg ggt tat agc gtt

Table 2.3. Gel recipes.

A. Denaturing gel. **B.** Native gradient gel. Prior to addition of ammonium persulfate and TEMED gel solutions were filtered through 0.2 µm Millipore filters to remove dust. Ammonium persulfate and TEMED were added immediately prior to gel pouring. Quantities given are sufficient to pour 2 denaturing gels or 4 native gradient gels. 40% acrylamide was obtained from BioRad. Acrylamide-bis solution contained 48% acrylamide, 1.5% bisacrylamide (49.5%T 3%C) and was cleaned with Amberlite MB-1 resin overnight prior to first use. 3x gel buffer contained 1.5 M 6-aminocaproic acid and 150 mM bistris pH 7.

A	Stacking gel	Resolving gel			
	3%	10%	12.5%	15%	20%
3.75 M Tris pH 8.6	-	920 µl	920 µl	920 µl	920 µl
0.5 M Tris pH 6.8	500 µl	-	-	-	-
40% Acrylamide (37:5:1)	450 µl	2.5 ml	3.1 ml	3.7 ml	4.9 ml
20% (w/v) SDS	25 µl	46 µl	46 µl	46 µl	46 µl
Urea	1.8 g	3.25 g	3.25 g	3.25 g	3.25 g
ddH_2O	3.25 ml	4.1 ml	3.5 ml	2.9 ml	1.7 ml
10% (w/v) Ammonium persulfate	25 µl	44 µl	44 µl	44 µl	44 µl
TEMED	3 µl	6 µl	6 µl	6 µl	6 µl

B	Stacking gel	Resolving gel	
	4%	8%	16%
Acrylamide-bis	0.5 ml	1.98 ml	3.25 ml
3x Gel buffer	2.0 ml	3.96 ml	3.3 ml
Glycerol	-	-	1.98 g
ddH_2O	3.5 ml	5.86 ml	1.7 ml
10% (w/v) Ammonium persulfate	50 µl	70 µl	35 µl
TEMED	5 µl	7 µl	3.5 µl

Table 2.4. Solutions used in western blotting.

Dissociation buffer	50 mM Tris-HCl pH 6.8 12% (w/v) glycerol 4% (w/v) SDS 2% (v/v) β-mercaptoethanol 0.01% (w/v) bromophenol blue
Running buffer	25 mM Tris 192 mM glycine 1% (w/v) SDS
Towbin's buffer	25 mM Tris-base 192 mM glycine 20% (v/v) methanol
Cathode buffer	50 mM tricine 15 mM bistris 0.02% (w/v) Serva blue G pH 7.0
Anode buffer	50 mM bistris pH 7.0
Solubilising solution	1 M 6-aminocaproic acid 50 mM bistris
Loading buffer	1 M 6-aminocaproic acid 5% (w/v) Serva blue G
PBS	0.01 M phosphate buffered saline pH 7.4 0.138 M sodium chloride 00027 M potassium chloride
PBST	0.01 M phosphate buffered saline pH 7.4 0.138 M sodium chloride 00027 M potassium chloride 0.3% (v/v) Tween 20

Table 2.5. Antibodies.

All the antibodies are monoclonal and raised in the mouse, except the polyclonal rabbit antiserum against Cox7p/Cox7ap and the polyclonal antiserum against cyt c_1. [a]Antibodies were diluted in PBST. [b]The exposure time required for two-dimensional blots was slightly longer than that stated. [c]Detection of Cox8p on two-dimensional blots additionally required the tertiary antibody PAP at 1:600 dilution.

Antigen	Primary antibody					Secondary antibody	
				Exposure time			
	Name	Dilution[a]	SDS gel (%)	SDS[b]	Native	Name	Dilution [a]
Cox1p	111D8-B7	1:400	10	2 min	15s	BioRad	1:4000
Cox2p	4B12-A5	1:4000	12.5	1 min	4 min	Dako	1:2000
Cox3p	DA5	1:4000	12.5	30s	15s	Dako	1:2000
Cox4p	1A12-A12	1:20,000	12.5	30s	2 min	BioRad	1:4000
Cox5p	13E2-F5	1:1000	15	30s	4 min	Dako	1:2000
Cox6p	11D11-H6	1:250	15	15s	30s	BioRad	1:4000
Cox6ap	7E3	1:2000SDS; 1:400 native	15	1 min	4 min	Dako	1:2000
Cox7p/7ap		1:500	15	10s	15s	BioRad rabbit	1:4000
Cox8p[c]	20B5	1:10	15	30s	1 min	BioRad	1:4000
Cyt c_1		1:6000	12.5	30s	-	BioRad	1:4000
Porin	16G9-E6	1:20,000	12.5	10s	-	BioRad	1:4000

Table 2.6. Primers used for amplification in (RT)q-PCR

Gene	Forward primer	Reverse primer
CYC7	tcc gag tac ttg acg aac cca	tcc ttt tcc ttc ttc aac ccg
CTT1	aga aag agt tcc gga gcg tg	tct ggt atg gag cgg cgt at
GPM2	gca agc aca cca tcc aat gt	gct tag cgt caa tcc aac cac
HSP26	tgt tcc cat ctg gtt tcg gt	acc agg aac cac gac ttt caa
GTT2	tgc ctt ggc tga gaa gaa ca	ctt ctt gtg ctc tcc ctt cca
OYE3	tgg tca gcg tgc tca aag ac	cga cct gct cat cag acc aa
ACT1	ttg gat tcc ggt gat ggt gt	cga ttc tca aaa tgg cgt ga

Chapter 3

SUBCOMPLEXES OF CYTOCHROME OXIDASE

3.1. INTRODUCTION

3.1.1. Temporal pathway of cytochrome oxidase assembly

While much is known about the array of assembly factors involved in the various stages of cytochrome oxidase assembly, relatively little is known about the order in which the subunits of cytochrome oxidase join together to form the fully assembled enzyme. Assembly of mammalian cytochrome oxidase is believed to occur in an ordered sequence. Work by Nijtmans *et al.* (Nijtmans et al., 1998) and Williams *et al.* (Williams et al., 2004) has outlined the temporal pathway of assembly in human cells. In yeast, there is only one previous report of cytochrome oxidase subassemblies (Church et al., 2005), but no subassembly containing any of the core subunits Cox1p, Cox2p or Cox3p has yet been identified.

3.1.2. Aims

The aim of this work was to gain more information on the assembly of cytochrome oxidase, in particular the order of subunit assembly, using yeast as a model system. I used a random mutagenesis approach to generate respiratory deficient mutants of the *COX2* gene, encoding the core subunit Cox2p. In addition to mutations which completely abolished cytochrome oxidase assembly I was able to identify mutants in which assembly was impaired but not completely abolished. I characterised these mutants and their subunit composition and identified novel cytochrome oxidase subcomplexes.

3.2. RESULTS

3.2.1. Selection and initial characterisation of the mutant strains

The strain BM1/1-16 had been previously subjected to moderate mutagenesis by overnight incubation with 8 mM of the mtDNA mutagen manganese chloride (Meunier et al., 1993). 29 mutants had previously been mapped to the *COX2* gene, by crossing of the haploid with a *COX2* rho$^-$ strain (large deletion of mtDNA, amplification of the remaining sequence) (see 2.1.5). I confirmed the mapping using the same method and identified the mutations by sequencing (see 2.2.3). The majority were stop or frameshift changes, but nine strains with one or more missense mutation in the *COX2* coding region were identified, as in the example shown in Figure 3.1. The mutants chosen for further study were transferred via cytoduction (see 2.1.6) into the W303-1B nuclear background to facilitate genetic analysis, since the BM1/1-16 strain contains the *op1* mutation in the major ADP/ATP carrier of the IMM, causing respiratory deficiency.

All the mutations were located in the C-terminal globular domain of Cox2p (Figure 3.2A). Three mutants harboured double mutations (Table 3.1). To determine which mutation caused the respiratory defect, I isolated revertants from the double mutants and identified any reversion mutations in *COX2* (Table 3.1) (see 2.1.7). Revertants are colonies which have acquired secondary mutations restoring competency to grow on respiratory medium. For two of the double mutants (Y146N + M232K and D162N + V169M), analysis of the reversions showed that only one of the double mutations was causing the respiratory defect (M232K or D162N). The second mutation by itself (Y146N or V169M) had little effect on the respiratory growth competence. The third double mutant, C221W + L245W, failed to yield reversion in *COX2*, suggesting that both mutations conferred respiratory deficient phenotype. For the remaining mutants, except G156E and R159K, reversion to wild type at each mutated site was identified, confirming that the mutation was responsible for the respiratory deficiency. The exception was P170H which failed to yield any mitochondrial reversions.

3.2.2. Analysis of cytochrome oxidase assembly by optical spectroscopy

The effect of the mutations on cytochrome oxidase content of whole cells was analysed. In yeast, unassembled subunits, especially the core subunits Cox1p, Cox2p and Cox3p, are rapidly degraded by AAA proteases (Nakai et al., 1995; Pearce and Sherman, 1995; Guelin et al., 1996). So in the absence of assembly the optical spectrum of the yeast cells alters, and the characteristic absorbance peak at 603 nm due to the heme aa_3 of

Cox1p is absent (Tzagoloff and Dieckmann, 1990; Brown et al., 1993; Meunier and Rich, 1998). Heme aa_3 signal was absent in seven of the nine mutants: Y146N + M232K, D162N + V169M, P170H, R213M, G219E, C221W + L245W and G226E (see 2.3.2). Therefore in these seven strains, mutation in *COX2* abolished assembly of cytochrome oxidase. The optical spectrum of the double mutant C221W + L245W is shown in Figure 3.3.

However, two *COX2* mutants, strain G156E (not shown) and R159K (Figure 3.3), showed a significant amount of cytochrome oxidase present in optical spectra although they were unable to grow on respiratory medium. For both mutants the amplitude of heme aa_3 signal was reduced to around 50% of the wild type level. In addition, the absorbance peak was shifted from 603 nm to 599 nm, indicating a perturbation of the heme environment. The phenotype of these two mutants was unusual since normally an assembly defect in yeast leads to a complete absence of aa_3 signal. The mutants were therefore investigated in further detail to establish what interesting information on cytochrome oxidase assembly they could provide.

3.2.3. Activity of cytochrome oxidase in the mutants R159K and G156E

Cytochrome oxidase activity was determined to see whether the mutations impaired enzyme function as well as its assembly. Varying concentrations of reduced cytochrome *c* were supplied to mitochondrial membranes and oxygen consumption was measured (see 2.3.3). Data obtained were used to construct Lineweaver-Burke plots from which V_m and K_m values were determined (Figure 3.4). Both mutants showed a decreased V_m and increased K_m for cytochrome *c* (Table 3.2). The increase in K_m is suggestive of a weakened interaction between the reaction partners, probably arising from a distortion of the binding site for cytochrome *c* on the surface of Cox2p.

3.2.4. Reversion mutations in the copper-binding domain of Cox2p

To understand the molecular nature of the effects of the mutations, I generated revertants which partially compensated the defects caused. As described in 2.1.7., the revertants were classified according to their mitochondrial or nuclear origin. For R159K, 9 nuclear and 6 mitochondrial revertants were identified and candidate genes were amplified and sequenced: *COX1*, *COX2* and *COX3* for mitochondrial reversions; *COX12* (coding for Cox6bp) and *COX9* (coding for Cox7ap) due to the close proximity of Cox6bp and Cox7ap to Cox2p, *OXA1* and *SCO1* for nuclear reversions. No reversions were identified in genes other than *COX2*. For both G156E and R159K, revertants were obtained with secondary mutations at residues D187 or S222 of Cox2p

(Table 3.1 and Figure 3.2B). These residues are located 25-30Å from the primary sites and are in the copper-binding domain. This might suggest that the Cu_A site is perturbed in the mutants and that the reversions restore its correct structure. The revertants R159K + D187N and R159K + S222Y were further studied. These reversion mutations restored respiratory growth yield to around half of wild type level and increased cytochrome oxidase content, though this was still lower than in the wild type (Table 3.2). Furthermore, cytochrome oxidase activity was closer to wild type; V_m was restored to wild type value and K_m (cyt *c*) was lower than in the mutant (Table 3.2).

3.2.5. No evidence for a role of Oxa1p or Sco1p in the suppression of the defect caused by R159K.

The assembly chaperone Oxa1p is required for export of the N-terminal region of cytochrome oxidase, and may also play a role in C-terminal export (Hell et al., 1997). It is possible that the mutation R159K might impair the interaction of Oxa1p with Cox2p, preventing insertion of Cox2p into the membrane. In this case, overexpression of *OXA1* might re-establish the membrane insertion of Cox1p. The R159K mutant was transformed with an *OXA1* overexpression plasmid (obtained from A. Tzagoloff, see 2.2.5). Growth of the resultant strain on respiratory medium did not differ from that of the parent R159K mutant, indicating that Oxa1p could not suppress the defect in the R159K mutant. However, the level of Oxa1p overexpression was not determined, therefore it cannot be ruled out that a concentration-dependent effect may be in operation and a higher level of Oxa1p expression may have elicited a growth difference. However, since the R159K mutation is located in the C-terminal region of Cox2p it seems unlikely that it would have an effect on Oxa1p function. Moreover, no nuclear revertants of the R159K strain were found to contain *OXA1* mutation.

More likely is that the mutation could interfere with the action of the copper chaperone Sco1p, which binds to the C-terminus of Cox2p to deliver copper to the Cu_A site (Lode et al., 2000; Glerum et al., 1996b). Since R159K is located in the C-terminal region a distortion here could easily be imagined to impair the interaction between Cox2p and Sco1p. Addition of copper to the growth medium might be expected to relieve problems caused by impaired interaction of Sco1p, since supplementation of copper to human cells deficient in the homologous SCO2 rescued their cytochrome oxidase deficiency (Jaksch et al., 2001; Salviati et al., 2002). To test this, growth medium (both respiratory and non-respiratory) was supplemented with copper (50-200 μM copper chloride) and growth of the R159K strain was monitored. No differences in

growth were observed in the presence of copper, which was not deleterious to wild type growth. Again, no nuclear revertants of R159K could be assigned to the *SCO1* gene.

3.2.6. Steady state subunit levels

The mutants G159E and R159K, and the revertants R159K + D187N and R159K + S222Y, were further investigated through western blotting analysis to determine the nature of the assembly failure (see 2.4.1 and 2.4.4). Mitochondrial membrane samples of the mutants and revertants were compared to serial dilutions of wild type membranes on denaturing gels to allow estimation of steady state enzyme content as a percentage of wild type (Figure 3.5). The mutant C221W + L245W, lacking heme aa_3 signal, was also used for comparison. Antibodies raised against several cytochrome oxidase subunits were used and an antibody against porin was employed as a control for equal loading of mitochondrial protein; the concentration of porin should not be affected by alteration in cytochrome oxidase level (Taanman et al., 1997).

Characteristic of the phenotype of yeast mutants with impaired assembly of cytochrome oxidase, C221W + L245W lacked most of the cytochrome oxidase subunits assessed, with the exception of Cox4p. Cox4p is a matrix-side extrinsic polypeptide which has been shown to be present in soluble form when assembly is disrupted, suggesting that it is relatively stable compared to other subunits (Glerum and Tzagoloff, 1997). Furthermore, in a yeast Cox3p point mutant the level of Cox4p was decreased to a lesser extent than most other subunits (Meunier and Taanman, 2002). The levels of each subunit compared to wild type could reflect partly the intrinsic stability of the subunit, and partly the content of that subunit in the misassembled complex. A small amount of Cox7p and/or Cox7ap (the antiserum detects both co-migrating subunits) could also be seen, since the signal was very strong; however, there was still less than 10% of this subunit present. Surprisingly, the mutant contained a small amount of Cox2p, though less than 10% of wild-type level.

In the mutants G156E and R159K the levels of the core subunits Cox1p and Cox3p were around 25% of the wild type level, the amount of Cox5p was between 25 and 50%, and the levels of Cox6p, Cox6ap, Cox7p and/or 7ap, and Cox8p were around 50% of wild type level. The amount of Cox4p was higher, at 75-100% of wild type level. Cox2p level in these mutants was exceptionally low, at less than 10% of wild type levels, clearly lower than the level of the other core subunits.

In the revertants R159K + D187N and R159K + S222Y the level of each subunit increased compared to the mutant, but was still lower than in the wild type, with the

exception of Cox4p which remained at high levels. Unexpectedly, the amount of Cox2p, while greater than in the mutant, remained at less than 10% of wild type levels. It might have been expected that Cox2p content in the revertants should have been similar to the levels of the other subunits, since enzyme activity was closer to the wild type rate (Table 3.2).

The level of cytochrome c_1 in the strains was also assessed (Figure 3.5). This was found to be at 50% of wild type level or higher in all mutants and revertants except C221W + L245W, containing less than 10% of wild type level. Since the amount of bc_1 complex seems affected by a decrease in cytochrome oxidase content, this may provide further evidence for the existence of a supracomplex containing both bc_1 and cytochrome oxidase (Schagger and Pfeiffer, 2000; Cruciat et al., 2000).

3.2.7. Subcomplexes of cytochrome oxidase

To investigate further the specific decrease in Cox2p, I performed western analysis of blue native gels, which allow isolation of membrane protein complexes (Schagger and von Jagow, 1991) (see 2.4.2 and 2.4.4). The neutral detergent laurylmaltoside extracts proteins from the membrane, and Serva blue G dye confers a negative charge on the proteins. Mitochondrial membrane samples were subjected to native electrophoresis and the same antibodies as above were used to detect any complexes or subcomplexes (resulting from assembly or degradation) of cytochrome oxidase (Figure 3.6).

3.2.7.1. Major subcomplexes present in the wild type

In the control wild type two bands were detected by most of the antibodies tested. The upper band, denoted *a*, was assumed to correspond to the monomeric holoenzyme complex due to it being the highest molecular weight band (migrating close to the 232 kDa marker). In-gel staining for cytochrome oxidase activity showed that both bands *a* and *b* represented active forms of the enzyme (Figure 3.7). The lower band *b* seems likely to be a partially degraded complex lacking Cox6ap, since it was not detected on probing with the antibody raised against this subunit. The relative proportions of bands *a* and *b* were not equal, and complex *b* tended to be present at higher levels. This suggests that Cox6ap is only loosely associated with the enzyme complex and that subtle variations in sample treatment prior to loading on the gel can alter the extent of Cox6ap attachment. Several lines of evidence in the literature corroborate this. Solubilisation of yeast cytochrome oxidase with Triton X-100 removes Cox6ap and Cox6bp (Taanman and Capaldi, 1992). Furthermore, chromatography (FPLC) of the purified bovine enzyme demonstrated that in various buffers containing 1 mM

laurylmaltoside and 400 mM salt the enzyme eluted from columns as two major peaks; a fully assembled 13-subunit form and an 11-subunit form lacking COX6A and COX6B (Liu et al., 1995). This suggests that loss of the homologous yeast subunits Cox6ap and Cox6bp (which I did not probe for) may occur during sample preparation for blue native gel electrophoresis. Finally, in humans, an assembly complex has been identified in which COX6A and COX7A are absent (Nijtmans et al., 1998; Williams et al., 2004).

Surprisingly, although Cox4p was present in band *b* it did not appear to be present in band *a* (Figure 3.6). This may be because the Cox4p epitope is not accessible to the anti-Cox4p antibody in the fully assembled monomer due to shielding by Cox6ap. In the bovine enzyme the N-terminus of COX5B, equivalent to yeast Cox4p, is in close vicinity to the N-terminal region of COX6A, the yeast Cox6ap counterpart (Figure 3.8). The N-terminal sequence of yeast Cox4p is extended by 25 amino acids compared to COX5B, while the region N-terminal of the membrane-spanning α-helix in Cox6ap is 35 amino acids compared with 12 in COX6A. The folding of these extended N-terminal sequences is unknown. However, it is quite possible that the extended N-terminal region of Cox4p is shielded by the extended Cox6ap N-terminal region. The location of the Cox4p epitope recognised by antibody has not been determined, but if it lies in the N-terminal region it may be inaccessible to antibody and thus not identified in the monomeric holoenzyme. It is well recognised that antibodies raised against polypeptides are not necessarily useful in detection of the natively folded protein.

3.2.7.2. Subcomplex c *identified only in the mutants and revertants*

No complexes were detected in the mutant C221W + L245W, as would be expected on consideration of the denaturing western blot (Figure 3.5). The mutants G156E and R159K contained less than 10% of wild type levels of complexes *a* and *b*. However, a faster migrating band *c*, not detectable in the wild type, was present. Band *c* was not detected by antibodies raised against Cox2p, Cox4p, Cox6ap, Cox7p and Cox7ap, or Cox8p, suggesting that these subunits were absent from subcomplex *c*. The band comprised Cox1p, Cox3p, Cox5p and Cox6p. The revertants contained band *c* in addition to bands *a* and *b*. Revertant R159K + S222Y had about 25-50% the level of bands *a* and *b* as the wild type, while revertant R159K + D187N appeared to have less than 10% of bands *a* and *b* compared to wild type. There is some difficulty in estimating this since the relative contributions of *a* and *b* to the assembled enzyme population vary with each sample, possibly due to subtle variations in sample treatment, as suggested earlier. However, both revertants seem to contain more of complexes *a* and *b* than the

parent mutant R159K. The quantity of band *c* in the revertants seems to be similar or slightly less than that in the mutants. Therefore the secondary mutations increase the content of fully assembled enzyme.

3.2.7.3. Other subcomplexes

Four other subcomplexes were identified in all wild type, mutant (except C221W + L245W) and revertant samples tested. Three faster migrating bands were identified separately by antibodies raised against Cox7p and Cox7ap (band *d*), Cox8p (band *e*) and Cox1p (band *f*). Additionally, a slower migrating band was identified by the Cox8p antibody (band *z*). Band *d* appeared less prominent in the mutants, while bands *e* and *f* were more prominent in the mutants and revertants than in the wild type.

As mentioned earlier, antibodies which work well in the detection of denatured proteins do not necessarily work well in detecting native protein. Non-specific binding may occur (Williams et al., 2004). To determine whether the detection of the bands *d*, *e*, *f* and *z* was specific and whether they did indeed represent subcomplexes containing Cox7p and/or Cox7ap, Cox8p and Cox1p (and also to confirm specificity of bands *a*, *b* and *c*), I ran two-dimensional gels, native in the first dimension then denaturing in the second dimension (Figure 3.9) (see 2.4.3 and 2.4.4). This allowed the components of each of the bands identified in the one-dimensional native blots to be determined. I used the revertant R159K + S222Y in this analysis since this strain contained high levels of all the bands detected.

When the two-dimensional blots were probed with antiserum against Cox3p, three spots corresponding to bands *a*, *b* and *c* were clearly visible at the correct migration for Cox3p, indicating that the detection was specific (Figure 3.9A). To determine whether band *f* was specific, two-dimensional blots were probed with the antibody raised against Cox1p. Four spots corresponding to bands *a*, *b*, *c* and *f* were detected, all migrating at the same rate on the second dimension denaturing gel, and the remainder of the blot was clear (Figure 3.9A). This suggests that bands *a*, *b*, *c* and *f* all contained Cox1p and that the bands were not non-specific signals. Band *f* runs on native gel between 66 and 140 kDa, therefore it was possible that it might in fact represent unassembled Cox1p. To determine whether this was the case, Cox1p was isolated from purified yeast cytochrome oxidase (see 2.4.6) and electrophoresed alongside the R159K + S222Y revertant on native gel (Figure 3.10). Band *f* co-migrated with purified Cox1p, therefore represents unassembled Cox1p. However, it is not clear why band *f* should be absent in the mutant C221W + L245W.

It can be noted that both Cox1p and Cox3p appear to migrate on two-dimensional gels at a faster rate than might be expected due to their molecular weight. This is most likely due to the difficulty in assembling these gels and ensuring that molecular weight marker is aligned correctly with the native gel slice. Lower molecular weight complexes tend to be more difficult to resolve on second dimension denaturing gel. On probing two-dimensional blots with Cox7p/Cox7ap antiserum, spots corresponding to bands *a* and *b* could be distinguished, migrating at the correct molecular weight for Cox7p/Cox7ap. However, the signal then extended in a streak, making identification of further spots problematic. The absence of any other spots corresponding to the migration of band *d*, though, suggests that band *d* is indeed a subcomplex containing Cox7p and/or Cox7ap. Band *d* was not identified by any of the other cytochrome oxidase antibodies tested, suggesting that it represents a subcomplex containing Cox7p and/or Cox7ap along with other unidentified proteins.

The final two bands, *e* and *z*, were both identified only by the Cox8p antibody. On probing the two-dimensional blot, two spots were present corresponding to bands *a* and *b* (Figure 3.9B). No spot corresponding to band *c* was visible, in accordance with the absence of band *c* in the one-dimensional native blot (Figure 3.6). Spots corresponding to bands *e* and *z* were also identifiable, but these did not co-migrate with spots *a* and *b*, indicating that the recognition of bands *e* and *z* by the Cox8p antibody was due to non-specific binding. In addition to the spots, several smears were present on the blot. Detection of spots with the Cox8p antibody required use of a tertiary antibody since the signal was weak. Incubation of a companion blot with only secondary and tertiary antibody demonstrated that the smears were due to non-specific reaction of the tertiary antibody used in conjunction with Cox8p antiserum.

3.2.8. Membrane insertion of the Cox2p N-terminal domain by Oxa1p

In parallel to this work I attempted to investigate possible involvement of the assembly factor Oxa1p in translocation of charged residues across the IMM. Oxa1p has been suggested to facilitate translocation of negatively charged regions, including the Cox2p N-terminal transmembrane domain, while more neutral regions position themselves in the membrane by other means (Saint-Georges et al., 2001; Herrmann and Bonnefoy, 2004).

I attempted the construction of two strains in which the N-terminal transmembrane domain of Cox2p would lose part of its negative charge. First, a strain with the mutation D41N in *COX2*, i.e. replacement of a negatively charged residue with

an uncharged polar residue in the N-terminal transmembrane domain of Cox2p. Second, a strain with the nearby mutation F45K, i.e. replacement of an uncharged residue with a positively charged residue. A human mutation (M29K) causing myopathy was found at an equivalent residue, though there is poor sequence conservation in this region (Rahman et al., 1999). I aimed to determine whether Oxa1p was still required for the insertion of Cox2p into the membrane when its N-terminal transmembrane domain was less negatively charged. In the absence of Oxa1p cytochrome oxidase cannot be assembled (Altamura et al., 1996). I planned to introduce the mutated *COX2* gene into a strain with deletion of the *OXA1* gene and see whether cytochrome oxidase could still be assembled in the mutants. Of course, this was subject to the mutations not causing assembly problem due to structural changes. For example, the crystal structure of bovine cytochrome oxidase suggests that residue D25 (equivalent to yeast D41) could form a salt bridge with an conserved arginine 2.5Å away on bovine COX6C (yeast Cox7ap) (Figure 3.11). Disruption of this would prevent neutralisation of the arginine charge, so assembly may be affected. Furthermore, D41 could be involved in tethering the transmembrane domain in place.

I attempted to generate the mutant strains through biolistic transformation as described in 2.2.6. Unfortunately I was not successful in generating the mutants. However the D41N mutant, but not the F45K mutant, was later successfully made by another member of our lab. The mutant did not have a respiratory deficient phenotype, suggesting that the D41 residue was not required for assembly of cytochrome oxidase. In another lab D41N was introduced into a mutant with temperature-sensitive Oxa1p function (see (Bauer et al., 1994; Hell et al., 2001)). Accumulation and degradation of Cox2p was studied after incubation at the permissive temperature of 28°C and non-permissive temperature of 34°C. No difference was observed between the control D41 and mutant D41N, and the work has not been pursued further (G. Dujardin, personal communication).

3.3. DISCUSSION

Nine strains containing mutations in the *COX2* gene have been analysed. All the mutations are located in the C-terminal globular domain of Cox2p. In yeast, unassembled subunits, especially the core subunits Cox1p, Cox2p and Cox3p, are rapidly degraded by AAA proteases, hence in the absence of assembly the characteristic peak at 603 nm due to the heme aa_3 of Cox1p is absent. In seven of the mutants an absence of heme aa_3 signal was observed in optical spectra. Therefore in these seven strains the *COX2* mutation(s) abolished assembly of cytochrome oxidase, explaining the respiratory growth deficiency observed. Two mutant strains, G156E and R159K, had an unusual optical spectrum: heme aa_3 signal was diminished but not abolished, and the absorbance peak was blue shifted to 599 nm. In these mutants, unusually, assembly was impaired but not abolished.

3.3.1. *COX2* mutations abolishing cytochrome oxidase assembly

In the absence of cytochrome oxidase assembly unassembled subunits are normally rapidly degraded. One of the seven mutants with no heme aa_3 signal (C221W + L245W) was analysed by western blotting and was found to contain less than 10% of wild type levels of all cytochrome oxidase subunits tested, except Cox4p, known to be a relatively stable subunit.

As shown in Figure 3.2A, some of the mutations are located close to the Cu_A centre. C221 is a copper ligand, and it has been shown previously that replacement of the copper ligands resulted in an assembly failure and absence of heme aa_3 signal (Speno et al., 1995). Residues M232, G219 and G226 are also in the Cu_A-binding domain. Mutation at these residues may abolish or diminish copper binding through alteration of the backbone fold or sidechain packing at the β-hairpin structure of the Cu_A site. The mutations could also hinder the metallation of the Cu_A site by impairing the interaction between Cox2p and copper chaperones through distorting the binding surface. Failure to bind copper is likely to result in degradation of Cox2p and therefore prevent complex assembly.

The remaining five deleterious residues are located away (>20 Å) from the Cu_A site. The corresponding residue to P170 initiates a β-turn in the bovine cytochrome oxidase, so mutation to histidine is likely to disrupt this. The corresponding bovine residue to D162 (E137) is likely to be involved in a stabilising sidechain ionic interaction with R122 (bovine numbering) in COX4 (yeast Cox5p) (Figure 3.12). However, since there is poor sequence conservation between the bovine and yeast

enzymes in this region of Cox2p no firm predictions can be made about the situation in yeast. R213 is located in a loop connecting β-strands in the bovine Cox2p structure, so mutation to methionine is likely to alter sidechain packing in this region. All these mutations are likely to disrupt the native fold of Cox2p.

Alteration of Cox2p metallation and/or folding is likely to be the cause of the assembly failure in these mutants. Unassembled Cox2p is a substrate of the AAA protease Yme1p (Nakai et al., 1995; Pearce and Sherman, 1995). The enzyme senses the folding state of solvent-exposed domains and degrades unfolded membrane proteins (Leonhard et al., 1999). It is probable that Cox2p is rapidly proteolytically degraded and consequently cannot associate with Cox1p to stabilise the nascent complex. This would result in degradation of the subunits and absence of a heme aa_3 signal.

3.3.2. *COX2* mutations allowing partial cytochrome oxidase assembly

The optical spectra of the mutants G156E and R159K showed the presence of a significant amount (approx. 50% wild type level) of cytochrome oxidase, despite the respiratory deficiency of the mutants (Table 3.2). However, the signal peak was shifted, indicating perturbation of the heme environment. The enzyme also had decreased activity and increased K_m for cytochrome *c*, suggesting a weakened interaction. Revertant mutations in the Cu_A-binding domain partially restored respiratory competence and cytochrome oxidase assembly. Interestingly, in a mutant of Sco1p, a copper chaperone which provides copper atoms to the Cu_A site, the optical spectrum also exhibited a blue-shifted and diminished heme aa_3 signal (Dickinson et al., 2000). It can be hypothesised that the primary mutations might have a long-range effect on folding of the Cu_A site, and the reversion mutations would alter the folding such that the enzyme can still be assembled. In the two R159K revertants analysed V_m was also restored, while K_m (cyt *c*) was still high but closer to wild type level. So the reversions increase the functionality of the cytochrome *c* binding site even in the presence of the mutation R159K. This might be expected since replacement of arginine with lysine is a semi-conservative structural change.

Analysis of subcomplexes of the cytochrome oxidase present in the mutant strains showed that a large proportion of the cytochrome oxidase is present as a newly identified subcomplex *c*. A total of five complexes or subcomplexes could be identified by blue native electrophoresis. The wild type contained *a*, the monomeric holoenzyme; *b*, the monomeric holoenzyme lacking Cox6ap; *d*, containing Cox7p and/or Cox7ap but none of the other cytochrome oxidase subunits tested; and *f*, unassembled Cox1p. The

mutant strains contained lower levels of *a* and *b* but additionally contained high levels of the faster migrating *c*, lacking Cox2p, Cox4p, Cox6ap, Cox7p, Cox7ap and Cox8p, but containing Cox1p, Cox3p, Cox5p and Cox6p. I did not probe with an antibody against Cox6bp. The revertants contained *c* in addition to levels of *a* and *b* intermediate between those observed in the wild type and mutants. The absence of Cox2p in the major population of cytochrome oxidase in the mutants would explain the perturbation of the heme environment observed in optical spectra. It could also help to explain the high K_m for cytochrome *c*, since part of the binding site for cytochrome *c* is located in Cox2p (Bisson et al., 1982; Lappalainen et al., 1995; Witt et al., 1995; Zhen et al., 1999). K_m would be closer to wild type in the revertants due to an increased proportion of enzyme containing Cox2p.

3.3.3. Origin of band *c*

There are several possibilities regarding the identity of band *c*:

3.3.3.1. Degradation product

Band *c* could represent a degradation product of the fully or partially assembled cytochrome oxidase. The G156E and R159K mutations may allow assembly of the complex. However, the mutations would alter the Cox2p structure such that it would be rendered unstable and especially susceptible to proteases. Cox2p would be proteolytically degraded and the attachment of some of the peripheral subunits would be weakened, while some of the remaining subunits (Cox1p, Cox3p, Cox5p and Cox6p) remained attached to each other in a stable subcomplex. It is not clear whether the entire Cox2p polypeptide would be extracted from the complex, or whether only the soluble extramembrane domain might be affected. Although the exact location of the Cox2p antibody epitope is not known, it is most likely to be in the exposed C-terminal region.

3.3.3.2. Assembly intermediate

Alternatively, band *c* could be an assembly intermediate accumulating due to the absence of Cox2p, rapidly degraded because of its mutations, but required in a subsequent assembly step. It is quite possible that Cox1p could interact with the core subunit Cox3p before interacting with Cox2p, since in the less complex cytochrome oxidase of *R. sphaeroides* Cox1p can associate with either of these subunits first (Hiser and Hosler, 2002). However, since *c* does not accumulate in the double mutant C221W + L245W this suggests that its formation requires the presence of Cox2p. Furthermore, the absence of heme aa_3 in the other Cox2p mutants suggests that Cox2p is required at

least for the formation of a heme-containing subcomplex. It seems unlikely that band *c* represents a simple assembly intermediate.

3.3.3.3. Partially degraded assembly intermediate

Instead, band *c* could represent a degradation product of an assembly intermediate containing Cox2p. Initial folding of Cox2p may be comparatively normal in the G156E and R159K mutants, allowing the formation of an assembly intermediate containing Cox1p, Cox2p, Cox3p, Cox5p and Cox6p (Figure 3.13). Assembly would halt at this point, perhaps due to an inability of nuclear subunits to bind the altered Cox2p, or an unstable interaction with a chaperone protein. Cox2p would be unprotected and susceptible to proteases, so it would be removed (either fully or partially) from the assembling complex, the rest of which remains stable and intact but cannot proceed with assembly in the absence of Cox2p. Hence band *c* would represent an assembly intermediate which has undergone processing to remove Cox2p. In the other *COX2* mutants the folding defect would be too severe to allow the transient assembly of Cox2p and formation of a stable subcomplex.

A small proportion of the Cox2p-containing assembly intermediate would escape proteolysis and persist to form fully assembled enzyme (Figure 3.13). In the revertants R159K + D187N and R159K + S222Y there are significantly higher levels of complex *a* and subcomplex *b* compared to the mutants (Figure 3.6), suggesting that the secondary mutations increase the stability of the Cox2p-containing assembly complex so that the proportion of fully assembled enzyme would increase. However, this does not seem in agreement with the data obtained using denaturing electrophoresis. The amount of Cox2p detected by this method was less than 10% of wild type level for both mutants and revertants. However, sample treatment prior to denaturing electrophoresis is harsher than that required for native electrophoresis. The stability of the revertant Cox2p is likely to be intermediate between that of the parent mutant and the wild type, so a high degree of Cox2p degradation may occur in the revertants during denaturing sample preparation, but not during native sample preparation. The mitochondrial membrane samples used were not treated with protease inhibitors during extraction, and in denaturing gel electrophoresis multiple bands were present beneath the Cox2p bands of the mutants and revertants but to a lesser extent in the wild type (Figure 3.5). These most likely represent Cox2p degradation products.

3.3.4. Band *d*

The other interesting subcomplex, *d*, containing Cox7p and/or Cox7ap, was detected in all samples except the mutant C221W + L245W. This may be a subassembly complex containing Cox7p and/or Cox7ap together with other as yet undetermined proteins. Recently, Church *et. al.* used sucrose gradient fractionation to identify a yeast cytochrome oxidase subcomplex containing Cox7p and Cox7ap in addition to Cox8p and the assembly factor Pet100p (Church et al., 2005). My analysis did not reveal the presence of Cox8p in subcomplex *d*, however, it would be interesting to know whether Pet100p was associated with the band.

3.3.5. Conclusions

This is the first instance of detection of the cytochrome oxidase subassemblies described, and only the second report of detection of subassemblies in yeast (see (Church et al., 2005)). The subassembly *c* is particularly interesting since it contains two of the core subunits of cytochrome oxidase. These results provide interesting data on the cytochrome oxidase assembly pathway and will aid understanding of the temporal order of subunit interaction. The work demonstrates that yeast, which has been invaluable in detecting assembly factors involved in assembly, can also be useful in delineating the sequential pathway of cytochrome oxidase assembly. It would be interesting now to analyse further yeast mutants in the same way.

The next chapter considers the effect of the cytochrome oxidase inhibitor and antimicrobial agent NO on yeast. A severe decrease in cytochrome oxidase content was observed after treatment with NO/RNS, suggesting that these substances can interfere with the assembly of cytochrome oxidase.

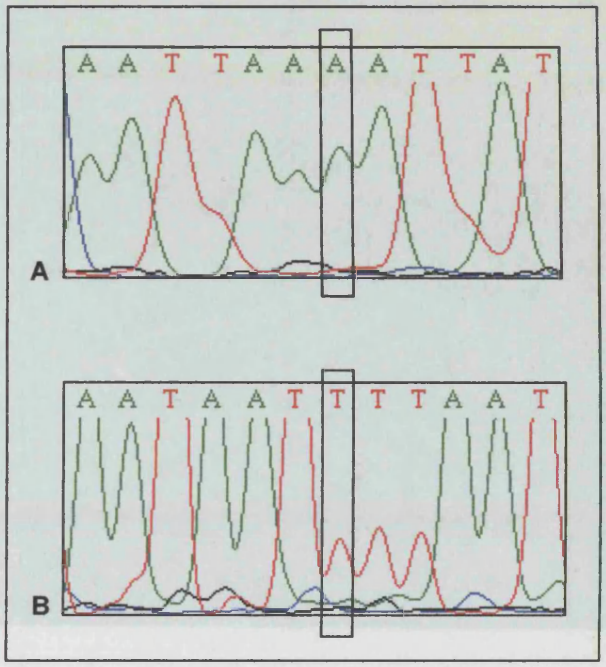

Figure 3.1. The R159K mutation in *COX2*.

The amino acid change arginine to lysine caused by mutation of guanine to adenine at nucleotide position 476 of the *COX2* cDNA is highlighted. **A.** Coding sequence (primer PL32). **B.** Reverse sequence (primer PL27).

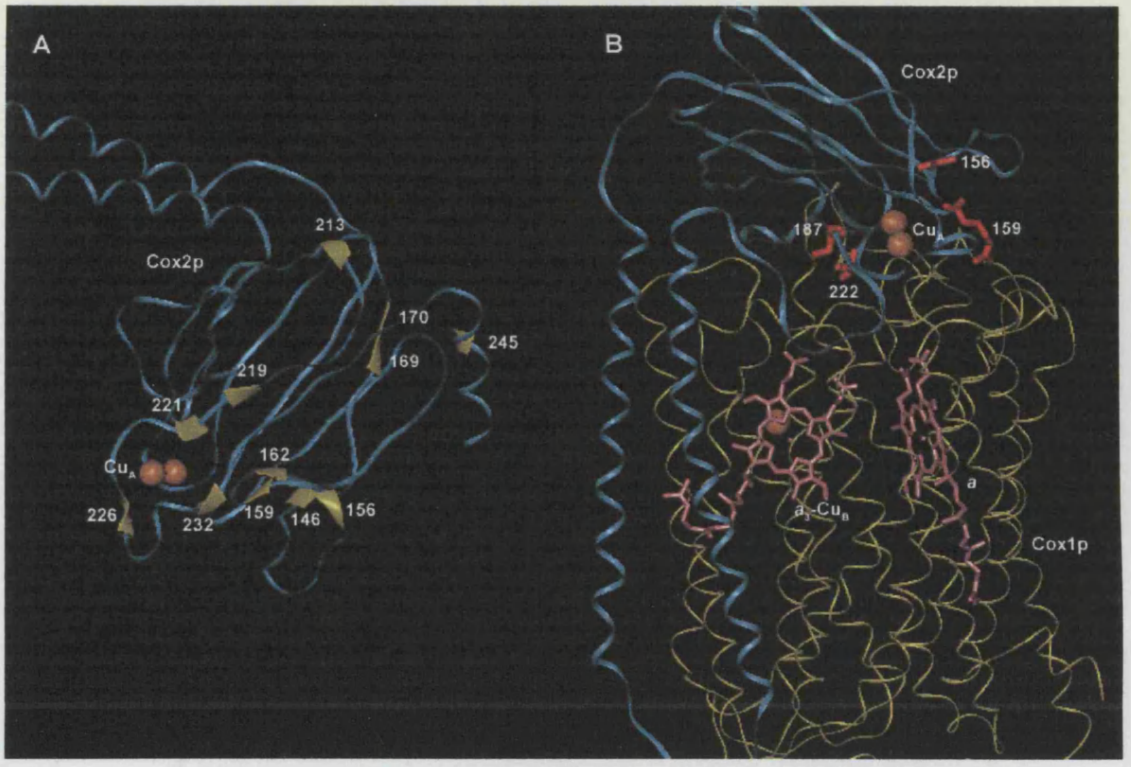

Figure 3.2. Location of Cox2p mutations and reversions.

A. Cox2p only is shown. The locations of all the missense mutations identified in the respiratory deficient mutants are indicated. **B.** Cox1p and Cox2p only are displayed. The locations of the mutations G156E and R159K are indicated, together with the reversion positions 187 and 222. The atomic structure is from the bovine enzyme (PDB 1OCC), but residues are identified by yeast numbering. Copper atoms are shown in orange and heme groups in pink.

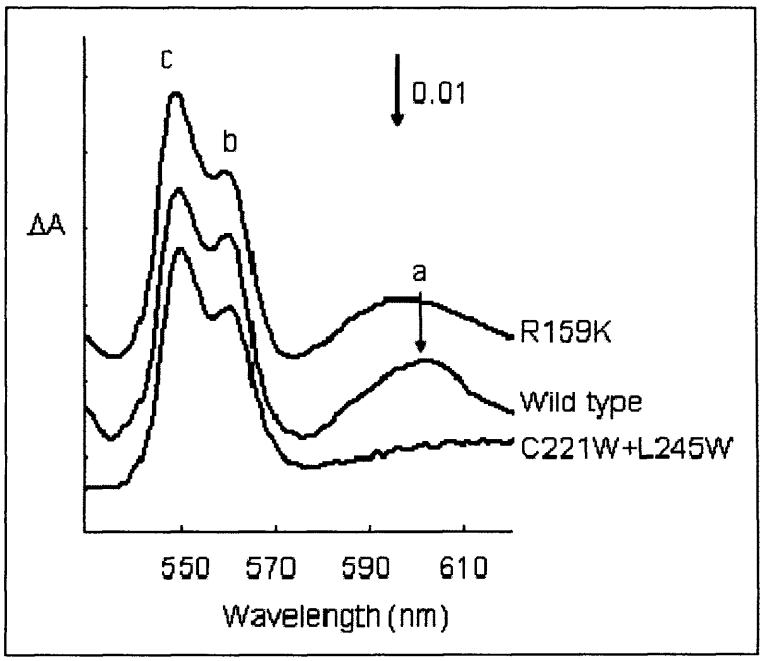

Figure 3.3. Cytochrome levels in mutant and wild type cells.

Optical spectra of fully reduced whole cell suspensions were obtained as described in 2.3.3. c, cytochrome *c*, b, cytochrome *b*, a, cytochrome oxidase (heme aa_3).

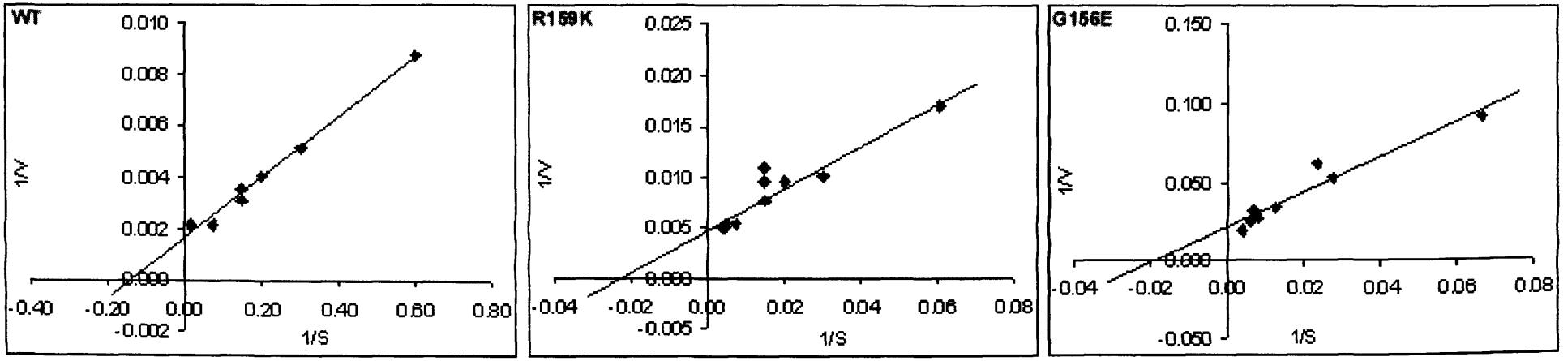

Figure 3.4. Cytochrome oxidase activity in mutants and wild type.

Lineweaver-Burke plots were constructed after measuring oxygen consumption by mitochondrial membranes supplied with varying concentrations of cytochrome *c*.

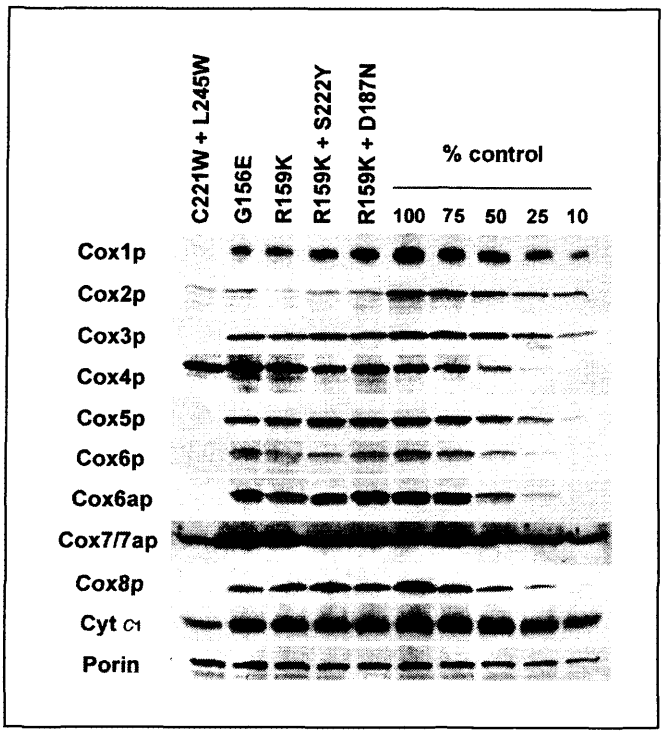

Figure 3.5. Steady state levels of cytochrome oxidase subunits in mutants and revertants.
Steady state subunit levels in mutants and revertants were compared to serial dilutions of the wild type on denaturing western blots loaded with 10-20 μg of protein, by probing with antibodies specific for cytochrome oxidase subunits Cox1p, Cox2p, Cox3p, Cox4p, Cox5p, Cox6p, Cox6ap, Cox7p and Cox7ap (Cox7/7ap), and Cox8p, and the bc_1-complex subunit cytochrome c_1 (see 2.4.1 and 2.4.4). An antibody specific for porin was used as control for equal loading.

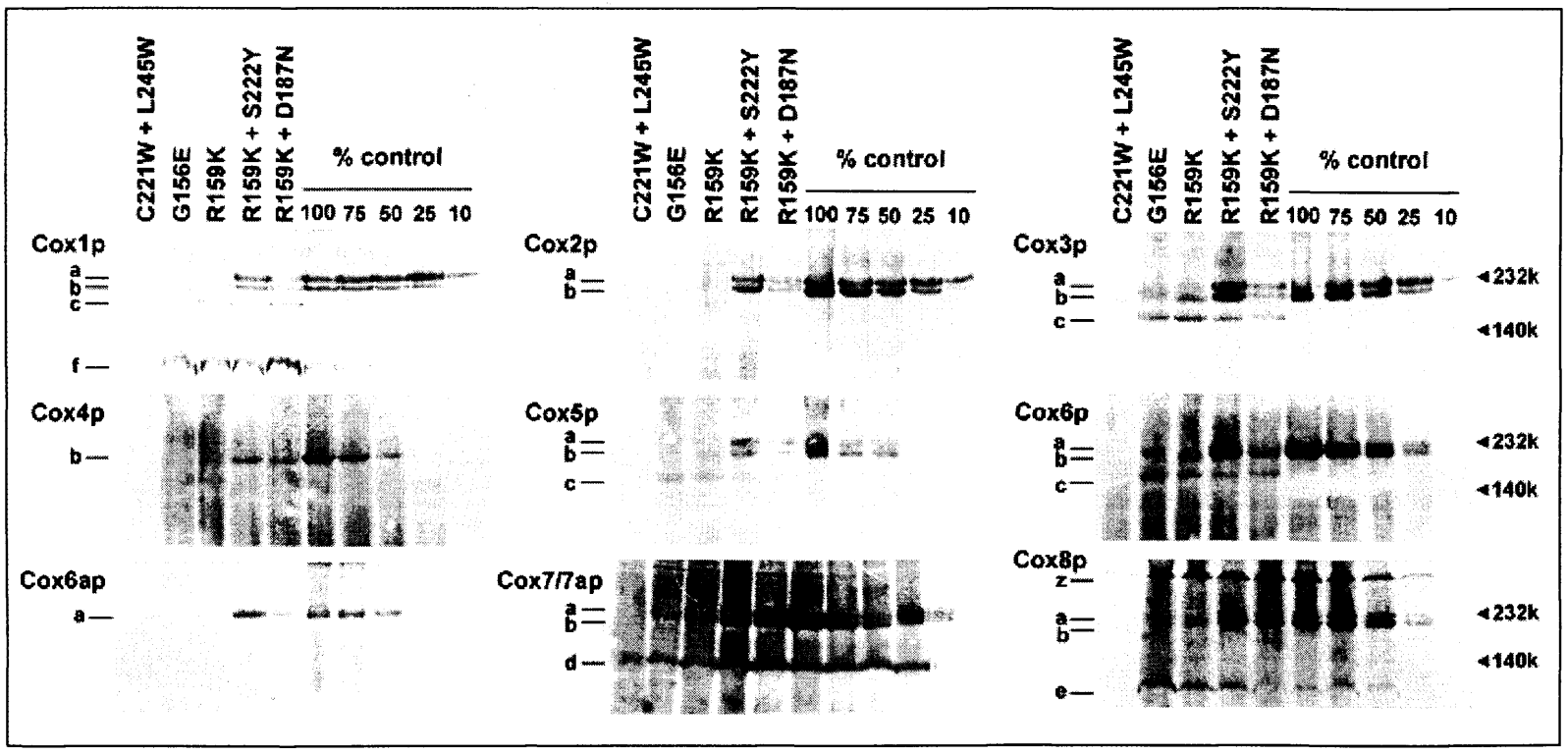

Figure 3.6. Subcomplexes of cytochrome oxidase in wild type and Cox2p mutants and revertants.

Immunoblots of native gels loaded with 60 μg of protein from mutants, revertants and wild type were probed with subunit-specific antibodies against Cox1p, Cox2p, Cox3p, Cox4p, Cox5p, Cox6p, Cox6ap, Cox7p and Cox7ap (Cox7/7ap), and Cox8p, to determine the existence and composition of subcomplexes. Equal loading was confirmed by denaturing western blot probed with antiserum against porin. Bands a-z represent possible complexes or subcomplexes of cytochrome oxidase. Molecular weight markers are shown on the right hand side.

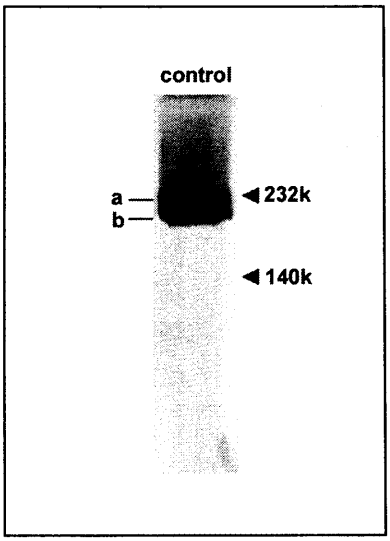

Figure 3.7 Cytochrome oxidase activity of complexes *a* and *b* in the wild type.
Wild type protein (60 µl) was resolved on blue native gel then stained for cytochrome oxidase activity, as described in 2.4.5.

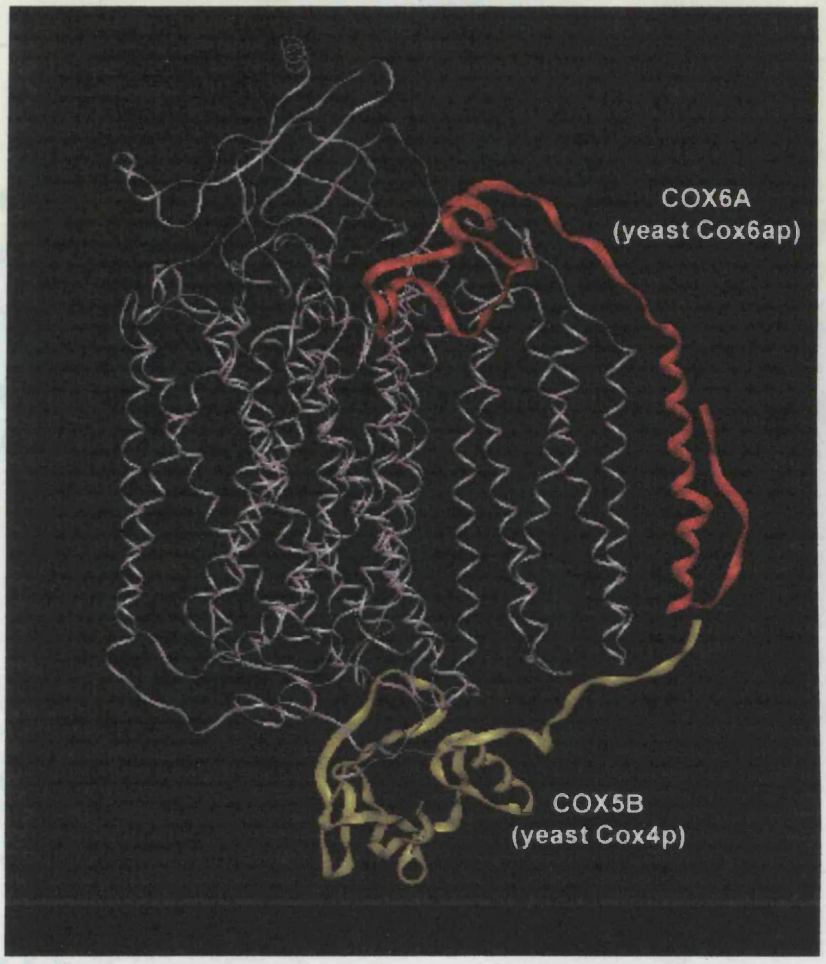

Figure 3.8. Proximity of the N-terminal regions of COX6A and COX5B.

The atomic structure is from the bovine enzyme (PDB 1OCC). The core subunits are shown in white, COX6A (yeast Cox6ap) is shown in red and COX5B (yeast Cox4p) is shown in yellow. In yeast, the Cox4p N-terminal sequence is extended by 25 amino acids and the Cox6ap N-terminal sequence by 23 amino acids.

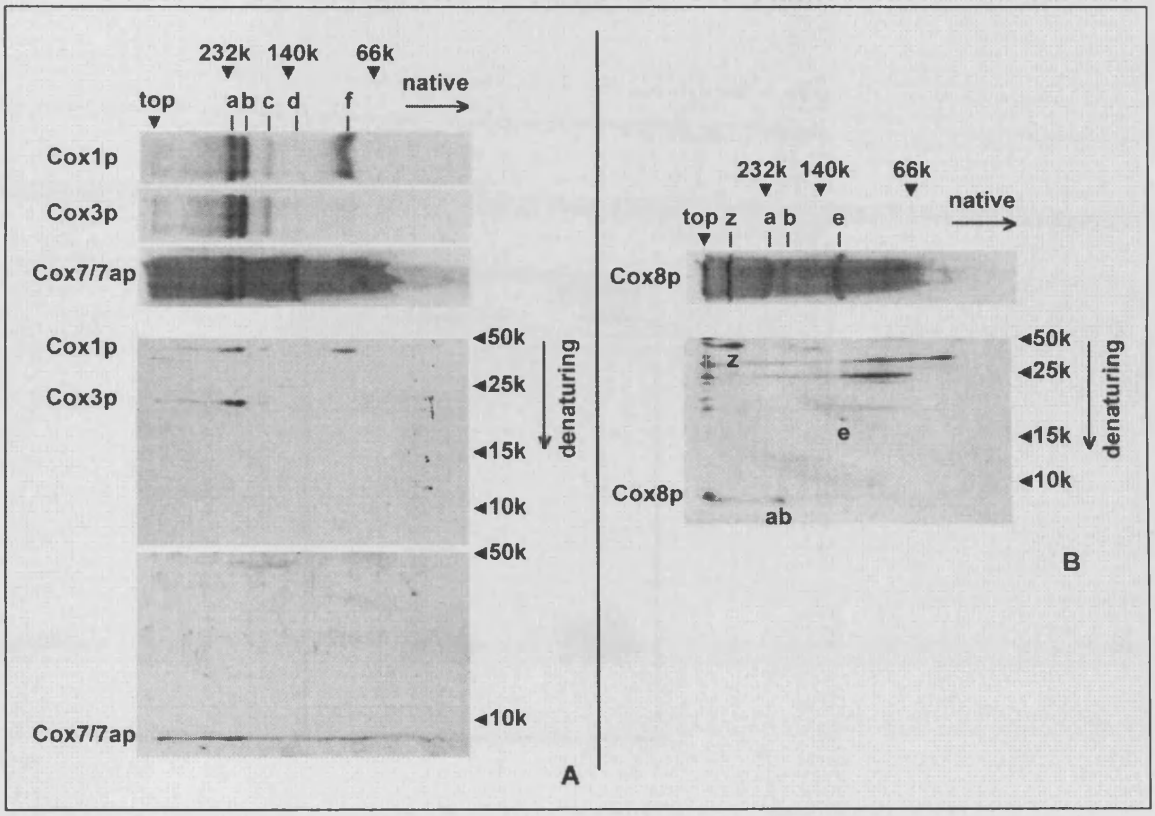

Figure 3.9 Subunit composition of cytochrome oxidase subcomplexes in the R159K + S222Y revertant verified by two-dimensional electrophoresis.

Blue native gel strips loaded with 60 µl protein were electophoresed then mounted horizontally and resolved by denaturing electrophoresis, before immunoblotting (see 2.4.3). Other gel strips from the same native gels were directly immunoblotted and are shown above the two-dimensional blots to aid identification of spots. **A.** The upper two-dimensional blot was probed with antibodies specific to Cox1p and Cox3p, while the lower blot was probed with antiserum recognising Cox7p and Cox7ap. In both cases, 15% denaturing gels was used. **B.** The two-dimensional blot, from a 20% denaturing gel, was probed with antibody raised against Cox8p.

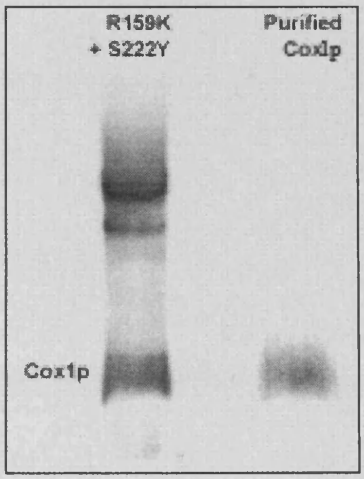

Figure 3.10. Identity of band *f*

Cox1p was isolated from purified yeast cytochrome oxidase and electrophoresed adjacent to the R159K + S222Y revertant on native gel, then the blot was incubated with antiserum against Cox1p.

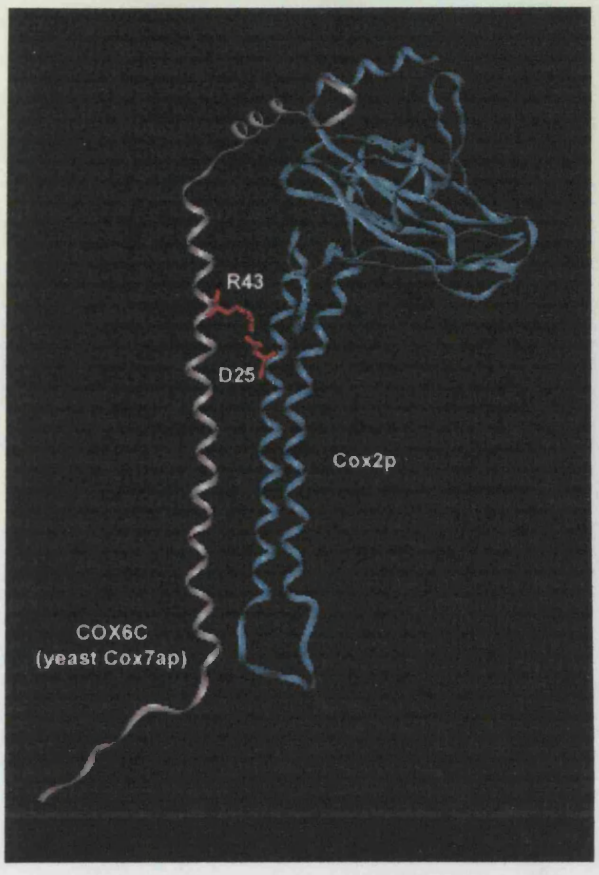

Figure 3.11. Possible salt bridge between Cox2p and Cox7ap.

The atomic structure is from the bovine enzyme (PDB 1OCC). Bovine residue D25 in COX2 (yeast Cox2p D41) may form a salt bridge with residue R43 in COX6C (yeast Cox7ap).

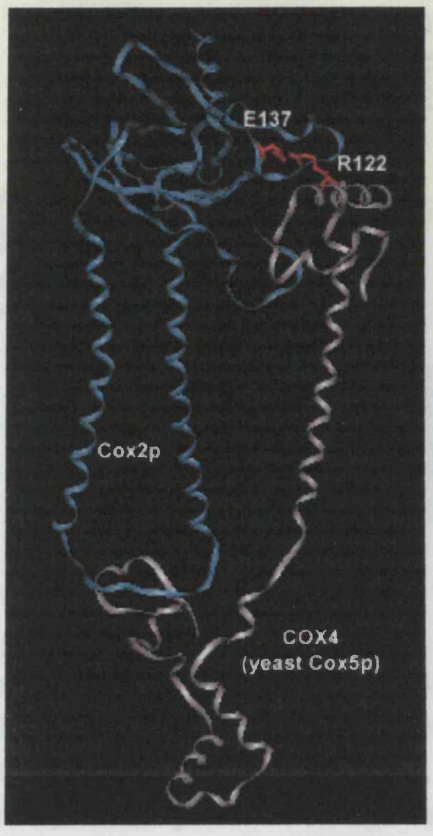

Figure 3.12. Possible stabilising sidechain interaction between Cox2p and Cox5p.
The atomic structure is from the bovine enzyme (PDB 1OCC). Bovine residue E137 in COX2 (yeast Cox2p D162) could interact with R122 in COX4 (yeast Cox5p).

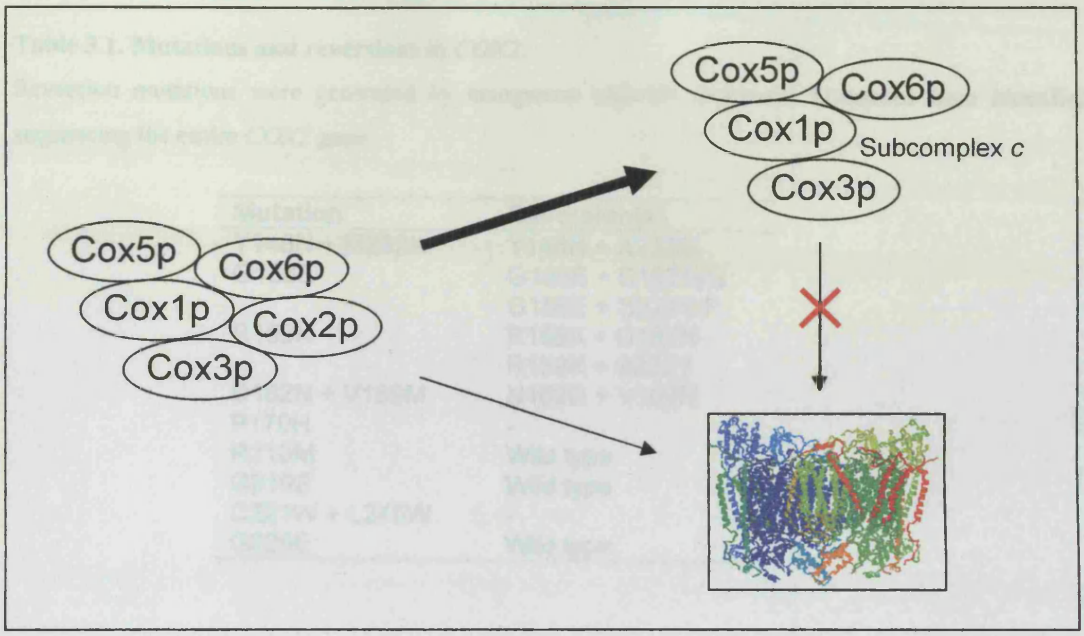

Figure 3.13. Formation of a partially degraded assembly intermediate of cytochrome oxidase. Initial folding of Cox2p would be comparatively normal, allowing formation of an assembly intermediate containing Cox1p, Cox2p, Cox3p, Cox5p and Cox6p. However, Cox2p would be unstable and proteolytically degraded, while the remaining subunits remain attached. Some assembly intermediate would escape degradation of Cox2p and persist to form fully assembled cytochrome oxidase.

Table 3.1. Mutations and reversions in *COX2*.

Reversion mutations were generated by manganese chloride treatment. Mutations were identified by sequencing the entire *COX2* gene.

Mutation	Reversion(s)
Y146N + M232K	Y146N + K232M
G156E	G156E + D187N/G
	G156E + S222Y/F
R159K	R159K + D187N
	R159K + S222Y
D162N + V169M	N162D + V169M
P170H	-
R213M	Wild type
G219E	Wild type
C221W + L245W	-
G226E	Wild type

Table 3.2. Cytochrome oxidase content and activity in mutants and revertants.

[a]The cells were incubated in YPG, and the optical density of the culture was determined after 3 days. [b]The cytochrome oxidase (CcO) content was determined from the amplitude of the heme aa_3 optical spectra of dithionite-reduced whole cell suspensions (see 2.3.2). [c]The cytochrome oxidase activity of membrane samples was measured using an oxygen electrode. Initial rates were measured as a function of cytochrome *c* concentration, and V_m and K_m values were derived from Lineweaver-Burke plots as in Figure 3.4. (see 2.3.3).

Mutation	Growth yield[a] (% wild type)	CcO content[b] (nmol.g cells^{-1})	CcO activity[c]	
			V_m (s^{-1})	K_m (μM cyt *c*)
Wild type	100	0.8	625	7.4
G156E	<5	0.4	47	53
R159K	<5	0.4	208	43
R159K + D187N	60	0.6	650	14
R159K + S222Y	40	0.5	580	16

Chapter 4

EFFECT OF NO/RNS ON CELL PROLIFERATION AND THE RESPIRATORY CHAIN

4.1. INTRODUCTION

4.1.1. Antimicrobial activity of nitric oxide

On infection with pathogenic bacteria, viruses, parasites and fungi, the mammalian immune system releases high levels of nitric oxide (NO), an effective antimicrobial agent (MacMicking et al., 1997). However the specific cellular targets of this antimicrobial activity are not well understood. NO reversibly inhibits cytochrome oxidase by high affinity binding at the active site. At high concentrations and/or on prolonged exposure NO reacts with other molecules to form species collectively described as reactive nitrogen species (RNS). These species have varying reactivity and stability, and extend the range of targets which NO can affect to include thiols, tyrosines, DNA and lipids. RNS have also been shown to irreversibly inhibit respiration. RNS, together with reactive oxygen species (ROS), form the first line of host cell defence against pathogens, and their breadth of targets would account for the broad spectrum antimicrobial activity observed.

4.1.2. Aims

The aim of the work described in this chapter, in conjunction with the work described in Chapter 5, was to assess the nature of the antimicrobial effect of NO and the responses it elicits in the cell, using the model *Saccharomyces cerevisiae*. My aim has not been to distinguish between the various RNS which could be involved, rather to study the effects of the collective RNS to which pathogens may be exposed. I have used the NO donor DETA NONOate as a source of NO, since it releases NO over an extended period of time (Hrabie and Klose, 1993). In this chapter I have considered the effects of prolonged NO exposure of yeast cells on cell proliferation and on the cytochromes of the respiratory chain. Since NO and RNS have been demonstrated to inhibit several respiratory chain enzymes it seems likely that part of their antimicrobial action could be achieved through disruption of respiration. I have also assessed the involvement of oxidative stress defence genes in the sensitivity of yeast cells to the growth inhibition to determine the involvement of ROS in the antimicrobial action.

4.2. RESULTS

4.2.1. Inhibition of yeast respiration by NO donor

NO is well known to inhibit mammalian respiration at sub-micromolar concentrations by reversibly inhibiting cytochrome oxidase. However yeast contain a very efficient NO oxidoreductase encoded by the *YHB1* gene, and Yhb1p is likely to be the main protective mechanism against NO in some microorganisms (Gardner et al., 2000; Liu et al., 2000). It might then be expected that the presence of Yhb1p would prevent inhibition of respiration by NO.

In Figure 4.1 cells were grown to late exponential phase (approx. 6.10^7 cells per ml) then resuspended in fresh growth medium before addition of the NO donor DETA NONOate, and oxygen consumption was measured (see 2.3.3). NO donor had only a mild effect, even at high concentration (3 mM), on respiration of wild type yeast, reducing oxygen consumption from 77 to 56 μM O_2 per second. However in a strain with deletion of *YHB1* (Δ*yhb1*) oxygen consumption was severely inhibited by 0.1 mM DETA NONOate, from 75 to 3 μM O_2 per second. So yeast respiration can be inhibited by NO, but the presence of Yhb1p is sufficient to defend against respiratory inhibition by even high concentrations of NO donor.

4.2.2. Inhibition of yeast proliferation by NO donor

The efficacy of Yhb1p in the removal of NO is also demonstrated by comparing the growth of wild type and Δ*yhb1* yeast in the presence of DETA NONOate. In all experiments cells were grown in galactose medium (YPGal) since this carbon source can be used for either respiration or fermentation by yeast cells, and induces much lower levels of repression of respiratory chain gene expression and mitochondrial biogenesis than glucose (Lagunas, 1986). At late exponential phase (approx. 6.10^7 cells per ml) cultures were divided into aliquots and varying concentrations of DETA NONOate added, then cell density was monitored for a period of 12 hours until stationary phase was attained (the experimental detail is described in 2.1.8).

Figure 4.2A shows that high concentration of DETA NONOate had no effect on the growth of wild type yeast. In the absence of DETA NONOate growth of the Δ*yhb1* mutant was similar to the wild type, confirming that the Δ*yhb1* mutation itself did not affect yeast growth. However proliferation of these cells was sensitive to NO donor. Addition of 0.1 mM DETA NONOate had no effect on growth, but the presence of 3 mM resulted in severe growth repression (Figure 4.2B). Control cultures underwent

between 3 and 4 doublings during 12 hours while 3 mM DETA NONOate-treated cells reached only between 2 and 3 doublings within the same time frame, to reach less than half the cell density of control cells. When 1 mM DETA NONOate was added, the effect was not so severe and the culture underwent more than 3 doublings. With this concentration cell proliferation decreased to a similar level to that observed on incubation with 8 μM myxothiazol (Figure 4.2C). Myxothiazol is a specific inhibitor of the bc_1 complex, and the concentration used here has been previously demonstrated to be sufficient to fully inhibit respiratory function (Bourges et al., 2005).

The effect of high concentration of DETA NONOate on proliferation of Δ*yhb1* cells which had already been allowed to reach early stationary phase (approx. 3.10^8 cells per ml) was also assessed (Figure 4.2B). Incubation with 3 mM DETA NONOate caused cells to undergo less than one doubling before reaching a plateau compared to between one and two doublings in the control, and the culture appeared as if in a premature stationary phase after about 4 hours. As with the late exponential phase cells, density after 12 hours of 3 mM NO donor treatment was approximately half that observed in the control.

These data clearly demonstrate that the *YHB1* gene is effective at removal of NO, and highlight the importance of flavohemoglobins as a protective mechanism against NO in some microorganisms. The objective of this study was to assess the antimicrobial action of NO, comprising the nature of the stresses sensed by the cell and the response of the cell to these stresses. Since Yhb1p is so remarkably efficient at protecting against NO/RNS I have performed all the experiments described subsequently in strains with deletion of the *YHB1* gene, to detect other proteins that contribute to the defence against NO/RNS.

To verify that NO and/or RNS, rather than another degradation product of DETA NONOate, was causing the inhibition of growth, the effect on cell proliferation of DETA NONOate which had been allowed to decompose for varying lengths of time was assessed (Figure 4.3). After one day of decomposition 3 mM DETA NONOate had a similar effect to fresh DETA NONOate. After 4 and 6 days decomposition the proliferation of treated cells became progressively closer to that observed in untreated cells. However, after 6 days decomposition the growth was still only about 70% of that observed in the untreated cells. The half life of DETA NONOate is 20 hours at 37°C and 57 hours at 24°C at pH 7.4 (Hrabie and Klose, 1993), so some DETA release might still be expected even after 6 days. Nevertheless, it is still possible that some of the deleterious effect on growth observed could be due to compounds other than NO and

RNS. However, when wild type cells were treated with 3 mM DETA NONOate which had been allowed to decompose for 4 days the cell proliferation observed was similar to that observed with 3 mM fresh DETA NONOate (Figure 4.3). Since the substrate for Yhb1p is NO, this data suggests that the growth inhibition in Δ*yhb1* cells is not due to an unknown degradation product of DETA NONOate.

To estimate the concentration of NO which causes the severe decrease in cell proliferation I used an NO electrode to measure NO release from 3 mM DETA NONOate (see 2.3.4). Cells were grown to late exponential phase in YPGal, then an aliquot was removed and placed in the chamber of the NO electrode. 3 mM DETA NONOate was added and NO concentration measured over the following 24 hours (Figure 4.4). NO levels rose to 15-18 μM rapidly after addition of DETA NONOate, and remained at around this level for 4 hours. The concentration then decreased to 10-12 μM after 6 hours then to 3 μM after 12 hours, after which it remained steady. In the experiments described in this chapter I have worked at 28°C and an initial pH of around 5.6, therefore the half life of NO donor might be expected to be less than the 20 hours recorded at 37°C and pH 7.4. Since the conditions in the NO electrode chamber were not identical to those used when monitoring cell growth (different stirring speed due to use of magnetic stirrer used instead of platform shaker; different oxygen concentration due to different surface area exposed to air) the results can only be an approximation of the concentrations sensed by the cells.

4.2.3. NO donor at 3 mM does not impair cell viability

Having established that 3 mM DETA NONOate exerts an antimicrobial effect on Δ*yhb1* yeast, I assessed cell survival to determine the nature of the inhibition of cell proliferation. Since RNS can act on a wide variety of targets incubation with DETA NONOate is likely to cause damage to several cellular components, which could lead to lethality. The viability stain methylene blue does not stain viable yeast cells since it is rapidly metabolised to a colourless product, but in non-living cells the stain appears blue. Comparison of methylene blue stained cells under the light microscope showed no differences between DETA NONOate-treated and control cell populations after 12 hours (see 2.1.9). Although the methylene blue stain has been reported to overestimate yeast viability (O'Connor-Cox et al., 1997), almost no stained cells could be identified. The efficacy of the assay was confirmed by the high proportion of cells staining after short ethanol incubation.

To further confirm the absence of lethality the percentage of cells able to form colonies after treatment with 3 mM DETA NONOate was monitored. After 12 hours treatment cell density was measured then cultures were diluted to 3000 cells per ml and aliquots were plated onto YPGal medium, then after 2 days incubation the colonies were counted. Viability of NO donor-treated cells was 77 ± 9% (n = 2) compared to the control. As a final test, I assessed the effect of replacing the growth medium after 12 hour treatment with NO donor. I took a culture which had been treated with NO donor, harvested the cells, washed them twice with water, and used resuspended cells to inoculate a new YPGal culture to A_{600nm} = 0.05. After 13 hours of growth the new culture reached late exponential phase. Growth was then monitored for a further 7.5 hours, after which time density of the culture derived from treated cells had reached about 80% of the density of a control culture treated in the same way (Figure 4.5). The small amount of growth inhibition observed may be due to residual NO donor, NO or RNS which had not been effectively washed from the cells, or a cytotoxic effect of DETA NONOate on a small proportion of the cells used to inoculate the culture. When this set of results is combined it seems that NO, at least at 3 mM, has a cytostatic rather than a cytotoxic effect on yeast.

4.2.4. NO donor does not cause rho$^-$ accumulation

I also evaluated the mutagenic effect of DETA NONOate. Deletions in mtDNA are called rho$^-$ mutations, and accumulation of rho$^-$ mutations reflects the mutagenic effect of a compound on mtDNA. Such mutations occur spontaneously in cultures at a frequency of around 0.1%. ROS are mutagenic: treatments which enhance ROS production or diminish yeast cell defences against ROS (such as disruption of *SOD2*) increase the frequency of rho$^-$ accumulation (Piper, 1999). mtDNA is particularly susceptible to the mutagenic effects of endogenous ROS production, and its location close to the respiratory chain, lack of protective histones and the apparent incapability of mitochondria to perform nucleotide-excision repair probably contribute to this (Yakes and Van Houten, 1997).

It seems possible that RNS could also have a mutagenic effect on mtDNA. Since the mtDNA encodes components of the respiratory chain, rho$^-$ mutations cause respiratory deficiency. The plates used in colony counting (see 4.2.3) were replicated onto respiratory medium (YPG) and the number of colonies unable to grow (respiratory deficient) was recorded. No respiratory deficient colonies were present, consequently it seems that RNS do not have a mutagenic effect on the mtDNA.

4.2.5. ROS do not appear to be involved in the effect of NO donor on cell proliferation

The respiratory chain is the major source of endogenous ROS production in yeast. Inhibition of the respiratory chain by NO acting on cytochrome oxidase will impede the flow of electrons, making the respiratory chain more reduced and increasing the likelihood of superoxide formation (Poderoso et al., 1996). Superoxide can combine with NO to form highly reactive peroxynitrite, which has a wide range of targets and may contribute to the antimicrobial action of NO. To determine the involvement of ROS in the observed response to NO donor, the effect of NO donor on proliferation of strains with deletion of genes involved in the oxidative stress response was monitored. The genes deleted were *SOD1* (cytosolic superoxide dismutase), *SOD2* (mitochondrial superoxide dismutase), *CCT1* (cytosolic catalase T) and *CCP1* (cytochrome *c* peroxidase). The superoxide dismutases are of particular interest since they are thought to perform one of the most important antioxidant activities in aerobic cells.

Cell density in the presence of 3 mM DETA NONOate was monitored over a 12 hour period from late exponential phase. The inhibitory effect of NO donor on growth of the deletion strains was not significantly different to that observed in the control (Figure 4.6A). The Δ*sod1* strain did appear slightly less sensitive than the control. However, this is likely due to the comparatively slow growth of this strain in the absence of DETA NONOate; it seems that deletion of the cytoplasmic superoxide dismutase is in itself deleterious, as has been reported previously (Longo et al., 1996). The data did not provide any evidence to suggest involvement of ROS in the cytostatic effect of NO donor.

4.2.6. The NO donor has a deleterious effect on cell proliferation in the absence of a respiratory chain

NO is a potent inhibitor of cytochrome oxidase. Additionally, RNS have been demonstrated to damage several components of the respiratory chain. Therefore it seems possible that the antimicrobial action of NO could be a consequence of deleterious action on the respiratory chain. To investigate whether a respiratory chain was required for the cytostatic effect I assessed the effect of DETA NONOate on cells with impaired respiratory function: cells treated with 8 μM myxothiazol immediately prior to addition of DETA NONOate (intact but inhibited respiratory chain); and rho^0 cells (absent respiratory chain). In both cases growth before addition of NO donor was decreased by around 25% compared to the control, since the cells could rely only on fermentation.

When 3 mM DETA NONOate was added growth was further inhibited by 30-35% after 12 hours, while 1 mM DETA NONOate had little or no effect (Figure 4.6B). These data suggest that at a high concentration, the NO donor has an inhibitory effect on yeast growth independently of a functional respiratory chain. However, at lower concentration this does not seem to be the case. The apparent weaker cytostatic effect of 3 mM NO donor observed in cells with impaired respiratory function might be due to their slower growth prior to NO donor addition, mirroring the situation with the Δ*sod1* strain described in 4.2.5. Slower growing cells could be less sensitive to NO/RNS damage, perhaps due to their having more time in each cell cycle to repair the damage.

4.2.7. Sites of ROS production in yeast

Although I did not find evidence to implicate ROS in the antimicrobial action of DETA NONOate, it was interesting to attempt to determine the main sites of ROS production in yeast, with a view to determining the effect of NO on ROS production. To this end, I used a number of yeast strains with deletion of components of various respiratory complexes: the internal NADH dehydrogenase, the two external NADH dehydrogenases, succinate dehydrogenase, the bc_1 complex and cytochrome oxidase, in addition to a strain with deletion of *CAT5*, involved in quinol biosynthesis. The strains were exposed to probes (dihydrorhodamine 123, carboxy-H_2DCFDA, dihydroethidium) designed to fluoresce when in contact with ROS. Dihydrorhodamine 123 and carboxy-H_2DCFDA both detect hydrogen peroxide and peroxynitrite. Carboxy-H_2DCFDA also detects peroxyl radicals ($ROO^{\cdot}$), and dihydroethidium detects superoxide. Quantitation of fluorescence was attempted by fluorimetry and confocal microscopy (as described in 2.1.10 and 2.1.11).

In fluorimetry, a low cell number (3.10^5 cells) per assay exhibited a similar fluorescence to no cells, with any concentration of probe used. Increasing the cell number resulted in higher signals, especially if a high concentration of probe was used, but fluorescence was not strikingly higher, indicating that the cells may be quenching the fluorescence. The yeast cells had a high degree of natural fluorescence, measured by both fluorimetry and confocal analysis, which varied with strain. Such autofluorescence has been observed previously in yeast and was suggested to be due to sources including reduced nicotinamide nucleotides and oxidised flavins (Knight et al., 1999; Billinton and Knight, 2001). Fluorescence in the presence of probe often did not therefore increase above that observed in the absence of probe. Use of higher concentrations of probe served to increase the autofluorescence, so did not alleviate the problem.

Additionally, replicates were variable and results were not comparable between different experiments. Significant error was likely to be introduced through washing the cells, but this was required to remove the growth medium, which itself fluoresced. To assess whether this error was important I corrected results for cell density of the resuspended cells, but the variations observed could not explain the results.

To determine whether the small increases in fluorescence observed in the presence of probe were due to ROS, antimycin, well documented to increase ROS production (for example (Boveris and Cadenas, 1975; Rasmussen et al., 2003)), was added to wild type cells. However, antimycin caused an increase in autofluorescence, again allowing only small changes in fluorescence on addition of probe. In conclusion, I was not able to show that it was ROS which were measured by the fluorescence changes on addition of probe, differences in fluorescence were very small anyway, and the results were highly variable. Therefore I did not pursue this line of research further.

4.2.8. Prolonged treatment with NO donor severely decreased cytochrome oxidase content

Prolonged incubation of mammalian cells with NO, especially at high concentrations, causes irreversible damage to respiratory function (see for example (Clementi et al., 1998)). To further investigate the effect of NO donor on the yeast respiratory chain, cytochrome levels were assessed after prolonged incubation with DETA NONOate. Firstly, as a control, the variations in cytochrome (c + c_1, b, a + a_3) levels and oxygen consumption were assessed at stages of growth from late exponential phase (9.10^7 cells per ml) through early stationary phase (3.10^8 cells per ml) to stationary phase (8.10^8 cells per ml), in the absence of DETA NONOate. Cells were grown in the same way as described previously, and at several time points were harvested and washed. Cytochrome content was assessed by spectroscopy (see 2.3.2) and oxygen consumption was assessed with an oxygen electrode (see 2.3.3). The results are shown in Table 4.1. Levels of all the cytochromes measured had a tendency to increase over growth. The overall oxygen uptake of the cells seemed reasonably constant, but cytochrome oxidase activity decreased after cells had reached stationary phase, falling from around 500 to around 330 electrons per second.

To test the effect of prolonged NO donor incubation on the respiratory chain, cells were cultured from late exponential phase in the presence of 3 mM DETA NONOate, then harvested for analysis at intervals over the next 12 hours. Pellets were washed thoroughly to remove any residual NO reversibly bound to cytochrome oxidase.

The change in cytochrome level with duration of treatment is shown in Figures 4.7A and B. Cytochrome level (pmol per 10^6 cells) was compared with that measured immediately prior to addition of NO donor. The NO donor had a differential effect on the cytochromes. By 4 hours of DETA NONOate treatment (approx. one cell division) the levels of all the cytochromes measured had decreased to around 50% of their original levels. After this, cytochromes *b* and $c + c_1$ levels began to increase and recovered to their original levels after 12 hours (approx. two cell divisions). In contrast, cytochrome oxidase exhibited a further dramatic decrease to just 10% of the original level.

The effect of different concentrations of DETA NONOate on cytochrome oxidase was also assessed (Figure 4.7C). Addition of 0.1 mM DETA NONOate had no effect on cytochrome oxidase levels after 12 hours. After 12 hour treatment with 1 mM NO donor the concentrations of cytochromes $c + c_1$, *b* and $a + a_3$ were 0.30, 0.18 and 0.04 pmol per 10^6 cells, respectively. This is compared to 0.29, 0.21 and 0.01 pmol per 10^6 cells in 3 mM-treated cells, indicating a less severe effect on cytochrome oxidase.

The analysis was repeated with another strain, FY1679 Δ*yhb1*. The growth rate of this strain showed a similar sensitivity to NO donor as BY4741 Δ*yhb1* (Figure 4.8, compare to Figure 4.2B). However the effect on cytochrome oxidase content was more rapid, and cytochrome oxidase was completely abolished after 6 hours incubation (Figure 4.9). By this point no oxygen consumption could be measured. Cytochrome *c* level in this strain was 0.08 pmol per 10^6 cells compared to 0.15 pmol per 10^6 cells in untreated cells after 6 hours, which may reflect the decrease observed after 6 hours in the BY4741 Δ*yhb1* strain. Cytochrome *b* level, however, did not appear to be sensitive to NO donor treatment after 6 hours.

4.2.9. The decrease in cytochrome oxidase content is specific to NO donor

Since NO donor inhibits respiration, the dramatic effect on cytochrome oxidase content might have been caused in some way by blockage of the respiratory chain. If this were the case it might be expected that a similar effect would be observed if the respiratory chain was blocked by another means. To test this the effect of carbon monoxide, which acts specifically at the active site of cytochrome oxidase, on late exponential phase cells was monitored (see 2.1.8 for experimental detail). Cytochrome content was not diminished. After 6.5 hour incubation cytochrome levels increased: $c + c_1$ from 0.29 to 0.62; *b* from 0.16 to 0.40; $a + a_3$ from 0.05 to 0.13 pmol per 10^6 cells. However, in this experiment the concentration of carbon monoxide was not measured, so it is not clear

whether the amount of carbon monoxide supplied to the cells was sufficient to inhibit respiration, or to what degree respiration was inhibited. Additionally, the experimental conditions differed slightly from those used in the other experiments described in this chapter (see 2.1.8), so the results may not be directly comparable.

As a further test, late exponential phase cells were treated with an inhibitory dose (8 μM) of the bc_1 complex specific inhibitor myxothiazol (see Figure 4.2C) and cytochrome content was measured after 6 and 12 hours of incubation (Table 4.2). Although yeast growth rate was decreased to around that observed on incubation with 1 mM DETA NONOate, levels of all the cytochromes increased throughout growth, as observed in the control (Table 4.1). Taken together, these data suggest that the decrease in cytochrome oxidase observed after treatment with NO donor is specifically due to NO/RNS, and not simply due to an inhibition of respiration.

4.2.10. NO donor has little effect on cytochrome content in stationary phase cells

In 4.2.8 I showed that NO donor had a severe effect on cytochrome oxidase level when added to rapidly dividing cultures in late exponential phase. I wanted to determine whether the same was true for slowly dividing cultures. The analysis was therefore repeated for cells which had been grown to early stationary phase (approx 3.10^8 cells per ml) prior to addition of NO donor. As shown in Figure 4.2B, these cultures undergo only one doubling before reaching stationary phase. The results are presented in Table 4.3. In contrast to the late exponential phase cells, the levels of all the cytochromes measured remained steady, even after 26 hours of treatment with NO donor. The activity of cytochrome oxidase fell from 591 to around 300 electrons per second after 6-12 hours treatment, mirroring the decrease in activity observed in untreated cells: when cells were grown from a density of about 3.10^8 to about 8.10^8 cells per ml (6 hours) in the absence of NO donor, cytochrome oxidase activity decreased from 591 to 333 electrons per second. This indicates that in early stationary phase cells NO donor does not irreversibly inhibit cytochrome oxidase, at least after 6-12 hours of incubation. However NO does seem to arrest cell proliferation and the accumulation of cytochromes; as untreated cells progress through stationary phase an increase, almost a doubling, in the levels of all the cytochromes is observed (Table 4.1), but this is not seen in NO donor-treated cells (Table 4.3). Additionally, cellular oxygen consumption progressively decreased over the 26 hours of NO donor treatment. This is likely due to the lower amount of cytochrome oxidase present per cell when compared to untreated cells.

4.3. DISCUSSION

4.3.1. Inhibitory effect of NO on cell proliferation

Proliferation of yeast cultures was inhibited by DETA NONOate, but only in the absence of the *YHB1* gene (Figure 4.2A). 3 mM DETA NONOate was required to elicit a severe growth repression, while 1 mM caused slight repression and 0.1 mM had no effect (Figure 4.2B).

However, the oxygen electrode data showed that a low concentration (0.1 mM) of NO donor was sufficient to completely inhibit respiration in Δ*yhb1* cells added to fresh medium in the oxygen electrode chamber (Figure 4.1). It might therefore have been expected that this concentration of NO donor would have had some deleterious effect on yeast growth. In galactose, when respiration is abolished, the growth rate should decrease as demonstrated by the effect of an inhibitory concentration of myxothiazol, a specific inhibitor of the bc_1 complex (Figure 4.2C). However, 0.1 mM of NO donor did not affect growth rate. It seems that the two systems, growth curve and oxygen electrode, give rise to differing sensitivities to NO donor. The ratio of cells to DETA NONOate was four times higher at the beginning of the growth curve experiment than in the oxygen consumption assay (approx. 2.10^7 compared to 5.10^6 cells per μmol DETA NONOate). This might help to explain why cells in the growth assay appear less sensitive to NO donor. Another possibility is that, due to harvesting and resuspension, cells are more stressed when they are placed in the oxygen electrode chamber, which may mean that defence systems are not able to deal adequately with the NO supplied. Furthermore, it is difficult to be sure that the concentration of NO released in the two systems is the same. The pH of the media used in growth curves at the point of NO donor addition was lower than that of the fresh media in the electrode chamber, since cells had already been growing in it (see 2.1.8). Therefore NO release might have been expected to be higher in the growth assays. However, the growth assay media may have been modified in such a way by metabolic products that NO release by DETA NONOate, or the concentration of NO/RNS sensed by the cells, was lower than in the fresh media. In addition to this, the oxygen consumption was measured during the first few minutes after NO inhibition, while the cell proliferation was monitored over a much longer time frame. It may be that initially respiration is completely inhibited by 0.1 mM NO donor, but the cells respond to this in such a way that the repression is relieved, perhaps by upregulating defence systems involved in removal of NO or RNS, as will be discussed in the following chapter.

I did not find evidence to suggest that DETA NONOate has a cytotoxic effect on *S. cerevisiae*, rather a cytostatic effect seems to be in operation. In addition to this NO donor did not appear to exert any mutagenic effect on the mtDNA. In this study I did not attempt to distinguish between NO and NO-derived RNS, but was interested in the overall effect of NO as an antimicrobial agent. However, I did assess the involvement of ROS in the antimicrobial effect. I monitored the effect of the NO donor on proliferation of strains with deletion of genes involved in oxidative stress defence (Figure 4.6A) and found no evidence to suggest involvement of ROS in the observed deleterious effect. Moreover, in the absence of a respiratory chain, the main site of ROS production, inhibition of cell proliferation still occurred with 3 mM NO donor (see next paragraph), further suggesting no major ROS involvement.

Since NO is a powerful inhibitor of cytochrome oxidase, and RNS have been demonstrated to damage respiratory chain components, the inhibition of yeast proliferation could be a consequence of adverse action on the respiratory chain. However, the effect of 3 mM DETA NONOate cannot be exclusively due to this since a deleterious effect was observed even when the respiratory chain was absent or compromised (Figure 4.6B). In contrast, 1 mM DETA NONOate failed to cause further decrease in growth from that due to the respiratory deficiency. It may be that at lower concentrations DETA NONOate inhibits the respiratory chain to cause an antimicrobial effect, while at high concentrations the growth inhibition is due to the combined effects of inhibition of the respiratory chain and further deleterious effects on other targets. Inhibition of the respiratory chain, whether reversible or irreversible, cannot solely account for the observed cytostatic effect on yeast.

4.3.2. Possible mechanisms for the inhibition of proliferation

NO has two particular targets, which are well characterised: the heme of the soluble guanylate cyclase, and the binuclear centre of cytochrome oxidase. It is feasible that NO could target other heme-containing enzymes. However RNS have a much wider range of targets. In similar conditions to those used here, it was shown that Δ*yhb1* yeast grown for an hour in the presence of 3 mM DETA NONOate had a ten-fold higher level of nitrosylation of multiple high mass complexes than wild type yeast treated in the same way (Liu et al., 2000). Since cells in my experiments were exposed to NO donor for a much longer time period, it seems likely that high levels of protein nitrosylation could be occurring in these experiments. Additionally, Ramachandran *et al.* showed that prolonged exposure of bovine endothelial cells to DETA NONOate caused an increase

in the levels of cysteine S-nitrosothiols and other nitrosated species (e.g. iron nitrosyl compounds, N-nitrosamines) (Ramachandran et al., 2004). NO and RNS could conceivably react with many targets to impair essential cellular activities and lead to cell growth inhibition.

Ribonucleotide reductase, the rate-limiting enzyme in DNA synthesis, has been documented as a target of NO/RNS. NO generated by macrophages caused growth arrest in tumour cells partly through inhibition of ribonucleotide reductase (Kwon et al., 1991). Such inhibition could be implicated in the inhibition of yeast growth. Another possiblility could be inhibition of enzymes involved in ergosterol biosynthesis. Ergosterol is a vital fungal cell wall constituent, and the ergosterol biosynthetic pathway is a major target of antifungal drugs (Lupetti et al., 2002). Several enzymes in the ergosterol biosynthesis pathway contain cytochrome P450, which is known to be inhibited by NO (Minamiyama et al., 1997; Roberts et al., 1998; Quaroni et al., 2004). DETA NONOate has been shown to inhibit steroid hormone synthesis in mammalian cells by inhibiting activity of several cytochrome P450-containing enzymes (Hanke et al., 1998). Effects of NO on other targets will be further discussed in the following chapter.

4.3.3. Severe decrease in cytochrome oxidase level after NO donor exposure

Prolonged exposure of late exponential phase cells to high concentrations of NO donor caused a severe decrease in cytochrome oxidase content, as judged by the heme aa_3 signal (Figure 4.7). The same effect was not observed for cytochromes *b* and $c + c_1$. The severe decrease could be due to a dissociation or degradation of cytochrome oxidase induced by DETA NONOate. Alternatively NO donor may be hampering synthesis of new cytochrome oxidase. As discussed in the previous chapter, failure to assemble cytochrome oxidase results in rapid degradation of subunits, in particular the core subunits Cox1p, Cox2p and Cox3p, resulting in an absence of the heme aa_3 signal.

There have been several reports in the literature regarding NO/RNS-induced loss of cytochrome oxidase. Ramachandran *et al.* showed that in bovine endothelial cells prolonged exposure to 0.5 mM DETA NONOate resulted in a decrease of NADH dehydrogenase, succinate dehydrogenase and cytochrome oxidase protein levels and activities (Ramachandran et al., 2004). The decrease in activity was reversible for succinate dehydrogenase and cytochrome oxidase when NO was removed (NADH dehydrogenase was not assessed), but in the case of cytochrome oxidase this reversibility was dependent on new protein synthesis.

Prolonged incubation of smooth muscle cells with azide caused an irreversible loss of cytochrome oxidase activity and loss of heme aa_3 signal (Leary et al., 2002). No decrease in mRNAs encoding several cytochrome oxidase subunits was observed, and steady state subunit levels were unaltered. However, significant pools of unassembled mitochondrial subunits were detected on blue native gels and cytochrome oxidase content as determined by absorbance spectra was decreased. The authors suggested that the treatment caused structural damage, likely around the heme groups, and dissociation of existing cytochrome oxidase (Leary et al., 2002).

Additionally, Sharpe and Cooper demonstrated that peroxynitrite treatment caused irreversible inhibition of purified cytochrome oxidase. This was associated with loss of the Cu_A absorption band and, at higher peroxynitrite concentrations, loss of hemes *a* and a_3 (Sharpe and Cooper, 1998).

4.3.4. Possible disruption of cytochrome oxidase synthesis

In the data presented here, cytochrome oxidase levels only decreased on DETA NONOate treatment of late exponential phase cells, and not early stationary phase cells. In this discussion, to simplify, I will refer to late exponential phase cells as 'dividing cells' and early stationary phase cells as 'non-dividing cells'. Even after 26 hours of exposure to DETA NONOate no decrease in cytochrome oxidase content was observed in non-dividing cells. Therefore it seems unlikely that the low level of cytochrome oxidase in dividing cells after NO donor treatment could be solely due to degradation of existing enzyme. It is more likely that the decreased cytochrome oxidase content is due to a lower synthesis of the enzyme in the presence of NO donor. In dividing cultures there is both a higher energy demand and a requirement for new enzymes for daughter cells, hence respiratory complex synthesis will be higher than in non-dividing cultures. Therefore the effects of NO donor on cytochrome oxidase levels would be more evident in this type of culture. Decreased synthesis of cytochrome oxidase could be brought about through various mechanisms including alteration of mRNA synthesis or stability, or a defect in the process of subunit assembly (involving cytochrome oxidase subunits or one of the many assembly factors).

4.3.4.1. mRNA changes

Several studies have reported specific modifications in mRNA levels of mitochondrially-encoded proteins as a result of NO treatment. Gou *et al.* and Wei *et al.* showed that on prolonged treatment of macrophages with LPS (which induces iNOS synthesis) the levels of cytochrome *b* and Cox1p mRNA and protein decreased (Gou et

al., 2001; Wei et al., 2002). This was not due to repressed transcription, rather to increased mRNA degradation, which the authors suggested was perhaps to be expected since the mitochondrial genes are transcribed as polycistronic precursor RNAs. However, Nicoletti *et al.* showed that LPS induction of iNOS in mixed cortical and astroglial cultures caused an increase in mRNAs for Cox1p, Cox2p and Atp6p (Nicoletti et al., 1998). This was reversed by addition of superoxide dismutases and catalase, indicating an involvement of ROS. The authors proposed that the cells were attempting to compensate for the accumulation of damaged subunits of the respiratory chain. In a study using the NO donor DEA NONOate, Lehrer-Graiwer *et al.* also showed that macrophage Cox1p mRNA and protein levels increased after short treatment (Lehrer-Graiwer et al., 2000). There seems to be no consensus on the effect of NO on mRNA levels, and observations may depend on the length of treatment and system used.

In the following chapter I describe the effect of short DETA NONOate exposure on genomic expression profiles. After 60 minutes the treatment resulted in a decrease in expression of a number of genes encoding subunits of respiratory chain complexes, and levels remained low even after 2 hours (Table 4.4). Subunits or assembly factors of all respiratory chain complexes were repressed in the analysis. The repression was not specific to cytochrome oxidase subunits: components of the bc_1 complex, for example, were repressed to a similar, if not more severe, extent. This repression may therefore account for the decrease in levels of cytochromes $c + c_1$, b and $a + a_3$ after 2 to 6 hours of DETA NONOate treatment, but is unlikely to be the cause of the further severe decrease in cytochrome oxidase content after prolonged exposure. However, mRNA levels were followed over only a 2 hour period, so the possibility remains that transcription of genes encoding cytochrome oxidase subunits could remain suppressed over a longer period, while genes encoding subunits of other respiratory complexes could have an increased expression later on, helping to restore levels of these enzymes in the cell. While it is possible that alterations in mRNA expression or stability may cause a specific decrease in cytochrome oxidase levels, the evidence does not point in favour of this.

4.3.4.2. Alterations in cytochrome oxidase assembly

The differential effect of DETA NONOate on the cytochrome oxidase level in dividing and non-dividing cells might be explained by its interfering with the physical assembly of cytochrome oxidase. Assembling enzyme might be particularly susceptible to interference by NO or RNS as potentially reactive sites could be more accessible.

Insertion of the heme or copper centres into the enzyme may be subject to interference. NO and RNS have been shown to react with protein-bound metal centres, with thiols and with tyrosines. There are therefore several possible targets in cytochrome oxidase for NO and its derivatives.

One target could be the cysteine ligands of the Cu_A site. The copper atoms of the *P. denitrificans* and bovine enzymes are bridged by two cysteine residues of Cox2p (Iwata et al., 1995; Ostermeier et al., 1997; Tsukihara et al., 1996) and in yeast they are likely to be bound in a similar manner. Sharpe and Cooper demonstrated that peroxynitrite treatment caused irreversible inhibition of purified cytochrome oxidase associated with irreversible loss of the Cu_A signal. It was suggested that peroxynitrite reacts with the Cu_A site, through oxidation of the thiol ligands (Sharpe and Cooper, 1998). It is possible that RNS may react with these cysteines in the nascent enzyme, and S-nitrosation or oxidation of the thiol groups is likely to hinder the binding of copper in the assembling enzyme. In Chapter 3, I showed that mutations in the Cu_A site caused assembly of cytochrome oxidase to be abolished. It can be suggested that in these mutants formation of the Cu_A site is impaired, hindering the folding of Cox2p, and leading to impaired enzyme assembly and consequent degradation of cytochrome oxidase subunits. The cysteine ligands may be particularly vulnerable to S-nitrosation in the nascent enzyme but protected in the assembled enzyme.

A second possibility is reaction with radical tyrosines to form nitrotyrosine. Cox1p contains several tyrosine residues which are conserved between yeast, human and cow (yeast residues 18, 130, 232, 245, 262, 304, 371, 372, 379 and 443). Peroxynitrite has been shown to induce formation of nitrotyrosine in other proteins (Ischiropoulos, 1998), so tyrosine residues could be targets of RNS in cytochrome oxidase. A highly conserved residue of particular interest is the redox-active tyrosine 245 (yeast numbering), which forms a radical tyrosyl in a catalytic intermediate of cytochrome oxidase (Proshlyakov et al., 2000). NO is likely to be very reactive with this radical. The equivalent residue tyrosine 244 in the bovine enzyme is close to the heme a_3-Cu_B centre, and is covalently linked to histidine 240 (yeast H241), a ligand of Cu_B (Ostermeier et al., 1997) (Figure 4.10). Site-directed mutagenesis of the equivalent tyrosine residue (Y288) in the *Escherichia coli* cytochrome bo_3 ubiquinol oxidase, part of the heme-copper oxidase superfamily, demonstrated that it was essential for the assembly of the Cu_B site (Thomas et al., 1994). Mutants Y288A/F/H/S had an inactive enzyme, assembled hemes *b* and o_3, but had a highly disrupted environment around heme o_3 and a loss of Cu_B. Y288F was also studied in *R. sphaeroides* by optical and

Raman spectroscopy. The enzyme was again inactive, and found to have hemes *a* and a_3 present but Cu_B absent (Das et al., 1998). So, alteration of this tyrosine causes the structure of the binuclear centre to be severely disrupted. It was postulated that in Y288F, the cross-link between Y288 and the histidine could not form, and that this cross-link holds the heme a_3-Cu_B structure in the correct configuration to allow catalytic activity (Das et al., 1998). It is possible that RNS may nitrate tyrosine 245 during assembly of cytochrome oxidase, impairing Cu_B binding. This is likely to cause disruption of assembly of the heme a_3-Cu_B centre and consequent disruption of enzyme assembly.

4.3.5. Conclusions

Prolonged incubation with high concentration of NO/RNS had a severe inhibitory effect on growth of yeast with deletion of the *YHB1* gene encoding the highly efficient NO oxidoreductase Yhb1p. However, the treatment was not cytotoxic and did not cause mtDNA mutation. The effect on cell proliferation did not seem to involve ROS, and was still observed when the respiratory chain was absent or compromised by myxothiazol, indicating that it was not simply due to inhibition of the respiratory chain. The levels of respiratory chain complexes were, however, altered by NO/RNS treatment, and in particular the assembly of cytochrome oxidase seemed to be compromised. To further characterise the antimicrobial activity of NO/RNS on yeast, alterations in gene expression caused by NO donor were next assessed.

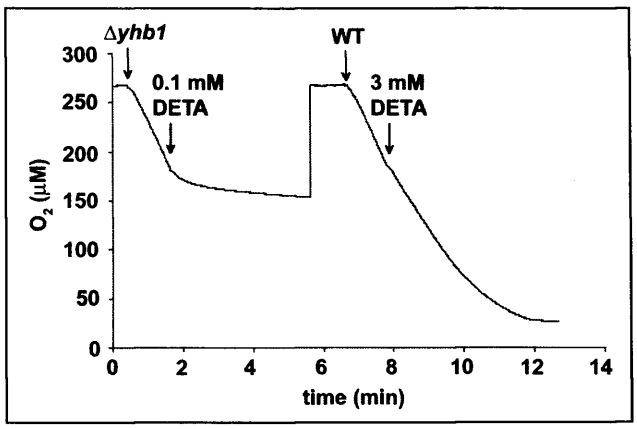

Figure 4.1. Effect of NO donor on oxygen consumption by yeast cells.

Wild type BY4741 cells and BY4741 Δ*yhb1* cells lacking the NO-scavenging enzyme Yhb1p were grown to late exponential phase and oxygen consumption measured. DETA NONOate (concentrations indicated) was added and the effect on oxygen consumption monitored.

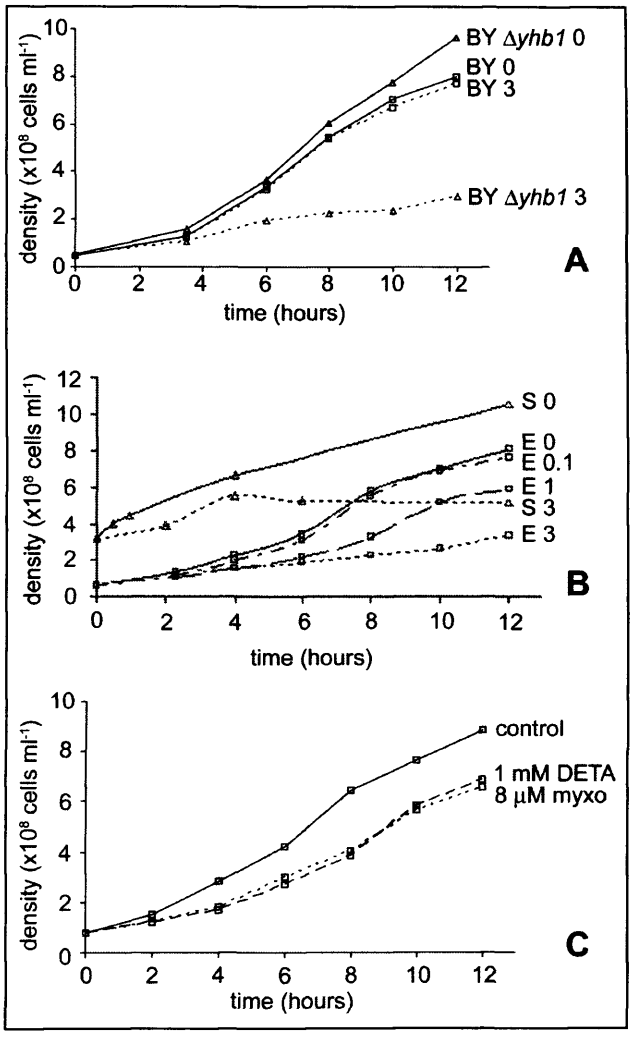

Figure 4.2. Effect of NO donor on yeast proliferation.

A. Wild type BY4741 and mutant BY4741 Δ*yhb1* cells were grown to late exponential phase then incubated with 0 or 3 mM DETA NONOate for 12 hours. **B.** BY4741 Δ*yhb1* cells were grown to late exponential (E) or early stationary (S) phase then incubated with 0, 0.1, 1 or 3 mM DETA NONOate for 12 hours. **C.** BY4741 Δ*yhb1* cells were grown to late exponential phase then incubated untreated (control), or with 1 mM DETA or 8 μM myxothiazol (a specific inhibitor of the bc_1 complex) for 12 hours. Cell density was measured at intervals. The graphs are representative of at least 3 independent experiments.

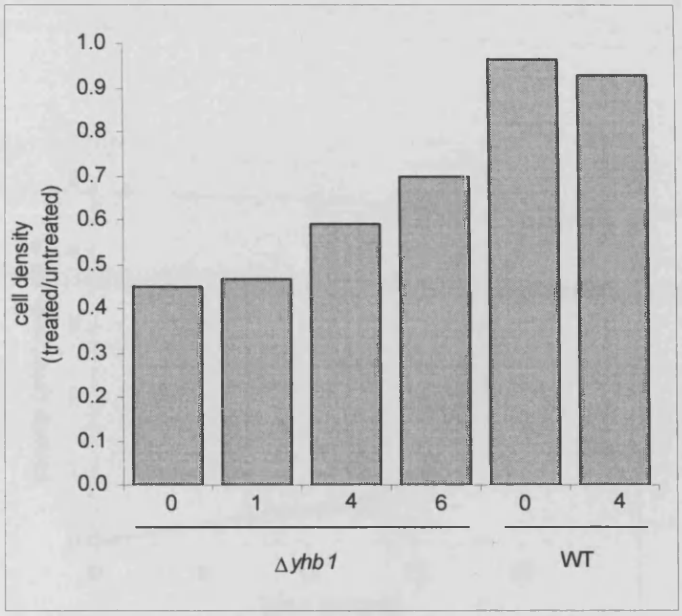

Figure 4.3. Effect of decomposed NO donor on yeast proliferation.
Growth of wild type and Δ*yhb1* cells after 12 hours incubation with 3 mM decomposed DETA NONOate was compared to growth of untreated cells. 0, 1, 4 and 6 denote the number of days DETA NONOate was allowed to decompose at 37°C prior to addition to cultures.

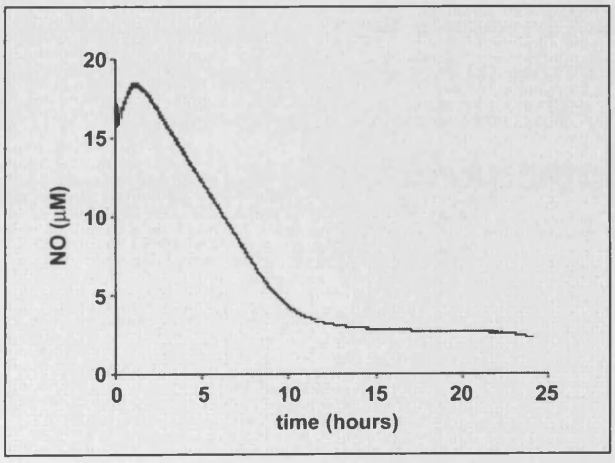

Figure 4.4. NO released upon addition of 3 mM DETA NONOate to the culture medium.
Cells were grown to late exponential phase, an aliquot was transferred to the NO electrode chamber, and 3 mM DETA NONOate was added. The concentration of NO was monitored for 24 hours. The graph is representative of two experiments.

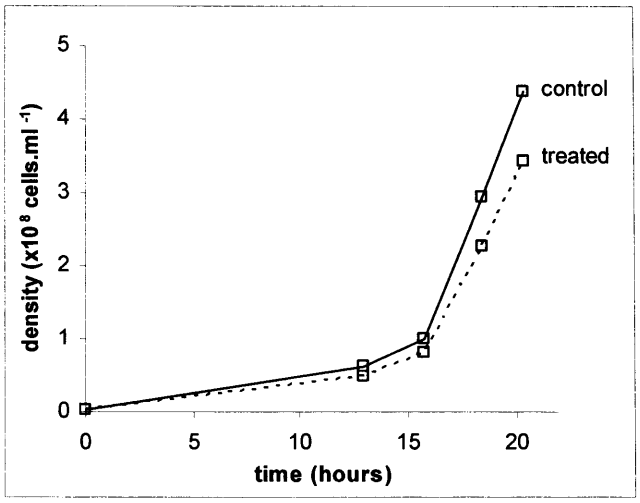

Figure 4.5. Viability of yeast cells after NO donor exposure.

Cultures were grown in the presence of 0 or 3 mM DETA NONOate for 12 hours. Cells were harvested, washed twice with water, then resuspended cells were used to inoculate fresh YPGal media to A_{600nm} = 0.05. After 13 hours growth the new cultures reached late exponential phase, and cell density was monitored over the 7.5 hours following this.

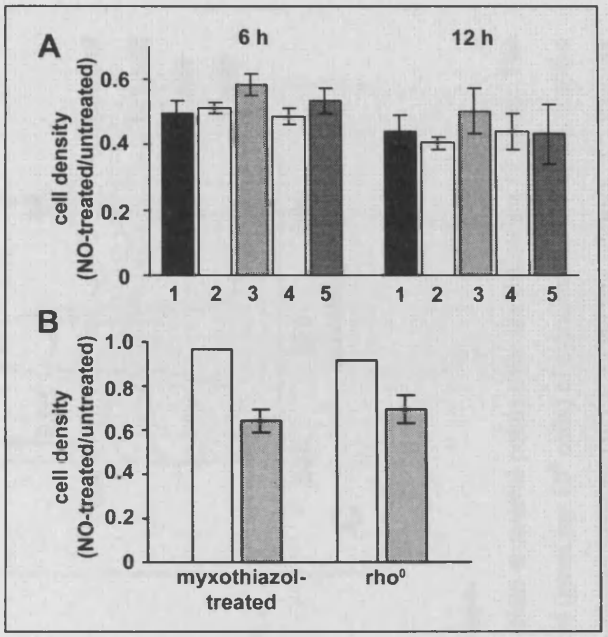

Figure 4.6. Effect of NO donor on the growth of cells with a non-functional respiratory chain, and on cells lacking components of the oxidative stress response system.

A. Cells were grown to late exponential phase then incubated with 0 or 3 mM DETA NONOate for 12 hours, and cell density measured at intervals. Density of NO donor-treated cultures is shown at two time points for several Δ*yhb1* strains lacking components of the oxidative stress response system: 1, FY1679; 2, FY1679 Δ*ctt1*; 3, FY1679 Δ*sod1*; 4, FY1679 Δ*sod2*; 5, FY1679 Δ*ccp1*. **B.** BY4741 Δ*yhb1* and BY4741 Δ*yhb1* rho^0 cells were grown to late exponential phase. 8 μM myxothiazol was added to the BY4741 cells then 0, 1 or 3 mM DETA was added to both BY4741 and BY4741 rho^0 cells. Cell density was monitored over 12 hours, and density of cultures treated with 1 mM (white) or 3 mM (grey) NO donor compared to untreated cells after 12 hours is shown. Where error bars are shown these represent ± the standard deviation from at least two independent experiments.

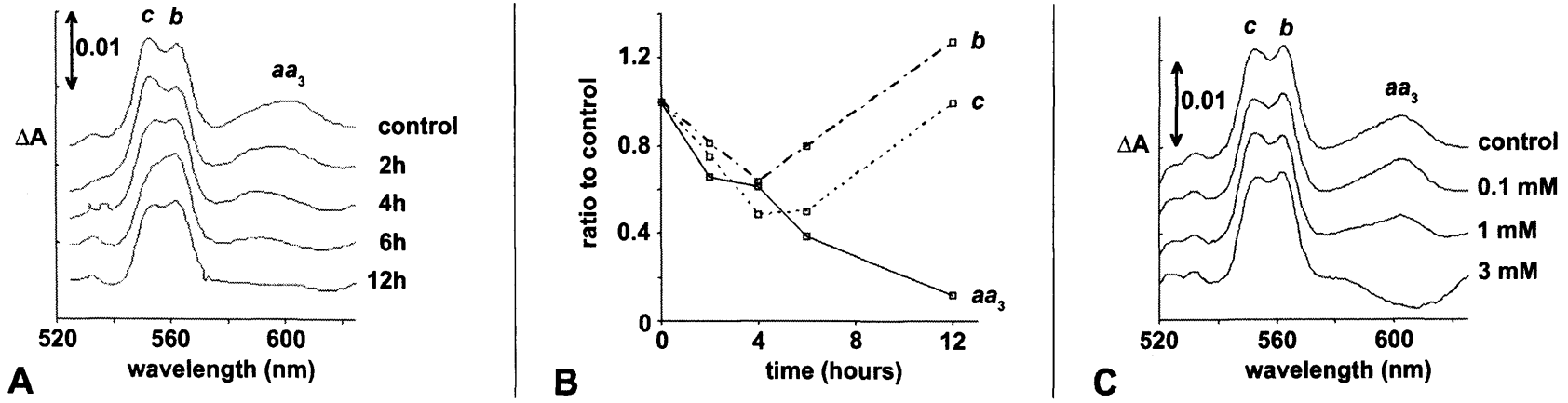

Figure 4.7. Change in cytochrome content on NO donor treatment of cells in late exponential phase.

A. 3 mM DETA was added to BY4741 Δ*yhb1* cells at 9.10^7 cells per ml density and spectra were taken at several points over the following 12 hours. The spectra were normalised for cytochrome *b* signal. Data are representative of 5 experiments. **B.** Content (pmol per 10^6 cells) of cytochromes $c + c_1$ (c), *b* and $a + a_3$ (aa_3) after addition of 3 mM NO donor is expressed as a ratio compared to control values obtained prior to DETA NONOate addition. **C.** Varying concentrations of DETA NONOate were added to cells at 9.10^7 cells per ml density and cytochrome content was measured after 12 hours. The spectra were normalised for cytochrome *b* signal.

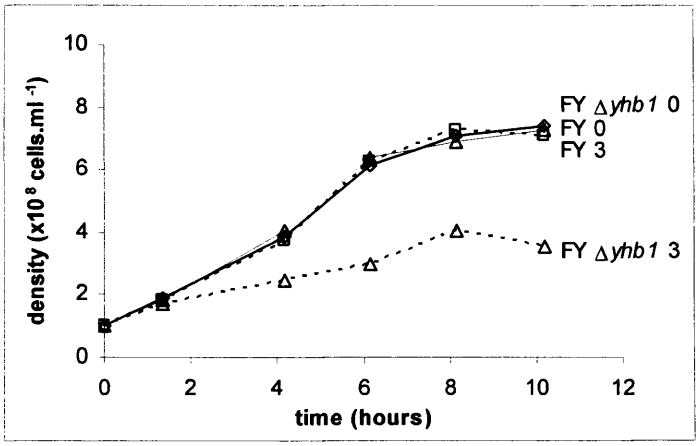

Figure 4.8. Effect of NO donor on FY1679 proliferation.

FY1679 wild type and Δ*yhb1* cells were grown to late exponential phase then incubated with 0 or 3 mM DETA NONOate for 12 hours. The graphs are representative of two independent experiments.

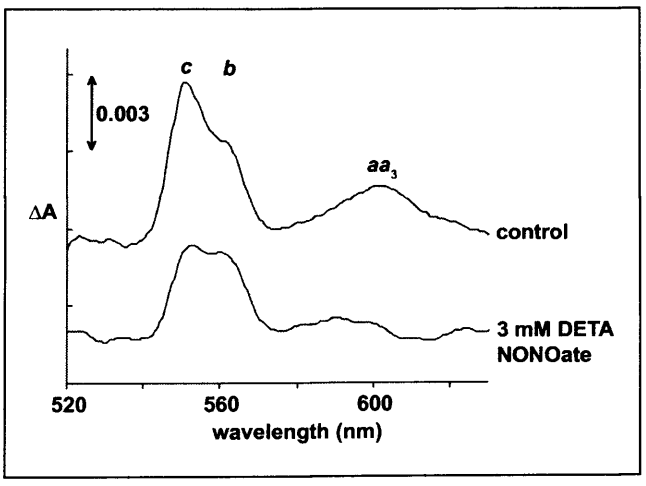

Figure 4.9. Cytochrome levels after NO donor treatment of FY1679 Δ*yhb1*.

3 mM DETA NONOate was added to exponential phase cells and spectra were taken after 6 hours incubation.

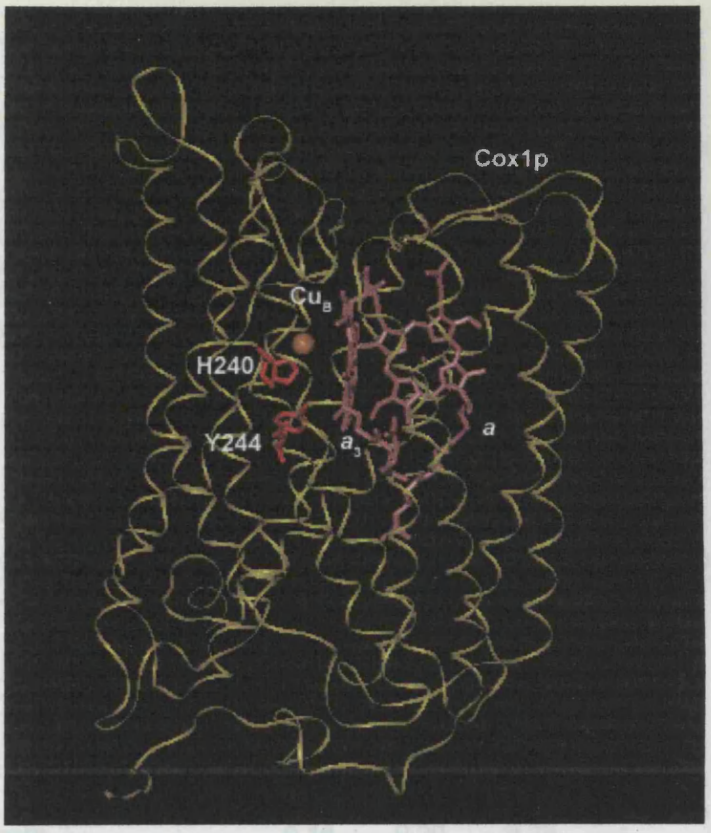

Figure 4.10. Tyrosine 244 in bovine COX1.

The atomic structure is from the bovine enzyme (PDB 1OCC), and residues are identified using the bovine numbering. Cu_B is shown in orange and hemes a and a_3 in pink.

Table 4.1. Variation in cytochrome levels and oxygen consumption in control cells.

BY4741 Δ*yhb1* cells were grown in YPGal and harvested at several growth stages. Cytochrome content and oxygen consumption were determined as described in 2.3.2 and 2.3.3. Time points represent hours from late exponential phase (0 = late exponential, 6 = early stationary, 12 = stationary phase). Data are representative of three experiments.

Time (hours)	0	6	12
Density ($x10^8$ cells ml^{-1})	0.9	2.6	7.8
Cytochrome content			
$c + c_1$ (pmol.10^6 cells^{-1})	0.29	0.20	0.39
b (pmol.10^6 cells^{-1})	0.16	0.14	0.27
$a + a_3$ (pmol.10^6 cells^{-1})	0.05	0.04	0.09
Oxygen consumption			
pmoles e^-.10^6 cells^{-1}.s^{-1}	23	23	30
e^-.cytochrome oxidase^{-1}.s^{-1}	458	591	333

Table 4.2. Cytochrome levels after myxothiazol treatment.

BY4741 Δ*yhb1* cells were grown until late exponential phase. 8 μM myxothiazol was added to aliquots of the culture and cytochrome content was measured after 6 and 12 hours (see 2.3.2).

Hours after myxothiazol addition	0	6	12
Density ($x10^8$ cells ml^{-1})	0.9	2.3	5.6
Cytochrome content			
$c + c_1$ (pmol.10^6 cells^{-1})	0.29	0.34	0.34
b (pmol.10^6 cells^{-1})	0.16	0.20	0.23
$a + a_3$ (pmol.10^6 cells^{-1})	0.05	0.11	0.14

Table 4.3. Change in cytochrome content on NO donor treatment of cells in early stationary phase.

BY4741 Δ*yhb1* cells were grown to early stationary phase then split into aliquots and 3 mM DETA NONOate added. Cells were incubated then harvested and washed at intervals, and cytochrome content and oxygen consumption assessed. Data are representative of 3 experiments.

Hours after NO donor addition	0	2	4	6	12	26
Density ($x10^8$ cells.ml^{-1})	2.6	3.9	5.5	5.3	5.2	5.6
Cytochrome content						
$c + c_1$ (pmol.10^6 cells^{-1})	0.20	0.31	0.28	0.29	0.30	0.26
b (pmol.10^6 cells^{-1})	0.14	0.21	0.20	0.20	0.20	0.17
$a + a_3$ (pmol.10^6 cells^{-1})	0.04	0.04	0.03	0.03	0.03	0.04
Oxygen consumption						
pmoles e^-.10^6 cells^{-1}.s^{-1}	23	20	15	10	9	3
e^-.cytochrome oxidase^{-1}.s^{-1}	591	557	459	354	277	58

Table 4.4. Gene expression changes after treatment with 3 mM DETA NONOate.

BY4741 Δ*yhb1* cells at exponential phase (cell density around 1.5 x 10^7 cells per ml) were incubated with 3 mM DETA NONOate for 10 to 120 minutes before RNA isolation and microarray analysis (as described in 2.5.1). Gene expression is represented as fold change compared to values obtained prior to treatment.

Complex	Gene	Description	10 min	30 min	60 min	120 min
NADH dehydrogenase	*NDE1*	External dehydrogenase	0.67	0.15	0.42	0.67
	NDI1	Internal dehydrogenase	1.10	0.25	0.12	0.08
Succinate dehydrogenase	*SDH1*	Flavoprotein subunit	0.74	0.21	0.12	0.09
	SDH2	Iron-sulfur protein	0.71	0.14	0.10	0.08
	SDH3	Cytochrome *b*	0.81	0.27	0.15	0.11
	SDH4	Membrane anchor subunit	0.85	0.35	0.17	0.14
Cytochrome *c*	*CYC1*	Isoform 1	0.79	0.05	0.02	0.01
	CYC7	Isoform 2	2.36	0.52	0.19	0.41
bc_1 complex	*CYT1*	Cytochrome c_1	0.50	0.17	0.08	0.07
	RIP1	Rieske iron-sulfur protein	0.75	0.21	0.13	0.14
	COR1	Core subunit	0.77	0.38	0.27	0.18
	QCR2	40 kDa subunit	0.86	0.29	0.17	0.14
	QCR6	17 kDa subunit	0.64	0.29	0.17	0.17
	QCR9	7.3 kDa subunit	0.75	0.42	0.32	0.35
	QCR10	8.5 kDa subunit	0.75	0.33	0.28	0.34
Cytochrome oxidase	*COX4*	Subunit 4	0.72	0.42	0.35	0.28
	COX5A	Subunit 5a	0.62	0.22	0.21	0.17
	COX6	Subunit 6	0.67	0.50	0.34	0.37

Chapter 5

TRANSCRIPTIONAL CHANGES INDUCED BY NO/RNS

5.1. INTRODUCTION

Reactive nitrogen species (RNS) have multiple targets and are likely to have a wide range of actions on the cell. In Chapter 4 I characterised the effect of prolonged exposure to nitric oxide (NO) donor on cell proliferation and on the cytochromes of the respiratory chain. NO donor had a cytostatic effect and caused a specific decrease in the level of cytochrome oxidase.

5.1.1. Aims

To gain more information on the stresses sensed by the cell on NO/RNS treatment, and the responses to these stresses, I used microarray technology to perform a genome-wide analysis of expression changes in response to short NO donor treatment. I monitored gene expression during the first two hours of exposure since the major alterations in gene expression are expected to be observed within this time frame. I measured the time-course effect of 3 mM DETA NONOate, a concentration which significantly inhibited growth of late exponential phase cells. I also assessed the response to varying concentrations of DETA NONOate. Additionally I used the transcriptional response of Δ*yhb1* rho^0 cells to determine the involvement of the respiratory chain in the gene expression changes caused by NO donor. The transcription factors Msn2/4p and Yap1p have been implicated in the general and the oxidative stress responses, respectively, so I investigated their involvement in the regulation of the genes altered by NO donor. I compared the results of the time-course analysis with those obtained from a study of the effect of the respiratory chain inhibitor myxothiazol on gene expression (Bourges et al., 2005) to enable identification of genes specifically altered in response to NO donor. Finally, several of the genes identified are known to be regulated by the transcription factor Hap1p, so I attempted to assess possible involvement of Hap1p in the NO donor-induced changes in gene expression.

5.2. RESULTS

5.2.1. W303-1B Δ*yhb1* sensitivity to NO donor

The strain used for the majority of the microarray analysis was W303-1B Δ*yhb1*, rather than BY4741 Δ*yhb1* used in Chapter 4. A previous microarray analysis in our lab, designed to investigate the effect of the bc_1 complex inhibitor myxothiazol on gene expression (Bourges et al., 2005), had been performed using this strain, and I wanted to be able to reliably compare my results with this study. To confirm that NO donor had the same deleterious effect on growth of the W303-1B Δ*yhb*1 strain I incubated cells from late exponential phase with 3 mM NO donor (see 2.1.8). Growth was severely inhibited by the addition of 3 mM DETA NONOate, while the control wild type strain was not affected (Figure 5.1), mirroring the effect observed on BY4741 and FY1679 (Figure 4.2A and Figure 4.8)

5.2.2. Time-course response to NO donor treatment

After growth to mid exponential phase cells were incubated for a period of 10, 30, 60 or 120 minutes with 3 mM DETA NONOate, harvested, then their RNA was extracted and used to prepare labelled cDNA for hybridisation to Affymetrix GeneChip expression arrays. The experimental procedure is described in 2.5.1. Control samples to which NO donor was not added were harvested at time zero. Data was analysed as described in 2.5.1.6. Of a total of about 6,400 nuclear genes (plus around 600 other targets including putative ORFs and mitochondrial genes) represented on the array, expression of 731 genes (after exclusion of chromosomes, *TY* elements and non-annotated SAGE ORFs) was altered after treatment at at least one time point compared to the control. These were categorised into 14 functional groups, and the number of genes altered in each group is shown in Table 5.1. Treatment with NO donor resulted in an increased number of transcripts for approximately half of these genes, with the remainder having fewer transcripts after treatment. The full set of expression data is available at http://www.ebi.ac.uk/arrayexpress/ and can be retrieved using the accession number E-MEXP-580.

Overall, the maximum repression of genes was usually observed early on, after 10 or 30 minutes of treatment. Analysis of the complete set of data showed that around 40% of the 385 repressed genes had a lowest expression after 10 minutes of treatment, and around 33% after 30 minutes. Induction of genes was more evenly spread, with

30% of the 346 overexpressed genes having maximum induction at 10 minutes, 20% at 30 minutes, 12% at 60 minutes and 38% at 120 minutes of NO donor incubation.

Many genes showed a time-course response similar to that induced by several environmental changes: immediately after the shift to stressful environment, cells respond with large changes in the expression of genes, and after a while the transcripts return to normal levels (Gasch et al., 2000). This type of transient response is typical of the environmental stress response. The most striking feature apparent from Table 5.1 is that a large number of genes (195) belonging to the category "DNA structure, replication, transcription and translation" are repressed on NO donor treatment. More than 75% of these are involved in transcription and translation. These genes typify the transient response, with repression early on in the time course and expression restored closer to control levels after 60 minutes (Figure 5.2A and B). For the overexpressed genes, such transient change was most clearly seen in the category "Protein folding and modification". Between 10 and 30 minutes of NO exposure, the expression increased 2 to 20 fold depending on the gene. Later, between 30 and 60 minutes of treatment, the expression decreased to a level closer to that observed in untreated cells. (Figure 5.2C).

Other genes showed a very different pattern of expression. For instance, the expression level of genes in the category "Response to oxidative stress" increased during the 30 minutes after NO donor addition, but transcript levels did not return to normal during the remainder of the time-course (Figure 5.2C). Similarly, expression of genes of the category "Electron transfer and ADP/ATP translocator" showed a prolonged increase (Figure 5.2C). Further analysis of transcriptional changes have been performed after 60 minutes treatment with NO donor, to obtain more information on the longer-lasting effects of NO/RNS.

5.2.3. Validation of microarray results by (RT)q-PCR

To independently validate the results of the microarray I prepared fresh cDNA from untreated cells and from cells incubated for 60 minutes with 3 mM NO donor. The samples were subjected to (RT)q-PCR analysis to determine the relative expression levels of six genes after treatment, as described in 2.5.2. The genes selected were chosen to represent the range of signal strengths and expression changes observed in microarray analysis. They were *CYC7*, repressed by 5-fold after 60 minutes; *CTT1*, repressed by 2-fold after 60 minutes; and *GPM2*, *HSP26*, *OYE3* and *GTT2*, induced by between 10 and 37-fold after 60 minutes. *ACT1* was used as a reference since it did not alter in any microarray experiment. The (RT)q-PCR data are presented in comparison to the

microarray data in Table 5.2. Although the extent of repression or upregulation observed by (RT)q-PCR is not identical to that observed by microarray analysis, the pattern of expression seen is alike.

5.2.4. Effect of different concentrations of NO donor on gene expression

The concentration of DETA NONOate used in these experiments was 3 mM, that required to significantly inhibit yeast growth (Figure 5.1). It was also interesting to determine what effect a lower inhibitory dose (1 mM) or a sub-inhibitory dose (0.1 mM) (see Figure 4.2B) had on gene expression, and whether such treatment caused a different type of response. The microarray analysis was repeated on cells incubated for 60 minutes in the presence of 1 mM and 0.1 mM DETA NONOate. When cells were treated with 3 mM NO donor, 291 genes had a significantly altered expression after 60 minutes. Of these genes, only 172 were also altered at 1 mM NO donor, and just 83 at 0.1 mM (Figure 5.3A). The average fold change in expression of the 291 genes was closer to 1 the lower the concentration of NO donor used (Figure 5.3B). When all the genes which showed alteration at any time point after 3 mM NO donor treatment, or after 60 minute treatment with 1 or 0.1 mM NO, were considered, 1 mM NO donor appeared to elicit a stronger response than 3 mM NO donor in just 48 genes of a total of 869. There were only three genes which had an altered expression level at 0.1 mM DETA but did not show a significant change at 1 or 3 mM. It seems therefore that the extent of the modification of gene expression increases with increasing concentration of NO donor, and that a novel pattern of gene expression is not observed at a sub-inhibitory dose of DETA NONOate.

5.2.5. Dependence of NO donor-induced gene expression on the respiratory chain

To assess whether the changes in gene expression observed after 3 mM DETA NONOate treatment were dependent on the respiratory chain, the strain W303-1B Δ*yhb1* rho^0, lacking mtDNA, was incubated for 60 minutes with 3 mM NO donor and the microarray analysis repeated. When the 291 genes altered after 60 minutes treatment in the control strain were analysed, the average fold change of gene expression between treated and untreated samples was closer to 1 in the rho^0 strain than in the control (3.74 versus 5.29 for the overexpressed genes, 1.19 versus 1.85 for the repressed genes), suggesting that NO donor elicited a weaker response in the rho^0 cells. The ratio "fold change in rho^0 / fold change in control" (R_1) was calculated and genes were categorised according to the impact the presence of a respiratory chain had on their expression (Table 5.3A).

An R_1 value of ≤ 0.25 (for overexpressed genes) or ≥ 4 (for repressed genes) represents a clear dependence on the respiratory chain. 35 genes of the total 291 altered in the control after 60 minutes treatment fell into this category. However 14 of these genes were already overexpressed or repressed in the untreated rho^0 compared to the untreated control; the absence of the respiratory chain caused expression change, which was not further altered by NO donor exposure. Therefore only 21 genes (7%, the majority belonging to the categories "Glycolysis, gluconeogenesis, carbohydrate storage pathway" and "Unknown genes") were found to be heavily dependent on the respiratory chain for modulation of expression. The expression change of these genes could be due to the inhibition of the respiratory chain by NO, or an indirect effect of a respiratory chain product such as ROS. The dependency of 7% of genes could not be clearly assigned to a category, while the expression of 26% of genes was clearly not affected by the absence of the respiratory chain. 161 genes (55%) had some weak reliance on the respiratory chain (R_1 value between 0.25 and 0.75). The data suggests that the overall transcriptional change is not simply due to inhibition of the respiratory chain by NO.

5.2.6. Comparison with transcriptional changes induced by myxothiazol treatment

A similar microarray analysis of the effect of an inhibitory concentration of myxothiazol, a respiratory chain inhibitor acting specifically on the bc_1 complex, on gene expression was recently performed in our lab (Bourges et al., 2005). Wild type W303-1B cells were treated with 8 μM myxothiazol for 2 to 120 minutes and the experiment was conducted using the same culture medium, conditions and method of analysis as those described here. The strain used in the myxothiazol study did not have deletion of the *YHB1* gene. To determine whether absence of *YHB1* caused significant modification of basal gene expression, I compared gene expression in untreated Δy*hb1* cells to expression in the untreated wild type cells. Only 17 genes exhibited a greater than two-fold alteration in expression between the two samples, hence it is still possible to make reliable comparison between the studies. After 2-120 minute treatment with myxothiazol, 879 genes, compared to 731 genes after 10-120 minute of NO donor treatment, were altered (Table 5.1). The larger number is probably due to the additional two minute time point. To identify those alterations in gene expression after NO donor exposure which could be classified as due to a general stress response induced by inhibition of the respiratory chain, and those which were more specific to NO donor treatment, I compared the two data sets.

5.2.6.1. Genes commonly altered by NO donor and myxothiazol

Most (477) of the 731 genes altered after DETA NONOate treatment were common to both NO donor and myxothiazol treatments (Table 5.1). For most categories, over 50% of the genes altered after DETA NONOate treatment were also altered after myxothiazol treatment. In general, the expression changes of these genes were transient on both NO donor and myxothiazol treatment (Figure 5.4A). This was particularly evident in the category "DNA structure, replication, transcription and translation", where 88% of the genes repressed in response to NO donor were also repressed by myxothiazol treatment (Figure 5.4B). Many of these genes have previously been observed to be repressed in response to several environmental changes (Causton et al., 2001). Most of the genes are involved in transcription and translation, and their transient repression represents a response to sudden environmental change associated with transient growth arrest. Similar transient responses were also observed in categories such as "Protein folding and modification" (Figure 5.2C) and "Glycolysis, gluconeogenesis and carbohydrate storage pathway" (Figure 5.2D).

5.2.6.1. Genes specifically altered in response to NO donor

265 genes were induced by NO donor incubation but not by myxothiazol incubation. The analysis of gene expression was repeated with another strain, BY4741 Δ*yhb1*, after 60 minutes exposure to 3 mM DETA NONOate, and results were similar to those observed in W303-1B Δ*yhb1* cells. Combining the results from both strains, 117 genes had a clearly altered expression after NO donor treatment, while their expression was not altered, or was altered in a different manner (induced rather than repressed), after myxothiazol treatment (Table 5.4). These 72 repressed and 45 induced genes could therefore be considered to be altered specifically in response to the NO donor and not due to a general respiratory chain inhibition stress. The expression change of none of these genes was heavily dependent on the respiratory chain (Table 5.3A).

In contrast to the pattern observed for the genes altered in response to both myxothiazol and NO donor, the modification of expression of the NO-specific genes generally persisted over the course of the experiment; overall, expression is altered in the first 10 to 30 minutes and does not return to control levels during the 2 hours assessed (Figure 5.5). This is especially striking in the category "Electron transfer and ADP/ATP translocator" (Table 5.4). 24 genes of this category were repressed specifically after NO donor treatment, half of them by 10-fold or more, and transcript

levels tended to progressively decrease over time. The overexpressed categories "Response to oxidative stress" and "Transporter and targeting" also typify the response.

5.2.7. Role of the transcription factors Yap1p, Msn2p and Msn4p

The transcription factor Yap1p is involved in the response to oxidative stress (Rodrigues-Pousada et al., 2004). Therefore it is possible that Yap1p might be involved in the regulation of gene expression by NO donor. The redundant transcription factors Msn2p and Msn4p have been shown to regulate genes of the general stress and environmental stress response (Martinez-Pastor et al., 1996; Schmitt and McEntee, 1996; Causton et al., 2001). Since several genes altered after NO donor exposure show the characteristic expression pattern of these responses, Msn2p and Msn4p are two more candidate transcription factors.

To test the involvement of Yap1p and Msn2/4p in the regulation, microarray data was obtained after 60 minutes of 3 mM DETA NONOate treatment of a strain with deletion of the *YAP1* gene (W303-1B Δ*yhb1* Δ*yap1*) and a strain with double deletion of *MSN2* and *MSN4* (W303-1B Δ*yhb1* Δ*msn2/4*). The ratios "fold change in Δ*yap1* or Δ*msn2/4* / fold change in control" (R_2 and R_3, respectively) were calculated for each of the 291 genes altered after 60 minutes of 3 mM NO donor treatment of the control, and genes were assigned to one of five categories depending on the transcription factors found to regulate their induction or repression (Table 5.3B). Alteration of gene expression was considered to be dependent on a transcription factor when R was lower than 0.75 (for up-regulated genes) or higher than 1.33 (for repressed genes). Yap1p was found to be involved in the regulation of 67 genes (23%) and Msn2/4p in the regulation of 77 genes (26%). Varying levels of reliance were exhibited, for example R values for overexpresssed genes varied from 0.05 (highly dependent) to 0.75 (weak dependence). Regulation was not able to be clearly assigned for 3.4% of the genes, and more than 55% of the genes were regulated by neither Yap1p nor Msn2/4p. Of the highly dependent genes ($R < 0.5$ for upregulated genes and $R > 2$ for repressed genes), sixteen (*AAD6, YKL071W, YOL155C, YNR064C, YLL056C, CYB2, HMX1, SUE1, HMG1, UBX6, HPA2, YBR056w-a, FLR1, CTA1, PCS60* and *YBR242W)* were specifically altered in response to NO/RNS and appear in Table 5.4.

A similar study was carried out to assess dependence of myxothiazol-induced gene expression changes on these transcription factors (Bourges et al., 2005). 301 genes with altered expression after 10 minutes of 8 μM myxothiazol treatment were assessed. Yap1p was found to be involved in the regulation of 30% of these genes, a similar

situation to that observed with NO donor. Msn2/4p had a much clearer involvement, being required for regulation of 84% of the genes, in combination or not with Yap1p. It might be that the regulators involved in responding to myxothiazol and NO donor stress are different.

To further investigate the involvement of Msn2/4p in the NO donor-induced response, I monitored the translational changes of an *MSN2/4*-driven *LacZ* reporter gene in the strain W303-1B Δ*yhb1*. Msn2/4p bind to the stress response element (STRE) to activate transcription (Estruch and Carlson, 1993; Schmitt and McEntee, 1996). β-galactosidase activity was measured in untreated cells and in 3 mM DETA NONOate-treated cells over 2 hours (Figure 5.6). A background β-galactosidase activity of 15-20 Units was observed in the untreated cells at time zero; this was also seen in the untreated control and in the NO donor-resistant wild type W303-1B after 120 minutes of treatment. After 10 minutes of incubation, no alteration of β-galactosidase activity was observed. However, after 60 and 120 minutes the activity almost doubled, to reach a level close to that observed after heat shock and after 120 minute treatment with 8 μM myxothiazol. When the strain W303-1B Δ*yhb1* Δ*msn2/4* containing the reporter gene was monitored no β-galactosidase activity was observed. These results mirror those obtained in the same experiment using the wild type strain to assess the transcription factors involved in myxothiazol-induced stress (Bourges et al., 2005). It seems therefore that DETA NONOate does induce the activation of STRE by Msn2/4p.

I also planned to assess the involvement of ROS in the Msn2/4p-regulated response to NO donor, using strains with inducible overexpression of *SOD1* (in addition to the Sod1p assembly factor *CSS1*, which is required for activity of overexpressed Sod1p (Harris et al., 2005)) or *CTT1*. *SOD1* overexpression resulted in a high basal level of β-galactosidase activity. This was not due to the presence of the vector since when expression was not induced the basal β-galactosidase level was low. This basal stress could be due to high levels of hydrogen peroxide produced by Sod1p which cannot be removed quickly enough by cells. Consequently the overexpression strain could not be used to assess whether increased Sod1p decreased the magnitude of response to NO donor. Overexpression of *CTT1* required growth in glycerol, but the β-galactosidase assay gave variable results using cells grown in glycerol, so the effect of NO donor in this strain could also not be assessed.

5.2.8. Role of the transcription factor Hap1p

Hap1p is an oxygen-responsive zinc finger transcription factor which regulates expression of genes of the respiratory chain, and heme, sterol and fatty acid synthesis. Its activity is regulated by heme levels. Since many genes of the respiratory chain, and involved in the synthesis of sterols and fatty acids, were repressed on NO donor exposure (Table 5.4) a potential involvement of Hap1p in the transcriptional response to NO donor was investigated. It seems possible that Hap1p could be inactivated on exposure to NO donor. One possibility is that NO/RNS could interfere with the heme synthesis pathway, resulting in a lower level of heme available for the activation of Hap1p. Supplying heme to the cells might result in re-activation of Hap1p.

To investigate this, I wanted to show in an independent assay that a reporter gene driven by Hap1p is repressed by NO donor, and use this assay to test compounds (heme, or precursors of heme) that might alleviate the Hap1p inactivation by NO donor. To this end, I monitored translational changes using a *LacZ* reporter gene under the control of the *CYC1* promoter (Guarente and Ptashne, 1981). *CYC1* is known to be induced by Hap1p. In the microarray analysis, *CYC1* was repressed by up to 100-fold. In the absence of NO donor, β-galactosidase activity was high at around 170 Units when cells were grown aerobically, but no activity was detected under anaerobic conditions (see 2.5.3), as expected since *HAP1* expression requires heme, the synthesis of which requires oxygen. Addition of 3 mM NO donor to aerobically grown cells caused a decrease in β-galactosidase activity of around one quarter after one hour, a much milder decrease than that observed by microarray (Figure 5.7). One possible reason for this could be that the assay was measuring a decreased level of protein. This would require degradation of existing β-galactosidase protein, which might be expected to take longer than the 1 hour period tested. The assay was repeated after 12 hours incubation of cells with NO donor, and this time a 5-fold decrease in β-galactosidase activity was observed. This could be interpreted to mean that RNS inhibits new synthesis of β-galactosidase but since the enzyme is very stable only mild effects on activity are observed. Alternatively, the turnover of the enzyme may be quick but the expression of β-galactosidase would be only partially inhibited by NO donor. When the assays were repeated with 8 μM myxothiazol similar effects on β-galactosidase activity were noted (Figure 5.7). However, myxothiazol was shown by microarray not to affect *CYC1* expression (Bourges et al., 2005). Therefore the decrease in β-galactosidase activity is likely to be due to a more general stress, for example the inhibition of respiration, and not specifically due to NO/RNS. It seems that the stability of the enzyme is most likely

the problem, and enzyme activity is not a sensitive probe for repression of transcription. To circumvent this problem, another possibility was to add NO donor to an anaerobic culture and assess the recovery of β-galactosidase activity. However the recovery proved very slow in control cells, with activity beginning to appear only after 8 hours of aerobic growth, so this approach was not experimentally feasible. In conclusion, this assay was not useful in assessing the involvement of the transcription factor Hap1p in transcriptional changes induced by NO donor.

In the next experiment, I used (RT)q-PCR to monitor *CYC7* gene expression and the effects of deuteroporphyrin (dpIX), a stable analogue of protoporphyrin, precursor of the final step of heme synthesis (heme itself cannot be used since it cannot pass the cell wall). Exogenously supplied dpIX has been shown to activate Hap1p (Hon et al., 2003). In the microarray analysis *CYC7* was repressed by up to five-fold after NO donor treatment. I treated cells for 60 minutes with 200 μg per ml of dpIX in the presence of 3 mM NO donor, then prepared cDNA and analysed expression of the gene *CYC7* using (RT)q-PCR. As a control I used cells treated with dpIX alone. The relative quantity of the *CYC7* gene after addition of NO donor was 0.053, while in the presence of dpIX the relative quantity was 0.020. Hence dpIX did not appear to relieve the NO donor-induced repression of *CYC7*. However, I did not show that a strain defective in heme synthesis could be rescued with the concentration of dpIX used, so the results do not allow complete rejection of the possibility of NO interfering with the heme level.

5.3. DISCUSSION

5.3.1. Overview of results

After 10-120 minutes treatment with an inhibitory dose of DETA NONOate the transcript levels of 731 genes were altered compared to the untreated control. Alterations of transcript levels may be due to alteration in the expression of genes (the number of mRNAs produced), or to a modification of the stability of mRNAs. Changes in stability of mRNAs can vary according to the cellular environment. In particular, as discussed in 4.3.4.1, studies have shown that induction of NO synthesis in mammalian cells led to specific decreases in levels of some respiratory chain mRNAs which were caused by an increase in mRNA degradation rather than a decrease in their expression (Gou et al., 2001; Wei et al., 2002).

At lower concentrations of DETA NONOate the extent of alteration of expression was decreased, and it seems that NO donor elicits a concentration-dependent effect. The requirement for a respiratory chain in the gene expression changes observed was assessed and the expression of most genes was found to have no reliance or only a weak reliance on the presence of a respiratory chain, indicating that the gene expression changes are not due simply to inhibition of the respiratory chain. This would also suggest that ROS do not play a major role in the gene expression changes, since the respiratory chain is the main site of ROS production.

The data was compared to that obtained in a similar analysis of the effects of myxothiazol on gene expression, and the majority of the genes (477 of 731) were found to be altered after both DETA NONOate and myxothiazol treatment. These genes tended to be expressed in a transient manner, with expression being highly altered at early time points but returning to control levels later on; this is the signature of the general stress response induced to allow cells to adapt to their new environment. Similar induction of the general stress response has been seen before in *Saccharomyces cerevisiae* (Sarver and DeRisi, 2005).

117 genes were clearly altered in response to NO donor but not myxothiazol treatment (Table 5.4). These generally exhibited a more prolonged response, with expression levels staying altered until the end of the two hour time course. Analysis of these genes might provide useful information on the nature of the stresses sensed by the cell and the responses induced by it. Cellular damage by ROS is prevented by antioxidant defences that neutralise ROS and detoxification defences which repair damage or remove damaged cellular components. When the cell is stressed so that

levels of ROS exceed the antioxidant capacity of the cell, it must respond to this. It is likely that a similar system exists to defend against RNS. At least 50% of the genes clearly upregulated by DETA NONOate but not by myxothiazol were also upregulated by hydrogen peroxide (Gasch et al., 2000; Causton et al., 2001), suggesting that RNS stress shares some features with oxidative stress.

5.3.2. Activation of antioxidant/detoxification enzymes

5.3.2.1. Yhb1p

The first line of defence against RNS in yeast seems to be the NO oxidoreductase Yhb1p, product of the *YHB1* gene, which consumes NO very efficiently (Gardner et al., 2000; Liu et al., 2000; Sarver and DeRisi, 2005). In recent microarray studies using *S. cerevisiae* and *Candida albicans*, *YHB1* was found to be highly induced on exposure to RNS (Sarver and DeRisi, 2005; Hromatka et al., 2005). Since I have utilised a strain with deletion of *YHB1*, no changes in the expression of the gene are observed in this study, allowing other less dominant defences to become apparent.

5.3.2.2. Superoxide dismutase, catalase and cytochrome c peroxidase

The first line of defence against ROS would be upregulation of genes encoding enzymes such as superoxide dismutase, catalase and cytochrome *c* peroxidase, which detoxify ROS (Moradas-Ferreira et al., 1996). The *SOD1*, *SOD2*, *CTT1* and *CCP1* genes were all upregulated in the presence of hydrogen peroxide (Gasch et al., 2000; Causton et al., 2001). However, none of these genes were induced on NO donor exposure. Instead, *CCP1* encoding cytochrome *c* peroxidase and *CTA1* encoding catalase A were in fact repressed, suggesting that ROS are not significantly involved in the NO donor-induced stress.

5.3.2.3. Glutathione

Glutathione is the most abundant thiol peptide in cells and is involved in many processes including detoxification of ROS. Glutathione forms S-conjugates with a wide range of toxins which can then be transported out of the cytosol to the vacuole. Two genes of this system, *GTT2* and *YCF1*, were upregulated. *GTT2* encodes glutathione S-transferase which catalyses conjugate formation, and was highly overexpressed, even in the presence of 0.1 mM DETA NONOate. It shares some functional overlap with *GTT1*, and *GRX1* and *GRX2* which encode glutaredoxins, however none of these genes had altered expression. *YCF1*, encoding a glutathione conjugate transporter, was upregulated

by 10-fold. *GSH1*, required for the synthesis of glutathione, was upregulated by 3-fold after NO donor incubation, but was not significantly altered in the BY4741 strain. In *C. albicans* several genes of the glutathione system, such as *YCF1*, *GTT1* and *GLR1* (glutathione reductase) were also overexpressed on nitrosative stress (Hromatka et al., 2005). In total, about a quarter of the clearly NO-specific overexpressed genes (including *SSU1*, *OYE3*, *GSH1*, *YNL134C*, *DRE2*, *FRE5*, *FLR1*, *ARN1*, *DDR48*) were upregulated in this organism.

5.3.2.4. Peroxiredoxins

Yeast contain five peroxiredoxins, a family of conserved antioxidant enzymes which use thioredoxin to scavenge hydrogen peroxide and alkyl hydroperoxides (Chae et al., 1994; Netto et al., 1996). The peroxiredoxin Tsa2p was found to have peroxynitrite reductase activity, and its expression was induced on exposure to peroxynitrite or a NO donor (Wong et al., 2002). Tsa2p was suggested to cooperate with Tsa1p, the major cytosolic thioredoxin peroxidase, to remove ROS and RNS. Here, *TSA2* was upregulated by around 4-fold by both NO donor (even at 0.1 mM) and myxothiazol, and the mitochondrial peroxiredoxin Prx1p, encoded by *PRX1*, was induced 3-fold in the W303-1B strain (but not in the BY4741 strain). On exposure to oxidants, cysteine-sulfinic (Cys-SOH) acid groups form in the 2-Cys peroxiredoxins Tsa1p, Tsa2p and Ahp1p. In most cases these groups are attacked by a cysteine residue of the other subunit of the homodimer to form a disulfide bond, but sometimes the cysteine-sulfinic acid is further oxidised to sulphinic acid (Cys-SO_2H). Sulfiredoxin, encoded by *SRX1*, reduces sulfinic acid groups in Tsa1p and Tsa2p, and facilitates formation of the disulfide bond (Biteau et al., 2003). *SRX1* was induced by up to 25-fold after DETA NONOate treatment. These data suggest that the cells may be exposed to hydrogen peroxide or peroxynitrite, and are attempting to remove these reactive molecules.

5.3.2.5. Lipid peroxidation

Lipid peroxidation is a major type of oxidative damage, and several genes involved in the repair of such damage were induced after exposure to NO donor. Phospholipid hydroperoxide glutathione peroxidases reduce hydrogen peroxide and larger hydroperoxides, including lipid peroxides. Oxidation of polyunsaturated lipids occurs by an autocatalytic process to produce fatty acid hydroperoxides. These undergo fragmentation to highly reactive epoxides, aldehydes and alkanes, which can cause further damage to the cell by reaction with proteins and DNA. Phospholipid hydroperoxides are central intermediates in the lipid peroxidation chain reaction,

therefore phospholipid hydroperoxide glutathione peroxidases are considered a main line of defence against oxidative damage to membranes. Three such enzymes have been identified in yeast; one of them, *GPX2*, was upregulated by around 4-fold after NO donor exposure. This gene was shown by Inoue *et. al.* (Inoue et al., 1999) to be under the control of Yap1p, but I did not observe this. The homologous gene *GPX1* was upregulated by about 4-fold by both NO donor and myxothiazol. Both genes were induced even at low (0.1 mM) concentration of NO donor.

The gene *YNR064C* was upregulated by up to 70-fold after NO donor treatment. This protein has characteristics of an epoxide hydrolase belonging to the α/β hydrolase fold family (Elfstrom and Widersten, 2005). Such enzymes inactivate reactive epoxides which might otherwise alkylate proteins and DNA. A microarray study showed that exposure to the DNA alkylating agent methyl methanesulfonate (MMS) caused 30-fold overexpression of the gene, suggesting that it may indeed function as an epoxide hydrolase (Jelinsky and Samson, 1999). In fact, many of the genes mentioned here were induced on MMS treatment of yeast. Exposure to an alkylating agent will bring into force a program to eliminate, repair or replace alkylated components from the cell.

Three putative aryl alcohol dehydrogenases, *AAD4*, *AAD6* and *AAD16*, were highly induced, between 11 and 40-fold, after DETA NONOate exposure. These share high sequence homology with the aryl alcohol dehydrogenase from the lignin-degrading fungus *Phanerochaete chryosporium*, which converts aromatic aldehydes arising from oxidation of lignocellulose into aromatic alcohols (Delneri et al., 1999a). The protein products may be involved in removing the damage done to lipids by peroxidation. However, function has not yet been assigned since deletion of the seven *AAD* genes did not reveal a phenotype (Delneri et al., 1999b). Overexpression of three of the seven genes suggests that they play an important role in the response to NO donor-stress. All seven genes were also found to be upregulated in oxidative stress caused by transfer to growth in oleate (Groot Koerkamp et al., 2002). Several of the *AAD* genes (3, 6, 10, 14 and 15) were overexpressed on transfer from fermentative to respiratory growth in the presence of a *YAP1* overexpression plasmid compared to a control strain, and it was suggested that the *AAD* genes might play an important protective role during oxidative stress (DeRisi et al., 1997). The promoter regions of *AAD4* and *AAD6* contain Yap1p control elements, and *AAD6* expression was found to be regulated by Yap1p (Groot Koerkamp et al., 2002). Here, I found *AAD6* to be clearly under the control of Yap1p, though *AAD4* was not. Finally, another alcohol dehydrogenase, *YNL134C*, was also upregulated, by around 5-fold, on exposure to NO donor.

5.3.2.6. DNA repair system

Oxidation of nucleic acids leads to damage such as base modification, single strand breaks and DNA-protein crosslinks. Two genes encoding proteins involved in the repair of DNA damage were upregulated after NO treatment. *HUG1* was not initially overexpressed, but expression had increased by 65-fold after 2 hours (26-fold in BY4741 after 1 hour). Hug1p is involved in the Mec1p-mediated checkpoint pathway that responds to DNA damage or replication arrest, and its transcription is induced by DNA damage (Basrai et al., 1999). *DDR48* encodes a DNA damage responsive protein and was induced by 4-fold after DETA NONOate treatment. Its expression was also increased after MMS treatment. The cells may be sensing DNA damage caused by exposure to RNS. However, this would appear to be limited since in 4.2.5 I demonstrated that even long exposure to DETA NONOate did not increase rho$^-$ (deletion in mtDNA) production.

5.3.3. Modification of iron homeostasis

Several genes involved in iron homeostasis were upregulated after exposure of yeast to NO donor. *ISU2*, encoding a conserved mitochondrial matrix protein which performs a scaffolding function during iron-sulfur cluster assembly and is required for the synthesis of iron-sulfur proteins (Schilke et al., 1999), was upregulated by up to 20-fold on NO donor exposure. *NFU1* and *ISA2*, with similar function (Schilke et al., 1999; Pelzer et al., 2000), were also upregulated, albeit to a lesser extent. *FRE5* encodes a putative ferric reductase, is part of a family of nine homologous genes thought to be involved in iron uptake, and is induced during iron depletion through the iron-regulated transcription factor Rcs1p. *FRE5* underwent a 6-fold increase in expression after NO donor exposure. The homologous *FRE7* was also upregulated, but not so clearly in the BY4741 strain. *ARN1* and *ARN2*, members of the ARN family of transporters that specifically recognize siderophore-iron chelates (Yun et al., 2000), were upregulated. *CCC1,* involved in transporting iron for storage in the yeast vacuole (Li et al., 2001), was repressed after NO donor exposure.

This data suggests that cells are attempting to acquire more iron. Possibly the iron already available in the cell is not in a 'free' form available for use. Superoxide radicals oxidise iron-sulfur clusters in proteins, releasing iron from the cluster and inactivating the enzyme. Despite having high levels of iron, *SOD1*-deficient mutants are iron-deficient, suggesting that the iron released accumulates in a form that cannot be used for the biosynthesis of new clusters (De Freitas et al., 2000; Srinivasan et al.,

2000). Genes encoding iron acquisition proteins were also shown to be upregulated in *Histoplasma capsulatum* (Nittler et al., 2005) and *C. albicans* (Hromatka et al., 2005) after exposure to NO donors. Increased iron demand may reflect the efforts of the cell to reconstitute iron-sulfur cluster-containing proteins to replace those which have been inactivated by RNS.

5.3.4. Induction of transporters

ARR2 was also highly induced after NO donor exposure. The arsenate reductase Arr2p converts arsenate to arsenite, which can then be exported from the cell (Mukhopadhyay and Rosen, 1998). The reason for upregulation of this gene is unclear, however, the equivalent of *ARR3*, encoding an arsenite transporter, was found to be upregulated in a microarray study of the effect of nitrosative stress on *C. albicans* (Hromatka et al., 2005). Several other transporters were also upregulated after NO donor exposure: *FLR1* (multidrug transporter), *MCH4* (monocarboxylic acid transporter), *YHR048W* and *SSU1* (sulfite transporter). *SSU1* was also upregulated after nitrosative stress in another *S. cerevisiae* study, and was suggested to transport RNS metabolites out of the cell (Sarver and DeRisi, 2005). A similar function could be suggested for the other transporters.

5.3.5. Repression of fatty acid and sterol synthesis

Eight genes involved in the synthesis of fatty acids and sterols were repressed on DETA NONOate treatment. *ERG7* encodes lanosterol synthase which catalyses cyclisation of squalene 2,3-epoxide, in ergosterol biosynthesis; *HMG1* encodes an isozyme of HMG-CoA reductase which catalyses a rate-limiting step in sterol biosynthesis; *MVD1* encodes mevalonate pyrophosphase decarboxylase, essential for sterol biosynthesis; *ATO1* encodes an acetate transporter. *FAS2* encodes a subunit of fatty acid synthetase, *OLE1* encodes a fatty acid desaturase, and *CYB5* is involved in both sterol and fatty acid synthesis. The number of genes increases to 15 if those genes which were not clearly also repressed in the BY4741 strain are included. In contrast, only one gene promoting lipid biosynthesis was repressed by both NO donor and myxothiazol. Most striking was the overexpression by a factor of more than 200 (the highest upregulation observed for any gene) of *FRM2*, encoding a protein of unknown function involved in the fatty acid signaling pathway. *FRM2* mutation prevented repression of *OLE1* by unsaturated fatty acids (McHale et al., 1996). A similar upregulation of *FRM2* was also observed on nitrosative stress in the *S. cerevisiae* study mentioned earlier (Sarver and DeRisi, 2005). As discussed in 4.3.2, a decrease in sterol synthesis might be expected to have a severe effect on cell proliferation, since ergosterol is essential for cell viability. However,

addition of ergosterol to the growth medium of NO donor-treated cells did not appear to relieve the inhibition of proliferation (although appropriate controls were not carried out).

5.3.6. Severe repression of respiratory chain genes

One of the most striking effects of NO donor exposure was the severe repression of many genes encoding respiratory chain subunits or involved in the assembly of respiratory complexes. A large majority of these genes were repressed by NO donor but not myxothiazol. Four cytochrome oxidase genes (three subunits), seven bc_1 complex genes (six subunits), four succinate dehydrogenase genes and one NADH dehydrogenase gene were repressed. This was in addition to three genes relating to cytochrome *c* and one gene required for ubiquinone biosynthesis. Repression reached as high as 100-fold. More than a third of these genes were also repressed after NO donor treatment of *C. albicans* (*SDH1*, *SDH2*, *CYC1*, *RIP1*, *YOR356W*, *COX4*, *QCR1*, *COX5A*, *QCR2*), along with several other respiratory chain genes which were not observed here (Hromatka et al., 2005). It seems that repression of the respiratory chain is of great importance in the response of cells to NO donor-induced stress. In the recent study of nitrosative stress in *S. cerevisiae*, repression of respiratory chain genes was observed in rich medium but not in synthetic medium (Sarver and DeRisi, 2005).

Nine respiratory chain genes (*CYT1*, *SDH2*, *NDI1*, *SDH1*, *QCR6*, *SDH4*, *QCR2*, *COX5A*, *COX1*, *ATP9*) were repressed by more than 3-fold in the untreated rho^0 strain compared to the untreated control. Downregulation of respiratory chain genes in the absence of mtDNA has been observed before (Epstein et al., 2001).

NO is a potent inhibitor of the respiratory chain, and blockage of the respiratory chain would be expected to increase production of ROS. If lowering transcription of respiratory chain genes leads to a decrease in levels of respiratory chain proteins the cells might be expected to produce less ROS, thus this could represent a strategy to protect the cells from further oxidative damage. However, when I monitored cell growth and gene expression in the absence of a respiratory chain, or cell growth in strains lacking components of the ROS defence system, I found no major role for ROS or the respiratory chain in the NO donor induced stress. Therefore it seems unlikely that this is a plausible rationale for decreased expression of respiratory chain genes.

5.3.7. Transcription factors involved in the genomic response to NO/RNS

5.3.7.1. Hap1p

Hap1p is a zinc finger transcription factor involved in regulating the transcriptional changes induced by altered oxygen tension. It is localised in the nucleus where its activity is controlled by heme, which in turn is dependent on oxygen level. Two steps in the heme biosynthetic pathway use oxygen as a substrate (enzymes Hem13p and Hem14p), while the final step in the pathway (enzyme Hem15p) has been shown to be faster in the presence of oxygen (Hon et al., 2003). In anaerobiosis heme is absent and Hap1p is bound to other proteins to form a high molecular weight complex (HMC) (Fytlovich et al., 1993; Zhang and Guarente, 1994; Zhang et al., 1998). In aerobic conditions, heme is synthesised and liberates Hap1p from the HMC, allowing Hap1p to bind DNA and activate transcription of aerobic genes encoding proteins involved in respiratory chain, heme, sterol and fatty acid synthesis. Heme is also a component of many of these enzymes, providing an additional level of control.

17 of the 36 known or putative Hap1p-regulated genes described in (Ter Linde and Steensma, 2002) were found to be repressed after NO donor treatment (Table 5.5). Most of the genes were unchanged on myxothiazol treatment, although 6 were overexpressed. One of the genes Hap1p is known to induce is *ROX1*, encoding a transcription factor which represses hypoxic genes in aerobic conditions. Although *ROX1* did not appear to be upregulated in my data, several of its known or putative target genes were upregulated (Table 5.5). This suggests that NO or RNS might be able to interfere somehow, directly or indirectly, with Hap1p, to impair its activity. The mechanism of interference could be through several means. It may be that on NO donor exposure the cells sense conditions resembling low oxygen tension. I compared the pattern of gene expression observed in anaerobiosis (Ter Linde et al., 1999) to that observed on NO donor exposure. Of the genes clearly specifically altered in response to NO donor, only a few were also altered in a similar manner in anaerobiosis, and this was more obvious in the repressed genes than the overexpressed genes. Also, some of the RNS-specific upregulated genes were downregulated in anaerobiosis. Therefore it seems that rather than a general low oxygen tension being sensed, NO/RNS may alter Hap1p activity more specifically. One possibility is inhibition of one of the enzymes involved in the heme synthesis pathway, resulting in decreased heme levels and therefore decreased Hap1p activity. I attempted to investigate this using a reporter gene, however this assay did not work well. I then assessed repression of the *CYC7* gene by

(RT)q-PCR, and the heme precursor dpIX did not relieve the repression caused by NO donor exposure. However, this would need to be repeated with a proper control. In conclusion, I did not find evidence to support an involvement of heme level in the gene repression, and was also not able to directly demonstrate involvement of Hap1p (since the reporter gene assay was unsuccessful). The possible role of Hap1p is inferred from the microarray data and from previous results of other groups, therefore more work needs to be done.

5.3.7.2. Msn2/4p

Msn2p and Msn4p are mediators of the general response to stress. After both myxothiazol and NO donor treatment, a transient gene expression response characteristic of the general stress response was observed, therefore it might be expected that Msn2/4p could play a role. Indeed, 84% of the genes altered after 10 minutes of myxothiazol treatment showed some dependence on Msn2/4p (Bourges et al., 2005). Gene expression after 60 minutes treatment with NO donor, however, was found to have only limited dependence on Msn2/4p, with 26% of genes showing dependency. However the involvement of transcription factors was assessed at different time points; 60 minutes for NO donor and 10 minutes for myxothiazol. To clarify this I assessed transcription of a *LacZ* reporter gene controlled by a STRE in the presence of NO donor. The β-galactosidase activity displayed a similar pattern of response to that seen after myxothiazol treatment, suggesting that the involvement of Msn2/4p is largely an early event. No STRE activation is detected at 10 minutes, presumably because the early alterations of transcription have not yet resulted in changes at the protein level. However, after 60 minutes the early transcriptional changes will have become detectable at the protein level. It seems likely that Msn2/4p are involved early on in transient transcriptional regulation of a large set of genes. After 60 minutes of NO donor incubation this involvement will not be seen in microarray analysis. It would be interesting to assess involvement of Msn2/4p at an earlier time point to confirm this.

5.3.7.3. Yap1p

Yap1p is specifically involved in the response to oxidative stress. After 60 minutes of NO donor treatment 23% of genes were found to be regulated by Yap1p, a similar number to those regulated by Msn2/4p. The strain W303-1B used in the majority of the experiments described carries a mutation in the gene encoding Ybp1p, which forms a stress-induced complex with Yap1p and influences its nuclear localisation in response to hydrogen peroxide (Veal et al., 2003). The mutation causes some loss of function and

increased sensitivity to hydrogen peroxide. Possible inhibition of the Yap1p system might therefore have affected some of the results. However, in the analysis of Yap1p involvement in the gene expression response due to myxothiazol, the experiment was repeated using the *YAP1* deletion in the BY4741 parent strain, which does not harbour the *YBP1* mutation, and similar results were found. Additionally, when gene expression changes after NO donor treatment were measured in the BY4741 strain, similar results were obtained to those in the W303-1B strain. Therefore it is unlikely that the mutations in *YBP1* affect the response to NO donor stress.

Interestingly, while the expression of *YAP1* was not altered after NO donor treatment, *YAP2* (another member or the AP-1 family) was induced on NO donor exposure. Yap2p has some overlapping function with Yap1p, but seems to be more involved in the control of genes involved in the stabilisation of proteins (Cohen et al., 2002).

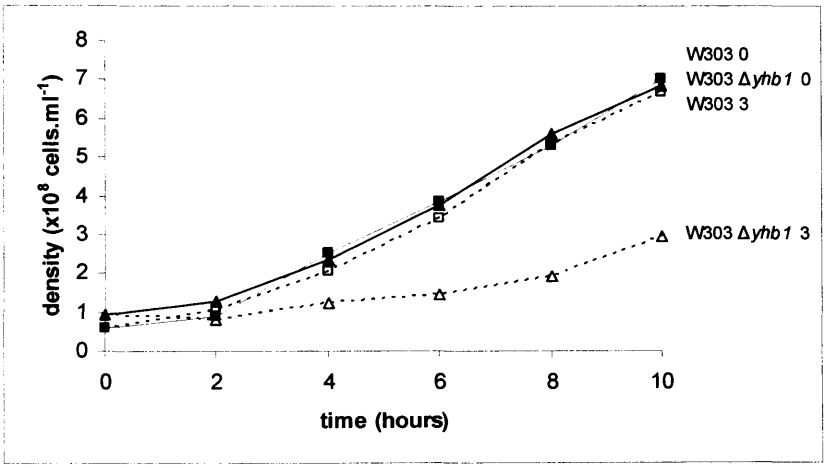

Figure 5.1. Effect of NO donor on yeast proliferation.

W303-1B and W303-1B Δ*yhb1* cells were grown in YPGal in the presence of 0 or 3 mM DETA NONOate. Growth was monitored by measuring cell density at 600 nm.

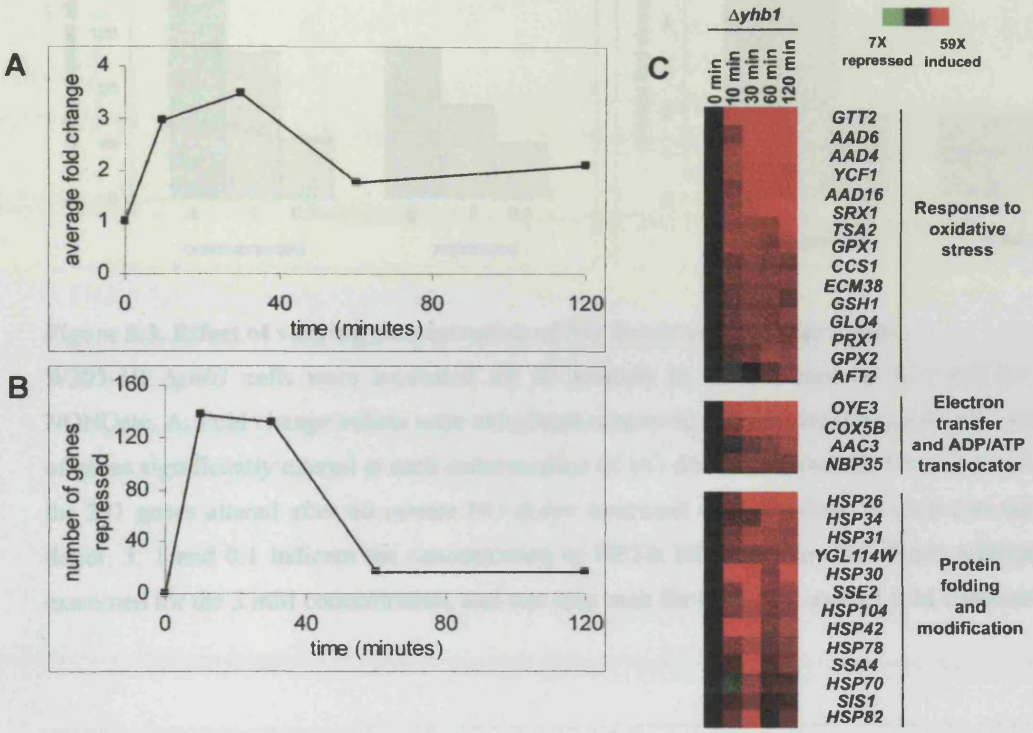

Figure 5.2. Changes in gene expression after NO donor treatment.

Fold change values were calculated relative to untreated cells. **A.** average fold decrease and **B.** number of genes repressed at each time point in the category "DNA structure, replication, transcription and translation". **C.** heat map showing overexpression of genes in the categories "Response to oxidative stress", "Electron transfer and ADP/ATP translocator" and "Protein folding and modification". The number of replicate chips for each time point is stated in 2.5.1.6.

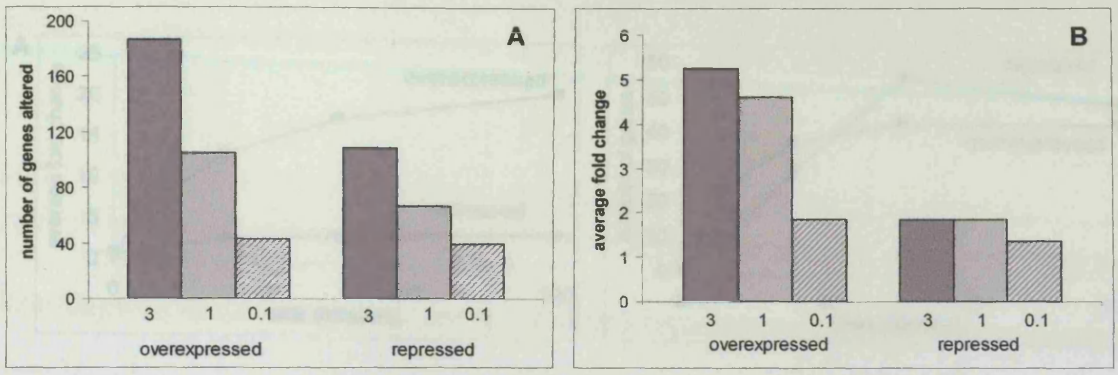

Figure 5.3. Effect of varying concentration of NO donor on gene expression.

W303-1B Δ*yhb1* cells were incubated for 60 minutes in the presence of 3, 1 and 0.1 mM DETA NONOate. **A.** Fold change values were calculated relative to the relevant untreated strain and the number of genes significantly altered at each concentration of NO donor is shown. **B.** The average fold change of the 291 genes altered after 60 minute NO donor treatment was calculated at each concentration of NO donor. 3, 1 and 0.1 indicate the concentration of DETA NONOate in mM. Three replicate chips were examined for the 3 mM concentration, and one chip each for the 1 mM and 0.1 mM concentrations.

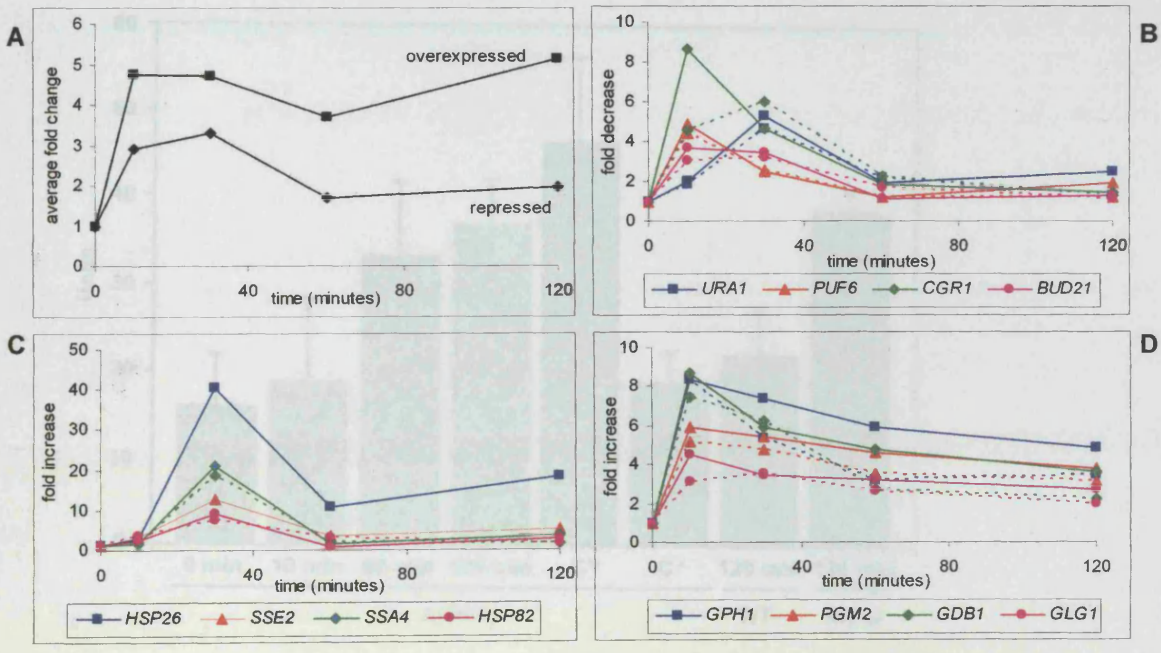

Figure 5.4. Genes commonly altered by NO donor and myxothiazol.

Fold change values were calculated relative to the relevant untreated strain. **A.** Average fold changes in response to NO donor for all genes (211 overexpressed, 266 repressed) with expression altered by both NO donor and myxothiazol treatment. **B, C, D.** Expression profiles of 4 representative genes after NO donor (solid line) and myxothiazol (dashed line) treatment, for the categories "DNA structure, replication, transcription and translation" (B), "Protein folding and modification" (C) and "Glycolysis, gluconeogenesis and carbohydrate storage" (D). The number of replicate chips examined for each time point is stated in 2.5.1.6.

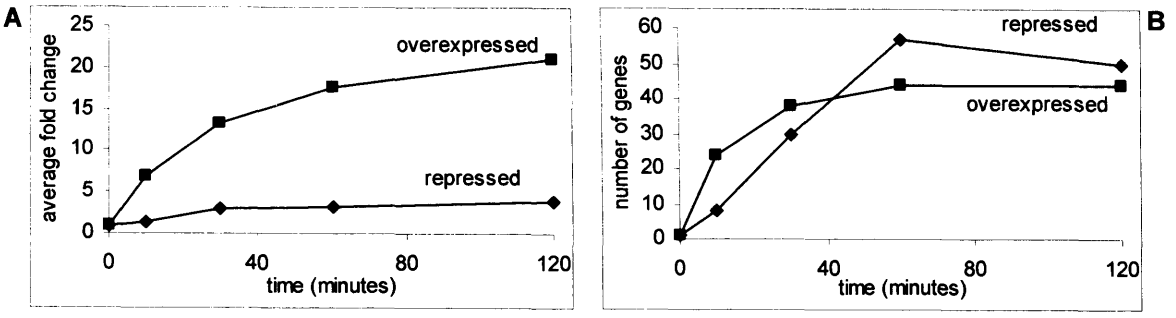

Figure 5.5. Genes altered specifically by NO donor.

Fold change values were calculated relative to the untreated strain. **A.** Average fold changes in response to NO donor for all genes (45 overexpressed, 72 repressed) with expression altered by NO donor but not myxothiazol treatment. **B.** Number of genes altered at each time point. The number of replicate chips examined for each time point is stated in 2.5.1.6.

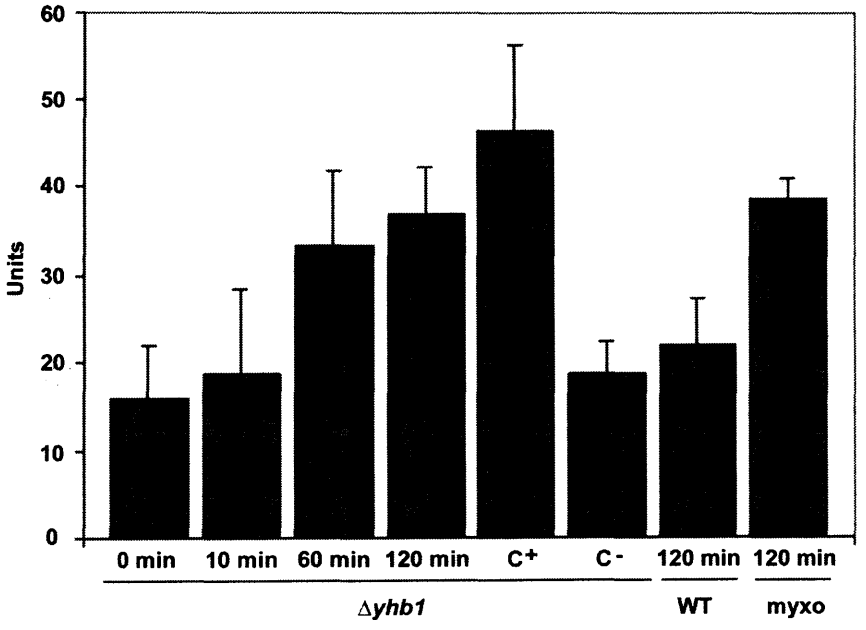

Figure 5.6. STRE activation by Msn2/4p induced by NO donor.

W303-1B Δ*yhb1* cells harbouring the reporter gene *LacZ* under the control of a STRE-containing promoter were cultivated for 8 hours in YPGal at 28°C, then exposed to 3 mM NO donor for 10, 60 or 120 min. The cells were harvested and the expression of the reporter gene was followed. Controls were as follows: after 8 hours growth at 28°C, W303-1B Δ*yhb1* cells were cultivated without NO donor for 60 min at 37°C (C^+), or for 120 hours at 28°C (C^-) or with 8 μM myxothiazol for 120 min at 28°C; W303-1B cells, with an active Yhb1p, were exposed to 3 mM NO donor for 120 min. The mean and standard deviation (±) of the values obtained for β-galactosidase activity are shown.

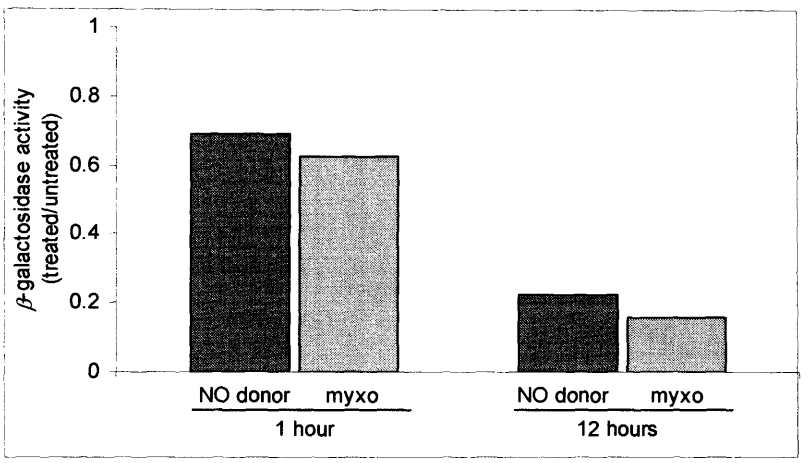

Figure 5.7. *CYC1* repression in the presence of NO donor and myxothiazol.

W303-1B Δ*yhb1* cells harbouring the reporter gene *LacZ* under the control of the *CYC1* promoter were cultivated for 8 hours in YPGal at 28°C, then exposed to 3 mM NO donor or 8 μM myxothiazol for 1 or 12 hours. The cells were harvested and the expression of the reporter gene monitored.

Table 5.1. Number of genes with altered expression as a result of incubation with NO donor.
W303-1B Δ*yhb1* cells were treated for 10-120 minutes with 3 mM DETA NONOate or for 2-120 minutes with 8 μM myxothiazol. For each gene, the number of transcripts in treated cells was compared to the number of transcripts in untreated cells and a fold change value calculated at each time point. The number of replicate chips examined for each time point is stated in 2.5.1.6. The over-expressed and repressed genes were grouped into functional categories. The table shows the number of genes in each functional category which had a fold change value judged significant at at least one time point (see 2.5.1.6). Of the genes altered after 3 mM DETA NONOate exposure, the number altered common to both treatments is indicated.

Category	Overexpressed genes			Repressed genes		
	NO	myxo	common	NO	myxo	common
Response to oxidative stress	15	6	4	4	2	2
Electron transfer and ADP/ATP translocator	4	8	2	31	4	5
Glycolysis, gluconeogenesis, carbohydrate storage pathway	48	68	40	13	11	9
Peroxisome, fatty acid and lipid metabolism	7	16	5	18	3	3
Amino acid metabolism, catabolism and transport	21	14	9	12	13	5
Ion homeostasis	7	4	1	4	3	2
Transporter and targeting	28	33	11	13	16	10
Protein folding and modification	13	13	10	3	2	2
Response to variable stress	8	6	5	1	3	1
Kinase, phosphorylase and signal transduction	9	24	7	1	3	1
Cellular organisation and biogenesis	33	61	19	27	33	13
DNA structure, replication, transcription and translation	14	28	9	195	251	171
Other	18	11	7	14	14	8
Unknown genes	121	154	82	49	75	34
Total	346	446	211	385	433	266

Table 5.2. Validation of microarray results by (RT) qPCR analysis.

For six representative genes, fold change value obtained after 60 minutes NO donor treatment in microarray analysis is listed adjacent to relative quantity obtained in (RT)q-PCR analysis. Values were calculated as described in 2.5.1.6 and 2.5.2 and are the average of results from at least two independent cell preparations (microarray) or at least three separate assays with each sample processed in duplicate ((RT)q-PCR).

	Microarray signal T0	**signal T60**	**fold change**	**(RT)q-PCR relative quantity**
CYC7	33	6.4	0.19	0.05
CTT1	6.5	3.5	0.54	0.23
HSP26	11	116	11	7.1
GPM2	7.6	93	12	9.8
OYE3	67	1173	18	44
GTT2	37	1378	37	55

Table 5.3. Dependence of NO donor-induced changes in gene expression on the respiratory chain, and on the transcription factors Msn2/4p and Yap1p.

The gene expression in the mutants Δ*yhb1* rho^0 (mtDNA-less), Δ*yhb1* Δ*msn2/4* and Δ*yhb1* Δ*yap1* after 60 minutes treatment with 3 mM NO donor was compared with gene expression in the control under the same conditions. 3 replicate chips were examined for the control and one chip for all other samples. The ratio "fold change in mutant / fold change in control" (R) was calculated for each gene. Assignment of genes into categories utilised the cut-off values for R indicated in the Table. R_1, R_2 and R_3 are the ratios in, respectively, rho^0, Δ*yap1* and Δm*sn2/4*. [a]Number of genes already altered in the untreated rho^0. [b]The genes exhibiting strong dependence on the respiratory chain are *GPH1*, *MAL32*, *TSL1*, *GDB1*, *GLC3*, *SUC4*, *SUC2*, *HSP26*, *HSP24*, *GPG1*, *YPR013C*, *DCS2*, *YIL057C*, *YNR034w-a*, *YNR073C*, *YER067W*, *YCL042W*, *YFR017C* (overexpressed), *RKI1*, *SPS4* and *RPL7B* (repressed); [c]Yap1p dependent genes: *AAD6*, *SRX1*, *ECM38*, *PRX1*, *GLO4*, *OYE3*, *TDH1*, *GPH1*, *OSM1*, *GDH3*, *BDH1*, *GSY2*, *GLG1*, *SUC4*, *SUC2*, *SRY1*, *ATR1*, *HSP26*, *SNO4*, *YGP1*, *WSC4*, *PKH2*, *HAP1*, *PHO5*, *YGR287C*, *PHO11*, *YKL071W*, *YCL042W*, *YFR017C*, *YRO2*, *YLR047C* (overexpressed), *COX23*, *CBP6*, *ACO1*, *RKI1*, *HNM1*, *RPL7B*, *FMP10* and *YFR026C* (repressed); [d]Msn2/4p dependent genes: *GTT2*, *TSA2*, *GSH1*, *NTH1*, *YNL274C*, *TSL1*, *GDB1*, *TPS2*, *LEU2*, *PAI3*, *TFS1*, *HSP31*, *GIP2*, *GPG1*, *HUG1*, *YOL155C*, *KTR2*, *DDR48*, *ANB1*, *YHR087W*, *YNR064C*, *SOL4*, *YLL056C*, *YMR090W*, *YLR346C* (overexpressed), *CYC1*, *CYB2*, *HMX1*, *CYC7*, *SUE1*, *SLS1*, *ADH1*, *JEN1*, *HXT2*, *HMG1*, *MVD1*, *ERG13*, *ERG25*, *INO2*, *PUT4*, *YMR009W*, *UBX6*, *SSA2*, *PTR2*, *TEC1*, *SST1*, *HPA2*, *RSM24* and *YBR056w-a* (repressed); [e]Yap1p and Msn2/4p dependent genes: *AAC3*, *YEL047C*, *MAL32*, *YHR048W*, *FLR1*, *YDR089W*, *YOL155C*, *YOL057W*, *GPM2*, *YPR013C*, *YNR034w-a*, *YNR073C*, *YER067W*, *YML131W*, *YER067c-a* (overexpressed), *CTA1*, *ADH2*, *FBP1*, *PCK1*, *ICL1*, *STL1*, *PXA2*, *ARG8*, *ADY2*, *MRPL1*, *PCS60*, *MSF1* and *YBR242W* (repressed).

A	Effect of respiratory deficiency	Number of genes
Overexpressed genes	Strong[b] ($R_1 \leq 0.25$)	30 (12[a])
	Weak ($0.25 < R_1 < 0.75$)	115
	None ($0.9 \leq R_1$)	32
	Unclear ($0.75 \leq R_1 < 0.9$)	7
Repressed genes	Strong ($R_1 \geq 4$)	5 (2[a])
	Weak ($4 > R_1 > 1.33$)	46
	None ($1.11 \geq R_1$)	42
	Unclear ($1.33 \geq R_1 > 1.33$)	14

B	Regulation	Number of genes
Overexpressed genes	Yap1p only[c] ($R_2 < 0.75$; $0.9 \leq R_3$)	31
	Msn2/4p only[d] ($R_3 < 0.75$; $0.9 \leq R_2$)	25
	Yap1p and Msn2/4p[e] (R_2 and $R_3 < 0.75$)	15
	Other (R_2 and $R_3 \geq 0.9$)	107
	Unclear ($0.75 \leq R_2$ and $R_3 < 0.9$)	6
Repressed genes	Yap1p only[c] ($R_2 > 1.33$; $1.11 \geq R_3$)	8[b]
	Msn2/4p only[d] ($R_3 > 1.33$; $1.11 \geq R_2$)	24[c]
	Yap1p and Msn2/4p[e] (R_2 and $R_3 > 1.33$)	13[d]
	Other (R_2 and $R_3 \leq 1.11$)	58
	Unclear ($1.11 < R_2$ and $R_3 \leq 1.33$)	4

Table 5.4. Genes with altered expression after NO donor treatment but not myxothiazol treatment.

Trancriptional responses to 3 mM DETA NONOate (Δ*yhb1* strain) and 8 μM myxothiazol were compared in the W303-1B background. 265 genes were found to be altered by NO donor but not by myxothiazol. 117 genes which were clearly altered specifically in response to NO donor after comparison to results obtained using another strain (BY1471 Δ*yhb1*) are listed in the table together with the fold change values obtained in the W303-1B Δ*yhb1* strain after 10-120 minutes treatment with DETA NONOate. [a]Gene overexpressed after myxothiazol treatment. Numbers in parenthesis indicate the total number of genes in that category altered after NO donor treatment (see Table 5.1).

A. Genes overexpressed after NO donor treatment

Category	Number of genes	Gene	Function	Fold change			
				10 min	30 min	60 min	120 min
Response to oxidative stress	7 (15)	*AAD4*	Putative aryl-alcohol dehydrogenase	5.1	15.2	27.0	29.6
		AAD6	Putative aryl-alcohol dehydrogenase	3.4	20.6	30.0	37.9
		AAD16	Putative aryl-alcohol dehydrogenase	3.5	10.0	10.4	11.0
		GPX2	Phospholipid hydroperoxide glutathione peroxidase	1.8	2.7	4.8	4.1
		GTT2	Glutathione S-transferase	11.5	30.6	37.1	36.8
		SRX1	Sulfiredoxin	4.1	9.0	13.8	24.1
		YCF1	Glutathione S-conjugate transporter	5.3	10.9	10.7	9.3
Electron transfer and ADP/ATP translocator	1 (4)	*OYE3*	NADPH dehydrogenase	8.4	16.0	17.6	13.6
Glycolysis, gluconeogenesis and carbohydrate storage pathway	3 (48)	*GDH3*	Glutamate dehydrogenase	2.9	4.2	4.2	5.6
		YEL047C	Fumarate reductase	1.5	3.0	5.7	9.3
		YNL134C	Alcohol dehydrogenase	3.6	5.9	5.4	4.6
Peroxisome, fatty acid and lipid metabolism	1 (7)	*FRM2*	Integration of lipid signaling pathways with cellular homeostasis	136.1	206.5	226.0	224.6
Amino acid metabolism, catabolism and transport	2 (21)	*GCV1*	Glycine decarboxylase complex T subunit	1.7	9.7	8.5	5.3
		SDL1	L-serine dehydratase	5.8	15.8	22.2	24.4
Ion homeostasis	2 (7)	*ISU2*	Synthesis of iron-sulfur proteins	10.0	14.4	19.2	21.5
		FRE5	Putative ferric reductase	1.9	3.1	5.7	4.5

Category	Number of genes	Gene	Function	Fold change			
				10 min	30 min	60 min	120 min
Transporter and targeting	7 (28)	*ARN1*	Siderophore-iron transporter	1.6	3.3	6.0	6.5
		ARN2	Siderophore-iron transporter	1.9	2.9	5.0	9.7
		ATR1	Major facilitator drug efflux pump	2.0	4.5	7.0	4.8
		FLR1	Major facilitator drug transporter	2.0	7.9	13.5	11.3
		MCH4	Transporter with similarity to mammalian onocarboxylate permeases	3.9	4.4	4.5	4.3
		SSU1	Major facilitator sulfite pump	2.3	2.9	9.3	10.1
		YHR048W	Drug transporter	3.5	13.0	21.0	20.6
Protein folding and modification	1 (13)	*HSP31*	Heat-shock protein 31	2.8	5.9	5.2	4.4
Response to variable stress	1 (8)	*YAP2*	Basic leucine zipper transcription factor	3.5	4.1	3.7	4.9
Cellular organisation and biogenesis	5 (33)	*DAN4*	Cell wall mannoprotein	2.9	3.3	4.9	4.9
		HUG1	Mec1p-mediated checkpoint pathway	0.9	0.9	5.3	65.3
		PKH2	Serine/threonine protein kinase involved in cell wall integrity	2.1	3.1	5.5	7.9
		SDP1	MAP kinase phosphatase involved in cell wall integrity	11.3	9.3	5.6	15.2
		YOL155C	Involved in cell wall integrity	1.5	1.8	5.5	7.0
DNA structure, replication, transcription and translation	1 (14)	*DDR48*	DNA damage-responsive protein	3.8	4.4	4.1	4.2
Other	2 (18)	*ARR2*	Arsenate reductase	4.6	14.2	26.5	32.9
		YNR064C	Epoxide hydrolase	15.3	52.8	70.7	67.2
Unknown genes	12 (121)	–	–	–	–	–	–
Total	45 (346)	–	–	–	–	–	–

B. Genes repressed after NO donor treatment

Category	Number of genes	Gene	Function	Fold change			
				10 min	30 min	60 min	120 min
Response to oxidative stress	3 (4)	*CCP1*	Cytochrome *c* peroxidase	1.3	0.3	0.1	0.1
		CTA1[a]	Catalase A	1.1	0.5	0.3	0.4
		GRX4	Glutaredoxin	0.5	0.4	0.2	0.2
Electron transfer and ADP/ATP translocator	24 (31)	*CBP4*	Cytochrome *b* mRNA processing	1.4	0.8	0.3	0.3
		COQ2	Ubiquinone biosynthesis	0.5	0.4	0.4	0.3
		COX4	Cytochrome *c* oxidase subunit 4	0.7	0.4	0.4	0.3
		COX5A	Cytochrome *c* oxidase subunit 5a	0.6	0.2	0.2	0.2
		COX6	Cytochrome *c* oxidase subunit 6	0.7	0.5	0.3	0.4
		CYB2[a]	Cytochrome b_2	0.8	0.1	0.1	0.1
		CYC1	Iso-1-cytochrome *c*	0.8	0.05	0.02	0.01
		CYC7[a]	Iso-2-cytochrome *c*	2.4	0.5	0.2	0.4
		CYT1	Cytochrome c_1	0.5	0.2	0.1	0.1
		HEM15	Ferrochelatase	1.7	0.4	0.3	0.2
		HMX1[a]	Heme-binding peroxidase	0.1	0.1	0.1	0.1
		NDI1	NADH:ubiquinone oxidoreductase	1.1	0.3	0.1	0.1
		PET309	Translational activator for the *COX1* mRNA	0.5	0.4	0.4	0.3
		QCR1	bc_1 complex core subunit	0.8	0.4	0.3	0.2
		QCR2	bc_1 complex subunit 2	0.9	0.3	0.2	0.1
		QCR6	bc_1 complex subunit 6	0.6	0.3	0.2	0.2
		QCR9	bc_1 complex subunit 9	0.8	0.4	0.3	0.4
		RIP1	bc_1 complex Rieske iron-sulfur protein	0.8	0.2	0.1	0.1
		SDH1	Succinate dehydrogenase flavoprotein subunit	0.7	0.2	0.1	0.1
		SDH2	Succinate dehydrogenase iron-sulfur protein subunit	0.7	0.1	0.1	0.1
		SDH3	Succinate dehydrogenase cytochrome *b* subunit	0.8	0.3	0.2	0.1
		SDH4	Succinate dehydrogenase membrane anchor	0.9	0.4	0.2	0.1
		SUE1[a]	Degradation of unstable forms of cytochrome *c*	0.6	0.3	0.2	0.4
		YOR356W	Oxidoreductase activity	0.6	0.1	0.1	0.05

Category	Number of genes	Gene	Function	Fold change			
				10 min	30 min	60 min	120 min
Glycolysis, gluconeogenesis and	1 (13)	*ACO1*	Aconitase	0.5	0.1	0.3	0.7
Peroxisome, fatty acid and lipid metabolism	8 (18)	*ACH1*	Acetyl-CoA hydrolase	1.5	0.3	0.2	0.3
		CYB5	Cytochrome b_5	0.1	0.1	0.1	0.1
		ERG7	Lanosterol synthase	0.5	0.2	0.3	0.2
		FAS2	Alpha subunit of fatty acid synthetase	0.7	0.5	0.4	0.2
		HMG1	HMG-CoA reductase isozyme	0.4	0.2	0.2	0.2
		HNM1	Choline transporter	0.4	0.3	0.3	0.3
		MVD1	Mevalonate pyrophosphate decarboxylase	0.5	0.3	0.3	0.3
		OLE1	Fatty acid desaturase	0.3	0.3	0.7	0.8
Amino acid metabolism, catabolism and transport	4 (12)	*GLT1*	Glutamate synthase	0.8	0.2	0.3	0.3
		LEU9	Alpha-isopropylmalate synthase II	0.4	0.2	0.3	0.3
		PUT1[a]	Proline oxidase	0.9	0.6	1.1	0.1
		PUT4[a]	Proline permease	0.4	0.03	0.04	0.04
Ion homeostasis	1 (4)	*CCC1*	Homeostasis of calcium, iron and manganese ions	0.8	0.4	0.4	0.3
Transporter and targeting	3 (13)	*ATO1*[a]	Acetate transporter	1.8	0.3	0.3	0.3
		EMP70	Transporter activity	0.7	0.4	0.5	0.3
		UBX6[a]	Ubiquitin regulatory X	0.9	0.8	0.3	0.3
Protein folding and modification	1 (3)	*PTR2*	Peptide transporter	0.9	0.5	0.3	0.2
Cellular organisation and biogenesis	5 (27)	*KTR6*	Probable mannosylphosphate transferase	0.8	0.4	0.3	0.3
		NCS2	Role in urmylation and invasive/pseudohyphal growth	0.2	0.2	0.4	0.3
		SCM4	Potential regulatory effector of CDC4 function	0.2	0.2	0.1	0.2
		SST2	GTPase-activating protein for Gpa1p	0.9	0.4	0.3	0.3
		SUR7	Involved in sporulation	0.8	0.6	0.3	0.05

Category	Number of genes	Gene	Function	Fold change			
				10 min	30 min	60 min	120 min
DNA structure, replication, transcription and translation	11 (195)	*CLU1*	Involved in mitochondrial organisation	0.9	0.5	0.3	0.2
		DBP10	Protein involved in ribosome biogenesis	0.3	0.4	0.6	0.5
		GCD10	Subunit of tRNA methyltransferase	0.4	0.2	0.6	0.5
		HPA2[a]	Histone acetyltransferase	0.5	0.3	0.2	0.3
		HTB2	Histone H2B	0.9	0.4	0.4	0.2
		MEF1	Mitochondrial elongation factor	1.4	1.1	0.3	0.2
		NOP7	Protein involved in ribosome biogenesis	0.5	0.1	0.5	0.4
		PUS2	Putative pseudouridine synthase	1	0.4	0.4	0.2
		RPC34	RNA polymerase III subunit C34	0.3	0.3	0.8	0.6
		RRP3	Ribosomal RNA processing	0.3	0.4	0.6	0.5
		RSM24	Ribosomal small subunit of mitochondria	1	0.8	0.4	0.3
Other	5 (14)	*DUR1,2*	Urea amidolyase	0.8	0.3	0.4	0.2
		LIP5	Probable lipoic acid synthase	0.8	0.4	0.3	0.3
		MDV1	Mitochondrial fission	0.7	0.5	0.4	0.2
		MIS1	Mitochondrial C_1-tetrahydrofolate synthase	0.6	0.3	0.4	0.3
		PCS60[a]	AMP-binding protein	0.8	0.5	0.4	0.3
Unknown genes	6 (49)	–	–	–	–	–	–
Total	72 (385)	–	–	–	–	–	–

Table 5.5. Expression changes of known and putative Hap1p and Rox1p-regulated genes after NO donor and myxothiazol treatment.

The list of known and putative Hap1p-regulated genes is taken from (Ter Linde and Steensma, 2002). "+" = upregulated, "-" = repressed. The fold change values after treatment with 3 mM DETA NONOate are given. The number of replicate chips examined for each time point is given in 2.5.1.6.

	Fold change				myxothiazol
	10 min	30 min	60 min	120 min	
Known Hap1p-regulated genes					
CTT1	unchanged				
CYB2	0.79	0.09	0.07	0.10	+
CYC1	0.79	0.05	0.02	0.01	unchanged
CYC7	2.36	0.52	0.19	0.41	+
CYT1	0.50	0.17	0.08	0.07	unchanged
DLD1	unchanged				
ERG9	unchanged				
ERG11	unchanged				
HAP1	2.65	2.86	4.47	2.46	unchanged
HMG1	0.37	0.23	0.23	0.22	-
HYP2	0.62	0.48	0.35	0.37	unchanged
QCR1	0.77	0.38	0.27	0.18	unchanged
QCR2	0.86	0.29	0.17	0.14	unchanged
ROX1	unchanged				
SOD2	unchanged				
YHB1	unchanged				
Putative Hap1p-regulated genes (7 other candidates unchanged)					
CYB5	0.07	0.07	0.06	0.07	unchanged
GFD2	0.11	0.07	0.23	0.18	-
HMX1	0.13	0.09	0.07	0.13	+
HPA2	0.50	0.31	0.20	0.32	+
MLS1	0.76	0.87	1.53	4.39	unchanged
PCK1	1.03	0.47	0.32	0.33	unchanged
PUT1	0.85	0.62	1.12	0.14	+
PUT4	0.35	0.03	0.04	0.04	+
REG2	4.53	2.93	1.86	0.49	unchanged
SCM4	0.23	0.19	0.13	0.18	unchanged
STL1	0.41	0.07	0.12	0.08	-
Known Rox1p-regulated genes					
AAC3	0.83	2.57	3.72	5.86	+
ANB1	1.03	2.45	8.23	22.40	+
ATF1	unchanged				
COX5B	3.36	6.93	8.31	8.91	+
HEM13	unchanged				
HMG2	unchanged				
NCP1	unchanged				
SUT1	unchanged				
Putative Rox1p-regulated genes (23 other candidates unchanged)					
DIP5	3.05	0.64	1.27	2.29	+
FIT2	1.83	2.93	4.08	5.17	+
FIT3	1.74	2.80	3.69	4.19	unchanged
ISU2	9.95	14.37	19.18	21.48	unchanged
RTA1	1.07	1.60	1.68	4.82	unchanged
SCM4	0.23	0.19	0.13	0.18	unchanged
SPI1	6.03	8.87	5.05	12.34	+
YAL028W	4.60	5.14	3.52	4.37	+
YGR066C	7.15	3.00	5.60	10.51	unchanged
YGR035C	1.31	1.79	4.12	2.15	-
YHR048W	3.47	13.02	20.99	20.58	unchanged

Chapter 6

CONCLUSIONS AND FUTURE DIRECTIONS

This work was intended to address two separate areas, with the mitochondrial respiratory chain and the yeast *Saccharomyces cerevisiae* as central themes. First, the assembly of the respiratory chain enzyme cytochrome oxidase was investigated, using yeast as a model system. Second, the nature of the antimicrobial effect of nitric oxide (NO) and its derivatives reactive nitrogen species (RNS) was assessed in yeast.

6.1. CYTOCHROME OXIDASE ASSEMBLY

Cytochrome oxidase takes the form of a dimer, and in yeast each monomer is composed of 11 subunits of dual genetic origin. Added complexity comes from the presence of several metal cofactors and the integral membrane location of the assembled enzyme. It is therefore unsurprising that its assembly has been found to require a vast array of assembly factors (Table 1.2). Much progress has been made in identifying the mechanisms involved in insertion of subunits into the IMM and assembly of the cofactors. However, the processes by which the subunits themselves interact with each other to form the assembled enzyme complex are only just beginning to be elucidated. In the human system analysis of cells with defective assembly has led to the identification of assembly subcomplexes, providing some information on the sequential interaction between subunits (Nijtmans et al., 1998; Williams et al., 2004) (Figure 6.1).

Yeast have long been used as a model organism to investigate respiratory chain function, and the majority of the assembly factors known to be required for cytochrome oxidase assembly were first identified in yeast. However, the use of yeast in investigating the sequential assembly process of cytochrome oxidase has been limited by the efficient degradation of unassembled subunits, in particular the core subunits, by AAA proteases when assembly is impaired (Pearce and Sherman, 1995; Guelin et al., 1996). There has only been one previous report of cytochrome oxidase subassemblies in yeast. Church *et al.* identified three subcomplexes, two containing the nuclear subunits Cox7p, Cox7ap and Cox8p, with or without the chaperone Pet100p, and one containing Cox5ap and Cox6p, by sucrose gradient centrifugation and immunoprecipitation (Church et al., 2005). However, prior to the work described in this thesis no subassemblies containing the core mitochondrially-encoded subunits had been identified in yeast.

6.1.1. Mutations in *COX2* abolishing assembly

With a view to elucidating the involvement of the core subunit Cox2p in the assembly process, I analysed yeast strains with mutations in the *COX2* gene, causing amino acid alterations in the C-terminal soluble domain of Cox2p. Most of the mutations

completely abolished cytochrome oxidase assembly, reflecting the central location of Cox2p in the enzyme complex. To try to gain more information on the mutants I generated several revertant strains with additional mutation in the nuclear genome. The nature of the reversions could provide useful information about the mechanism by which the original mutation prevents assembly. Although I sequenced several candidate genes to try to identify the locations of the nuclear reversions, I was unsuccessful in locating them. A more profitable approach might be to construct genomic libraries from the revertant strains and transform them into the original mutant strains, select for those clones which have regained respiratory competence, and identify the genes responsible.

It may also be interesting to assess whether translocation of the C-terminal domain occurs in these mutants. C-terminal translocation is thought to involve the assembly factors Cox18p, Mss2p and Pnt1p (He and Fox, 1999; Broadley et al., 2001; Saracco and Fox, 2002). It is not clear whether it occurs before or after formation of the Cu_A site of Cox2p. The mutations could impair the binding of copper, or alter interaction with assembly factors, preventing translocation. Fox and colleagues have developed a system whereby a synthetic yeast mitochondrial gene *ARG8*^{m} is fused to *COX2* resulting in a fusion protein with Arg8^{m}p attached to the C-terminus of Cox2p (He and Fox, 1999). Soluble nuclear encoded Arg8p is normally imported into the matrix, where it participates in arginine biosynthesis. In the fusion protein Arg8p is exported to the IMM, and is unable to participate. If the nuclear-encoded Arg8p protein is nonfunctional, export of Arg8^{m}p to the IMM will cause an Arg$^-$ phenotype, hence defects in Cox2p C-terminal export can be identified by an Arg$^+$ phenotype.

6.1.2. Subcomplexes of cytochrome oxidase

Blue native electrophoresis allows separation of protein complexes in non-denaturing conditions (Schagger and von Jagow, 1991). I applied this technique to the separation of complexes present in mitochondrial membrane preparations of yeast, and used antibodies recognising subunits of cytochrome oxidase to try to identify subcomplexes of the enzyme. In wild type yeast I was able to identify one subcomplex of particular interest, containing Cox7p and/or Cox7ap (the antiserum used recognised both of these co-migrating subunits) (Figure 3.6). Due to the extent of migration of this subcomplex it seems likely that other proteins are associated with it, however the subcomplex did not contain any other cytochrome oxidase subunits (although I did not probe for Cox6bp). It is therefore unlikely to correspond to the complex identified by Church *et al.* containing Cox7p, Cox7ap and Cox8p (with or without Pet100p) (Church et al., 1996), although it

could be related to it, and it may be interesting to probe for the presence of Pet100p. Other chaperone proteins (see Table 1.2) could also be associated with the subcomplex.

Unusually, two of the *COX2* mutants screened (G156E and R159K) allowed partial assembly of cytochrome oxidase, permitting identification of a further subcomplex by blue native electrophoresis, this time containing core cytochrome oxidase subunits (Figure 3.6). The complex detected contained Cox1p, Cox3p, Cox5p and Cox6p, but not Cox2p, Cox4p, Cox6ap, Cox7p, Cox7ap or Cox8p. This novel subcomplex is likely to represent the degradation product of a subassembly containing the core subunits Cox1p, Cox2p and Cox3p, together with the nuclear subunits Cox5p and Cox6p. The existence of such a subcomplex is in agreement with the current model for assembly of mammalian cytochrome oxidase (Figure 6.1). Mammalian COX1, COX4 and COX5A, the equivalents of yeast Cox1p, Cox5p and Cox6p, respectively, are believed to interact first to form a subcomplex S2. Since Cox2p and Cox3p are core subunits, they would be expected to associate with S2 soon afterwards. It would be useful to perform a pulse chase experiment to compare the stability of Cox2p in the G156E and R159K mutants with that of the wild type Cox2p and the Cox2p in the assembly-abolished mutants. It might be expected that while Cox2p in the other mutants would be degraded rapidly, the G156E or R159K mutated Cox2p would persist for longer, although not as long as wild type Cox2p.

6.1.3. Perspectives

The residues R159 and G156 of *COX2* are conserved between species (Figure 6.2). Together with the similar phenotype resulting from mutation at both of these residues, this suggests that this region of Cox2p has a particular role in assembly. Interestingly, McFarland *et al.* identified a human mutation L135P at the equivalent residue to yeast L160, another highly conserved amino acid in this region (McFarland et al., 2004). The mutation caused rhabdomyolysis, the breakdown of muscle fibers with leakage of potentially toxic cellular contents into the circulation. The assembly defect caused by mutation of the nearby residues R159 and G156 in yeast in this conserved region may provide some clues as to the molecular defect in this patient. It seems likely that the human mutation could cause an assembly problem in cytochrome oxidase.

In conclusion, this work has demonstrated that yeast are a valuable model for further elucidation of the cytochrome oxidase assembly pathway. Other cytochrome oxidase mutant strains should now be analysed in a similar way to that described here,

in an attempt to identify further subassemblies which could provide information on the assembly process.

6.2. ANTIMICROBIAL EFFECT OF NO/RNS

NO is released in high concentrations by macrophages, and RNS together with ROS form the first line of host cell defence against pathogens. Release of NO is an important mediator of the activity of macrophages against several pathogenic fungi. Host resistance increases with iNOS expression and inhibition of NOS exacerbates infection (see for example (Lane et al., 1994; Lovchik et al., 1995)). The second part of my thesis investigated the antimicrobial action of NO/RNS, using the effect of the NO donor DETA NONOate on yeast as a model. I first assessed the effect of NO/RNS on yeast proliferation and on the cytochromes of the respiratory chain. I then measured the genomic response to NO/RNS to try and determine the nature of the stress sensed by the cells on exposure, and the factors which mediate the response to this stress. I also tried to assess whether ROS contributed significantly to the stress, and whether several candidate transcription factors were involved in mediating the responses to NO/RNS.

6.2.1. Yeast are extremely resistant to NO/RNS

Yeast contain a highly efficient NO oxidoreductase, which makes cells extremely resistant to NO/RNS even at high concentration (Figure 4.1, Figure 4.2A). To allow identification of other NO/RNS defence systems I therefore performed all my analyses in strains lacking the *YHB1* gene. However, even in the absence of Yhb1p yeast were very resistant to treatment. Very high doses of NO donor were required to affect cell proliferation; 0.1 mM and 1 mM of DETA NONOate had little effect. These results are in agreement with previous reports on the sensitivity of yeast growth to this particular NO donor (Liu et al., 2000; Matsumoto et al., 2003). Furthermore, even high doses of DETA NONOate did not cause cell death in yeast: a cytostatic rather than cytotoxic effect was observed. A similar result was also observed in the pathogen fungus *H. capsulatum* using an alternative NO donor DPTA NONOate (Nittler et al., 2005). When mammalian cells are subjected to similar doses a clear deleterious effect is observed. For example, in a human breast cancer cell line incubation with 0.1 mM DETA NONOate (concentration of 0.5 μM NO in the growth medium) led to cytostasis by 12 hours, followed by cytotoxicity (Pervin et al., 2001). Mammalian cells are highly susceptible to the high concentrations of NO generated by macrophages, however the macrophages themselves are relatively resistant, allowing them to persist to carry out their physiological functions. Activated macrophages synthesising NO seem to have an

atypical apoptotic cascade which makes the cell resistant to apotosis in the presence of NO (Boscá et al., 2005). Yeast also seem to be particularly resistant to NO/RNS, and this is not just because of Yhb1p, suggesting that, in addition to Yhb1p, yeast have other effective defence strategies against NO/RNS which make them particularly insensitive to these compounds.

6.2.3. General considerations about the microarray analysis

The analysis of global gene expression after NO donor treatment was intended to give clues as to the nature of the stress sensed by cells on exposure, on the defence mechanisms used to negate this stress, or repair or remove the damage caused by it.

When interpreting the microarray data it must be remembered that the correlation between mRNA and protein levels is not always straightforward. Post-translational mechanisms of control at the level of translation rate and protein stability mean that the relationship between the two can be variable. A study by Gygi *et al.* determined the relationship between mRNA and protein levels for 106 yeast genes (Gygi et al., 1999). A general trend of increased protein levels resulting from increased mRNA levels was found, but for genes with low mRNA or protein levels the correlation was much less apparent. The same group also looked at the correlation between mRNA and protein expression changes induced by growth of yeast on two different carbon sources, and found that, while in many cases changes in mRNA level corresponded with changes at the protein level, a significant number of changes did not show correlation (Griffin et al., 2002). So, while measurement of mRNA changes cannot give definitive conclusions as to the corresponding protein levels, they will frequently show correlation and can certainly identify trends. The next step regarding the microarray data would be to assess the protein levels of some of the genes exhibiting an interesting response to treatment to see if the transcript changes are translated into alteration at the protein level.

On a separate but related point, it must be considered that other mechanisms of enzyme regulation exist apart from modification of mRNA level. Activity of enzymes can be regulated by covalent modification (for example phosphorylation), or by subcellular distribution. Microarray data does not provide information relating to this, therefore there are likely to be other mechanisms of defence against RNS that have not been identified in this study. For example, the MnSOD of potato mitochondria (Bykovaet al., 2003) and pig heart mitochondria (Hopper et al., 2006) have been shown to be phosphorylated. Dephosphorylation of MnSOD on incubation with calcium

correlated with an increase in MnSOD activity, suggesting a potential link between phosphorylation and activity (Hopper et al., 2006). Therefore an involvement of superoxide dismutase in the response to RNS stress cannot be excluded solely on the basis of an absence of induction in the microarray data. Additionally, NO can lead to S-nitrosation of cysteine thiols, which has been implicated in protein regulation (Hess et al., 2005).

6.2.4. Targets of NO/RNS and mechanisms of defence

Incubation with NO donor had a severe effect on the cytochrome oxidase content of yeast cells. NO donor also had an initial effect on other cytochromes, but the levels of these returned to normal over the period tested. The decrease in cytochrome oxidase content was observed only in dividing cells, not non-dividing cells, suggesting that NO/RNS was somehow interfering in the assembly of cytochrome oxidase. The microarray analysis showed that expression of several respiratory chain genes was repressed on NO donor treatment, however, this was not confined to cytochrome oxidase, therefore cannot fully explain the severe decrease in content observed, suggesting instead that NO/RNS interferes in some way with the physical assembly of the enzyme complex. It would be interesting to analyse the subunit profile of cytochrome oxidase after NO donor treatment, as performed for the *COX2* mutants in Chapter 3. A decrease in respiratory chain complexes would not affect the viability of *S. cerevisiae* because in the presence of NO, an inhibitor of cytochrome oxidase, the cells would have presumably switched to fermentation. However, in pathogens relying more heavily on respiration, the decrease in cytochromes could have a more deleterious effect.

When cell proliferation was diminished due to the absence of a respiratory chain, or an inhibited respiratory chain, addition of NO donor caused a further inhibition of cell proliferation, indicating that mechanisms other than simple inhibition of the respiratory chain must also be in operation. RNS can interact with and damage several protein moieties, and are likely to react with numerous proteins and other cellular constituents. This might cause a general cell stress which would slow growth rate while cells attempted to repair the damage. A large number of genes of the category "DNA structure, replication, transcription and translation" were repressed on incubation with NO donor, many linked with the response to sudden environmental change associated with growth arrest. However, the repression of such genes was largely transient, suggesting that this would not explain the prolonged growth inhibition.

Proteins with a more specific involvement in cell growth could be targets of RNS. One target pathway could be the biosynthesis of ergosterol, an essential constituent of the yeast cell wall. In the microarray analysis the expression of several genes involved in ergosterol biosynthesis was downregulated. Furthermore, NO may be able to inhibit those enzymes of the ergosterol biosynthetic pathway which contain cytochrome P450. A preliminary experiment to test the effect of addition of ergosterol to the growth medium did not demonstrate relief of the growth inhibition caused by NO donor. Nevertheless, it would be interesting to measure the ergosterol content in NO donor-treated cells, to see whether the decrease in gene expression or potential inhibition of the biosynthetic enzymes led to a decrease in ergosterol content. Another possible target is ribonucleotide reductase, the rate-limiting step in DNA synthesis. NO has been previously shown to have an inhibitory effect on this enzyme (Kwon et al., 1991). If non-functional, the synthesis of new DNA, and therefore cell proliferation, would be impaired. To test this deoxyribonucleosides could be added to the cell culture to see whether this leads to any decrease in the growth inhibition caused by NO donor.

The microarray data provides many other clues to the mechanism of inhibition of proliferation. As might be expected, upregulation of genes involved in removal of reactive species was observed. Several members of the peroxiredoxin and phospholipid hydroperoxide glutathione peroxidase family were upregulated. These enzymes are involved in the removal of hydrogen peroxide, alkyl hydroperoxides, and peroxynitrite. More prevalent than induction of genes involved in detoxification of RNS themselves was the upregulation of genes involved in the repair of cell damage. In particular several enzymes which could be implicated in the removal of lipid epoxides were highly upregulated, including the phospholipid hydroperoxide glutathione peroxidase family mentioned above, an epoxide hydrolase and several putative aryl alcohol dehydrogenases. In addition, the glutathione detoxification system, which may facilitate removal of toxic material from the cell, seemed to be activated, and enzymes of the DNA repair system were induced. Furthermore, genes involved in iron homeostasis were altered, perhaps in response to breakdown of iron-sulfur clusters.

Three papers have been published recently assessing gene expression changes in fungi in response to nitrosative stress. Firstly, Sarver and DeRisi studied the effect of the NO donor DPTA NONOate and NO gas on *S. cerevisiae* (Sarver and DeRisi, 2005). As in this study, the majority of the gene changes were associated with the general stress response. The study focused on a strong and long lasting induction of *YHB1*, *SSU1* (sulfite transporter), YNR064C (epoxide hydrolase) and two homologous ORFs

YNL335W and YFL061W. The transcription factor Fzf1p was shown to be involved in the regulation of these transcripts. The transcripts (with the obvious exception of *YHB1*) were also upregulated by NO donor treatment in my study. Secondly, Nittler et al. assessed the response to nitrosative stress caused by DPTA NONOate and GSNO in the pathogenic fungus *H. capsulatum* (Nittler et al., 2005). Several sets of genes were induced, including those involved in iron acquisition and DNA repair. Finally, Hromatka *et al.* looked at the effect of DPTA NONOate on another pathogenic fungus *C. albicans* (Hromatka et al., 2005). A large number of respiratory chain genes were repressed after treatment, as was also observed in my study.

The work described in this thesis seems to fit well with these reports, suggesting that nitrosative stress activates the same defence systems in *S. cerevisiae* and pathogenic fungi. It also expands on the data, in particular by assessing the involvement of several different transcription factors in the response to nitrosative stress, and the contribution of ROS and inhibition of the respiratory chain. It would now be interesting to generate strains with deletion of some of those genes found to be involved in the response to NO/RNS, and determine their sensitivity to NO donor. It may be that deletion of these genes potentiates the inhibition of cell proliferation caused by NO/RNS.

6.2.5. Involvement of ROS in the effect of NO/RNS

ROS are involved in the generation of some RNS. Additionally, NO increases the synthesis of ROS through inhibition of the respiratory chain (Poderoso et al., 1996). Previous studies in yeast did not find evidence for a major contribution of ROS in the antimicrobial effect of NO. Jakubowski *et al.* found only minor differences in growth inhibition caused by the NO donor GSNO on strains with deletions of antioxidant defence genes (Jakubowski et al., 1999). Chiang *et al.* found that the toxicity of NO was enhanced under aerobic conditions, but this was not due to the action of hydrogen peroxide or superoxide (Chiang et al., 2000). However, these studies did not utilise strains with deletion of *YHB1* so effects could have been overlooked. To clarify this, I reassessed the involvement of ROS in the antimicrobial effect of NO donor.

The majority of my data points away from a major involvement of ROS, at the level of both cell growth and gene expression. In the absence of a functional respiratory chain a high concentration of NO donor caused inhibition of cell proliferation; since the respiratory chain is the major site of ROS production this suggests that ROS do not provide a major contribution to the inhibition. Furthermore, deletion of genes encoding enzymes involved in the removal of ROS (superoxide dismutase, catalase and

cytochrome *c* peroxidase) did not alter the extent of inhibition of yeast growth by NO donor. However, double deletions (for example both *SOD1* and *SOD2* genes) were not assessed and it is possible that compensatory mechanisms could be involved. Notably absent in the transcriptional response to NO/RNS was the induction of these ROS defence genes, which are highly induced in the presence of hydrogen peroxide (Gasch et al., 2000; Causton et al, 2001). This lack of induction on NO donor treatment would suggest that the cell recognises RNS stress as distinct from ROS stress, and may also suggest that ROS do not have a major involvement in the RNS-induced stress. In the absence of a respiratory chain the overall gene expression response to NO donor was similar to the response observed in control cells, suggesting that the stress sensed was similar whether or not ROS were generated by the respiratory chain. However, several genes involved in the removal of peroxides were induced by NO donor treatment, and many of the genes upregulated were also upregulated by hydrogen peroxide (Gasch et al., 2000; Causton et al, 2001), suggesting that RNS stress does shares some features with oxidative stress. Furthermore, the transcription factor Yap1p, mediator of the response to oxidative stress, was involved in the expression alteration of 23% of genes.

In summary, the evidence does not exclude involvement of ROS in the RNS-induced stress, but suggests that a significant part of the stress does not involve the contribution of ROS and is specific to RNS. As discussed earlier it cannot be excluded that post-translational events affecting the activity of proteins involved in ROS metabolism could occur, and I have not investigated this.

6.2.6. Downregulation of Hap1p-activated genes by NO donor

The most striking observation made from the transcriptional analysis was the repression of a large number of respiratory chain genes and genes involved in fatty acid and sterol synthesis after NO donor treatment. In yeast, in aerobic conditions, the presence of heme liberates the transcription factor Hap1p from the complex (HMC) it forms with other proteins, enabling it to activate transcription of aerobic genes encoding proteins involved in the respiratory chain, and heme, sterol and fatty acid synthesis. One of the major genes activated is *ROX1*, the product of which represses transcription of several hypoxic genes. The microarray data showed that a large number of genes under the control of Hap1p were expressed at a lower level after addition of NO donor, resembling the situation in anaerobiosis, suggesting that Hap1p may be, directly or indirectly, affected by NO/RNS.

In mammalian cells the major transcription factor involved in the response to oxygen concentration is the heterodimeric HIF-1 (hypoxia-inducible factor-1). In low oxygen concentrations HIF-1 binds to promoters of hypoxia-inducible genes to activate transcription. One component of the heterodimeric protein is HIF-1α, the stability of which is regulated in response to oxygen concentration (Wang et al., 1995; Huang et al., 1996). In conditions of low oxygen the activity of a family of prolyl hydroxylases is inhibited and HIF-1α accumulates to form an active dimer with HIF-1β and activate expression of hypoxic genes (Ivan et al., 2005; Jaakkola et al., 2005). NO and other respiratory chain inhibitors have been shown to prevent the stabilisation of HIF-1α during hypoxia (Hagen et al., 2003). This is due to a lack of inhibition of prolyl hydroxylase, possibly due to the increased availability of oxygen, which has not been consumed by the respiratory chain. However, high concentrations of NO have the converse effect and stabilise HIF-1α, even at high oxygen concentration (Mateo et al., 2003), allowing it to activate transcription of hypoxic genes. This stabilisation is independent of the respiratory chain, and has been suggested among other things to be due to S-nitrosation of thiols in HIF-1α or inactivation of prolyl hydroxylase by NO. It seems therefore that in mammalian cells high concentrations of NO cause the cell to sense a hypoxic state and activate hypoxic genes. In yeast, NO seems to have a similar effect in preventing the transcription of aerobic genes.

I attempted to determine whether Hap1p activity was decreased after NO donor treatment, however, the β-galactosidase assay I used was unsuitable. The gene expression profile, though, strongly suggests that Hap1p is affected in some way by NO/RNS. One possible hypothesis could be that NO/RNS might affect Hap1p by interfering with heme synthesis, thereby decreasing heme levels and preventing Hap1p release from the inhibitory HMC. The mammalian equivalent of Hem15p, catalysing the final step of heme biosynthesis, is inhibited by NO through destruction of its iron-sulfur centre, though the yeast enzyme does not contain this cluster and is unaffected by NO (Sellers et al., 1996). However, several heme biosynthetic enzymes contain cytochrome P450, and NO has been shown to inhibit members of this superfamily. I made a preliminary attempt to assess the effect on transcription of adding a heme precursor to the NO donor-treated cells and found no differences, but further investigation would be required to confirm this result, and it would be interesting to pursue this hypothesis further. Any decrease in heme synthesis might also be expected to result in a decrease in the levels of heme-containing proteins, including components of the respiratory chain as well as other proteins, possibly contributing to the decreased cell proliferation.

If alteration of heme level was discounted as a mechanism of Hap1p inactivation by NO donor, it might be possible that RNS could act directly on Hap1p. The DNA-binding domain of Hap1p is a Zn_2Cys_6 binuclear cluster domain. S-nitrosation at the cysteine residues may disrupt the coordination of zinc and hamper binding to DNA, thereby preventing the activity of Hap1p. Treatment of *K. lactis* with NO caused a decrease in DNA binding activity of the *LAC9* transcription factor, which contains a Zn_2Cys_6 domain (Krönke et al., 1994). Alternatively, perhaps NO/RNS could affect the other proteins of the HMC, which include Hsp90p, Ydj1p, Hsp70p and Sro9p (Hon et al., 2001) to prevent release of Hap1p.

6.2.7. Conclusions

In summary, yeast are highly resistant to the effects of NO/RNS, and antimicrobial effects are observed only with high concentrations of NO donor. The main defence mechanism against NO is the NO oxidoreductase Yhb1p. However, yeast also seem to contain several other defence mechanisms to counteract the damage caused by NO/RNS. These include enzymes which detoxify peroxides, in particular lipid epoxides, and enzymes involved in iron homeostasis and repair of DNA damage. RNS also seem to affect cytochrome levels, in particular cytochrome oxidase. The majority of the RNS-induced stress observed did not appear to rely on the presence of ROS. The pattern of gene expression induced by NO/RNS points to involvement of the oxygen-responsive transcription factor Hap1p. This work could provide valuable information on the strategies used by pathogens to defend against the antimicrobial action of RNS.

6.3. FINAL REMARKS

This thesis illustrates the versatility of the yeast *Saccharomyces cerevisiae* as a model organism which can be utilised in the investigation of subjects relevant to both higher and lower eukaryotes. In particular, *S. cerevisiae* is exceptionally useful in the investigation of matters relating to respiration, due to its capacity to remain viable even in the absence of a functional respiratory chain.

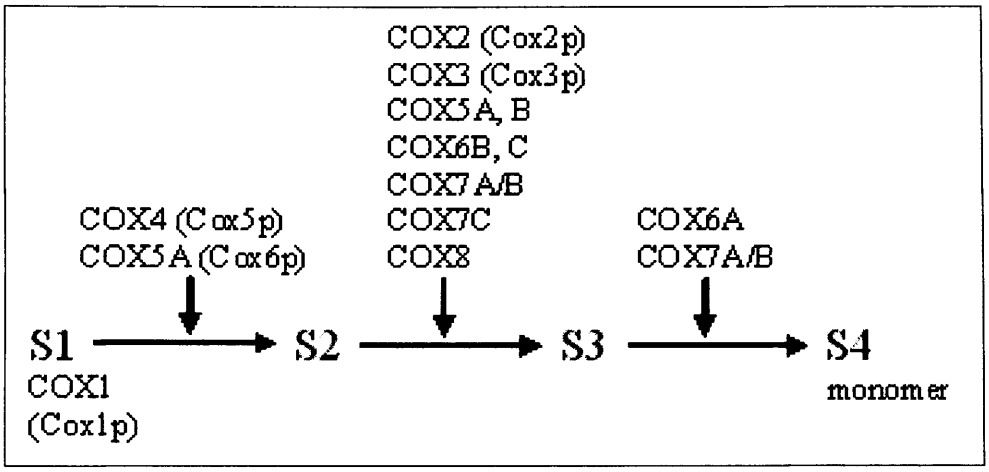

Figure 6.1. Mammalian cytochrome oxidase assembly pathway.

Several assembly subcomplexes have been identified in human cells (Nijtmans et al., 1998; Williams et al., 2004). Yeast counterparts of some of the human subunits are given in parenthesis.

Yeast	V	I	P	D	E	L	L	E	E	**G**	Q	L	**R**	L	L	D	T	D	T	S	M	V	V	P
Human	M	L	P	P	L	F	L	E	P	**G**	D	L	**R**	L	L	D	V	D	N	R	V	V	L	P
Mouse	M	I	P	T	N	D	L	K	P	**G**	E	L	**R**	L	L	E	V	D	N	R	V	V	L	P
Rat	M	I	P	T	N	D	L	K	P	**G**	E	L	**R**	L	L	E	V	D	N	R	V	V	L	P
Bovine	M	I	P	T	S	E	L	K	P	**G**	E	L	**R**	L	L	E	V	D	N	R	V	V	L	P
Xenopus	M	I	P	T	N	D	L	T	P	**G**	Q	F	**R**	L	L	E	V	D	N	R	M	V	V	P

Figure 6.2. Sequence comparison of the *COX2* gene showing the conserved residues G156 and R159.

Sequences were obtained from NCBI and alignment was made using ClustalW (http://www.ebi.ac.uk/clustalw/)

REFERENCE LIST

Aggeler,R. and Capaldi,R.A. (1990). Yeast cytochrome *c* oxidase subunit VII is essential for assembly of an active enzyme. Cloning, sequencing, and characterization of the nuclear-encoded gene. J. Biol. Chem. *265*, 16389-16393.

Alderton,W.K., Cooper,C., and Knowles,R.G. (2001). Nitric oxide synthases: structure, function and inhibition. Biochem. J. *357*, 593-615.

Altamura,N., Capitanio,N., Bonnefoy,N., Papa,S., and Dujardin,G. (1996). The *Saccharomyces cerevisiae* OXA1 gene is required for the correct assembly of cytochrome *c* oxidase and oligomycin-sensitive ATP synthase. FEBS Lett. *382*, 111-115.

Aulak,K.S., Miyagi,M., Yan,L., West,K.A., Massilon,D., Crabb,J.W., and Stuehr,D.J. (2001). Proteomic method identifies proteins nitrated in vivo during inflammatory challenge. Proc. Natl. Acad. Sci. USA *98*, 12056-12061.

Avery,A.M. and Avery,S.V. (2001). *Saccharomyces cerevisiae* expresses three phospholipid hydroperoxide glutathione peroxidases. J. Biol. Chem. *276*, 33730-33735.

Balatri,E., Banci,L., Bertini,I., Cantini,F., and Ciofi-Baffoni,S. (2003). Solution structure of Sco1: A thioredoxin-like protein involved in cytochrome *c* oxidase assembly. Structure *11*, 1431-1443.

Ballinger,S.W., Patterson,C., Yan,C.N., Doan,R., Burow,D.L., Young,C.G., Yakes,F.M., Van Houten,B., Ballinger,C.A., Freeman,B.A., and Runge,M.S. (2000). Hydrogen peroxide- and peroxynitrite-induced mitochondrial DNA damage and dysfunction in vascular endothelial and smooth muscle cells. Circ. Res. *86*, 960-966.

Barrientos,A., Barros,M.H., Valnot,I., Rotig,A., Rustin,P., and Tzagoloff,A. (2002). Cytochrome oxidase in health and disease. Gene *286*, 53-63.

Barros,M.H., Nobrega,F.G., and Tzagoloff,A. (2001). Involvement of mitochondrial ferredoxin and Cox15p in hydoxlation of heme O. FEBS Lett. *492*, 133-138.

Barros,M.H., Johnson,A., and Tzagoloff,A. (2004). COX23, a homologue of COX24, is required for cytochrome oxidase assembly. J. Biol. Chem. *279*, 31943-31947.

Barros,M.H., Myers,A.M., Van Driesche,S., and Tzagoloff,A. (2006). COX24 codes for a mitochondrial protein required for processing of the COX1 transcript. J. Biol. Chem. *281*, 3743-3751.

Basrai,M.A., Velculescu,V.E., Kinzler,K.W., and Hieter,P. (1999). NORF5/HUG1 is a component of the MEC1-mediated checkpoint response to DNA damage and replication arrest in *Saccharomyces cerevisiae*. Mol. Cell. Biol. *19*, 7041-7049.

Bauer,M., Behrens,M., Esser,K., Michaelis,G., and Pratje,E. (1994). PET1402, a nuclear gene required for proteolytic processing of cytochrome oxidase subunit 2 in yeast. Mol. Gen. Genet. *245*, 272-278.

Beckman,J.S., Beckman,T.W., Chen,J., Marshall,P.A., and Freeman,B. (1990). Apparent hydroxyl radical production by peroxynitrite: Implications for endothelial injury from nitric oxide and superoxide. Proc. Natl. Acad. Sci. USA *87*, 1620-1624.

Beckman,J.S., Ischiropoulos,H., Zhu,L., van der Woerd,M., Smith,C., Chen,J., Harrison,J., Martin,J.C., and Tsai,M. (1992). Kinetics of superoxide dismutase- and iron-catalysed nitration of phenolics by peroxynitrite. Arch . Biochem. Biophys. *298*, 438-445.

Beers,J., Glerum,D.M., and Tzagoloff,A. (1997). Purification, characterisation, and localization of yeast Cox17p, a mitochondrial copper shuttle. J. Biol. Chem. *272*, 33191-33196.

Behrens,M., Michaelis,G., and Pratje,E. (1991). Mitochondrial inner membrane protease 1 of *Saccharomyces cerevisiae* shows sequence similarity to the *Escherichia coli* leader peptidase. Mol. Gen. Genet. *228*, 167-176.

Beltran,B., Orsi,A., Clementi,E., and Moncada,S. (2000). Oxidative stress and S-nitrosylation of proteins in cells. British. J. Pharmacol. *129*, 953-960.

Billinton,N. and Knight,A.W. (2001). Seeing the wood through the trees: A review of techniques for distinguishing green fluorescent protein from endogenous autofluorescence. Anal. Biochem. *291*, 175-197.

Bisson,R., Steffens,G.C.M., Capaldi,R.A., and Buse,G. (1982). Mapping of the cytochrome *c* binding site on cytochrome *c* oxidase. FEBS Lett. *144*, 359-363.

Biteau,B., Labarre,J., and Toledano,M.B. (2003). ATP-dependent reduction of cysteine-sulphinic acid by *S. cerevisiae* sulphiredoxin. Nature *425*, 980-984.

Bolanos,J.P., Peuchen,S., Heales,S.J.R., Land,J.M., and Clark,J.B. (1994). Nitric oxide-mediated inhibition of the mitochondrial respiratory chain in cultured astrocytes. J. Neurochem. *63*, 910-916.

Borutaite,V., Budriunaite,A., and Brown,G.C. (2000). Reversal of nitric oxide-, peroxynitrite- and S-nitrosothiol-induced inhibition of mitochondrial respiration or complex I activity by light and thiols. Biochim. Biophys. Acta *1459*, 405-412.

Boscá,L., Zeini,M., Través,P.G., and Hortelano,S. (2005). Nitric oxide and cell viability in inflammatory cells: a role for NO in macrophage function and fate. Toxicol. *208* 249-258.

Bourges,I., Horan,S., and Meunier,B. (2005). Effect of inhibition of the bc_1 complex on gene expression profile in yeast. J. Biol. Chem. *280*, 29743-29749.

Boveris,A. and Cadenas,E. (1975). Mitochondrial production of superoxide anions and its relationship to the antimycin insensitive respiration. FEBS Lett. *54*, 311-314.

Boveris,A., Cadenas,E., and Stoppani,A.O. (1976). Role of ubiquinone in the mitochondrial generation of hydrogen peroxide. Biochem. J. *156*, 435-444.

Bratton,M., Mills,D., Castleden,C.K., Hosler,J., and Meunier,B. (2003). Disease-related mutations in cytochrome *c* oxidase studied in yeast and bacterial models. Eur. J. Biochem. *270*, 1-9.

Broadley,S.A., Demlow,C.M., and Fox,T.D. (2001). Peripheral mitochondrial inner membrane protein, Mss2p, required for export of the mitochondrially coded Cox2p C tail in *Saccharomyces cerevisiae*. Mol. Cell. Biol. *21*, 7663-7672.

Brookes,P.S., Pinner,A., Ramachanran,A., Coward,L., Barnes,S., Kim,H., and Darley-Usmar,V.M. (2002). High throughput two-dimensional blue-native electrophoresis: a tool for functional proteomics of mitochondria and signaling complexes. Proteomics *2*, 969-977.

Brown,G.C. and Cooper,C.E. (1994). Nanomolar concentrations of nitric oxide reversibly inhibit synaptosomal respiration by competing with oxygen at cytochrome oxidase. FEBS Lett. *356*, 295-298.

Brown,G.C. (1995a). Nitric oxide regulates mitochondrial respiration and cell functions by inhibiting cytochrome oxidase. FEBS Lett. *369*, 136-139.

Brown,G.C. (1995b). Reversible binding and inhibition of catalase by nitric oxide. Eur. J. Biochem. *232*, 188-191.

Brown,G.C., Foxwell,N., and Moncada,S. (1998). Transcellular regulation of cell respiration by nitric oxide generated by activated macrophages. FEBS Lett. *439*, 321-324.

Brown,N.G., Costanzo,M.C., and Fox,T.D. (1994). Interaction among three proteins that specifically activate translation of the mitochondrial COX3 mRNA in *Saccharomyces cerevisiae*. Mol. Cell. Biol. *14*, 1045-1053.

Brown,S., Colson,A.-M., Meunier,B., and Rich,P.R. (1993). Rapid screening of cytochromes of respiratory mutants of *Saccharomyces cerevisiae* – application to the selection of strains containing novel forms of cytochrome *c* oxidase. Eur. J. Biochem. *213*, 137-145.

Butzer,U., Weidenbach,H., Gansauge,S., Gansauge,F., Beger,H.G., and Nussler,A.K. (1999). Increased oxidative stress in the RAW 264.7 macrophage cell line is partially mediated via the S-nitrosothiol-induced inhibition of glutathione reductase. FEBS Lett. *445*, 274-278.

Bykova,N.V., Egsgaard,H. and Moller,I.M. (2003). Identification of 14 new phosphoproteins involved in important plant mitochondrial processes. FEBS Lett. *540,* 141-146.

Cadenas,E., Boveris,A., Ragan,C.I., and Stoppani,A.O.M. (1977). Production of superoxide radicals and hydrogen peroxide by NADH-ubiquinone reductase and ubiquinol-cytochrome *c* reductase from beef-heart mitochondria. Arch. Biochem. Biophys. *180*, 248-257.

Calder,K.M. and McEwen,J.E. (1990). Nucleotide sequence of the gene encoding cytochrome *c* oxidase subunit VII from *Saccharomyces cerevisiae*. Nucl. Acid. Res. *18*, 1632.

Carlson,C.G., Barrientos,A., Tzagoloff,A., and Glerum,D.M. (2003). COX16 encodes a novel protein required for the assembly of cytochrome oxidase in *Saccharomyces cerevisiae*. J. Biol. Chem. *278*, 3770-3775.

Carr,H.S. and Winge,D.R. (2003). Assembly of cytochrome *c* oxidase within the mitochondrion. Acc. Chem. Res *36*, 309-316.

Carr,H.S., Georges,G.N., and Winge,D.R. (2002). Yeast Cox11, a protein essential for cytochrome *c* oxidase assembly, is a Cu (I)-binding protein. J. Biol. Chem. *277*, 31237-31242.

Cassina,A. and Radi,R. (1996). Differential inhibitory action of nitric oxide and peroxynitrite on mitochondrial electron transport. Arch. Biochem. Biophys. *328*, 309-316.

Castro,L.A., Robalinho,R.L., Cayota,A., Meneghini,R., and Radi,R. (1998). Nitric oxide and peroxynitrite-dependent aconitase inactivation and iron-regulatory protein-1 activation in mammalian fibroblasts. Arch . Biochem. Biophys. *359*, 215-224.

Caughey,W.S., Smythe,G.A., O'Keeffe,D.H., Maskasky,J.E., and Smith,M.L. (1975). Heme A of cytochrome oxidase. Structure and properties: comparisons with hemes B, C, and S and derivatives. J. Biol. Chem. *250*, 7602-7622.

Causton,H.C., Ren,B., Koh,S.S., Harbison,C.T., Kanin,E., Jennings,E.G., Lee,T.I., True,H.L., Lander,E.S., and Young,R.A. (2001). Remodelling of yeast genome expression in response to environmental changes. Mol. Biol. Cell *12*, 323-337.

Chacinska,A., Pfannschmidt,S., Wiedemann,N., Kozjak,V., Sanjuan Szklarz,L.K., Schulze-Specking A, Truscott KN, Guiard B, Meisinger C, and Pfanner N. (2004). Essential role of Mia40 in import and assembly of mitochondrial intermembrane space proteins. EMBO J. *23*, 3735-3746.

Chae,H.Z., Chung,S.J., and Rhee,S.G. (1994). Thioredoxin-dependent peroxide reductase from yeast. J. Biol. Chem. *269*, 27670-27678.

Chiang,K.T., Switzer,C.H., Akali,K.O., and Fukuto,J.M. (2000). The role of oxygen and reduced oxygen species in nitric oxide-mediated cytotoxicity: studies in yeast *Saccharomyces cerevisiae* model system. Toxicol. Appl. Pharmacol. *167*, 30-36.

Chinenov,Y.V. (2004). Cytochrome *c* oxidase assembly factors with a thioredoxin fold are conserved among prokaryotes and eukaryotes. J. Mol. Med. *78*, 239-242.

Church,C., Chapon,C., and Poyton,R.O. (1996). Cloning and characterization of PET100, a gene required for the assembly of yeast cytochrome *c* oxidase. J. Biol. Chem. *271*, 18499-18507.

Church,C., Goehring,B., Forsha,D., Wazny,P., and Poyton,R.O. (2005). A role for Pet100p in the assembly of yeast cytochrome *c* oxidase. Interaction with a subassembly that accumulates in a pet100 mutant. J. Biol. Chem. *280*, 1854-1863.

Cleeter,M.W.J., Cooper,J.M., Darley-Usmar,V.M., Moncada,S., and Schapira,A.H.V. (1994). Reversible inhibition of cytochrome *c* oxidase, the terminal enzyme of the mitochondrial respiratory chain, by nitric oxide. Implications for neurodegenerative diseases. FEBS Lett. *345*, 50-54.

Clementi,E., Brown,G.C., Feelisch,M., and Moncada,S. (1998). Persistent inhibition of cell respiration by nitric oxide. Proc. Natl. Acad. Sci. USA *95*, 7631-7636.

Cohen,B.A., Pilpel,Y., Mitra,R.D., and Church,G.M. (2002). Discrimination between paralogs using microarray analysis: Application to the Yap1p and Yap2p transcription network. Mol Biol Cell. *13*, 1608-1614.

Collinson,E.J. and Grant,C.M. (2003). Role of yeast glutaredoxins as glutathione S-transferases. J. Biol. Chem. *278*, 22492-22497.

Collinson,E.J., Wheeler,G.L., Garrido,E.O., Avery,A.M., Avery,S.V., and Grant,C.M. (2002). The yeast glutaredoxins are active as glutathione peroxidases. J. Biol. Chem. *277*, 16712-16717.

Conde,J. and Fink,G.R. (1976). A mutant of *Saccharomyces cerevisae* defective for nuclear fusion. Proc. Natl. Acad. Sci. USA *73*, 3651-3655.

Cooper,C.E. (1999). Nitric oxide and iron proteins. Biochim. Biophys. Acta *1411*, 290-309.

Costanzo,M.C. and Fox,T.D. (1986). Product of *Saccharomyces cerevisiae* nuclear gene PET494 activates translation of a specific mitochondrial mRNA. Mol Cell Biol. *6*, 3694-3703.

Costanzo,M.C., Seaver,E.C., and Fox,T.D. (1986). At least two nuclear gene products are specifically required for translation of a single yeast mitochondrial mRNA. EMBO J. *5*, 3637-3641.

Cruciat,C.-M., Brunner,S., Baumann,F., Neupert,W., and Stuart,R.A. (2000). The cytochrome bc_1 and cytochrome *c* oxidase complexes associate to form a single supracomplex in yeast mitochondria. J. Biol. Chem. *275*, 18093-18098.

Cumsky,M.G., Ko,C., Trueblood,C.E., and Poyton,R.O. (1985). Two nonidentical forms of subunit V are functional in yeast cytochrome *c* oxidase. Proc. Natl. Acad. Sci. USA *82*, 2235-2239.

Das,T.K., Pecoraro,C., Tomson,F.L., Gennis,R.B., and Rousseau,D.L. (1998). The post-translational modification in cytochrome *c* oxidase is required to establish a functional environment of the catalytic site. Biochemistry *37*, 14471-14476.

De Freitas,J.M., Liba,A., Meneghini,R., Valentine,J.S., and Gralla,E.B. (2000). Yeast lacking Cu-Zn superoxide dismutase show altered iron homeostasis. Role of oxidative stress in iron metabolism. J. Biol. Chem. *275*, 11645-11649.

De Groote,M.A., Ochsner,U.A., Shiloh,M.U., Nathan,C., McCord,J.M., Dinaeur,M.C., Libby,S.J., Vazquez-Torres,A., Xu,Y., and Fang,F.C. (1997). Periplasmic superoxide dismutase protects Salmonella from products of phagocyte NADPH-oxidase and nitric oxide synthase. Proc. Natl. Acad. Sci. USA *94*, 13997-14001.

Dedon,P.C. and Tannenbaum,S.R. (2004). Reactive nitrogen species in the chemical biology of inflammation. Arch. Biochem. Biophys. *423*, 12-22.

Delneri,D., Gardner,D.C.J., and Oliver,S.G. (1999a). Analysis of the seven-member AAD gene set demonstrates that genetic redundancy in yeast may be more apparent than real. Genetics *153*, 1591-1600.

Delneri,D., Gardner,D.C.J., Bruschi,C.V., and Oliver,S.G. (1999b). Disruption of seven hypothetical aryl alcohol dehydrogenase genes from *Saccharomyces cerevisae* and construction of a multiple knock-out strain. Yeast *15*, 1681-1689.

Denninger,J.W. and Marletta,M.A. (1999). Guanylate cyclase and the NO/cGMP signaling pathway. Biochim. Biophys. Acta *1411*, 334-350.

DeRisi,J.L., Lyer,V.R., and Brown,P.O. (1997). Exploring the metabolic and genetic control of gene expression on a genomic scale. Science *278*, 680-686.

Dickinson,E.K., Adams,D.L., Schon,E., and Glerum,D.M. (2000). A human SCO2 mutation helps define the role of Sco1p in the cytochrome oxidase assembly pathway. J. Biol. Chem. *275*, 26780-26785.

Dimmeler,S., Lottspeich,F., and Brune,B. (1992). Nitric oxide causes ADP-ribosylation and inhibition of glyceraldehyde-3- phosphate dehydrogenase. J. Biol. Chem. *267*, 16771-16774.

Dowhan,W., Bibus,C.R., and Schatz,G. (1985). The cytoplasmically-made subunit IV is necessary for assembly of cytochrome *c* oxidase in yeast. EMBO J. *4*, 179-184.

Drapier,J.-C. and Hibbs,J.B. (1986). Murine cytotoxic activated macrophages inhibit aconitase in tumor cells. J. Clin. Invest. *78*, 790-797.

Elfstrom,L.T. and Widersten,M. (2005). The Saccharomyces cerevisiae ORF YNR064c protein has characteristics of an 'orphaned' epoxide hydrolase. Biochim. Biophys. Acta *1748*, 213-221.

Epstein,C.B., Waddle,J.A., Hale IV,W., Dave,V., Thornton,J., Macatee,T.L., Garner,H.R., and Butow,R.A. (2001). Genome-wide responses to mitochondrial dysfunction. Mol. Biol. Cell *12*, 297-308.

Estruch,F. and Carlson,M. (1993). Two homologous zinc finger genes identified by multicopy suppression in a SNF1 protein kinase mutant of *Saccharomyces cerevisiae*. Mol Cell Biol. 13, 3872-3881.

Funes,S., Nargang,F.E., Neupert,W., and Herrmann,J.M. (2004). The Oxa2 protein of *Neurospora crassa* plays a critical role in the biogenesis of cytochrome oxidase and defines a ubiquitous subbranch of the Oxa1/YidC/Alb3 protein family. Mol. Biol. Cell *15*, 1853-1861.

Fytlovich,S., Gervais,M., Agrimonti,C., and Guiard,B. (1993). Evidence for an interaction between the CYP1 (HAP1) activator and a cellular factor during heme-dependent transcriptional regulation in the yeast *Saccharomyces cerevisiae*. EMBO J. *12*, 1209-1218.

Gardner,P.R., Costantino,G., Szabo,C., and Salzman,A.L. (1997). Nitric oxide sensitivity of the aconitases. J. Biol. Chem. *272*, 25071-25076.

Gardner,P.R., Gardner,A.M., Martin,L.A., Dou,Y., Li,T., Olson,J.S., Zhu,H., and Riggs,A.F. (2000). Nitric-oxide dioxygenase activity and function of flavohemoglobins. Sensitivity to nitric oxide and carbon monoxide inhibition. J. Biol. Chem. *275*, 31581-31587.

Gasch,A.P., Spellman,P.T., Kao,C.M., Carmel-Harel,O., Eisen,M.B., Storz,G., Botstein,D., and Brown,P.O. (2000). Genomic expression programs in the response of yeast cells to environmental changes. Mol. Biol. Cell *11*, 4241-4257.

Geng,Y., Hansson,G.K., and Holme,E. (1992). Interferon-gamma and tumor necrosis factor synergize to induce nitric oxide production and inhibit mitochondrial respiration in vascular smooth muscle cells. Circ. Res. *71*, 1268-1276.

Ghafourifar,P. and Richter,C. (1997). Nitric oxide synthase activity in mitochondria. FEBS Lett. *418*, 291-296.

Gietz,R.D. and Woods,R.A. (2002). Transformation of yeast by lithuim acetate/single stranded carrier DNA/polyethylene glycol method. Methods Enzymol. *350*, 87-96.

Glerum,D.M., Koerner,T.J., and Tzagoloff,A. (1995). Cloning and characterization of COX14, whose product is required for assembly of yeast cytochrome oxidase. J. Biol. Chem. *270*, 15585-15590.

Glerum,D.M., Shtanko,A., and Tzagoloff,A. (1996a). Characterization of COX17, a yeast gene involved in copper metabolism and assembly of cytochrome oxidase. J. Biol. Chem. *271*, 14504-14509.

Glerum,D.M., Shtanko,A., and Tzagoloff,A. (1996b). SCO1 and SCO2 act as high copy suppressors of a mitochondrial copper recruitment defect in *Saccharomyces cerevisiae*. J. Biol. Chem. *271*, 20531-20535.

Glerum,D.M. and Tzagoloff,A. (1997). Submitochondrial distributions and stabilities of subunits 4, 5 and 6 of yeast cytochrome oxidase in assembly defective mutants. FEBS Lett. *412*, 410-414.

Gou,H., Wei,J., and Kuo,P.C. (2001). Nitric oxide inhibits expression of cytochrome *b* in endotoxin-stimultaed murine macrophages. Biochem. Biophys. Res. Comm. *289*, 993-997.

Griffin,T.J., Gygi,S.P., Ideker,T., Rist,B., Eng,J., Hood,L., and Aebersold,R. (2002). Complementary profiling of gene expression at the transcriptome and proteome levels in *Saccharomyces cerevisiae*. Mol. Cell Proteom. *1,* 323-333.

Groot Koerkamp,M., Rep,M., Bussemaker,H.J., Hardy,G.P.M.A., Mul,A., Piekarska,K., Al-Khalili Szigyarto,C., Teixeira de Mattos,J.M., and Tabak,H.F. (2002). Dissection of transient oxidation stress response in *Saccharomyces cerevisiae* by using DNA microarrays. Mol. Biol. Cell *13*, 2783-2794.

Gross,W.L., Bak,M.I., Ingwall,J.S., Arstall,M.A., Smith,T.W., Balligand,J.L., and Kelly,R.A. (1996). Nitric oxide inhibits creatine kinase and regulates rat heart contractile reserve. Proc. Natl. Acad. Sci. USA *93*, 5604-5609.

Guarente,L. and Ptashne,M. (1981). Fusion of *Escherichia coli* LacZ to the cytochrome *c* gene of *Saccharomyces cerevisiae*. Proc. Natl. Acad. Sci. USA *78*, 2199-2203.

Guelin,E., Rep,M., and Grivell,L.A. (1996). Afg3p, a mitochondrial ATP-dependent metalloprotease, is involved in degradation of mitochondrially-encoded Cox1, Cox3, Cob, Sub6, Sub8 and Sub9 subunits of the inner membrane complexes III, IV and V. FEBS Lett. *381*, 42-46.

Gygi,S.P., Rochon,Y., Franza,B.R., and Aebersold,R. (1999). Correlation between protein and mRNA abundance in yeast. Mol Cell Biol. *19,* 1720-1730.

Hagen,T., Taylor,C.T., Lam,F., and Moncada,S. (2003). Redistribution of intracellular oxygen in hypoxia by nitric oxide: effect on HIF1α. Science *302,* 1975-1978.

Haltia,T., Finel,M., Harms,N., Nakari,T., Raitio,M., Wikström,M., and Saraste,M. (1989). Deletion of the gene for subunit III leads to defective assembly of bacterial cytochrome oxidase. EMBO J. *8*, 3571-3579.

Hamel,P., Lemaire,C., Bonnefoy,N., Brivet-Chevillotte,P., and Dujardin,G. (1998). Mutations in the membrane anchor of yeast cytochrome c_1 compensate for the absence of Oxa1p and generate carbonate-extractable forms of cytochrome c_1. Genetics *150*, 601-611.

Hanke,C.J., Drewett,J.G., Myers,C.R., and Campbell,W.B. (1998). Nitric oxide inhibits aldosterone synthesis by a guanylyl cyclase-independent effect. Endocrinology *139*, 4053-4060.

Harris,N., Costa,V., MacLean,M., Mollapour,M., Morades-Ferreira,P., and Piper,P. (2003). MnSOD overexpression extends the yeast chronological (G_0) life span but acts independently of Sir2p histone deacetylase to shorten the replicative life span of dividing cells. Free Rad. Biol. Med. *34,* 1599-1606.

Harris,N., Bachler,M., Costa,V., Moradas-Ferreira,P., and Piper,P.W. (2005). Overexpressed Sod1p acts either to reduce or to increase the lifespans and stress resistance of yeast, depending on whether it is Cu_2^+-deficient or an active Cu,Zn-superoxide dismutatse. Aging Cell *4*, 41-52.

Hausladen,A. and Fridovich,I. (1994). Superoxide and peroxynitrite inactivate aconitases, but nitric oxide does not. J. Biol. Chem. *269*, 29405-29408.

Hausladen,A., Gow,A.J., and Stamler,J.S. (1998). Nitrosative stress: Metabolic pathway involving the flavohemoglobin. Proc. Natl. Acad. Sci. USA *95*, 14100-14105.

He,S. and Fox,T.D. (1997). Membrane translocation of mitochondrially coded Cox2p: Distinct requirements for export of N and C termini and dependence on the conserved protein Oxa1p. Mol. Biol. Cell *8*, 1449-1460.

He,S. and Fox,T.D. (1999). Mutations affecting a yeast mitochondrial inner membrane preotein, Pnt1p, block export of a mitochondrially synthesised fusion protein from the matrix. Mol. Cell. Biol. *19*, 6598-6607.

Heales,S.J., Bolanos,J.P., Land,J.M., and Clark,J.B. (1994). Trolox protects mitochondrial complex IV from nitric oxide-mediated damage in astrocytes. Brain Res. *668*, 243-245.

Heaton,D.N., George,G.N., Garrison,G., and Winge,D.R. (2001). The mitochondrial copper metallochaperone Cox17 exists as an oligomeric, polycopper complex. Biochemistry *40*, 743-751.

Hell,K., Herrmann,J., Pratje,E., Neupert,W., and Stuart,R.A. (1997). Oxa1p mediates the export of the N- and C-termini of pCoxII from the mitochondrial matrix to the intermembrane space. FEBS Lett. *418*, 367-370.

Hell,K., Herrmann,J.M., Pratje,E., Neupert,W., and Stuart,R.A. (1998). Oxa1p, an essential component of the N-tail protein export machinery in mitochondria Proc. Natl. Acad. Sci. USA *95*, 2250-2255.

Hell,K., Tzagoloff,A., Neupert,W., and Stuart,R.A. (2000). Identification of Cox20p, a novel protein involved in the maturation and assembly of cytochrome oxidase subunit 2. J. Biol. Chem. *275*, 4571-4578.

Hell,K., Neupert,W., and Stuart,R.A. (2001). Oxa1p acts as a general membrane insertion machinery for proteins encoded by mitochondrial DNA. EMBO J. *20*, 1281-1288.

Henry,Y., Lepoivre,M., Drapier,J.C., Ducrocq,C., Boucher,J.L., and Guissani,A. (1993). EPR characterisation of molecular targets for NO in mammalian cells and organelles. FASEB J. *7*, 1124-1134.

Herrmann,J.M. and Bonnefoy,N. (2004). Protein export across the inner membrane of mitochondria: The nature of translocated domains determines the dependence on the Oxa1 translocase. J. Biol. Chem. *279*, 2507-2512.

Hess,D.T., Matsumoto,A., Kim,S.-O., Marshall,H.E., and Stamler,J.S. (2005). Protein S-nitrosylation: Purview and parameters. Nature Rev. Mol. Cell Biol. *6*, 150-166.

Hibbs,J.B., Jr., Vavrin,Z., and Taintor,R.R. (1987). L-arginine is required for expression of the activated macrophage effector mechanism causing selective metabolic inhibition in target cells. J. Immunol. *138*, 550-565.

Hiltunen,J.K., Mursula,A.M., Rottensteiner,H., Wierenga,R.K., Kastaniotis,A.J., and Gurvitz,A. (2003). The biochemistry of peroxisomal ß-oxidation in the yeast *Saccharomyces cerevisiae*. FEMS Microbiol. Rev. *27*, 35-64.

Hiser,L., Di Valentin,M., Hamer,A.G., and Hosler,J.P. (2000). Cox11p is required for stable formation of the Cu_B and magnesium centers of cytochrome *c* oxidase. J. Biol. Chem. *275*, 619-623.

Hiser,L. and Hosler,J.P. (2002). Heme A is not essential for assembly of the subunits of cytochrome *c* oxidase of *Rhodobacter sphaeroides*. J. Biol. Chem. *276*, 45403-45407.

Hon,T., Dodd,A., Dirmeier,R., Gorman,N., Sinclair,P.R., Zhang,L., and Poyton,R.O. (2003). A mechanism of oxygen sensing in yeast. Multiple oxygen-responsive steps in the heme biosynthetic pathway affect Hap1 activity. J. Biol. Chem. *278*, 50771-50780.

Hon,T., Lee,H.C., Hach,A., Johnson,J.L., Craig,E.A., Erdjument-Bromage,H., Tempst,P., and Zhang,L. (2001). The Hsp70-Ydj1 molecular chaperone represses the activity of the heme activator protein Hap1 in the absence of heme. Mol. Cell Biol. *21* 7923-7932.

Hopper,R.K., Carroll,S., Aponte,A.M., Johnson,D.T., French,S., Shen,R.-F., Witzmann,F.A., Harris.,R.A., and Balaban,R.S. (2006). Biochemistry *45,* 2524-2536.

Horng,Y.C., Cobine,P.A., Maxfield,A.B., Carr,H.S., and Winge,D.R. (2004). Specific copper transfer from the Cox17 metallochaperone to both Sco1 and Cox11 in the assembly of yeast cytochrome *c* oxidase. J. Biol. Chem. *279*, 35334-35340

Hrabie,J.A. and Klose,J.R. (1993). New nitric oxide-releasing zwitterions derived from polyamines. J. Org. Chem. *58*, 1472-1476.

Hromatka,B.S., Noble,S.M., and Johnson,A.D. (2005). Transcriptional response of *Candida albicans* to nitric oxide and the role of the YHB1 gene in nitrosative stress and virulence. Mol. Biol. Cell. *16*, 4814-4826.

Huang,L.E., Arany,Z., Livingston,D.M., and Bunn,H.F. (1996). Activation of hypoxia-inducible transcription factor depends primarily on redox-sensitive stabilisation of its α-subunit. J Biol. Chem. *271*, 32253-32259.

Ignarro,L.J., Buga,G.M., Wood,K.S., Byrns,R.E., and Chaudhuri,G. (1987). Endothelium-derived relaxing factor produced and released from artery and vein is nitric oxide. Proc. Natl. Acad. Sci. USA *84*, 9265-9269.

Inoue,Y., Matsuda,T., Sugiyama,K., Izawa,S., and Kimura,A. (1999). Genetic analysis of glutathione peroxidase in oxidative stress response of *Saccharomyces cerevisiae*. J. Biol. Chem. *274*, 27002-27009.

Ischiropoulos,H. (1998). Biological tyrosine nitration: A pathophysiological function of nitric oxide and reactive oxygen species. Arch . Biochem. Biophys. *356*, 1-11.

Ivan,M., Kondo,K., Yang,H., Kim,W., Valiando,J., Ohh,M., Salic,A., Asara,J.M., Lane,W.S., and Kaelin Jr, W.G. (2001). HIFalpha targeted for VHL-mediated destruction by proline hydroxylation: implications for O_2 sensing. Science *292*, 464-468.

Iwata,S., Ostermeier,C., Ludwig,B., and Michel,H. (1995). Structure at 2.8 Å resolution of cytochrome *c* oxidase from *Paracoccus denitrificans*. Nature *376*, 660-669.

Jaakkola,P., Mole,D.R.,Tian,Y.M., Wilson,M.I., Gielbert,J., Gaskell,S.J., Kriegsheim,AV.,Hebestreit,H.F., Mukherji,M., Schofield,C.J., Maxwell,P.H., Pugh,C.W., and Ratcliffe,P.J. (2001). Targeting of HIF-alpha to the von Hippel-Lindau ubiquitylation complex by O_2-regulated prolyl hydroxylation. Science *292*, 468-472.

Jaksch,M., Paret,C., Stucka,R., Horn,N., Muller-Hocker,J., Horvath,R., Trepesch,N., Stecker,G., Freisinger,P., Thirion,C., Muller,J., Lunkwitz,R., Rodel,G.,

Jakubowski,W., Bilinski,T., and Bartosz,G. (1999). Sensitivity of antioxidant-deficient yeast *Saccharomyces cerevisae* to peroxynitrite and nitric oxide. Biochim. Biophys. Acta *1472*, 395-398.

Jelinsky,S.A. and Samson,L.D. (1999). Global response of *Saccharomyces cerevisiae* to an alkylating agent. Proc. Natl. Acad. Sci. USA *96*, 1486-1491.

Kadenbach,B., Napiwotzki,J., Frank,V., Arnold,S., Exner,S., and Hüttemann,M. (1998). Regulation of energy transduction and electron transfer in cytochrome *c* oxidise by adenine nucleotides. J. Bioenerg. Biomemb. *30*, 25-34.

Khalimonchuk,O., Ostermann,K., and Rodel,G. (2005). Evidence for the association of yeast mitochondrial ribosomes with Cox11p, a protein required for the Cu_B site formation of cytochrome *c* oxidase. Curr. Genet. *47*, 223-233.

Kim,S.O., Orii,Y., Lloyd,D., Hughes,M.N., and Poole,R.K. (1999). Anoxic function for the *Escherichia coli* flavohaemoglobin (Hmp): Reversible binding of nitric oxide and reduction to nitrous oxide. FEBS Lett. *445*, 389-394.

King,P.A., Anderson,V.E., Edwards,J.O., Gustafson,G., Plumb,R.C., and Suggs,J.W. (1992). A stable solid that generates hydroxyl radical upon dissolution in aqueous solutions: Reaction with proteins and nucleic acid. J. Am. Chem. Soc *114*, 5430-5432.

Kirichenko,A., Vygodina,T., Mkrtchyan,M., and Konstantinov,A. (1998). Specific cation binding site in mammalian cytochrome oxidase. FEBS Lett. *423*, 329-333.

Klebanoff,S.J. (1971). Intraleukocytic microbicidal defects. Ann. Rev. Med. *22*, 39-62.

Kloeckener-Gruissem,B., McEwen,J.E., and Poyton,R.O. (1988). Identification of a third nuclear protein-coding gene required specifically for posttranscriptional expression of the mitochondrial COX3 gene in *Saccharomyces cerevisiae*. J. Bacteriol. *130*, 1399-1402.

Knight,A.W., Goddard,N.J., Fielden,P.R., Barker,M.G., Billinton,N., and Walmsley,R.M. (1999). Fluorescence polarisation of green fluorescent protein (GFP). A strategy for improved wavelength discrimination for GFP determinations. Anal. Commun. *36*, 113-117.

Konorev,E.A., Hogg,N., and Kalyanaraman,B. (1998). Rapid and irreversible inhibition of creatine kinase by peroxynitrite. FEBS Lett. *427*, 171-174.

Krems,B., Charizanis,C., and Entian,K.D. (1996). The response regulator-like protein Pos9/Skn7 of *Saccharomyces cerevisiae* is involved in oxidative stress resistance. Curr. Genet. *29*, 327-334.

Krönke,K.D., Fehsel,K., Schmidt,T., Zenke,F.T., Dasting,I., Wesener,J.R., Bettermann,H., Breunig,K.D., and Kolb-Bachofen,V. (1994). Nitric oxide destroys zinc-sulfur clusters including zinc release from metallothoinein and inhibition of the zinc finger-type yeast transcription activator LAC9. Biochim. Biophys. Res. Comm. *200*, 1105-1110.

Krummeck,G. and Rödel,G. (1990). Yeast SCO1 protein is required for a post-translational step in the accumulation of mitochondrial cytochrome *c* oxidase subunits I and II. Curr. Genet. *18*, 13-15.

Kuge,S., Jones,N., and Nomoto,A. (1997). Regulation of yAP-1 nuclear localization in response to oxidative stress. EMBO J. *16*, 1710-1720.

Kwon,M., Chong,S., Han,S., and Kim,K. (2003). Oxidative stresses elevate the expression of cytochrome *c* peroxidase in *Saccharomyces cerevisiae*. Biochim. Biophys. Acta *1623*, 1-5.

Kwon,N.S., Stuehr,D.J., and Nathan,C.F. (1991). Inhibition of tumor cell ribonucleotide reductase by macrophage-derived nitric oxide. J. Exp. Med. *174*, 761-767.

Lagunas,R. (1986). Misconceptions about the energy metabolism of *Saccharomyces cerevisiae*. Yeast *2*, 211-228.

LaMarche,A.E.P., Abate,M.I., Chan,S.H.P., and Trumpower,B.L. (1992). Isolation and characterization of COX12, the nuclear gene for a previously unrecognized subunit of *Saccharomyces cerevisiae* cytochrome *c* oxidase. J. Biol. Chem. *267*, 22473-22480.

Lancaster,J.R., Jr. (1994). Simulation of the diffusion and reaction of endogeneously produced nitric oxide. Proc. Natl. Acad. Sci. *91*, 8137-8141.

Lane,T.E., Otero,G.C., Wu-Hsieh,B.A., and Howard,D.H. (1994). Expression of inducible nitric oxide synthase by stimulated macrophages correlates with their antihistoplasma activity. Infect. Immun. *62* 1478-1479.

Lappalainen,P., Watmough,N.J., Greenwood,C., and Saraste,M. (1995). Electron transfer between cytochrome *c* and the isolated CuA domain: Identification of substrate-binding residues in cytochrome *c* oxidase. Biochemistry *34*, 5824-5830.

Leary,S.C., Hill,B.C., Lyons,C.N., Carlson,C.G., Michaud,D., Kraft,C.S., Ko,K., Glerum,D.M., and Moyes,C.D. (2002). Chronic treatment with azide in situ leads to an irreversible loss of cytochrome *c* oxidase activity via holoenzyme dissociation. J. Biol. Chem. *277*, 11321-11328.

Lee,J., Godon,C., Lagniel,G., Spector,D., Garin,J., Labarre,J., and Toledano,M.B. (1999). Yap1 and Skn7 control two specialized oxidative stress response regulons in Yeast. J. Biol. Chem. *274*, 16040-16046.

Leeuwenburgh,C., Hardy,M.M., Hazen,S.L., Wagner,P., Oh-ishi,S., Steinbrecher,U.P., and Heinecke,J.W. (1997). Reactive nitrogen intermediates promote low density lipoprotein oxidation in human atherosclerotic intima. J. Biol. Chem. *272*, 1433-1436.

Lehrer-Graiwer,J., Firestein,B.L., and Bredt,D.L. (2000). Nitric oxide mediated induction of cytochrome *c* oxidase mRNA and protein in a mouse macrophage cell line. Neurosci. Lett. *288*, 107-110.

Lemaire,C., Robineau,S., and Netter,P. (1998). Molecular and biochemical analysis of *Saccharomyces cerevisiae* cox1 mutants. Current Genetics *34*, 138-145.

Lemaire,C., Hamel,P., Velours,J., and Dujardin,G. (2000). Absence of the mitochondrial AAA protease Yme1p restores F_o-ATPase subunit accumulation in an oxa1 deletion mutant of *Saccharomyces cerevisiae*. J. Biol. Chem. *275*, 23471-23475.

Lemaire,G., Alvarez-Pachon,F.-J., Beuneu,C., Lepoivre,M., and Petit,J.-F. (1999). Differential cytostatic effects of NO donors and NO producing cells. Free Rad. Biol. and Med. *26*, 1274-1283.

Leonhard,K., Stiegler,A., Neupert,W., and Langer,T. (1999). Chaperone-like activity of the AAA domain of the yeast AAA Yme1 AAA protease. Nature *398*, 348-351.

Leonhard,K., Guiard,B., Pellecchia,G., Tzagoloff,A., Neupert,W., and Langer,T. (2000). Membrane protein degradation by AAA proteases in mitochondria: Extraction of substrates from either membrane surface. Mol. Cell *5*, 629-638.

Lepoivre,M., Flaman,J.M., Bobe,P., Lemaire,G., and Henry,Y. (1994). Quenching of the tyrosyl free radical of ribonucleotide reductase by nitric oxide. Relationship to cytostasis induced in tumor cells by cytotoxic macrophages. J. Biol. Chem. *269*, 21891-21897.

Li,L., Chen,O.S., Ward,D.M., and Kaplan,J. (2001). CCC1 is a transporter that mediates vacuolar iron storage in yeast. J. Biol. Chem. *276*, 29515-29519.

Li,Z.-S., Szczypka,M., Lu,Y.-P., Thiele,D.J., and Rea,P.A. (1996). The yeast cadmium factor protein (YCF1) is a vacuolar glutathione S-conjugate pump. J. Biol. Chem. *271*, 6509-6517.

Lightowlers,R., Chrzanowska-Lightowlers,Z., Marusich,M., and Capaldi,R.A. (1991). Subunit function in eukaryote cytochrome *c* oxidase. A mutation in the nuclear-coded subunit IV allows assembly but alters the function and stability of yeast cytochrome *c* oxidase. J. Biol. Chem. *266*, 7688-7693.

Liu,L., Zeng,M., Hausladen,A., Heitman,J., and Stamler,J.S. (2000). Protection from nitrosative stress by yeast flavohemoglobin. Proc. Natl. Acad. Sci. USA *97*, 4672-4676.

Liu,X., Miller,M.J.S., Joshi,M.S., Thomas,D.D., and Lancaster,J.R. (1998). Accelerated reaction of nitric oxide with O_2 within the hydrophobic interior of biological membranes. Proc. Natl. Acad. Sci. USA *95*, 2175-2179.

Liu,Y., Fiskum,G., and Schubert,D. (2002). Generation of reactive oxygen species by the mitochondrial electron transport chain. J. Neurochem. *80*, 780-787.

Liu,Y.C., Sowdal,L.H., and Robinson,N.C. (1995). Separation and quantitation of cytochrome *c* oxidase subunits by mono-Q fast protein liquid chromatography and C18 reverse- phase high-performance liquid chromatography. Arch. Biochem. Biophys. *324*, 135-142.

Livak,K.J. and Schmittgen,T.D. (2001). Analysis of relative gene expression data using real-time quantitative PCR and the 2-ΔΔCT method. Methods *25*, 402-408.

Lode,A., Kuschel,M., Paret,C., and Rodel,G. (2000). Mitochondrial copper metabolism in yeast: Interaction between Sco1p and Cox2p. FEBS Lett. *485*, 19-24.

Lode,A., Paret,C., and Rodel,G. (2002). Molecular characterization of *Saccharomyces cerevisiae* Sco2p reveals a high degree of redundancy with Sco1p. Yeast *19*, 909-922.

Longo,V.D., Gralla,E.B., and Valentine,J.S. (1996). Superoxide dismutase activity is essential for stationary phase survival in *Saccharomyces cerevisiae*. J. Biol. Chem. *271*, 12275-12280.

Lovchik,J.A., Lyons,C.R., and Lipscomb,M.F. (1995). A role for gamma interferon-induced nitric oxide in pulmonary clearance of *Cryptococcus neoformans*. Am. J. Respir. Cell Mol. Biol. *13*, 116-124.

Lupetti,A., Danesi,R., Campa,M., Tacca,M.D., and Kelly,S. (2002). Molecular basis of resistance to azole antifungals. Trends Mol. Med. *8*, 76-81.

MacMicking,J., Xie,Q.W., and Nathan,C. (1997). Nitric oxide and macrophage function. Ann. Rev. Immunol. *15*, 323-350.

Maneg,O., Malatesta,F., Ludwig,B., and Drosou,V. (2004). Interaction of cytochrome *c* with cytochrome oxidase: two different docking scenarios. Biochim. Biophys. Acta *1655*, 274-281.

Manthey,G.M. and McEwan,J.E. (1995). The product of the nuclear gene PET309 is required for translation of mature mRNA and stability of production of intron-containing RNAs derived from the mitochondrial COX1 locus of *Saccharomyces cerevisiae*. EMBO J. *14*, 4031-4043.

Marletta,M.A., Yoon,P.S., Iyengar,R., Leaf,C.D., and Wishnok,J.S. (1988). Macrophage oxidation of L-arginine to nitrite and nitrate: nitric oxide is an intermediate. Biochemistry *27*, 8706-8711.

Martinez-Pastor,M.T., Marchler,G., Schuller,C., Marchler-Bauer,A., Ruis,H., and Estruch,F. (1996). The Saccharomyces cerevisiae zinc finger proteins Msn2p and Msn4p are required for transcriptional induction through the stress response element (STRE). EMBO J. *15*, 2227-2235.

Mastroeni,P., Vazquez-Torres,A., Fang,F.C., Xu,Y., Khan,S., Hormaeche,C.E., and Dougan,G. (2000). Antimicrobial actions of the NADPH phagocyte oxidase and inducible nitric oxide synthase in experimental salmonellosis. II. Effects on microbial proliferation and host survival in vivo. J. Exp. Med. *192*, 237-248.

Mateo,J., Garcia-Lecea,M., Cadenas,S., Hernandez,C., and Moncada,S. (2003). Biochem. J. *376* 537-544.

Matsumoto,A., Comatas,K.E., Liu,L., and Stamler,J.S. (2003). Screening for nitric oxide-dependent protein-protein interactions. Science *301*, 657-661.

Maxfield,A.B., Heaton,D.N., and Winge,D.R. (2004). Cox17 is functional when tethered to the mitochondrial inner membrane. J. Biol. Chem. *279*, 5072-5080.

McCartney-Francis,N., Allen,J.B., Mizel,D.E., Albina,J.E., Xie,Q.W., Nathan,C.F., and Wahl,S.M. (1993). Suppression of arthritis by an inhibitor of nitric oxide synthase. J. Exp. Med. *178*, 749-754.

McEwan,J.E., Cumsky,M.G., Ko,C., Power,S.D., and Poyton,R.O. (2004). Mitochondrial membrane biogenesis: characterisation and use of pet mutants to clone the nuclear gene coding for subunit V of yeast cytochrome *c* oxidase. J. Cell Biochem. *24*, 229-242.

McEwen,J.E., Hong,K.H., Park,S., and Preciado,G.T. (1993). Sequence and chromosomal localization of two *PET* genes required for cytochrome *c* oxidase assembly in *Saccharomyces cerevisiae*. Curr. Genet. *23*, 9-14.

McFarland,R., Taylor,R.W., Chinnery,P.F., Howell,N., and Turnbull,D.M. (2004). A novel sporadic mutation in cytochrome *c* oxidase subunit II as a cause of rhabdomyolysis. Neuromusc. Disord. *14* 162-166.

McHale,M.W., Kroening,K.D., and Bernlohr,D.A. (1996). Identification of a class of *Saccharomyces cerevisiae* mutants defective in fatty acid repression of gene transcription and analysis of the frm2 gene. Yeast *12*, 319-331.

Meister,A. (1988). Glutathione metabolism and its selective modification. J. Biol. Chem. *263*, 17205-17208.

Meunier,B., Lemarre,P., and Colson,A.M. (1993). Genetic screening in *Saccharomyces cerevisiae* for large numbers of mitochondrial point mutations which affect structure and function of catalytic subunits of cytochrome-*c* oxidase. Eur. J. Biochem. *213*, 129-135.

Meunier,B. and Rich,P.R. (1998). Quantitation and characterisation of cytochrome *c* oxidase in complex systems. Anal. Biochem. *260*, 237-243.

Meunier,B. and Rich,P.R. (1998). Second-site reversion analysis is not a reliable method to determine distance in membrane proteins: an assessment using mutations in yeast cytochrome *c* oxidase subunits I and III. J. Mol. Biol. *283*, 727-730.

Meunier,B. (2001). Site-direct mutations in the mitochondrially-encoded subunits I and III of yeast cytochrome oxidase. Biochem. J. *354*, 407-412.

Meunier,B. and Taanman,J.-W. (2002). Mutations of cytochrome *c* oxidase subunits 1 and 3 in *Saccharomyces cerevisiae*: Assembly defect and compensation. Biochim. Biophys. Acta *1554*, 101-107.

Michel,H., Behr,J., Harrenga,A. and Knnt,A. (1998). Cytochrome *c* oxidase: structure and spectroscopy. Ann. Rev. Biophys. Biomol. Struct. *27*, 329-356.

Miller,B.R. and Cumsky,M.G. (1993). Intramitochondrial sorting of the precursor to yeast cytochrome *c* oxidase subunit Va. J. Cell. Biol. *121*, 1021-1029.

Minamiyama,Y., Takemura,S., Imaoka,S., Funae,Y., Tanimoto,Y., and Inoue,M. (1997). Irreversible inhibition of cytochrome P450 by nitric oxide. J. Pharmacol. Exp. Ther. *283*, 1479-1485.

Mitchell,P., and Moyle,J. (1967). Chemiosmotic hypothesis of oxidative phosphorylation. Nature *213*, 137-139.

Moncada,S., Palmer,R.M.J., and Higgs,E.A. (1991). Nitric oxide: physiology, pathophysiology, and pharmacology. Pharmac. Rev. *43*, 109-142.

Moncada,S. and Erusalimsky,J.D. (2002). Does nitric oxide modulate mitochondrial energy generation and apoptosis? Nature Rev. Mol. Cell Biol. *3*, 214-220.

Moradas-Ferreira,P., Costa,V., Piper,P.W., and Mager,W. (1996). The molecular defences against reactive oxygen species in yeast. Mol. Microbiol. *19*, 651-658.
Moreno,J.J. and Pryor,W.A. (1992). Inactivation of a1-proteinase inhibitor by peroxynitrite. Chem. Res. Toxicol. *5*, 425-431.

Morgan,B.A., Banks,G.R., Toone,W.M., Raitt,D., Kuge,S., and Johnston,L.H. (1997). The Skn7 response regulator controls gene expression in the oxidative stress response of the budding yeast *Saccharomyces cerevisiae*. EMBO J. *16*, 1035-1044.

Morgan,E.T., Ullrich,V., Daiber,A., Schmidt,P., Takaya,N., Shoun,H., McGiff,J.C., Okeyan,A., Hanke,C.J., Campbell,W.B., Park,C.-S., Kang,J.-S., Yi,H.-G., Cha,Y.-N., Mansuy,D., and Boucher,J.-L. (2001). Cytochromes P450 and flavin monooxygenases - targets and sources of nitric oxide. Drug Metab. Dispos. *29*, 1366-1376.

Mukhopadhyay,R. and Rosen,B.P. (1998). *Saccharomyces cerevisiae* ACR2 gene encodes an arsenate reductase. FEMS Microbiol. Lett. *168*, 127-136.

Mulero,J.J. and Fox,T.D. (1993). Alteration of *Saccharomyces cerevisiae* COX2 mRNA 5'-untranslated leader by mitochondrial gene replacement and functional interaction with the translational activator protein PET111. Mol. Biol. Cell. *4*, 1327-1335.

Naithani,S., Saracco,S.A., Butler,C.A., and Fox,T.D. (2003). Interactions among COX1, COX2, and COX3 mRNA-specific translational activator proteins on the inner surface of the mitochondrial inner membrane of *Saccharomyces cerevisiae*. Mol. Biol. Cell *14*, 324-333.

Nakai,T., Yasuhara,T., Fujiki,Y., and Ohashi,A. (1995). Multiple genes, including a member of the AAA family, are essential for degradation of unassembled subunit 2 of cytochrome *c* oxidase in yeast mitochondria. Mol. Cell. Biol. *15*, 4441-4452.

Nathan,C.F. and Root,R.K. (1977). Hydrogen peroxide release from mouse peritoneal macrophages. J. Exp. Med. *146*, 1648-1662.

Netto,L.E.S., Chae,H.Z., Kang,S.W., Rhee,S.G., and Stadtman,E.R. (1996). Removal of hydrogen peroxide by thiol-specific antioxidant enzyme (TSA) is involved with its antioxidant properties. TSA possesses thiol peroxidase activity. J. Biol. Chem. *271*, 15315-15321.

Nicoletti,V.G., Caruso,A., Tendi,E.A., Privitera,A., Console,A., Calabrese,V., Spadaro,F., Ravagna,A., Copani,A., and Giuffrida-Stella,A.M. (1998). Effect of nitric oxide synthase induction on the expression of mitochondrial respiratory chain enzyme subunits in mixed cortical and astroglial cell cultures. Biochimie *80*, 871-881.

Nijtmans,L.G.J., Spelbrink,J.N., Van Galen,M.J.M., Zwaan,M., Klement,P., and Van den Bogert,C. (1995). Expression and fate of the nuclearly encoded subunits of cytochrome-*c* oxidase in cultured human cells depleted of mitochondrial gene products. Biochim. Biophys. Acta *1265*, 117-126.

Nijtmans,L.G.J., Taanman,J.-W., Muijsers,A.O., Speijer,D., and Van den Bogert,C. (1998). Assembly of cytochrome *c* oxidase in cultured human cells. Eur. J. Biochem. *254*, 389-394.

Nittis,T., George,G.N., and Winge,D.R. (2001). Yeast Sco1, a protein essential for cytochrome *c* oxidase function, is a Cu (I)-binding protein. J. Biol. Chem. *276*, 42520-42526.

Nittler,M.P., Hocking-Murray,D., Foo,C.K., and Sil,A. (2005). Identification of *Histoplasma capsulatum* transcripts induced in response to reactive nitrogen species. Mol. Biol. Cell *16*, 4792-4813.

Nobrega,M.P., Bandeira,S.C.B., Beers,J., and Tzagoloff,A. (2002). Characterisation of COX19, a widely distributed gene required for expression of mitochondrial cytochrome oxidase. J. Biol. Chem. *277*, 40206-40211.

Nunnari,J., Fox,T.D., and Walter.P (1993). A mitochondrial protease with two catalytic subunits of overlapping specificities. Science *262*, 1997-2004.

O'Connor-Cox,E., Mochaba,F.M., Lodolo,E.J., Majara,M., and Axcell,B. (1997). Methylene blue staining: use at your own risk. Tech. Q. Master Brew. Assoc. Am. *34*, 306-312.

O'Donnell,V.B., Chumley,P.H., Hogg,N., Bloodsworth,A., Darley-Usmar,V., and Freeman,B.A. (1997). Nitric oxide inhibition of lipid peroxidation: Kinetics of reaction with lipid peroxyl radicals and comparison with a-tocopherol. Biochemistry *36*, 15216-15223.

Ostermeier,C., Harrenga,A., Ermler,U., and Michel,H. (1997). Structure at 2.7 Å resolution of the *Paracoccus denitrificans* two-subunit cytochrome coxidase complexed with an antibody Fv fragment. Proc. Natl. Acad. Sci. USA *94*, 10547-10553.

Otsuka,M., Mizuno,Y., Yoshida,M., Kagawa,Y., and Ohta,S. (1988). Nucleotide sequence of cDNA encoding human cytochrome oxidase subunit IVc. Nuc. Acid. Res. *16*, 10916.

Packer,M.A., Porteous,C.M., and Murphy,M.P. (1996). Superoxide production by mitochondria in the presence of nitric oxide forms peroxynitrite. Biochem. Mol. Biol. Int. *40*, 527-534.

Padgett,C.M. and Whorton,A.R. (1995). S-nitrosoglutathione reversibly inhibits GAPDH by S-nitrosylation. Am. J. Physiol. Cell Physiol *269*, C739-C749.

Palmer,R.M.J., Ferrige,A.G., and Moncada,S. (1987). Nitric oxide release accounts for the biological activity of endothelial-derived relaxing factor. Nature *327*, 524-526.

Paradies,G., Petrosillo,G., Pistolese,F., and Ruggiero,M. (2000). The effect of reactive oxygen species generated from the mitochondrial electron transport chain on the cytochrome *c* oxidase activity and on the cardiolipin content in bovine heart submitochondrial particles. FEBS Lett. *466*, 323-326.

Paret,C., Ostermann,K., Krause-Buchholz,U., Rentzsch,A., and Rodel,G. (1999). Human members of the SCO1 gene family:complementation analysis in yeast and intracellular localization. FEBS Lett. *447*, 65-70.

Park,S.G., Cha,M.K., Jeong,W., and Kim,I.H. (2000). Distinct physiological functions of thiol peroxidase isoenzymes in *Saccharomyces cerevisiae*. J. Biol. Chem. *275*, 5723-5732.

Patterson,T.E. and Poyton,R.O. (1986). Cox8, the structural gene for yeast cytochrome *c* oxidase subunit VIII. DNA sequence and gene disruption indicate that subunit VIII is required for maximal levels of cellular respiration and is derived from a precursor which is extended at both its NH_2 and COOH termini. J. Biol. Chem. *261*, 17192-17197.

Pearce,D.A. and Sherman,F. (1995). Degradation of cytochrome oxidase subunits in mutants of yeast lacking cytochrome *c* and suppression of the degradation by mutation of yme1. J. Biol. Chem. *270*, 20879-20882.

Pearce,L.L., Epperly,M.W., Greenberger,J.S., Pitt,B.R., and Peterson,J. (2001). Identification of respiratory complexes I and III as mitochondrial sites of damage following exposure to ionizing radiation and nitric oxide. Nitric Oxide *5*, 128-136.

Pelzer,W., Muhlenhoff,U., Diekert,K., Siegmund,K., Kispal,G., and Lill,R. (2000). Mitochondrial Isa2p plays a crucial role in the maturation of cellular iron-sulfur proteins. FEBS Lett. *476*, 134-139.

Perez-Martinez,X., Broadley,S.A., and Fox,T.D. (2003). Mss51p promotes mitochondrial Cox1p synthesis and interacts with newly synthesized Cox1p. EMBO J. *22*, 5951-5961.

Pervin,S., Singh,R., Gau,C.-L., Edamatsu,H., Tamanoi,F., and Chaudhuri,G. (2001). Potentiation of nitric oxide-induced apoptosis of MDA-MB-468 cells by farnesyltransferase inhibitor: implications in breast cancer. Canc. Res. *61*, 4701-4706.

Peterson,G.L. (1977). A simplification of the protein assay method of Lowry et al. which is more generally applicable. Anal. Biochem. *83*, 346-356.

Petruzzella,V., Tiranti,V., Fernandez,P., Ianna,P., Carrozzo,R., and Zeviani,M. (1998). Identification and characterization of human cDNAs specific to BCS1, PET112, SCO1, COX15, and COX11, five genes involved in the formation and function of the mitochondrial respiratory chain. Genomics *54*, 494-504.

Pfanner,N. and Geissler,A. (2001). Versatility of the mitochondrial protein import machinery. Nat. Rev. Mol. Cell Biol. *2*, 339-349.

Pfeiffer,K., Gohil,V., Stuart,R.A., Hunte,C., Brandt,U., Greenberg,M.L., and Schagger,H. (2003). Cardiolipin stabilizes respiratory chain supercomplexes J. Biol. Chem. *278*, 52873-52880.

Piper,P.W. (1999). Yeast superoxide dismutase mutants reveal a pro-oxidant action of weak organic food preservatives. Free Rad. Biol. Med. *27*, 1219-1227.

Poderoso,J.J., Carreras,M.C., Lisdero,C., Riobo,N., Schopfer,F., and Boveris,A. (1996). Nitric oxide inhibits electron transfer and increases superoxide radical production in rat heart mitochondria and submitochondrial particles. Arch. Biochem. Biophys. *328*, 85-92.

Poole,R.K. and Hughes,M.N. (2000). New functions for the ancient globin family: Bacterial responses to nitric oxide and nitrosative stress. Mol. Microbiol. *36*, 775-783.

Poyton,R.O. and Burke,P.V. (1992). Oxygen regulated transcription of cytochrome *c* and cytochrome *c* oxidase genes in yeast. Biochim. Biophys. Acta *1101*, 252-256.

Pratje,E., Mannhaupt,G., Michaelis,G., and Beyreuter,K. (1983). A nuclear mutation prevents processing of a mitochondrially encoded membrane protesin in *Saccharomyces cerevisiae*. EMBO J. *2*, 1049-1054.

Preuss,M., Leonhard,K., Hell,K., Stuart,R.A., Neupert,W., and Herrmann,J.M. (2001). Mba1, a novel component of the mitochondrial protein export machinery of the yeast *Saccharomyces cerevisiae*. J. Cell Biol. *153*, 1085-1096.

Preuss,M., Ott,M., Funes,S., Luirink,J., and Herrmann,J.M. (2005). Evolution of mitochondrial oxa proteins from bacterial YidC: Inherited and acquired functions of a conserved protein insertion machinery. J. Biol. Chem. *280*, 13004-13011.

Proshlyakov,D.A., Pressler,M.A., DeMaso,C., Leykam,J.F., DeWitt,D.L., and Babcock,G.T. (2000). Oxygen activation and reduction in respiration: involvement of redox-active tyrosine 244. Science *290*, 1588-1591.

Pryor,W.A. and Lightsey,J.W. (1981). Mechanisms of nitrogen dioxide reactions: initiation of lipid peroxidation and the production of nitrous acid. Science *214*, 435-437.

Quaroni,L.G., Seward,H.E., McLean,K.J., Girvan,H.A., Ost,T.W.B., Noble,M.A., Kelly,S.M., Price,N.C., Cheesman,M.R., Smith,W.E., and Munro,A.W. (2004). Interaction of nitric oxide with cytochrome P450 BM3. Biochemistry *43*, 16416-16431.

Radi,R., Beckman,J.S., Bush,K.M., and Freeman,B.A. (1991a). Peroxynitrite oxidation of sulfhydryls. The cytotoxic potential of superoxide and nitric oxide. J. Biol. Chem. *266*, 4244-4250.

Radi,R., Beckman,J.S., Bush,K.M., and Freeman,B.A. (1991b). Peroxynitrite-induced membrane lipid peroxidation: The cytotoxic potential of superoxide and nitric oxide. Arch. Biochem. Biophys. *288*, 481-487.

Radi,R., Rodriguez,M., Castro,L., and Telleri,R. (1994). Inhibition of mitochondrial electron transport by peroxynitrite. Arch. Biochem. Biophys. *308*, 89-95.

Rahman,S., Taanman,J.-W., Cooper,J.M., Nelson,I., Hargreaves,I., Meunier,B., Hanna,M.G., Garcia,J., Capaldi,R.A., Lake,B.D., Leonard,J.V., and Shapira,A.H.V. (1999). A mis-sense mutation of cytochrome oxidase subunit II causes defective assembly and myopathy. Am. J. Hum. Genet. *65*, 1030-1039.

Ramachandran,A., Ceaser,E., and Darley-Usmar,V. (2004). Chronic exposure to nitric oxide alters the free iron pool in endothelial cells: Role of mitochondrial respiratory complexes and heat shock proteins. Proc. Natl. Acad. Sci. USA *101*, 384-389.

Ramil,E., Agrimonti,C., Shechter,E., Gervais,M., and Guiard,B. (2000). Regulation of the CYB2 gene expression: transcriptional co-ordination by the Hap1p, Hap2/3/4/5p and Adr1p transcription factors. Mol. Microbiol. *37* 1116-1132.

Rasmussen,A.K., Chatterjee,A., Rasmussen,L.J., and Singh,K.K. (2003). Mitochondria-mediated nuclear mutator phenotype in *Saccharomyces cerevisiae*. Nuc. Acid. Res. *31*, 3909-3917.

Rep,M., Nooy,J., Guelin,E., and Grivell,L.A. (1996). Three genes for mitochondrial proteins suppress null-mutations in both Afg3 and Rca1 when over-expressed. Curr. Genet. *30*, 206-211.

Rich,P.R., Jünemann,S., and Meunier,B. (1998). Protonmotive mechanism of haem-copper oxidases. J. Bioenerg. Biomemb. *30*, 131-138.

Riobo,N.A., Clementi,E., Melani,M., Boveris,A., Cadenas,E., Moncada,S., and Poderoso,J.J. (2001). Nitric oxide inhibits mitochondrial NADH: ubiquinone reductase activity through peroxynitrite formation. Biochem. J. *359*, 139-145.

Roberts,E.S., Lin,H., Crowley,J.R., Vuletich,J.L., Osawa,Y., and Hollenberg,P.F. (1998). Peroxynitrite-mediated nitration of tyrosine and inactivation of the catalytic activity of cytochrome P450 2B1. Chem. Res. Toxicol. *11*, 1067-1074.

Rodrigues-Pousada,C.A., Nevitt,T., Menezes,R., Azevedo,D., Pereira,J., and Amaral,C. (2004). Yeast activator proteins and stress response: an overview. FEBS Lett. *567*, 80-85.

Roy,B., Lepoivre,M., Henry,Y., and Fontecave,M. (1995). Inhibition of ribonucleotide reductase by nitric oxide derived form thionitrites: reversible modification of both subunits. Biochemistry *34*, 5411-5418.

Saint-Georges,Y., Hamel,P., Lemaire,C., and Dujardin,G. (2001). Role of positively charged transmembrane segments in the insertion and assembly of mitochondrial inner-membrane proteins. Proc. Natl. Acad. Sci. USA *98*, 13814-13819.

Salviati,L., Hernendez-Rosa,E., Walker,W.F., Sacconi,S., DiMauro,S., Schon,E.A., and Davidson,M.M. (2002). Copper supplementation restores cytochrome *c* oxidase activity in cultured cells from patients with SCO2 mutations. Biochem. J. *363*, 321-327.

Saracco,S.A. and Fox,T.D. (2002). Cox18p is required for export of the mitochondrially encoded *Saccharomyces cerevisiae* Cox2p C-tail and interacts with Pnt1p and Mss2p in the inner membrane. Mol. Biol. Cell *13*, 1122-1131.

Sarti,P., Giuffre,A., Barone,M.C., Forte,E., Mastronicola,D., and Brunori,M. (2003). Nitric oxide and cytochrome oxidase: reaction mechanisms from the enzyme to the cell. Free Rad. Biol. Med. *34*, 509-520.

Sarver,A. and DeRisi,J. (2005). Fzf1p regulates an inducible response to nitrosative stress in *Saccharomyces cerevisiae*. Mol. Biol. Cell. *16*, 4781-4791.

Schagger,H. and von Jagow,G. (1991). Blue native electrophoresis for isolation of membrane protein complexes in enzymatically active form. Anal. Biochem. *199*, 223-231

Schagger,H. and Pfeiffer,K. (2000). Supercomplexes in the respiratory chains of yeast and mammalian mitochondria. EMBO J. 19, 1777-1783.

Schilke,B., Voisine,C., Beinert,H., and Craig,E. (1999). Evidence for a conserved system for iron metabolism in the mitochondria of *Saccharomyces cerevisiae*. Proc. Natl. Acad. Sci. USA *96*, 10206-10211.

Schmidt,B., McCracken,J., and Ferguson-Miller,S. (2003). A discrete water exit pathway in the membrane protein cytochrome *c* oxidase. Proc. Natl. Acad. Sci. USA *100*, 15539-15542.

Schmitt,A.P. and McEntee,K. (1996). Msn2p, a zinc finger DNA-binding protein, is the transcriptional activator of the multistress response in *Saccharomyces cerevisiae*. Proc. Natl. Acad. Sci. USA *93*, 5777-5782.

Schmitt,M.E., Brown,T.A., and Trumpower,B. (1990). A rapid and simple method for preparation of RNA from *Saccharomyces cerevisiae*. Nuc. Acid. Res. *18*, 3091-3092.

Sedlák,M. and Robinson,N.C. (1999). Phospholipase A2 digestion of cardiolipin bound to bovine cytochrome *c* oxidase alters both activity and quaternary structure. Biochemistry *38*, 14966-14972.

Sellers,V.M., Johnson,M.K. and Dailey,H.A. (1996). Function of the [2Fe-2S] cluster in mammalian ferrochelatase: a possible role as a nitric oxide sensor. Biochemistry *35*, 2699-1704.

Sharpe,M.A. and Cooper,C.E. (1998). Interaction of peroxynitrite with mitochondrial cytochrome oxidase. J. Biol. Chem. *273*, 30961-30972.

Shergill,J.K., Cammack,R., Cooper,C.E., Cooper,J.M., Mann,V.M., and Schapira,A.H.V. (1996). Detection of nitrosyl complexes in human substantia nigra, in relation to Parkinson's disease. Biochim. Biophys. Res. Commun. *228*, 298-305.

Shoubridge,E.A., and Lochmuller,H. (2001). Cytochrome oxidase deficiency due to mutations in SCO2, encoding a mitochondrial copper-binding potein, is rescued by copper in human myoblasts. Hum. Mol. Genet. *10*, 3025-3035.

Siep,M., van Oosterum,K., Neufeglise,H., van der Spek,H., and Grivell,L.A. (2000). Mss51p, a putative translational activator of cytochrome *c* oxidase subunit-1 (COX1) mRNA, is required for synthesis of Cox1p in *Saccharomyces cerevisiae*. Curr.Genet. *37*, 213-220.

Slonimski,P.P. and Tzagoloff,A. (1976). Localisation in yeast mitochondrial DNA of mutations expressed in a deficiency of cytochrome oxidase and/or coenzyme QH_2-cytochrome *c* reductase. Eur. J. Biochem. *61*, 27-41.

Smith,D., Gray,J., Mitchell,L., Antholine,W.E., and Hosler,J.P. (2005). Assembly of cytochrome-*c* oxidase in the absence of assembly protein Surf1p leads to loss of the active site heme. J. Biol. Chem. *280*, 17652-17656.

Souza,J.M. and Radi,R. (1998). Glyceraldehyde-3-phosphate dehydrogenase inactivation by peroxynitrite. Arch. Biochem. Biophys. *360*, 187-194.

Souza,R.L., Green-Willms N.S., Fox T.D., Tzagoloff A., and Nobrega F.G. (2000). Cloning and characterization of COX18, a *Saccharomyces cerevisiae* PET gene required for the assembly of cytochrome oxidase. J. Biol. Chem. *275*, 14898-14902.

Speno,H., Taheri,M.R., Sieburth,D., and Martin,C.T. (1995). Identification of essential amino acids within the proposed Cu_A binding site in subunit II of cytochrome *c* oxidase. J. Biol. Chem. *270*, 25363-25369.

Srinivasan,C., Liba,A., Imlay,J.A., Valentine,J.S., and Gralla,E.B. (2000). Yeast lacking superoxide dismutase(s) show elevated levels of "free iron" as measured by whole cell electron paramagnetic resonance. J. Biol. Chem. *275*, 29187-29192.

Stachowiak,O., Dolder,M., Wallimann,T., and Richter,C. (1998). Mitochondrial creatine kinase is a prime target of peroxynitrite-induced modification and inactivation. J. Biol. Chem. *273*, 16694-16699.

Susswein,A.J., Katzoff,A., Miller,N., and Hurwitz,I. (2004). Nitric oxide and memory. Neuroscientist *10*, 153-162.

Szyrach,G., Ott,M., Bonnefoy,N., Neupert,W., and Herrmann,J.M. (2003). Ribosome binding to the Oxa1 complex facilitates co-translational protein insertion in mitochondria. EMBO J. *22*, 6448-6457.

Taanman,J.W. and Capaldi,R.A. (1992). Purification of yeast cytochrome *c* oxidase with a subunit composition resembling the mammalian enzyme. J. Biol. Chem. *267*, 22481-22485.

Taanman,J.-W. and Capaldi,R.A. (1993). Subunit VIa of yeast cytochrome *c* oxidase is not necessary for assembly of the enzyme complex but modulates the enzyme activity. Isolation and characterization of the nuclear-coded gene. J. Biol. Chem. *268*, 18754-18761.

Taanman,J.-W. (1997). Human cytochrome *c* oxidase: Structure, function and deficiency. J. Bioenerg. Biomemb. *29*, 151-163.

Taanman,J.-W., Bodnar,A.G., Cooper,J.M., Morris,A.A.M., Clayton,P.T., Leonard,J.V., and Schapira,A.H.V. (1997). Molecular mechanisms in mitochondrial DNA depletion syndrome. Hum. Mol. Genet. *6*, 935-942.

Tamir,S., Burney,S., and Tannenbaum,S.R. (1996). DNA damage by nitric oxide. Chem. Res. Toxicol. *9*, 821-827.

Tatoyan,A. and Giulivi,C. (1998). Purification and characterisation of a nitric-oxide synthase from rat liver mitochondria. J. Biol. Chem. *273*, 11044-11048.

Tauer,R., Mannhaupt,G., Schnall,R., Pajic,A., Langer,T., and Feldmann,H. (1994). Yta10p, a member of a novel ATPase family in yeast, is essential for mitochondrial function. FEBS Lett. *353*, 197-200.

Ter Linde,J.J., Liang,H., Davis,R.W., Steensma,H.Y., van Dijken,J.P., and Pronk,J.T. (1999). Genome-wide transcriptional analysis of aerobic and anaerobic chemostat cultures of *Saccharomyces cerevisiae*. J. Bacteriol. *181*, 7409-7413.

Ter Linde,J.J. and Steensma,H.Y. (2002). A microarray-assisted screen for potential Hap1 and Rox1 target genes in *Saccharomyces cerevisiae*. Yeast *19*, 825-840.

Terziyska,N., Lutz,T., Kozany,C., Mokranjac,D., Mesecke,N., Neupert,W., Herrmann,J.M., and Hell,K. (2005). Mia40, a novel factor for protein import into the intermembrane space of mitochondria is able to bind metal ions. FEBS Lett. *579*, 179-184.

Thomas,J.W., Calhoun,M.W., Lemieux,L.J., Puustinen,A., Wikström,M., Alben,J.O., and Gennis,R.B. (1994). Site-directed mutagenesis of residues within helix VI in subunit I of the cytochrome bo_3 ubiquinol oxidase from *Escherichia coli* suggests that tyrosine 288 may be a Cu_B ligand. Biochemistry *33*, 13013-13021.

Torello,A.T., Overholtzer,M.H., Cameron,V.L., Bonnefoy,N., and Fox,T.D. (1997). Deletion of the leader peptide of the mitochondrially encoded precursor of *Saccharomyces cerevisiae* cytochrome *c* oxidase subunit II. Genetics *145*, 903-910.

Tsukihara,T., Aoyama,H., Yamashita,E., Tomizaki,T., Yamaguchi,H., Shinzawa-Itoh,K., Nakashima,R., Yaono,R., and Yoshikawa,S. (1995). Structures of metal sites of oxidized bovine heart cytochrome *c* oxidase at 2.8 Å. Science *269*, 1069-1074.

Tsukihara,T., Aoyama,H., Yamashita,E., Tomizaki,T., Yamaguchi,H., Shinzawa-Itoh,K., Nakashima,R., Yaono,R., and Yoshikawa,S. (1996). The whole structure of the 13-subunit oxidized cytochrome *c* oxidase at 2.8 Å. Science *272*, 1136-1144.

Turrens,J.F. and Boveris,A. (1980). Generation of superoxide anion by the NADH dehydrogenase of bovine heart mitochondria. Biochem. J. *191*, 421-427.

Tzagoloff,A., Capitanio,N., Nobrega,M.P., and Gatti,D. (1990). Cytochrome oxidase assembly in yeast requires the product of COX11, a homolog of the *P. denitrificans* protein encoded by ORF3. EMBO J. *9*, 2759-2764.

Tzagoloff,A., and Dieckmann,C.L. (1990). PET genes of *Saccharomyces cerevisiae*. Microbiol. Rev. *54*, 211-225.

Tzagoloff,A., Nobrega,M., Gorman,N., and Sinclair,P. (1993). On the functions of the yeast COX10 and COX11 gene products. Biochem. Mol. Biol. Int. *31*, 593-598.

van Gelder,B., and Slater,E.C. (1962). The extinction coefficient of cytochrome *c*. Biochim. Biophys. Acta *58,* 893-595.

van Loon,A.P.G.M., Pesold-Hurt,B., and Schatz,G. (1986). A yeast mutant lacking mitochondrial manganese-superoxide dismutase is hypersensitive to oxygen. Proc. Natl. Acad. Sci. USA *83*, 3820-3824.

Veal,E.A., Ross,S.J., Malakasi,P., Peacock,E., and Morgan,B.A. (2003). Ybp1 is required for the hydrogen peroxide-induced oxidation of the Yap1 transcription factor. J. Biol. Chem. *278*, 30896-30904.

Vesela,K., Hansikova,H., Tesarova,M., Martasek,P., Elleder,M., Houstek,J., and Zeman,J. (2004). Clinical, biochemical and molecular analyses of six patients with isolated cytochrome c oxidase deficiency due to mutations in the SCO2 gene. Acta Paediatr. *93*, 1312-1317.

Wang,G.L., Jiang,B.H., Rue,E.A. and Semenza,G.L. (1995). Hypoxia-inducible factor 1 is a basic-helix-loop-helix-PAS heterodimer regulated by cellular O_2 tension. Proc. Natl. Acad. Sci. USA *92*, 5510-5514.

Wei,J., Guo,H., and Kuo,P.C. (2002). Endotoxin-stimulated nitric oxide production inhibits expression of cytochrome *c* oxidase in ANA-1 murine macrophages. J. Immunol. *168*, 4721-4727.

Welter,R., Yu,L., and Yu.C-.A. (1996). The effects of nitric oxide on electron transport complexes. Arch. Biochem. Biophys. *331*, 9-14.

Wennmalm,A., Benthin,G., Edlund,A., Jungersten,L., Kieler-Jensen,N., Lundin,S., Westfelt,U.N., Petersson,A.S., and Waagstein,F. (1993). Metabolism and excretion of nitric oxide in humans. An experimental and clinical study. Circ. Res. *73*, 1121-1127.

Wikström,M., Morgan,J.E., and Verkhovsky,M.I. (1998). On the mechanism of proton translocation by respiratory enzyme. J. Bioenerg. Biomemb. *30,* 139-145.

Wikström,M. (2000) Proton translocation by cytochrome c oxidase: a rejoinder to recent criticism. Biochemistry *39*, 3515-9.

Williams,S.L., Valnot,I., Rustin,P., and Taanman,J.-W. (2004). Cytochrome *c* oxidase subassemblies in fibroblast cultures from patients carrying mutations in COX10, SCO1, or SURF1. J. Biol. Chem. *279*, 7462-7469.

Witt,H., Zickermann,V., and Ludwig,B. (1995). Site-directed mutagenesis of cytochrome *c* oxidase reveals two acidic residues involved in the binding of cytochrome *c*. Biochim. Biophys. Acta *1230*, 74-76.

Wolosker,H., Panizzutti,R., and Engelender,S. (1996). Inhibition of creatine kinase by S-nitrosoglutathione. FEBS Lett. *392*, 274-276.

Wong,C.-M., Zhou,Y., Ng,R.W.M., Kung,H., and Jin,D.-Y. (2002a). Cooperation of yeast peroxiredoxins Tsa1p and Tsa2p in the cellular defense against oxidative and nitrosative stress. J. Biol. Chem. *277*, 5385-5394.

Wright,R.M., Dircks,L.K., and Poyton,R.O. (1986). Characterization of COX9, the nuclear gene encoding the yeast mitochondrial protein cytochrome *c* oxidase subunit VIIa. Subunit VIIa lacks a leader peptide and is an essential component of the holoenzyme. J. Biol. Chem. *261*, 17183-17191.

Yakes,F.M. and Van Houten,B. (1997). Mitochondrial DNA damage is more extensive and persists longer than nuclear DNA damage in human cells following oxidative stress. Proc. Natl. Acad. Sci. USA *94*, 514-519.

Yamamoto,T., Maruyama,W., Kato,Y., Yi,H., Shamoto-Nagai,M., Tanaka,M., Sato,Y., and Naoi,M. (2002). Selective nitration of mitochondrial complex I by peroxynitrite: Involvement in mitochondria dysunction and cell death of dopaminergic SH-SY5Y cells. J. Neural. Transm. *109*, 1-13.

Yun,C.-W., Ferea,T., Rashford,J., Ardon,O., Brown,P.O., Botstein,D., Kaplan,J., and Philpott,C.C. (2000). Desferrioxamine-mediated iron uptake in *Saccharomyces cerevisiae*. Evidence for two pathways of iron uptake. J. Biol. Chem. *275*, 10709-10715.

Zhang,L. and Guarente,L. (1994). HAP1 is nuclear but is bound to a cellular factor in the absence of heme. J. Biol. Chem. *269*, 14643-14647.

Zhang,L., Hach,A., and Wang,C. (1998). Molecular mechanism governing heme signaling in yeast: A higher-Order complex mediates heme regulation of the transcriptional activator HAP1. Mol. Cell. Biol. *18*, 3819-3828.

Zhang,M., Mileykovskaya,E., and Dowhan,W. (2002). Gluing the respiratory chain together. Cardiolipin is required for supercomplex formation in the inner mitochondrial membrane. J. Biol. Chem. *277*, 43553-43556.

Zhen,Y., Hoganson,C.W., Babcock,G.T., and Ferguson-Miller,S. (1999). Definition of the interaction domain for cytochrome *c* on cytochrome *c* oxidase. I. Biochemical, spectral, and kinetic characterization of surface mutants in subunit II of *Rhodobacter sphaeroides* cytochrome aa_3. J. Biol. Chem. *274*, 38032-38041.

APPENDICES

Biochem. J. (2005) **390**, 703–708 (Printed in Great Britain) doi:10.1042/BJ20050598

Analysis of COX2 mutants reveals cytochrome oxidase subassemblies in yeast

Susannah HORAN*, Ingrid BOURGES*, Jan-Willem TAANMAN† and Brigitte MEUNIER*[1]

THE JOURNAL OF BIOLOGICAL CHEMISTRY

Vol. 280, No. 33, Issue of August 19, pp. 29743–29749, 2005
Printed in U.S.A.

Effect of Inhibition of the bc_1 Complex on Gene Expression Profile in Yeast*[S]

Received for publication, May 31, 2005
Published, JBC Papers in Press, June 20, 2005, DOI 10.1074/jbc.M505915200

Ingrid Bourges, Susannah Horan, and Brigitte Meunier‡

Yeast
Yeast 2006; **23**: 519–535.
Published online in Wiley InterScience (www.interscience.wiley.com). **DOI:** 10.1002/yea.1372

Research Article

Transcriptional response to nitrosative stress in *Saccharomyces cerevisiae*

Susannah Horan[1], Ingrid Bourges[1] and Brigitte Meunier[1,2]*

Yeast 2006; **23**: 519–535.

Yeast 2006; **23**: 519–535.

Yeast 2006; **23**: 519–535.

Yeast 2006; **23**: 519–535.

Yeast 2006; **23**: 519–535.

Yeast 2006; **23**: 519–535.

Yeast 2006; **23**: 519–535.

Yeast 2006; **23**: 519–535.

Yeast 2006; **23**: 519–535.

Yeast 2006; **23**: 519–535.

Yeast 2006; **23**: 519–535.

Yeast 2006; **23**: 519–535.

Yeast 2006; **23**: 519–535.